

New magnetic topological materials from high-throughput search

Íñigo Robredo,^{1, 2} Yuanfeng Xu,³ Yi Jiang,¹ Claudia Felser,² B. Andrei Bernevig,^{1, 4, 5} Luis Elcoro,⁶ Nicolas Regnault,^{4, 7} and Maia G. Vergniory^{1, 2, 8,*}

¹*Donostia International Physics Center, P. Manuel de Lardizabal 4, 20018 Donostia-San Sebastian, Spain*

²*Max Planck Institute for Chemical Physics of Solids, 01187 Dresden, Germany*

³*Center for Correlated Matter and School of Physics, Zhejiang University, Hangzhou 310058, China*

⁴*Department of Physics, Princeton University, Princeton, New Jersey 08544, USA*

⁵*IKERBASQUE, Basque Foundation for Science, 48013 Bilbao, Spain*

⁶*Department of Physics, University of the Basque Country UPV/EHU, Apartado 644, 48080 Bilbao, Spain*

⁷*Laboratoire de Physique de l'Ecole normale supérieure,*

ENS, Université PSL, CNRS, Sorbonne Université,

Université Paris-Diderot, Sorbonne Paris Cité, 75005 Paris, France

⁸*Département de physique et Institut quantique, Université de Sherbrooke, Sherbrooke, Québec, Canada J1K 2R1*

We conducted a high-throughput search for topological magnetic materials on 522 new, experimentally reported commensurate magnetic structures from [MAGNDATA](#), doubling the number of available materials on the [Topological Magnetic Materials](#) database. This brings up to date the previous studies [1–4] which had become incomplete due to the discovery of new materials. For each material, we performed first-principle electronic calculations and diagnosed the topology as a function of the Hubbard U parameter. Our high-throughput calculation led us to the prediction of 250 experimentally relevant topologically non-trivial materials, which represent 47.89% of the newly analyzed materials. We present five remarkable examples of these materials, each showcasing a different topological phase: [Mn₂AIB₂](#) (BCSID 1.508), which exhibits a nodal line semimetal to topological insulator transition as a function of SOC, [CaMnSi](#) (BCSID 0.599), a narrow gap axion insulator, [UAs](#) (BCSID 0.594) a 5f-orbital Weyl semimetal, [CsMnF₄](#) (BCSID 0.327), a material presenting a new type of quasi-symmetry protected closed nodal surface and [FeCr₂S₄](#) (BCSID 0.613), a symmetry-enforced semimetal with double Weyls and spin-polarised surface states.

I. INTRODUCTION

For decades, electronic topological systems have been a research hotspot in the field of condensed matter physics. The development of topological quantum chemistry (TQC) [2, 5] and symmetry-based indicators [6–10] has facilitated the prediction of topological quantum materials in realistic systems. In particular, it allowed for high-throughput searches of topological quantum materials resulting in extensive databases [3, 4, 11, 12] like the [Topological Quantum Chemistry website](#). Recent developments have shown that the interplay of spin and charge degrees of freedom in magnetic systems can realize new topological phases such as axion insulators (AXI) [13–17], or non-axionic magnetic higher-order topological insulators (MHOTI) [1, 2, 18–20]. These phases, unique to magnetic systems, combine the robustness of topological surface states with spin ordering, promising a wide array of applications, such as in materials for quantum computation [21], spintronics [22] and catalysis [23, 24]. The current focus now lies on finding materials that display the aforementioned topological properties and can be readily grown. To enable the prediction and diagnosis of magnetic topological phases of matter, the formalism of TQC was extended to magnetic TQC (MTQC) [2], resulting in the prediction of 137 new magnetic topological materials [1, 25].

In this work, we use MTQC to conduct a high-throughput analysis on the new entries in [MAGNDATA](#), extending the [Topological Magnetic Materials](#) [1] database from 372 to 894 entries and adding 522 new experimentally reported stoichiometric magnetic materials with commensurate magnetic order. The main result of our work is the prediction of 250 experimentally relevant topologically non-trivial materials. We define a material as topologically non-trivial if we diagnose it as topological for at least one value of the interaction strength, parameterized by the Hubbard U value [26]. Interestingly, we found several examples of interaction-driven topology: systems in which the interaction can onset a topological phase transition.

In our search, we found 98 new topological insulators (TI), which can be broken down into different topological classes. We found 84 axion insulators (AXI), 3 magnetic topological crystalline insulators (MTCI) and 34 3D quantum anomalous Hall (3DQAH) systems, as well as 50 magnetic obstructed atomic insulators (mOAI), a special case of topological insulators that can be explained in terms of localized orbitals but whose Wannier charge center is localized away from atomic positions [5, 25, 27–29]. The latter is relevant since their non-magnetic counterparts have been predicted to have good catalytic activity [24, 25]; and magnetic systems are known to improve some catalytic reactions, such as oxygen evolution reaction (OER) [30–32]. We therefore speculate that mOAI may be promising materials displaying both features. In this category, we find a promis-

* maia.vergniory@cpfs.mpg.de

ing candidate, CuFeO_2 (BCSID 1.347), which holds the same topological diagnosis for all values of the Hubbard parameter U . We also predict 182 new enforced semimetals (ES) with symmetry-enforced degeneracies at high-symmetry points, lines or planes. One of the most relevant magnetic semimetals are Weyl semimetals, due to various proposed effects and applications, such as Veselago lenses, quantized circular photogalvanic effect or unconventional charge to spin conversion[33–36]. Contrary to non-magnetic systems where predicting Weyl crossings is difficult in terms of symmetry indicators (SI) [37], the MTQC formalism can predict Weyl crossings in magnetic systems under certain conditions [2]. Based on SI, MTQC can predict the difference in the Chern numbers between high-symmetry planes, which assures the existence of a quantum critical point along the momentum separating them. This degeneracy point carrying topological charge forces the system to be semi-metallic, thus indicating the presence of Weyl nodes. These systems are also known as Smith index semimetals or symmetry indicated Weyl semimetals [1, 2, 38]. In our high-throughput search, we found 13 symmetry indicated Weyl semimetals, among which we found that the ferromagnetic Weyl semimetal $\text{Co}_3\text{Sn}_2\text{S}_2$ (BCSID 0.860), which has been well-studied previously[39–41], can be reinterpreted by a topological index $\eta_{4I} = 3$.

From our search results, we have identified five especially promising materials, two TIs and three ESs, which we selected for further analysis of their topological properties. First, we present Mn_2AlB_2 (BCSID 1.508), a layered antiferromagnetic system that displays a nodal line to TI transition when the spin-orbit coupling (SOC) is turned on. Then we consider materials within the Ce-FeSi family of small gap magnetic insulators [42]. We found that one material in the family, CaMnSi (BCSID 0.599), displays a band inversion that drives the topological transition to an AXI. In the ES class, we present three examples, namely UAsS (BCSID 0.594), CsMnF_4 (BCSID 0.327) and FeCr_2S_4 (BCSID 0.613). The first is a ferromagnetic Weyl and nodal line semimetal with double Fermi arcs on the surface. The second is a layered square net ferromagnetic system that displays a symmetry-protected nodal line. While already reported in Ref. [43], our analysis proves that there is a hidden quasi-symmetry [44, 45] that protects an almost closed 2D nodal surface, enhancing the semimetallic behavior at the Fermi level. Lastly, FeCr_2S_4 (BCSID 0.613) is a ferrimagnetic system with symmetry-protected nodal lines and topologically protected Weyl nodes, as well as double Weyl nodes [46].

This work is divided as follows. In Section II, we present the workflow and methods for the high-throughput search. In Section III, we summarize the topological properties of the five selected materials. Section IV provides the discussion of the main results of our search. In Appendix A we give an overview of the formalism of MTQC and explain the origin of the symmetry indicators and real space invariants (RSI) [25, 27] using

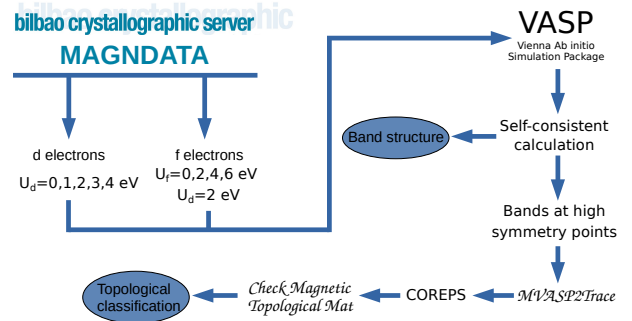


FIG. 1. High throughput flowchart. We categorize the materials in MAGNDATA database into two groups: one containing d electrons and no f electrons, and another one containing f electrons. We then conduct *ab initio* calculations using VASP [47–50] with multiple Hubbard U parameters to obtain the band structure as well as the magnetic coreps [2, 51]. Subsequently, the corresponding symmetry-data-vector can be uploaded to the BCS to obtain the topological classification.

magnetic space group (MSG) $P\bar{1}$ as an example. Appendix B gives the full analysis of the topological properties of the selected example materials. Finally, Appendices C, D, E and F contain the full tables summarizing the results of our materials search: Appendix C includes a comparison between experimental and calculated magnetic moments, Appendix D covers the topological classification and both direct and indirect gaps. Finally, in Appendix E we give the physical interpretation of the systems with non-trivial symmetry indicators and Appendix F contains detailed information on the crystal structure, magnetic space group, electronic band structure, and topological classification of all materials.

II. WORKFLOW

In this section we present the main symmetry-diagnosable categories of topological materials and our computational methods.

A. MTQC brief overview

The formalism of MTQC has been extensively described and reviewed in prior work [1, 2, 52, 53]. Here we briefly review the fundamental building blocks and the resulting topological classification. The electronic band structures of solids can be classified according to the symmetry properties of the Bloch wavefunctions at high-symmetry momenta. This information is encoded in a vector containing the multiplicity of the irreducible co-representations (coreps) of the occupied set of bands called symmetry-data-vector. A symmetry-data-vector is identified as topologically trivial if it can be expressed as a sum of elementary band representations (EBR) with

MSG	TI/OAI			ES/ESFD			MSG	TI/OAI			ES/ESFD			MSG	TI/OAI			ES/ESFD		
	$U=0$	$U=2$	$U=4$	$U=0$	$U=2$	$U=4$		$U=0$	$U=2$	$U=4$	$U=0$	$U=2$	$U=4$		$U=0$	$U=2$	$U=4$	$U=0$	$U=2$	$U=4$
$P\bar{1}$	1	1	1	0	0	0	$Pmm'n'$	0	0	0	2	2	1	$I\bar{4}'2d'$	0	0	0	1	1	0
$P_S\bar{1}$	4	2	2	0	0	0	P_Cbcn	1	0	1	0	1	0	$P4/mm'm'$	0	0	1	3	3	2
P_a2_1/m	1	1	1	0	0	0	P_Ibcn	2	2	0	0	1	3	P_c4/mcc	0	0	0	0	1	2
P_C2_1/m	1	0	0	0	0	0	P_Cbca	0	0	1	1	1	0	P_I4/nnc	2	1	3	9	16	15
$C2/m$	0	0	0	1	1	1	$Pnma$	4	1	0	0	0	0	$P4'/m'bm'$	1	1	1	1	2	2
$C2'/m'$	8	7	6	0	0	0	$Pn'm'a$	2	1	1	2	1	1	P_c4/mnc	0	0	0	0	1	1
C_c2/m	7	5	3	1	0	0	$Pn'm'a'$	1	0	0	2	2	1	P_I4/mnc	1	0	1	5	6	5
P_a2/c	1	0	0	0	0	0	$Pn'm'a'$	0	0	0	2	0	0	$P4'/n'm'm$	4	2	2	0	0	0
P_{21}/c	3	1	1	8	2	2	P_anma	2	2	2	1	0	0	$P4/nm'm'$	1	2	0	2	1	3
$P_{2'_1}/c'$	2	1	1	0	0	0	P_bnma	0	0	0	1	0	1	P_c4/ncc	0	1	1	1	0	0
P_a2_1/c	1	1	1	0	0	0	$Cm'cm$	0	0	0	2	2	1	$I4'/mmm'$	0	0	0	1	1	0
P_A2_1/c	1	1	1	0	0	0	$Cm'c'm$	0	0	2	3	4	2	$I4'/m'm'm$	2	3	1	0	0	2
P_C2_1/c	2	0	0	0	0	0	$Cmc'm'$	1	0	0	1	2	3	$I4/mm'm'$	0	0	0	2	5	5
$C2/c$	1	0	0	0	1	0	$Cm'cm'$	1	0	0	10	10	9	I_4/mcm	0	1	1	1	0	0
$C2'/c'$	2	2	2	0	0	0	C_cmc_m	2	0	2	0	2	0	$I4_1/am'd'$	0	0	0	0	1	0
C_c2/c	2	3	2	0	0	0	C_Amca	5	2	1	1	1	2	$R\bar{3}m$	0	0	0	0	1	0
C_a2/c	1	1	0	0	0	0	$Cmm'm'$	0	0	0	5	5	3	$R\bar{3}m'$	3	2	1	2	3	3
$Cmc'2'_1$	0	0	0	1	0	0	C_ammm	1	0	1	0	0	0	$R_I\bar{3}c$	1	1	1	0	0	0
$Am'm'2$	0	0	0	1	0	1	C_cccm	0	0	1	1	1	0	$P62'm'$	0	0	0	2	0	2
A_bbm2	0	0	0	1	0	0	C_{Accm}	1	1	0	0	0	0	$P6/mm'm'$	0	0	0	3	0	2
$Im'm2'$	0	0	0	6	6	5	C_{amma}	3	3	3	0	0	0	P_c6/mcc	0	0	0	1	1	0
$I_{ama}2$	0	0	0	1	0	0	C_{Acca}	1	1	1	0	0	0	$P6'_3/m'm'c$	2	1	1	0	0	0
$Pm'm'm$	0	0	1	1	1	0	$Fd'd'd$	0	0	0	1	0	0	$P6_3/mm'c'$	0	0	0	1	1	1
P_Bnnna	0	0	0	1	1	1	$Im'mm$	0	0	0	1	2	2	$P2_{13}$	0	0	0	0	0	2
P_{Bcca}	2	2	2	0	0	0	$Imm'a'$	0	0	0	1	1	1	$Fd\bar{3}m'$	2	1	0	0	0	0
P_{Innm}	0	0	0	0	2	2	P_C42_1m	0	0	1	0	0	0	$Im\bar{3}m'$	0	0	0	0	1	1
$Pm'm'n$	3	1	1	1	4	4	$I4m'2'$	0	0	0	0	1	1	Total	89	58	56	95	102	95

TABLE I. Summary of topologically nontrivial materials per MSG as a function of Hubbard U parameter. We group the topologically non-trivial systems into topological insulators (TI, which accounts for SEBR and NLC, and OAI) and enforced semimetals (both ES and ESFD). We display the U values 0, 2 and 4 (in units of eV), which are the ones in common for all material types, both containing d and f electrons. The table contains the classification as a function of magnetic space group.

positive integer coefficients. The trivial symmetry-data-vectors, also called band representations (BR), conform the space of trivial insulators. Physically, the sum of EBRs can be understood as the addition of trivial atomic insulators. If a system can be expressed as a collection of trivial insulators, the studied band structure can be adiabatically connected to a trivial insulator, and it is thus, diagnosed as topologically trivial.

There are 4 possible outcomes when we express a symmetry-data-vector in terms of EBRs:

- Linear combination of EBRs (LCEBR). In this case, the symmetry-data-vector can be expressed as linear combination of EBRs with positive integer coefficients. Therefore, the system is compatible with a description in terms of localized magnetic orbitals in real space. In addition to atomic insulators (AI) that are topologically trivial, a topologically distinct phase exists, i.e., the mOAI. In the latter case, the occupied electronic bands are induced from localized magnetic orbitals away from the atomic positions and there exists an obstruction to reverting them to the original atomic location. These systems exhibit special surface states pinned by crystalline symmetries that do not connect va-

lence and conduction bands and can be diagnosed via the RSI [25, 54].

- Linear combination of EBRs with, necessarily, at least one negative integer coefficient in the EBR decomposition (fragile). This solution is inconsistent with a trivial insulator, but the addition of extra orbitals to the system would render it topologically trivial [2, 5, 7–9].
- Topological insulator. The solution of the decomposition into EBRs has fractional coefficients and indicates stable topology. For instance, AXI, MTCI or (M)HOTIs [1, 55] belong to that category. They can be compactly diagnosed by symmetry indicators [2, 5, 7–9, 11] (see Appendix A for further details). There are two subcategories, split EBR (SEBR), in which the solution can be expressed in terms of EBRs and parts of split EBRs, and ‘non linear combination’ (NLC), in which case there is no decomposition into EBRs and parts of split EBRs.
- Enforced semimetal (ES). This case arises if the symmetry-data-vector [2, 5, 7, 9] is incompatible with an insulator. There are two types of ESs: first,

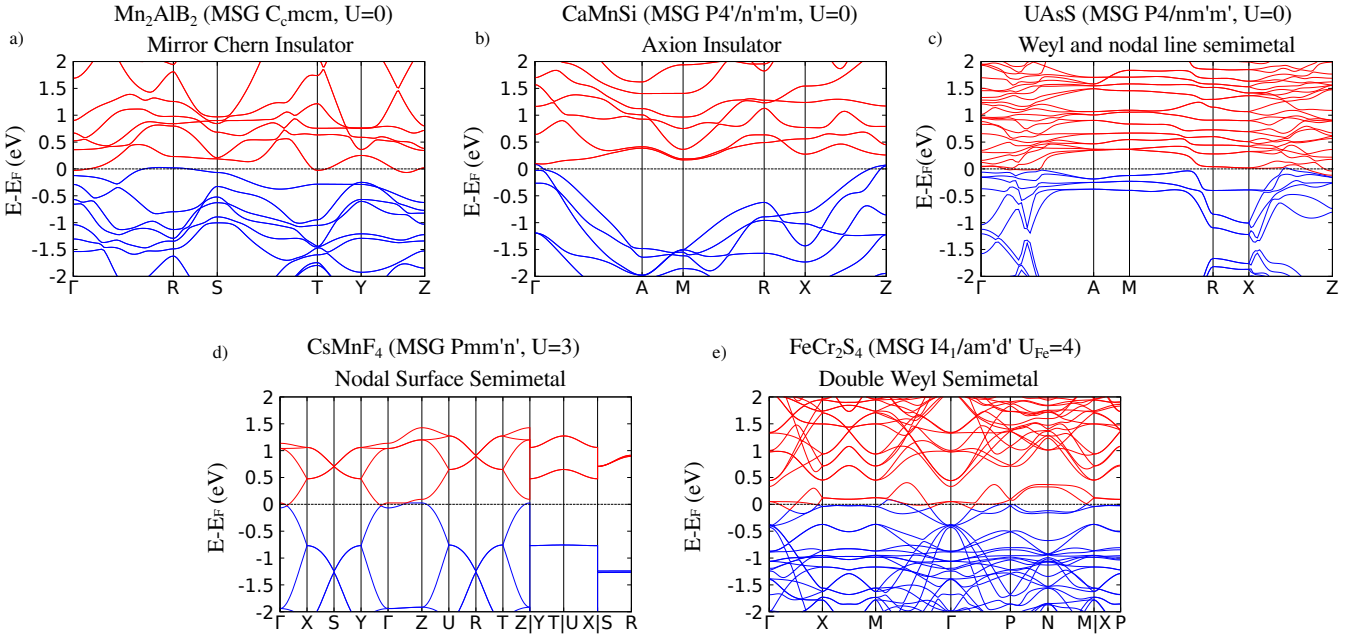


FIG. 2. Electronic band structures for the five ideal topological systems: a) Mn_2AlB_2 (BCSID 1.508), b) CaMnSi (BCSID 0.599), c) UAsS (BCSID 0.594), d) CsMnF_4 (BCSID 0.327) and e) FeCr_2S_4 (BCSID 0.613). The blue (red) color stands for the valence (conduction) bands according to the band index. In the title above each figure, we display the chemical formula, MSG and Hubbard U value used for the band structure and providing the best match for the magnetic moments. Under the title, we provide the topological classification.

if by electron counting, a corep at a high symmetry point is only partially filled, we classify the material as enforced semimetal with Fermi degeneracy (ESFD). In case the Fermi level is clean from electron or hole pockets, the Fermi energy would exactly intersect the degenerate crossing enforced by symmetry. Second, even if the bands are gapped at every high-symmetry k -point, if the compatibility relations are not satisfied[1, 2] the bands must be gapless at some point along a high-symmetry line or plane in the BZ. The formalism does not predict the exact point in which the crossing must occur, but it can predict certain high symmetry lines or planes in which the crossing happens.

- Smith-index SM (SISM). Unlike ESs in which the crossing is protected as well as predicted by symmetry, SISMs satisfy the compatibility relations [2, 5], i.e., the symmetry-data-vector is compatible with an insulator. However, a difference in the Chern number between high-symmetry planes assures the existence of a quantum critical point along the path [38]. This degeneracy point, carrying topological charge, forces the system to be semimetallic (e.g. Weyl semimetals).

The symmetry-based diagnosis poses certain limitations. In general, symmetry-based topological diagnosis is a sufficient condition to classify a compound as topologically non-trivial but it is not a necessary condition. Therefore, in cases with scarce symmetry, MTQC

can diagnose nontrivial topology as trivial. This formalism, however, serves as a computationally inexpensive diagnosing method (as opposed to, e.g., Wilson loops) for high-throughput prediction of topological materials [1, 3, 4, 11].

B. Methods

We start by selecting 522 new material entries from the BCS magnetic material database **MAGNDATA** [56, 57]. In this database, both the crystalline and magnetic structures have been derived from experiments. As the determination of the magnetic ground state is a computationally challenging task, we initialize our calculations with the experimental magnetization and ensure their self-consistent convergence. This is expected to yield much more accurate results than determining the magnetic ordering from first principles. The process will generally converge to distinct magnetic structures as a function of the Hubbard U parameter, which accounts for the localization properties of magnetic elements' electrons in d- and f-shells. We summarize the resulting magnetization as a function of the Hubbard U parameter in Appendix C. Based on these results, we can estimate the most probable topological classification for a given material, by selecting the one that deviates the least from the experimentally reported magnetic structure.

We performed DFT calculations as implemented in the Vienna ab initio simulation package (VASP) [47–50]. The

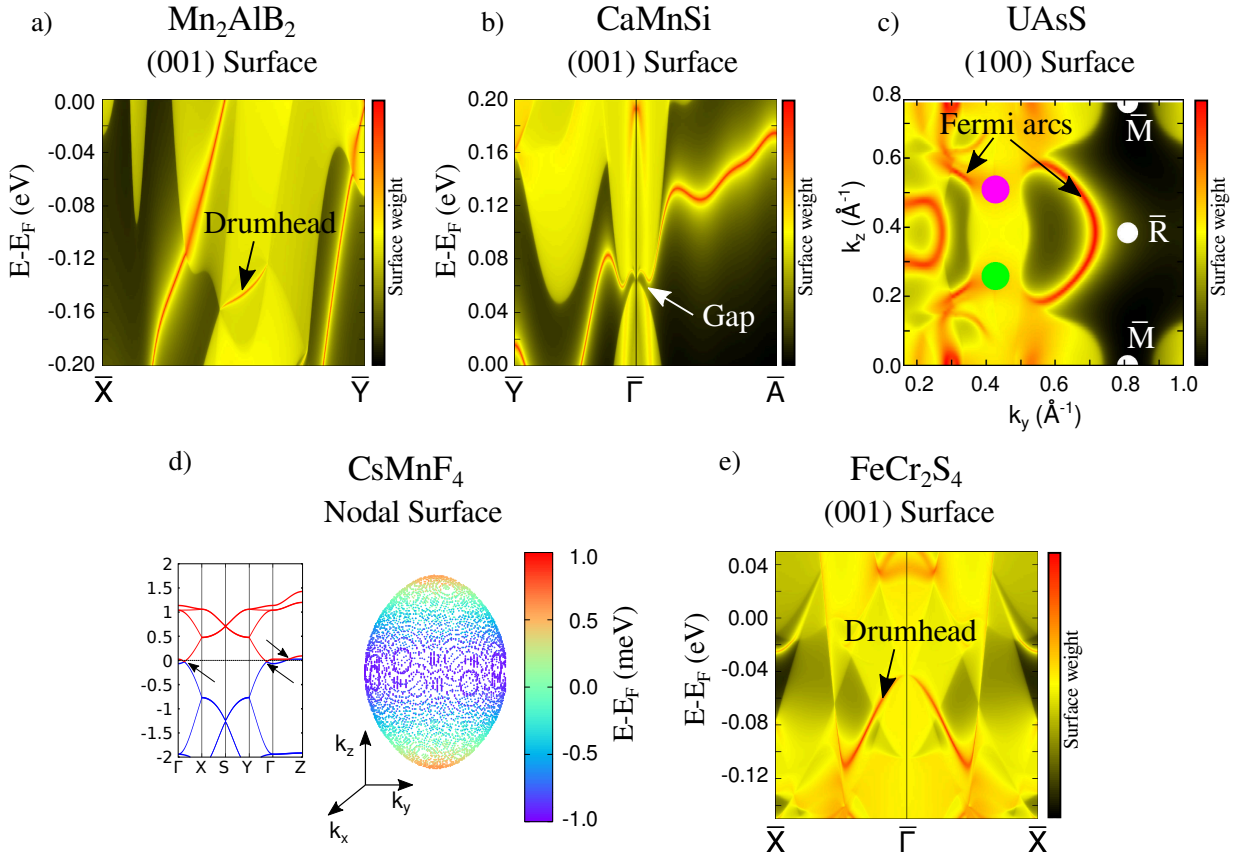


FIG. 3. Surface spectrum and topological properties of the high-quality systems. For a), b), c) and e) we provide the surface direction in the title of the plot. a) Drumhead surface states of Mn_2AlB_2 (BCSID 1.508) without SOC connecting the projections of the bulk nodal line in the surface. b) Gaped surface spectrum of CaMnSi (BCSID 0.599) axion insulator. c) Double Fermi arcs connecting the projection of Weyl nodes of UAsS (BCSID 0.594) at the Fermi level (Weyl projection of charge 2 in magenta, Weyl projection of charge -2 in green). d) 2D closed nodal surface enforced by quasi-symmetry of CsMnF_4 (BCSID 0.327). The arrows point at the nodal surface location in the band structure. e) Drumhead surface states of SOC FeCr_2S_4 (BCSID 0.613).

interaction between the ion cores and valence electrons was treated by the projector augmented-wave method [58], the generalized gradient approximation (GGA) was employed for the exchange-correlation potential with the Perdew–Burke–Ernzerhof functional for solid parameterization [59], and the spin-orbit coupling (SOC) was considered based on the second variation method [60]. A Γ -centered Monkhorst-Pack k-point grid of $(9 \times 9 \times 9)$ was used for reciprocal space integration and 500 eV energy cutoff of the plane-wave expansion. The grid density of the largest materials was reduced up to $(5 \times 5 \times 5)$ k-points. For materials with d-electron elements, we performed DFT+U calculations with Hubbard U parameter values of $U = 0, 1, 2, 3, 4$ eV. For f-electron elements, that tend to be more localized, we used larger Hubbard U values, $U = 0, 2, 4, 6$ eV. In the presence of both d- and f-electron elements, we set the Hubbard U value of the d-electron element to $U = 2$ eV and vary the f-electron element U parameter, following the criteria of Ref. [1]. All materials presented herein were converged self-consistently to a magnetic ground state with an accuracy of 10^{-5} eV per unit cell. We then run two non-self-

consistent band calculations; one along high symmetry lines to get the electronic band dispersion and another one at the high-symmetry points to obtain the wavefunctions. We use *MagVASP2trace* [1, 2] on the latter to obtain the magnetic coreps and BR of the occupied set of bands, which we then upload to the BCS server [61–63] for symmetry-based topological prediction. The workflow is schematically depicted in Fig. 1.

III. IDEAL TOPOLOGICAL MATERIALS

As representatives of the different topological classes found on this work, we selected five examples, each showcasing a different topological phase: Mn_2AlB_2 (BCSID 1.508), which exhibits a nodal line semimetal to topological insulator transition, CaMnSi (BCSID 0.599), a narrow gap axion insulator, UAsS (BCSID 0.594), a 5f-shell ferromagnetic Weyl and nodal line semimetal, CsMnF_4 (BCSID 0.327), a material presenting a new type of quasi-symmetry protected closed nodal surface, and FeCr_2S_4 (BCSID 0.613), a symmetry-enforced

ferrimagnetic semimetal with double Weyls and spin-polarised surface states.

As an example of interaction strength-dependent topology, we selected **Mn₂AlB₂** (BCSID 1.508) in MSG 63.466 (*C_cmcm*) (see Fig. 2a). Interestingly, the case with $U = 0$ most accurately reproduced the experimentally measured magnetic momenta. This is also the only U value for which the system is a topological insulator. This points to **Mn₂AlB₂** being an itinerant ferromagnet (Stoner model of magnetism [64–67]), in which magnetism does not originate from localized electrons. In particular, it is diagnosed as $\eta_{4I} = 2, \delta_{2m} = 1$. The $\eta_{4I} = 2$ symmetry indicator implies that the system is in the non-trivial axionic phase, that is, the axion angle is quantized to $\theta = \pi$. Therefore, if the surface is fully gapped, the system will present half-quantized values of surface anomalous Hall conductivity[17, 55, 68–70]. The other non-trivial symmetry indicator, $\delta_{2m} = 1$, indicates a difference in the mirror Chern number of the $k_z = 0, \pi$ planes. This forces the mirror Chern number to be nonzero in at least one of the planes, which implies the presence of symmetry-protected Dirac nodes on the surfaces preserving the mirror symmetry. Upon neglecting the SOC, we found symmetry-protected nodal lines, with their corresponding drumhead surface states (see Fig. 3a).

CaMnSi (BCSID 0.599), in MSG 129.416 ($P4'/n'm'm'$), is an example of AXI which is indicated by index $z_2 = 1$ (see Fig. 2b). One of the major distinctions between AXI and 3DTIs is that the topological surface Dirac cones of a 3DTI are gapped in the AXI phase because of the TRS breaking (Fig. 3b). As stated previously in the case of **Mn₂AlB₂**, if the AXI surface is fully gapped, it presents a half-quantized surface anomalous Hall conductivity [55, 69, 70]. AXIs are also predicted to display large magnetoelectric response, as well as quantized Kerr rotation [71]. AXI materials are also a promising platform to study Majorana edge modes [72]. The computed gap of **CaMnSi** using PBE functional is small, and the topology is extremely sensitive to gap closings. Thus, we improved the accuracy of gap prediction by repeating the calculation with a meta-GGA functional (modified Becke–Johnson functional [73]). The smallest direct gap using this functional is 6.1 meV, and the symmetry-based topological diagnosis remains unchanged, which reassures the topological diagnosis (see Appendix B for further details).

We choose **UAsS** (BCSID 0.594) in MSG 129.417 ($P4/n'm'm'$) as an example of 5f-electron heavy fermion ferromagnetic semimetal (see Fig. 2c). We selected this compound from the family due to its relative simplicity at the Fermi level. Having a clean Fermi surface allows an easier identification of topological signatures. Similar to **Mn₂AlB₂**, the Hubbard U value that fits best is $U = 0$ eV. We find Weyl nodes and nodal lines, both with their characteristic surface states. In particular, even though there are only single-Weyls (topological charge 1), when projecting on the (100) surface termination,

equal charge pairs of Weyl nodes are projected on the same point, thus giving rise to two Fermi arcs stemming from each of their surface projections (Fig. 3c). Heavy fermion Weyl semimetal systems are of particular interest to study the interplay of electronic correlations and topological protection of Weyl nodes, such as Weyl-Kondo systems [74, 75].

We also study a 3d-electron ferromagnetic enforced semimetal, **CsMnF₄** (BCSID 0.327), in MSG 59.410 ($Pmm'n'$) (see Fig. 2d). This material is an example of a ferromagnetic half metal, where one spin channel is fully gapped and the bands close to the Fermi level are spin polarized. Note that there are two different reported structures for this material [76, 77]. We choose the first structure for this work [76], which is the one available in MAGNDATA and has been studied with DFT before [43]. We find almost no change in magnetization with respect to the Hubbard U parameter: the system remains half-metallic for all U values but the band structure and topological properties are affected by U . Our calculations show that this system is an ES in the range $U \leq 3$ eV and presents a topological transition from enforced semimetal to trivial insulator at $U=4$ eV (see Appendix F). Further analysis identifies an approximate nodal surface in this phase (Fig. 3d). The bands close to the Fermi level mainly stem from Mn atoms, which form a square lattice with a 2x2 supercell. As we detail in Appendix B, the extra translational symmetry associated with the 2x2 supercell is responsible for folding the bands and creating the approximate nodal surface. The extra translational symmetry prevents the gap from opening (at first order), thereby demonstrating the recently proposed quasisymmetric-protected phase [44, 45], which can enforce small, non-vanishing gaps that can be sources of large Berry curvature. Full details on the system can be found in Appendix B.

Finally, we analyze **FeCr₂S₄** (BCSID 0.613) in MSG 141.557 ($I4_1/am'd'$), which is an example of ferrimagnetic system with a clean Fermi level, where the low-energy physics is governed by a few connected bands (see Fig. 2e). In particular, there are 4 bands close to the Fermi level, and the relevant crossings occur between the last valence and the first conduction bands. We observed multi-Weyl nodes with a topological charge of 2 along the Γ –M line and a mirror symmetry-protected nodal line at $k_z = 0$. The charge $C > 1$ of these Weyl nodes is enforced by the 4-fold symmetry axis that leaves the Γ –M line invariant [78–80] and gives rise to 2 Fermi arcs per node. The nodal line gives rise to drumhead surface states in the (001) surface termination, whereas the other remnant gapped nodal lines' drumhead states are also gapped. The 4 bands crossing the Fermi level are purely spin-polarised: the resulting surface states are also spin-polarised.

IV. DISCUSSION

In this study, we performed complete DFT+U calculations and topological diagnosis of 522 new experimentally reported materials from the [MAGNDATA](#) database. The main result is the addition of 250 new experimentally relevant topological materials to the [Topological Magnetic Materials](#) database, which now counts with 894 entries, out of which 43.29% are reported as topologically non-trivial. We present a summary of topologically classified materials in Table I. Among these, we report 50 new mOAI insulators, although most of them failed to satisfy our criteria of ideal topological material, in this case, having an indirect gap. The most promising candidate, [CuFeO₂](#) ([BCSID 1.347](#)) is an mOAI for all Hubbard U values. During the preparation of this manuscript it was predicted that [CrSb](#) ([BCSID 0.528](#)) is an altermagnet Weyl semimetal [81–83]. Since it has an even number of Weyl nodes in each half of the BZ, its topology cannot be diagnosed using symmetry indicators. However, we discovered that the system is an mOAI at the Fermi level, providing new insights into the topological properties of this highly interesting material.

Since all additions to the [Topological Magnetic Materials](#) database arise from experimentally reported systems, they are readily available to be grown and have their topological properties tested. Systems with stable topology as a function of the Hubbard U parameter are the most promising ones to display topological properties, like [CaMnSi](#). However, systems with variable topology can result in interesting platforms to study the interplay between topology and electron interactions, like the [Mn₂AIB₂](#) ([BCSID 1.508](#)) insulator or the [FeCr₂S₄](#) ([BCSID 0.613](#)) semimetal. The five materials we have selected exhibit the most distinct experimental signatures of their topological properties that can be measured experimentally.

V. ACKNOWLEDGEMENTS

M.G.V. and C.F. thank support from the Deutsche Forschungsgemeinschaft (DFG, German Research Foun-

dation) GA3314/1-1 -FOR 5249 (QUAST). M.G.V and I.R. thank support to the Spanish Ministerio de Ciencia e Innovacion grant PID2022-142008NB-I00 and the Ministry for Digital Transformation and of Civil Service of the Spanish Government through the QUANTUM ENIA project call - Quantum Spain project, and by the European Union through the Recovery, Transformation and Resilience Plan - NextGenerationEU within the framework of the Digital Spain 2026 Agenda. This project was partially supported by the European Research Council (ERC) under the European Union's Horizon 2020 Research and Innovation Programme (Grant Agreement No. 101020833). L.E. was supported by the Government of the Basque Country (Project IT1458-22) and the Spanish Ministry of Science and Innovation (PID2019-106644GB-I00). B.A.B was supported by the Gordon and Betty Moore Foundation through Grant No.GBMF8685 towards the Princeton theory program, the Gordon and Betty Moore Foundation's EPiQS Initiative (Grant No. GBMF11070), Office of Naval Research (ONR Grant No. N00014-20-1-2303), Global Collaborative Network Grant at Princeton University, BSF Israel US foundation No. 2018226, NSF-MERSEC (Grant No.MERSEC DMR 2011750), the Simons theory collaboration on frontiers of superconductivity, and Simons collaboration on mathematical sciences. Y.X. was supported by the National Natural Science Foundation of China (General Program no. 12374163) and the Fundamental Research Funds for the Central Universities (grant no. 226-2024-00200). Y.J. is supported by the European Research Council (ERC) under the European Union's Horizon 2020 research and innovation program (Grant Agreement No. 101020833) as well as by IKUR Strategy.

-
- [1] Yuanfeng Xu, Luis Elcoro, Zhi-Da Song, Benjamin J. Wieder, M. G. Vergniory, Nicolas Regnault, Yulin Chen, Claudia Felser, and B. Andrei Bernevig, “High-throughput calculations of magnetic topological materials,” [Nature](#) **586**, 702–707 (2020).
 - [2] Luis Elcoro, Benjamin J. Wieder, Zhida Song, Yuanfeng Xu, Barry Bradlyn, and B. Andrei Bernevig, “Magnetic topological quantum chemistry,” [Nature Communications](#) **12**, 5965 (2021).
 - [3] M. G. Vergniory, L. Elcoro, Claudia Felser, Nicolas Regnault, B. Andrei Bernevig, and Zhijun Wang, “A complete catalogue of high-quality topological materials,” [Nature](#) **566**, 480–485 (2019).
 - [4] Maia G. Vergniory, Benjamin J. Wieder, Luis Elcoro, Stuart S. P. Parkin, Claudia Felser, B. Andrei Bernevig, and Nicolas Regnault, “All topological bands of all nonmagnetic stoichiometric materials,” [Science](#) **376**, eabg9094 (2022).
 - [5] Barry Bradlyn, L. Elcoro, Jennifer Cano, M. G. Vergniory, Zhijun Wang, C. Felser, M. I. Aroyo, and B. Andrei Bernevig, “Topological quantum chemistry,” [Nature](#) **547**, 298–305 (2017).
 - [6] Liang Fu and C. L. Kane, “Time reversal polarization and a Z_2 adiabatic spin pump,” [Phys. Rev. B](#) **74**, 195312

- (2006).
- [7] Hoi Chun Po, Ashvin Vishwanath, and Haruki Watanabe, “Symmetry-based indicators of band topology in the 230 space groups,” *Nature Communications* **8**, 50 (2017).
 - [8] Zhida Song, Tiantian Zhang, Zhong Fang, and Chen Fang, “Quantitative mappings between symmetry and topology in solids,” *Nature Communications* **9**, 3530 (2018).
 - [9] Haruki Watanabe, Hoi Chun Po, and Ashvin Vishwanath, “Structure and topology of band structures in the 1651 magnetic space groups,” *Science Advances* **4**, eaat8685 (2018).
 - [10] Robert-Jan Slager, Andrej Mesaros, Vladimir Juričić, and Jan Zaanen, “The space group classification of topological band-insulators,” *Nature Physics* **9**, 98–102 (2013).
 - [11] Tiantian Zhang, Yi Jiang, Zhida Song, He Huang, Yuqing He, Zhong Fang, Hongming Weng, and Chen Fang, “Catalogue of topological electronic materials,” *Nature* **566**, 475–479 (2019).
 - [12] Feng Tang, Hoi Chun Po, Ashvin Vishwanath, and Xiangang Wan, “Comprehensive search for topological materials using symmetry indicators,” *Nature* **566**, 486–489 (2019).
 - [13] Rundong Li, Jing Wang, Xiao-Liang Qi, and Shou-Cheng Zhang, “Dynamical axion field in topological magnetic insulators,” *Nature Physics* **6**, 284–288 (2010).
 - [14] Roger S. K. Mong, Andrew M. Essin, and Joel E. Moore, “Antiferromagnetic topological insulators,” *Phys. Rev. B* **81**, 245209 (2010).
 - [15] Jiaheng Li, Yang Li, Shiqiao Du, Zun Wang, Bing-Lin Gu, Shou-Cheng Zhang, Ke He, Wenhui Duan, and Yong Xu, “Intrinsic magnetic topological insulators in van der Waals layered $MnBi_2Te_4$ -family materials,” *Science Advances* **5**, eaaw5685 (2019).
 - [16] Dongqin Zhang, Minji Shi, Tongshuai Zhu, Dingyu Xing, Haijun Zhang, and Jing Wang, “Topological axion states in the magnetic insulator $MnBi_2Te_4$ with the quantized magnetoelectric effect,” *Phys. Rev. Lett.* **122**, 206401 (2019).
 - [17] Yuanfeng Xu, Zhida Song, Zhijun Wang, Hongming Weng, and Xi Dai, “Higher-order topology of the axion insulator $EuIn_2As_2$,” *Phys. Rev. Lett.* **122**, 256402 (2019).
 - [18] Frank Schindler, Ashley M. Cook, Maia G. Vergniory, Zhijun Wang, Stuart S. P. Parkin, B. Andrei Bernevig, and Titus Neupert, “Higher-order topological insulators,” *Science Advances* **4**, eaat0346 (2018).
 - [19] Frank Schindler, Zhijun Wang, Maia G. Vergniory, Ashley M. Cook, Anil Murani, Shamashis Sengupta, Alik Yu. Kasumov, Richard Deblock, Sangjun Jeon, Ilya Drozdov, Hélène Bouchiat, Sophie Guéron, Ali Yazdani, B. Andrei Bernevig, and Titus Neupert, “Higher-order topology in bismuth,” *Nature Physics* **14**, 918–924 (2018).
 - [20] Bingrui Peng, Yi Jiang, Zhong Fang, Hongming Weng, and Chen Fang, “Topological classification and diagnosis in magnetically ordered electronic materials,” *Physical Review B* **105**, 235138 (2022).
 - [21] A.Yu. Kitaev, “Fault-tolerant quantum computation by anyons,” *Annals of Physics* **303**, 2–30 (2003).
 - [22] Dmytro Pesin and Allan H. MacDonald, “Spintronics and pseudospintrronics in graphene and topological insulators,” *Nature Materials* **11**, 409–416 (2012).
 - [23] Catherine R. Rajamathi, Uttam Gupta, Nitesh Kumar, Hao Yang, Yan Sun, Vicky Süß, Chandra Shekhar, Marcus Schmidt, Horst Blumtritt, Peter Werner, Binghai Yan, Stuart Parkin, Claudia Felser, and C. N. R. Rao, “Weyl semimetals as hydrogen evolution catalysts,” *Advanced Materials* **29**, 1606202 (2017).
 - [24] Guowei Li, Yuanfeng Xu, Zhida Song, Qun Yang, Yudi Zhang, Jian Liu, Uttam Gupta, Vicky Sus, Yan Sun, Paolo Sessi, Stuart S. P. Parkin, B. Andrei Bernevig, and Claudia Felser, “Obstructed surface states as the descriptor for predicting catalytic active sites in inorganic crystalline materials,” *Advanced Materials* **34**, 2201328 (2022).
 - [25] Yuanfeng Xu, Luis Elcoro, Guowei Li, Zhi-Da Song, Nicolas Regnault, Qun Yang, Yan Sun, Stuart Parkin, Claudia Felser, and B. Andrei Bernevig, “Three-dimensional real space invariants, obstructed atomic insulators and a new principle for active catalytic sites,” (2021).
 - [26] J. Hubbard and Brian Hilton Flowers, “Electron correlations in narrow energy bands,” *Proceedings of the Royal Society of London. Series A. Mathematical and Physical Sciences* **276**, 238–257 (1963).
 - [27] Zhi-Da Song, Luis Elcoro, and B. Andrei Bernevig, “Twisted bulk-boundary correspondence of fragile topology,” *Science* **367**, 794–797 (2020).
 - [28] Yuanfeng Xu, Luis Elcoro, Zhi-Da Song, M. G. Vergniory, Claudia Felser, Stuart S. P. Parkin, Nicolas Regnault, Juan L. Mañes, and B. Andrei Bernevig, “Filling-enforced obstructed atomic insulators,” *Phys. Rev. B* **109**, 165139 (2024).
 - [29] Jiacheng Gao, Yuting Qian, Huaxian Jia, Zhaopeng Guo, Zhong Fang, Miao Liu, Hongming Weng, and Zhijun Wang, “Unconventional materials: the mismatch between electronic charge centers and atomic positions,” *Science bulletin* **67**, 598–608 (2022).
 - [30] J. Gracia, “Spin dependent interactions catalyse the oxygen electrochemistry,” *Phys. Chem. Chem. Phys.* **19**, 20451–20456 (2017).
 - [31] Felipe A. Garces-Pineda, Marta Blasco-Ahicart, David Nieto-Castro, Núria López, and José Ramón Galán-Mascarós, “Direct magnetic enhancement of electrocatalytic water oxidation in alkaline media,” *Nature Energy* **4**, 519–525 (2019).
 - [32] Jianhua Yan, Ying Wang, Yuanyuan Zhang, Shuhui Xia, Jianyong Yu, and Bin Ding, “Direct magnetic reinforcement of electrocatalytic ORR/OER with electromagnetic induction of magnetic catalysts,” *Advanced Materials* **33**, 2007525 (2021).
 - [33] R. D. Y. Hills, A. Kusmartseva, and F. V. Kusmartsev, “Current-voltage characteristics of Weyl semimetal semiconducting devices, veselago lenses, and hyperbolic dirac phase,” *Phys. Rev. B* **95**, 214103 (2017).
 - [34] Fernando de Juan, Adolfo G. Grushin, Takahiro Morimoto, and Joel E. Moore, “Quantized circular photo-galvanic effect in Weyl semimetals,” *Nature Communications* **8**, 15995 (2017).
 - [35] Bing Zhao, Bogdan Karpak, Dmitrii Khokhriakov, Annika Johansson, Anamul Md. Hoque, Xiaoguang Xu, Yong Jiang, Ingrid Mertig, and Saroj P. Dash, “Unconventional charge–spin conversion in Weyl-semimetal WTe_2 ,” *Advanced Materials* **32**, 2000818 (2020).
 - [36] Dylan Rees, Kaustuv Manna, Baozhu Lu, Takahiro Morimoto, Horst Borrmann, Claudia Felser, J. E. Moore, Darius H. Torchinsky, and J. Orenstein, “Helicity-dependent

- photocurrents in the chiral Weyl semimetal RhSi,” *Science Advances* **6**, eaba0509 (2020).
- [37] Qunian Xu, Yang Zhang, Klaus Koepernik, Wujun Shi, Jeroen van den Brink, Claudia Felser, and Yan Sun, “Comprehensive scan for nonmagnetic Weyl semimetals with nonlinear optical response,” *npj Computational Materials* **6**, 32 (2020).
- [38] Hongming Weng, Chen Fang, Zhong Fang, B. Andrei Bernevig, and Xi Dai, “Weyl semimetal phase in noncentrosymmetric transition-metal monophosphides,” *Phys. Rev. X* **5**, 011029 (2015).
- [39] Qi Wang, Yuanfeng Xu, Rui Lou, Zhonghao Liu, Man Li, Yaobo Huang, Dawei Shen, Hongming Weng, Shanhai Wang, and Hechang Lei, “Large intrinsic anomalous hall effect in half-metallic ferromagnet $Co_3Sn_2S_2$ with magnetic Weyl fermions,” *Nature communications* **9**, 3681 (2018).
- [40] Enke Liu, Yan Sun, Nitesh Kumar, Lukas Muechler, Aili Sun, Lin Jiao, Shuo-Ying Yang, Defa Liu, Aiji Liang, Qunian Xu, *et al.*, “Giant anomalous Hall effect in a ferromagnetic kagome-lattice semimetal,” *Nature physics* **14**, 1125–1131 (2018).
- [41] DF Liu, AJ Liang, EK Liu, QN Xu, YW Li, C Chen, D Pei, WJ Shi, SK Mo, P Dudin, *et al.*, “Magnetic Weyl semimetal phase in a Kagomé crystal,” *Science* **365**, 1282–1285 (2019).
- [42] R. Welter, G. Venturini, E. Ressouche, and B. Malaman, “Neutron diffraction studies of the CeFeSi-type CaMnSi and CaMnGe compounds,” *Solid State Communications* **97**, 503–507 (1996).
- [43] Anuroopa Behatha, Argha Jyoti Roy, C V Anusree, L Ponvijayakanthan, Vineet Kumar Sharma, and V Kancharana, “Correlation driven topological nodal ring ferromagnetic spin gapless semimetal: $CsMnF_4$,” *Journal of Physics: Condensed Matter* **33**, 165803 (2021).
- [44] Chunyu Guo, Lunhui Hu, Carsten Putzke, Jonas Diaz, Xiangwei Huang, Kaustuv Manna, Feng-Ren Fan, Chandra Shekhar, Yan Sun, Claudia Felser, Chaoxing Liu, B. Andrei Bernevig, and Philip J. W. Moll, “Quasi-symmetry-protected topology in a semi-metal,” *Nature Physics* **18**, 813–818 (2022).
- [45] Lun-Hui Hu, Chunyu Guo, Yan Sun, Claudia Felser, Luis Elcoro, Philip J. W. Moll, Chao-Xing Liu, and B. Andrei Bernevig, “Hierarchy of quasisymmetries and degeneracies in the CoSi family of chiral crystal materials,” *Phys. Rev. B* **107**, 125145 (2023).
- [46] Chen Fang, Matthew J. Gilbert, Xi Dai, and B. Andrei Bernevig, “Multi-Weyl topological semimetals stabilized by point group symmetry,” *Phys. Rev. Lett.* **108**, 266802 (2012).
- [47] G. Kresse and J. Hafner, “Ab initio molecular dynamics for liquid metals,” *Phys. Rev. B* **47**, 558–561 (1993).
- [48] G. Kresse and J. Hafner, “Ab initio molecular-dynamics simulation of the liquid-metal–amorphous-semiconductor transition in germanium,” *Phys. Rev. B* **49**, 14251–14269 (1994).
- [49] G. Kresse and J. Furthmüller, “Efficiency of ab-initio total energy calculations for metals and semiconductors using a plane-wave basis set,” *Computational Materials Science* **6**, 15–50 (1996).
- [50] G. Kresse and J. Furthmüller, “Efficient iterative schemes for ab initio total-energy calculations using a plane-wave basis set,” *Phys. Rev. B* **54**, 11169–11186 (1996).
- [51] C.J. Bradley and A.P. Cracknell, *The mathematical theory of symmetry in solids: representation theory for point groups and space groups* (Clarendon Press, 1972).
- [52] Jennifer Cano, Barry Bradlyn, and M. G. Vergniory, “Multifold nodal points in magnetic materials,” *APL Materials* **7**, 101125 (2019).
- [53] Iñigo Robredo, Niels B. M. Schröter, Claudia Felser, Jennifer Cano, Barry Bradlyn, and Maia G. Vergniory, “Multifold topological semimetals,” *Europhysics Letters* (2024).
- [54] Zhi-Da Song, Luis Elcoro, and B. Andrei Bernevig, “Twisted bulk-boundary correspondence of fragile topology,” *Science* **367**, 794–797 (2020).
- [55] Nicodemos Varnava and David Vanderbilt, “Surfaces of axion insulators,” *Phys. Rev. B* **98**, 245117 (2018).
- [56] Samuel V. Gallego, J. Manuel Perez-Mato, Luis Elcoro, Emre S. Tasci, Robert M. Hanson, Koichi Momma, Mois I. Aroyo, and Gotzon Madariaga, “MAGNDATA: towards a database of magnetic structures. I. The commensurate case,” *Journal of Applied Crystallography* **49**, 1750–1776 (2016).
- [57] Samuel V. Gallego, J. Manuel Perez-Mato, Luis Elcoro, Emre S. Tasci, Robert M. Hanson, Mois I. Aroyo, and Gotzon Madariaga, “MAGNDATA: towards a database of magnetic structures. II. The incommensurate case,” *Journal of Applied Crystallography* **49**, 1941–1956 (2016).
- [58] P. E. Blöchl, “Projector augmented-wave method,” *Phys. Rev. B* **50**, 17953–17979 (1994).
- [59] John P. Perdew, Kieron Burke, and Matthias Ernzerhof, “Generalized gradient approximation made simple,” *Phys. Rev. Lett.* **77**, 3865–3868 (1996).
- [60] Soner Steiner, Sergii Khmelevskyi, Martijn Marsmann, and Georg Kresse, “Calculation of the magnetic anisotropy with projected-augmented-wave methodology and the case study of disordered $Fe_{(1-x)}Co_x$ alloys,” *Phys. Rev. B* **93**, 224425 (2016).
- [61] J. Perez-Mato, D Orobengoa, Emre Tasci, Gemma De la Flor Martin, and A Kirov, “Crystallography online: Bilbao crystallographic server,” *Bulgarian Chemical Communications* **43**, 183–197 (2011).
- [62] Mois Ilia Aroyo, Juan Manuel Perez-Mato, Cesar Capillas, Eli Kroumova, Svetoslav Ivantchev, Gotzon Madariaga, Asen Kirov, and Hans Wondratschek, “Bilbao crystallographic server: I. databases and crystallographic computing programs,” *Zeitschrift für Kristallographie - Crystalline Materials* **221**, 15 – 27 (01 Jan. 2006).
- [63] Mois I. Aroyo, Asen Kirov, Cesar Capillas, J. M. Perez-Mato, and Hans Wondratschek, “Bilbao Crystallographic Server. II. Representations of crystallographic point groups and space groups,” *Acta Crystallographica Section A* **62**, 115–128 (2006).
- [64] Edmund Clifton Stoner, “Collective electron ferromagnetism,” *Proceedings of the Royal Society of London. Series A. Mathematical and Physical Sciences* **165**, 372–414 (1938).
- [65] Rudolf Zeller, J. Grotendorst, S. Blügel, D. Marx (eds, Rudolf Zeller, and Forschungszentrum Jülich, “Spin-polarized dft calculations and magnetism,” (2006).
- [66] B. T. Matthias, A. M. Clogston, H. J. Williams, E. Corenzwit, and R. C. Sherwood, “Ferromagnetism in solid solutions of Scandium and Indium,” *Phys. Rev. Lett.* **7**, 7–9 (1961).

- [67] B. T. Matthias and R. M. Bozorth, “Ferromagnetism of a Zirconium-Zinc compound,” *Phys. Rev.* **109**, 604–605 (1958).
- [68] Changming Yue, Yuanfeng Xu, Zhida Song, Hongming Weng, Yuan-Ming Lu, Chen Fang, and Xi Dai, “Symmetry-enforced chiral hinge states and surface quantum anomalous hall effect in the magnetic axion insulator $B_{2-x}Sm_xSe_3$,” *Nature Physics* **15**, 577–581 (2019).
- [69] Chang Liu, Yongchao Wang, Hao Li, Yang Wu, Yaxin Li, Jiaheng Li, Ke He, Yong Xu, Jinsong Zhang, and Yayu Wang, “Robust axion insulator and chern insulator phases in a two-dimensional antiferromagnetic topological insulator,” *Nature Materials* **19**, 522–527 (2020).
- [70] Rafael González-Hernández, Carlos Pinilla, and Bernardo Uribe, “Axion insulators protected by C_2T symmetry, their K -theory invariants, and material realizations,” *Phys. Rev. B* **106**, 195144 (2022).
- [71] Junyeong Ahn, Su-Yang Xu, and Ashvin Vishwanath, “Theory of optical axion electrodynamics and application to the Kerr effect in topological antiferromagnets,” *Nature Communications* **13**, 7615 (2022).
- [72] Qing Yan, Hailong Li, Jiang Zeng, Qing-Feng Sun, and X. C. Xie, “A majorana perspective on understanding and identifying axion insulators,” *Communications Physics* **4**, 239 (2021).
- [73] Axel D. Becke and Erin R. Johnson, “A simple effective potential for exchange,” *The Journal of Chemical Physics* **124**, 221101 (2006).
- [74] Yuanfeng Xu, Changming Yue, Hongming Weng, and Xi Dai, “Heavy Weyl fermion state in $CeRu_4Sn_6$,” *Physical Review X* **7**, 011027 (2017).
- [75] C. Y. Guo, F. Wu, Z. Z. Wu, M. Smidman, C. Cao, A. Bostwick, C. Jozwiak, E. Rotenberg, Y. Liu, F. Steglich, and H. Q. Yuan, “Evidence for Weyl fermions in a canonical heavy-fermion semimetal $YPtBi$,” *Nature Communications* **9**, 4622 (2018).
- [76] W. Massa and M. Steiner, “Crystal and magnetic structure of the planar ferromagnet $CsMnF_4$,” *Journal of Solid State Chemistry* **32**, 137–143 (1980).
- [77] Michel Molinier and Werner Massa, “Die kristallstrukturen der tetrafluoromanganate(iii) $AMnF_4$ ($A = K, Rb, Cs$) / the crystal structures of the tetrafluoromanganates(iii) $AMnF_4$ ($A = K, Rb, Cs$)”, *Zeitschrift für Naturforschung B* **47**, 783–788 (1992).
- [78] Tiantian Zhang, Ryo Takahashi, Chen Fang, and Shuichi Murakami, “Twofold quadruple Weyl nodes in chiral cubic crystals,” *Phys. Rev. B* **102**, 125148 (2020).
- [79] Lei Jin, Xiaoming Zhang, Ying Liu, Xuefang Dai, Liying Wang, and Guodong Liu, “Fully spin-polarized double-weyl fermions with type-III dispersion in the quasi-one-dimensional materials X_2RhF_6 ($X=K, Rb, Cs$)” *Phys. Rev. B* **102**, 195104 (2020).
- [80] Y. J. Jin, Y. Xu, Z. J. Chen, and H. Xu, “Type-II quadratic and cubic Weyl fermions,” *Phys. Rev. B* **105**, 035141 (2022).
- [81] Sonka Reimers, Lukas Odenbreit, Libor Šmejkal, Vladimir N. Strocov, Prokopios Constantinou, Anna B. Hellenes, Rodrigo Jaeschke Ubiergo, Warley H. Campos, Venkata K. Bharadwaj, Atasi Chakraborty, Thibaud Denneulin, Wen Shi, Rafal E. Dunin-Borkowski, Suvadip Das, Mathias Kläui, Jairo Sinova, and Martin Jourdan, “Direct observation of altermagnetic band splitting in CrSb thin films,” *Nature Communications* **15**, 2116 (2024).
- [82] Cong Li, Mengli Hu, Zhilin Li, Yang Wang, Wanyu Chen, Balasubramanian Thiagarajan, Mats Leandersson, Craig Polley, Timur Kim, Hui Liu, Cosma Fulga, Maia G. Vergniory, Oleg Janson, Oscar Tjernberg, and Jeroen van den Brink, “Topological Weyl altermagnetism in CrSb,” (2024), arXiv:2405.14777 [cond-mat.mtrl-sci].
- [83] Wenlong Lu, Shiyu Feng, Yuzhi Wang, Dong Chen, Zihan Lin, Xin Liang, Siyuan Liu, Wanxiang Feng, Kohei Yamagami, Junwei Liu, Claudia Felser, Quansheng Wu, and Junzhang Ma, “Observation of surface fermi arcs in altermagnetic Weyl semimetal CrSb,” (2024), arXiv:2407.13497 [cond-mat.mtrl-sci].
- [84] Luis Elcoro, Zhida Song, and B. Andrei Bernevig, “Application of induction procedure and Smith decomposition in calculation and topological classification of electronic band structures in the 230 space groups,” *Phys. Rev. B* **102**, 035110 (2020).
- [85] J. Zak, “Symmetry specification of bands in solids,” *Phys. Rev. Lett.* **45**, 1025–1028 (1980).
- [86] J. Zak, “Band representations and symmetry types of bands in solids,” *Phys. Rev. B* **23**, 2824–2835 (1981).
- [87] J. Zak, “Band representations of space groups,” *Physical Review B* **26**, 3010–3023 (1982).
- [88] H. Bacry, L. Michel, and J. Zak, “Symmetry and classification of energy bands in crystals,” in *Group Theoretical Methods in Physics: Proceedings of the XVI International Colloquium Held at Varna, Bulgaria, June 15–20, 1987* (Springer Berlin Heidelberg, Berlin, Heidelberg, 1988) pp. 289–308.
- [89] M. G. Vergniory, L. Elcoro, Zhijun Wang, Jennifer Cano, C. Felser, M. I. Aroyo, B. Andrei Bernevig, and Barry Bradlyn, “Graph theory data for topological quantum chemistry,” *Phys. Rev. E* **96**, 023310 (2017).
- [90] Jennifer Cano, Barry Bradlyn, Zhijun Wang, L. Elcoro, M. G. Vergniory, C. Felser, M. I. Aroyo, and B. Andrei Bernevig, “Topology of disconnected elementary band representations,” *Phys. Rev. Lett.* **120**, 266401 (2018).
- [91] W. P. Su, J. R. Schrieffer, and A. J. Heeger, “Solitons in polyacetylene,” *Phys. Rev. Lett.* **42**, 1698–1701 (1979).
- [92] Fernando Aguado, Fernando Rodriguez, and Pedro Núñez, “Pressure-induced Jahn-Teller suppression and simultaneous high-spin to low-spin transition in the layered perovskite $CsMnF_4$,” *Phys. Rev. B* **76**, 094417 (2007).
- [93] Fernando Palacio, M.C. Moron, G. Antorrena, S. Clark, and A. Devine, *European Powder Diffraction* **4**, Materials Science Forum, Vol. 228 (Trans Tech Publications Ltd, 1996) pp. 855–862.

Appendix A: MTQC summary, symmetry indicators and real space invariants

In this section, we will provide a concise overview of key topics, including the theory of magnetic topological quantum chemistry (TQC) [2, 5], topological phases determined by symmetry eigenvalues [7–9, 84], the definition of OAIs and RSI [24, 25, 54].

1. Magnetic Topological Quantum Chemistry

Magnetic topological quantum chemistry (MTQC) integrates the principles of topological quantum chemistry (TQC) combined with magnetism and enables the investigation of topological phenomena emerging in magnetic materials. TQC [2, 5] is a theory that characterizes the topology of electronic bands in crystalline solids and it is constructed on the basis of trivial atomic limits, which transform as elementary band representations (EBRs) [85–88]. MTQC tabulates all the magnetic EBRs (MEBRs) in the 1651 magnetic space groups (MSGs). In particular, even within MSGs where symmetry eigenvalue labels cannot distinguish between trivial and topological states, the real-space indicators obtained from MEBRs describe stable and fragile topological insulating phases as well as magnetic OAIs. MTQC also tabulates all band co-representations, described in momentum space, induced from magnetic atomic (Wannier) orbitals in position space (Wyckoff positions). MTQC provides a complete characterization of the symmetry properties of an isolated band through its decomposition into irreducible co-reps, where only the multiplicities (m) of the decomposition into (co)-irreps ($\chi_{K_j}^i$) at the high symmetry momenta (maximal K-points) are necessary. In general, we compute the multiplicities for the first N_e bands (occupied bands, regardless of the Fermi level) and define the symmetry-data-vector B of the occupied bands as follows:

$$B = (m(\chi_{K_1}^1), m(\chi_{K_1}^2), \dots, m(\chi_{K_2}^1), \dots,), \quad (\text{A1})$$

where $m(\chi_{K_j}^i)$ denotes the multiplicity of the χ^i irrep of the little cogroup of K_j . The symmetry properties of a set of occupied bands are fully described by the symmetry-data-vector B . The set of bands (and then the compound itself) is diagnosed as trivial whenever it is possible to describe the symmetry data vector B as a linear integer (and positive) combination of the corresponding symmetry-data-vectors of the MEBRs. If such a combination does not exist, the set of bands is classified as topological.

Following the procedure that we will further detail in the next subsection, the solution of this problem can be encoded in a set of so-called symmetry indicators (SI) [2, 5, 7–9], that are mapped to topological invariants. As discussed in the main text, various topological phases of matter can be diagnosed based on this analysis (see Sec. II). However, a band representation is well-defined only for insulators that satisfy the compatibility relations [89, 90]. There are two main cases in which these relations are not satisfied: enforced semimetal with Fermi degeneracy (ESFD) and enforced semimetal (ES). In the former case, there is an n -dimensional corep at a high symmetry point which is occupied by d number of electrons, with $d < n$. There, the band structure can be adiabatically deformed until the Fermi level precisely intersects the degeneracy point, and the Fermi surface becomes a single point. This is why they are referred to as "enforced semimetal with Fermi degeneracy". The situation with enforced semimetals is more intricate, as the bands exhibit local gaps at each high-symmetry k-point in the Brillouin Zone (BZ). Consider two maximal k-points K_a , K_b and a path k_p connecting them, which means that the co-irreps of the little cogroup associated with k_p can be subduced from irreps at both K_a and K_b . If the subsets of coreps of the N_e occupied bands at both momentum maximal k-points (K_a and K_b) subduce into two different subsets of coreps at k_p , the N_e bands cannot be connected. At least one band (corep) at each maximal k-vector is connected to another band (corep) above the first N_e bands in the other maximal k-vector. Therefore, at least two bands cross along the path k_p and the Fermi level also crosses both bands. In this situation, the diagnosis is ES.

In the following sections we derive the symmetry indicators for stable topology in MSG 2.4 ($P\bar{1}$) as well as the real space invariants, which are analogous to the symmetry indicators and can diagnose magnetic obstructed atomic insulators (see Sec. II).

2. Symmetry indicators

For illustration purposes, in this section we will derive the symmetry indicators and real space invariants of SG $P\bar{1}$. In three dimensions, the high-symmetry k-points in the BZ are labeled $\Gamma = (0, 0, 0)$, $X = (\pi, 0, 0)$, $Y = (0, \pi, 0)$, $V = (\pi, \pi, 0)$, $Z = (0, 0, \pi)$, $U = (\pi, 0, \pi)$, $T = (0, \pi, \pi)$ and $R = (\pi, \pi, \pi)$. The irreps of this MSG are particularly simple and can be labeled by the inversion eigenvalue, $\pm 1 \equiv \pm$. The symmetry information for any set of bands

within this MSG can be encoded in an array that contains the multiplicities of the irreps, as previously described:

$$BR = \{n(\Gamma^+), n(\Gamma^-), n(R^+), n(R^-), n(T^+), n(T^-), n(U^+), n(U^-), \\ n(V^+), n(V^-), n(X^+), n(X^-), n(Y^+), n(Y^-), n(Z^+), n(Z^-)\}. \quad (\text{A2})$$

In MSG 2.4 ($P\bar{1}$) all lines connecting high-symmetry points have the trivial little cogroup, so the compatibility relations reduce to having the same number of occupied bands (electrons) at each high-symmetry point. In terms of the coreps:

$$n(\Gamma^+) + n(\Gamma^-) = n(X^+) + n(X^-) = n(Y^+) + n(Y^-) = n(V^+) + n(V^-) = \\ n(Z^+) + n(Z^-) = n(U^+) + n(U^-) = n(T^+) + n(T^-) = n(R^+) + n(R^-). \quad (\text{A3})$$

There are $2^8 = 256$ possible insulating band structures with $n(\rho^+) + n(\rho^-) = 1$ that satisfy the compatibility relations in MSG 2.4 ($P\bar{1}$). To classify the topological phases associated with all these band structures, we start with a basis of EBRs which span the space of trivial insulators within this specific MSG. This basis is not unique; we choose the convention of the BCS [61–63], and we write the EBR matrix from BANDREP. With the basis spanning the EBRs induced from alternating even/odd irreducible representations from the maximal 1a-1h Wyckoff positions:

$$EBR = \begin{pmatrix} 1 & 0 & 1 & 0 & 1 & 0 & 1 & 0 & 1 & 0 & 1 & 0 & 1 & 0 & 1 & 0 \\ 0 & 1 & 0 & 1 & 0 & 1 & 0 & 1 & 0 & 1 & 0 & 1 & 0 & 1 & 0 & 1 \\ 1 & 0 & 0 & 1 & 0 & 1 & 0 & 1 & 1 & 0 & 1 & 0 & 1 & 0 & 0 & 1 \\ 0 & 1 & 1 & 0 & 1 & 0 & 1 & 0 & 0 & 1 & 0 & 1 & 0 & 1 & 1 & 0 \\ 1 & 0 & 0 & 1 & 0 & 1 & 1 & 0 & 0 & 1 & 0 & 1 & 1 & 0 & 1 & 0 \\ 0 & 1 & 1 & 0 & 1 & 0 & 0 & 1 & 1 & 0 & 1 & 0 & 0 & 1 & 0 & 1 \\ 1 & 0 & 0 & 1 & 1 & 0 & 0 & 1 & 0 & 1 & 1 & 0 & 0 & 1 & 1 & 0 \\ 0 & 1 & 1 & 1 & 0 & 0 & 1 & 1 & 0 & 1 & 0 & 0 & 1 & 1 & 0 & 1 \\ 1 & 0 & 1 & 0 & 0 & 1 & 0 & 1 & 1 & 0 & 0 & 1 & 1 & 0 & 0 & 1 \\ 0 & 1 & 0 & 1 & 1 & 0 & 1 & 0 & 0 & 1 & 1 & 0 & 1 & 0 & 0 & 1 \\ 1 & 0 & 1 & 0 & 1 & 0 & 0 & 1 & 0 & 1 & 0 & 1 & 1 & 0 & 0 & 1 \\ 0 & 1 & 0 & 1 & 0 & 1 & 1 & 0 & 1 & 0 & 0 & 1 & 1 & 0 & 0 & 1 \\ 1 & 0 & 1 & 0 & 0 & 1 & 1 & 0 & 0 & 1 & 0 & 1 & 1 & 0 & 0 & 1 \\ 0 & 1 & 0 & 1 & 1 & 0 & 0 & 1 & 1 & 0 & 0 & 1 & 1 & 0 & 1 & 0 \\ 1 & 0 & 0 & 1 & 1 & 0 & 1 & 0 & 1 & 0 & 0 & 1 & 0 & 1 & 0 & 1 \\ 0 & 1 & 1 & 0 & 0 & 1 & 0 & 1 & 0 & 0 & 1 & 1 & 0 & 0 & 1 & 0 \end{pmatrix}, \quad (\text{A4})$$

where each column represents an EBR. The integers are multiplicities of the coreps in the same order as Eq. A2 of the corresponding EBR. These 16 EBRs represent the 16 different atomic limits in MSG 2.4 ($P\bar{1}$) (two bands induced from the two irreps of the site-symmetry group of each of the 8 Wyckoff positions a-h). The rest (240) of the band structures are then topologically non-trivial. We can use this matrix to answer the following question: given a band structure characterised by a symmetry vector B , can it be expressed in terms of EBRs? This question is equivalent to solving the following system of equations [2, 5, 7–9]:

$$EBR \cdot X = B \quad (\text{A5})$$

with X a vector of integer coefficients expressing the decomposition of B in terms of EBRs. We can simplify Eq. A5 through the Smith decomposition. Since EBR is an $m \times n$ integer matrix, there exists unimodular matrices L ($m \times m$) and R ($n \times n$) such that:

$$\Delta = L \cdot EBR \cdot R, \quad (\text{A6})$$

with Δ a matrix with non-zero entries only in the main diagonal, known as the Smith normal form of EBR . It is important to note that we can always choose L and R such that the first r entries in the main diagonal of Δ are non-zero, with $r = \text{rank}(EBR)$. We can now rewrite Eq. A5 as:

$$L^{-1} \cdot \Delta \cdot R^{-1} \cdot X = B, \quad LB = \Delta R^{-1}X, \quad C = \Delta Y, \quad (\text{A7})$$

where in the last step we redefined $C = LB$ and $Y = R^{-1}X$ for the sake of clarity. Because the matrix Δ only has non-zero entries in the main diagonal (denoted as $\Delta_{i,i}$), the system in Eq. A7 only has an integer solution if (and

only if) the following conditions are satisfied:

$$c_i = 0 \quad \text{for } i > r \quad (\text{A8})$$

$$c_i/\Delta_{i,i} \in \mathbb{Z} \quad \text{for } i = 1, \dots, r. \quad (\text{A9})$$

If such a solution exists, the X vector in Eq. A5 is:

$$X = R \cdot Y \quad \text{with } Y = (c_1/\Delta_{1,1}, \dots, c_r/\Delta_{r,r}, y_1, \dots, y_l) \quad (\text{A10})$$

with $l = m - r$ the number of 0 entries in the main diagonal of Δ and y_i free variable parameters. The existence of a solution requires that B satisfies both conditions defined in Eq. A8 and Eq. A9. Eq. A8 is equivalent to enforcing the compatibility relations we described earlier, while the condition in Eq. A9 gives us the *symmetry indicators*. We can rewrite the condition in Eq. A9 as:

$$c_i \equiv 0 \pmod{\Delta_{i,i}}. \quad (\text{A11})$$

We can apply the described procedure to the *EBR* matrix in Eq. A4. We compute the Smith normal decomposition and find:

$$\Delta = \begin{pmatrix} 1 & 0 & 0 & 0 & 0 & 0 & 0 & 0 & 0 & 0 & 0 & 0 & 0 & 0 & 0 & 0 \\ 0 & 1 & 0 & 0 & 0 & 0 & 0 & 0 & 0 & 0 & 0 & 0 & 0 & 0 & 0 & 0 \\ 0 & 0 & 1 & 0 & 0 & 0 & 0 & 0 & 0 & 0 & 0 & 0 & 0 & 0 & 0 & 0 \\ 0 & 0 & 0 & 1 & 0 & 0 & 0 & 0 & 0 & 0 & 0 & 0 & 0 & 0 & 0 & 0 \\ 0 & 0 & 0 & 0 & 1 & 0 & 0 & 0 & 0 & 0 & 0 & 0 & 0 & 0 & 0 & 0 \\ 0 & 0 & 0 & 0 & 0 & 1 & 0 & 0 & 0 & 0 & 0 & 0 & 0 & 0 & 0 & 0 \\ 0 & 0 & 0 & 0 & 0 & 0 & 2 & 0 & 0 & 0 & 0 & 0 & 0 & 0 & 0 & 0 \\ 0 & 0 & 0 & 0 & 0 & 0 & 0 & 2 & 0 & 0 & 0 & 0 & 0 & 0 & 0 & 0 \\ 0 & 0 & 0 & 0 & 0 & 0 & 0 & 0 & 2 & 0 & 0 & 0 & 0 & 0 & 0 & 0 \\ 0 & 0 & 0 & 0 & 0 & 0 & 0 & 0 & 0 & 4 & 0 & 0 & 0 & 0 & 0 & 0 \\ 0 & 0 & 0 & 0 & 0 & 0 & 0 & 0 & 0 & 0 & 0 & 0 & 0 & 0 & 0 & 0 \\ 0 & 0 & 0 & 0 & 0 & 0 & 0 & 0 & 0 & 0 & 0 & 0 & 0 & 0 & 0 & 0 \\ 0 & 0 & 0 & 0 & 0 & 0 & 0 & 0 & 0 & 0 & 0 & 0 & 0 & 0 & 0 & 0 \\ 0 & 0 & 0 & 0 & 0 & 0 & 0 & 0 & 0 & 0 & 0 & 0 & 0 & 0 & 0 & 0 \\ 0 & 0 & 0 & 0 & 0 & 0 & 0 & 0 & 0 & 0 & 0 & 0 & 0 & 0 & 0 & 0 \\ 0 & 0 & 0 & 0 & 0 & 0 & 0 & 0 & 0 & 0 & 0 & 0 & 0 & 0 & 0 & 0 \\ 0 & 0 & 0 & 0 & 0 & 0 & 0 & 0 & 0 & 0 & 0 & 0 & 0 & 0 & 0 & 0 \\ 0 & 0 & 0 & 0 & 0 & 0 & 0 & 0 & 0 & 0 & 0 & 0 & 0 & 0 & 0 & 0 \\ 0 & 0 & 0 & 0 & 0 & 0 & 0 & 0 & 0 & 0 & 0 & 0 & 0 & 0 & 0 & 0 \\ 0 & 0 & 0 & 0 & 0 & 0 & 0 & 0 & 0 & 0 & 0 & 0 & 0 & 0 & 0 & 0 \\ 0 & 0 & 0 & 0 & 0 & 0 & 0 & 0 & 0 & 0 & 0 & 0 & 0 & 0 & 0 & 0 \\ 0 & 0 & 0 & 0 & 0 & 0 & 0 & 0 & 0 & 0 & 0 & 0 & 0 & 0 & 0 & 0 \end{pmatrix} \quad (\text{A12})$$

and

$$L = \begin{pmatrix} 0 & 0 & 1 & 0 & 0 & 0 & 0 & 0 & 0 & 0 & 0 & 0 & 0 & 0 & 0 & 0 \\ 0 & 1 & 0 & 0 & 0 & 0 & 0 & 0 & 0 & 0 & 0 & 0 & 0 & 0 & 0 & 0 \\ 1 & 0 & 0 & 0 & 0 & 0 & 0 & 0 & 0 & 0 & 0 & 0 & 0 & 0 & -1 & 0 \\ 1 & 0 & 0 & 0 & 0 & 0 & 0 & 0 & 0 & 0 & 0 & -1 & 0 & 0 & 0 & 0 \\ 1 & 0 & 0 & 0 & 0 & 0 & 0 & 0 & 0 & 0 & -1 & 0 & 0 & 0 & 0 & 0 \\ 1 & 0 & 0 & 0 & 0 & 0 & 0 & 0 & 0 & -1 & 0 & 0 & 0 & 0 & 0 & 0 \\ 1 & 0 & 0 & 0 & 0 & 0 & 0 & 0 & 1 & 0 & -1 & 0 & -1 & 0 & 0 & 0 \\ 1 & 0 & 0 & 0 & 0 & 0 & 0 & 1 & 0 & 0 & -1 & 0 & 0 & 0 & -1 & 0 \\ 1 & 0 & 0 & 0 & 1 & 0 & 0 & 0 & 0 & 0 & 0 & -1 & 0 & -1 & 0 & 0 \\ 1 & 0 & -1 & 0 & 1 & 0 & 1 & 0 & 1 & 0 & -1 & 0 & -1 & 0 & -1 & 0 \\ -1 & -1 & 0 & 0 & 0 & 0 & 0 & 0 & 1 & 1 & 0 & 0 & 0 & 0 & 0 & 0 \\ -1 & -1 & 0 & 0 & 1 & 1 & 0 & 0 & 0 & 0 & 0 & 0 & 0 & 0 & 0 & 0 \\ -1 & -1 & 0 & 0 & 0 & 0 & 0 & 0 & 0 & 0 & 1 & 1 & 0 & 0 & 0 & 0 \\ -1 & -1 & 1 & 1 & 0 & 0 & 0 & 0 & 0 & 0 & 0 & 0 & 0 & 0 & 0 & 0 \\ -1 & -1 & 0 & 0 & 0 & 0 & 0 & 0 & 0 & 0 & 0 & 1 & 1 & 0 & 0 & 0 \\ -1 & -1 & 0 & 0 & 0 & 1 & 1 & 0 & 0 & 0 & 0 & 0 & 0 & 0 & 0 & 0 \\ -1 & -1 & 0 & 0 & 0 & 0 & 0 & 0 & 0 & 0 & 0 & 0 & 0 & 1 & 1 & 0 \end{pmatrix} \quad (\text{A13})$$

The Δ matrix for MSG 2.4 ($P\bar{1}$) has three diagonal elements $\Delta_{i,i} = 2$ ($i=6,7,8$) and one $\Delta_{9,9} = 4$, so there are 4 SI in the group and the classification is $\mathbb{Z}_2 \times \mathbb{Z}_2 \times \mathbb{Z}_2 \times \mathbb{Z}_4$, which is in agreement with previous work [2, 7, 8, 84]. From Eq. A7 we extract that $c_i = L_{ij} \cdot B_j$, so that the rows of L serve as symmetry indicators, which we denote as *Smith*

symmetry indicators (SSI):

$$\begin{aligned} z_{2,a} &= n(\Gamma^+) + n(V^+) - n(X^+) - n(Y^+) \pmod{2} \\ z_{2,b} &= n(\Gamma^+) + n(U^+) - n(X^+) - n(Z^+) \pmod{2} \\ z_{2,c} &= n(\Gamma^+) + n(T^+) - n(Y^+) - n(Z^+) \pmod{2} \\ z_4 &= n(\Gamma^+) - n(R^+) + n(T^+) + n(U^+) + n(V^+) - n(X^+) - n(Y^+) - n(Z^+) \pmod{4}. \end{aligned} \quad (\text{A14})$$

Notice that the SSI as given by Eq. A14 do not have the same form the usual [2, 8] indices found in the literature, which read:

$$z_{2I,i} = \sum_{K \in k_i=\pi} \frac{n(K^-) - n(K^+)}{2} \pmod{2} = \sum_{K \in k_i=\pi} \frac{n_K^- - n_K^+}{2} \pmod{2} \quad (\text{A15})$$

$$\eta_{4I} = \sum_{K \in \text{TRIM}} \frac{n(K^-) - n(K^+)}{2} \pmod{4} = \sum_{K \in \text{TRIM}} \frac{n_K^- - n_K^+}{2} \pmod{4}, \quad (\text{A16})$$

where the sum runs over the TRIM k-points in the $k_i = \pi$ planes ($i=x,y,z$) for Eq. A15 and it runs over all TRIM k-points for Eq. A16. Note that we introduce the compact notation $n_K^\pm = n(K^\pm)$ used in the literature [8]. The Smith decomposition scheme fully determines the product group of the symmetry indicators, $\mathbb{Z}_2 \times \mathbb{Z}_2 \times \mathbb{Z}_2 \times \mathbb{Z}_4$ in this case, and it gives a possible choice of symmetry indicators. As a consequence, distinct topological phases possess unique symmetry indicators, even though the translation from symmetry indicators to topological invariants is generally non-trivial [2, 7, 8]. To prove this idea, we select representatives of each of the $2 \times 2 \times 2 \times 4 = 32$ topological classes and compute the Fu-Kane-like symmetry indicators ($z_{2I,1}, z_{2I,2}, z_{2I,3}, \eta_{4I}$) as well as our SSI, showing that, even though the individual values are different, there is a one-to-one mapping between the topological invariants and our SSI (see Table S1).

In the context of MSG, the \mathbb{Z}_4 index of MSG 2.4 ($P\bar{1}$) (in the absence of TRS) we described was renamed η_{4I} [1, 2]. Interestingly, odd values of this symmetry indicator ($\eta_{4I} = 1, 3$) indicate a difference in Chern number parity between the $k_z = 0, \pi$ planes. This is only possible if there exists a quantum critical point at a finite $k_z = C$ plane at which the bands become degenerate. That is, an odd η_{4I} indicator implies the presence of an odd number of Weyl nodes in each half of the BZ. Thus, the η_{4I} indicator can diagnose Weyl semimetals from symmetry.

3. Real space invariants

In the previous section, we derived the symmetry indicators of MSG 2.4 ($P\bar{1}$) and determined the conditions for a non-trivial stable topological insulator. When all the symmetry indicators are 0, the band structure can be deconstructed as a sum of atomic insulators, and the possible phases are fragile (negative coefficients in the EBR decomposition), trivial, or obstructed atomic insulator. In the last case, the analyzed band structure can be induced by a sum of atomic insulators but the decomposition *necessarily* contains EBRs induced from unoccupied Wyckoff positions or positions that cannot be occupied by moving the atomic orbitals in a symmetry conserving fashion. There is thus a symmetry obstruction in which the charge is pinned on a non-occupied Wyckoff position, which represents a different atomic limit. This system can exhibit surface states inside the bulk gap that *do not* connect valence and conduction bands but are nevertheless pinned by symmetry at the surfaces [24, 25, 54, 91]. These bands are not pinned in energy and generically can move up and down in the conduction or valence band. In order to diagnose these states, the theory of real space invariants (RSI) has been recently developed [24, 25, 54]. We will now derive the RSI for MSG 2.4 ($P\bar{1}$) to illustrate the procedure.

Let us start by focusing on the 1a Wyckoff position $q_{1a} = (0, 0, 0)$ and its surroundings. The site-symmetry group of q_{1a} is $\bar{1}$, which has two 1-dimensional irreducible representations, A_g and A_u , which have opposite inversion eigenvalues (A_g is even while A_u is odd). If we place an orbital at a random position $q_r = (x, y, z)$, inversion symmetry forces us to place another orbital in the inversion-related position, $-q_r = (-x, -y, -z)$. These orbitals transform into each other under inversion symmetry, so that the matrix representation of inversion symmetry is $\rho(\mathcal{I}) = \begin{pmatrix} 0 & 1 \\ 1 & 0 \end{pmatrix}$, which

can be diagonalized to obtain $\rho(\mathcal{I}) = \begin{pmatrix} 1 & 0 \\ 0 & -1 \end{pmatrix} = A_g \oplus A_u$. The two states (orbitals) at $\pm q_r$ transform under the representation $A_g \oplus A_u$ at q_{1a} . Since this process is reversible, whenever we have a pair of orbitals transforming in

Band Representation	Fu-Kane-like symmetry indicators ($z_{2I,1}, z_{2I,2}, z_{2I,3}, \eta_{4I}$)	Smith symmetry indicators ($z_{2,a}, z_{2,b}, z_{2,c}, z_4$)
{1,0,1,0,1,0,1,0,1,0,1,0,1,0,1,0,1,0}	{0,0,0,0}	{0,0,0,0}
{1,0,0,1,1,0,0,1,0,1,1,0,0,1,0,1}	{0,0,0,1}	{1,1,1,1}
{2,0,0,2,2,0,1,1,1,2,0,1,1,1,1}	{0,0,0,2}	{0,0,0,2}
{1,0,1,0,1,0,1,0,1,0,0,1,0,1,0,1}	{0,0,0,3}	{1,1,1,3}
{0,1,0,1,0,1,1,0,0,1,0,1,0,1,1,0}	{0,0,1,0}	{1,0,0,2}
{0,1,1,0,1,0,0,1,0,1,1,0,1,0,1,0}	{0,0,1,1}	{0,1,1,3}
{0,1,1,0,0,1,1,0,0,1,1,0,1,0,0,1}	{0,0,1,2}	{1,0,0,0}
{1,0,0,1,0,1,1,0,1,0,0,1,0,1,0,1}	{0,0,1,3}	{0,1,1,1}
{0,1,0,1,0,1,0,1,1,0,1,0,0,1,0,1}	{0,1,0,0}	{0,1,0,2}
{0,1,1,0,0,1,1,0,0,1,1,0,1,0,1,0}	{0,1,0,1}	{1,0,1,3}
{0,1,1,0,1,0,0,1,0,1,1,0,1,0,0,1}	{0,1,0,2}	{0,1,0,0}
{1,0,0,1,1,0,0,1,1,0,0,1,0,1,0,1}	{0,1,0,3}	{1,0,1,1}
{0,1,0,1,0,1,1,0,1,0,1,0,0,1,0,1,0}	{0,1,1,0}	{1,1,0,0}
{0,1,1,0,0,1,0,1,0,1,1,0,1,0,0,1}	{0,1,1,1}	{0,0,1,1}
{0,1,1,0,0,1,0,1,0,1,0,1,0,1,0,1}	{0,1,1,2}	{1,1,0,2}
{1,0,0,1,1,0,1,0,1,0,0,1,0,1,1,0}	{0,1,1,3}	{0,0,1,3}
{1,0,0,1,1,0,1,0,0,1,1,0,1,0,1,0}	{1,0,0,0}	{0,0,1,2}
{1,0,1,0,1,0,0,1,1,0,1,0,0,1,0,1}	{1,0,0,1}	{1,1,0,3}
{1,0,0,1,1,0,0,1,1,0,1,0,0,1,0,1}	{1,0,0,2}	{0,0,1,0}
{1,0,0,1,1,0,1,0,0,1,0,1,0,1,0,1}	{1,0,0,3}	{1,1,0,1}
{0,1,1,0,1,0,1,0,0,1,1,0,0,1,0,1}	{1,0,1,0}	{1,0,1,0}
{0,1,0,1,0,1,1,0,1,0,0,1,0,1,1,0}	{1,0,1,1}	{0,1,0,1}
{0,1,1,0,0,1,0,1,0,1,0,1,0,1,0,1}	{1,0,1,2}	{1,0,1,2}
{1,0,0,1,1,0,1,0,1,0,0,1,1,0,0,1}	{1,0,1,3}	{0,1,0,3}
{0,1,1,0,1,0,1,0,0,1,0,1,1,0,0,1}	{1,1,0,0}	{0,1,1,0}
{0,1,1,0,0,1,0,1,0,1,0,1,1,0,1,0}	{1,1,0,1}	{1,0,0,1}
{0,1,1,0,0,1,0,1,0,1,1,0,0,1,0,1}	{1,1,0,2}	{0,1,1,2}
{1,0,0,1,1,0,1,0,1,0,1,0,0,1,1,0,1}	{1,1,0,3}	{1,0,0,3}
{0,1,0,1,0,1,0,1,0,1,0,0,1,1,0,0,1}	{1,1,1,0}	{1,1,1,2}
{1,0,0,1,0,1,1,0,1,0,0,1,0,1,0,1}	{1,1,1,1}	{0,0,0,3}
{0,1,1,0,1,0,0,1,0,1,0,1,1,0,1,0,1}	{1,1,1,2}	{1,1,1,0}
{0,1,0,1,1,0,1,0,1,0,0,1,0,1,0,1,0}	{1,1,1,3}	{0,0,0,1}

TAB. S1. Symmetry indicators for the 32 different topological phases in MSG 2.4 ($P\bar{1}$). In the first column we express the band representation as described in Eq. A2. In the second and third columns, we show the resulting Fu-Kane-like indicators ($z_{2I,1}, z_{2I,2}, z_{2I,3}, \eta_{4I}$) (Eq. A15,A16) and Smith symmetry indicators ($z_{2,a}, z_{2,b}, z_{2,c}, z_4$) (Eq. A14). Even though they do not coincide, there is a one-to-one mapping between the indicators.

the $A_g \oplus A_u$ representation at q_{1a} we can move them away from this position without breaking inversion symmetry. In general, when the number of A_g and A_u orbitals is exactly the same, it is possible to move them away from the $1a$ Wyckoff position keeping the inversion symmetry, i.e., the orbitals are not pinned. Conversely, if the numbers of both types of orbitals are different, not all of them can be moved away keeping the inversion symmetry and there will be a finite subset of orbitals pinned at the $1a$ position. Thus, the quantity $\delta_{1a} = n(A_g) - n(A_u)$ serves as an real space invariant representing the amount of symmetry pinned orbitals at the $1a$ Wyckoff position. This procedure is based on the subduction/induction relations of Wyckoff positions and high-symmetry lines, as sketched in the previous example, which can be generalized to all Wyckoff positions in all MSGs. The formulas for computing the different RSIs are listed in Ref. [54].

Appendix B: Detailed discussion on ideal topological materials

In this section we will provide an in depth analysis of the ideal topological materials outlined in the main text.

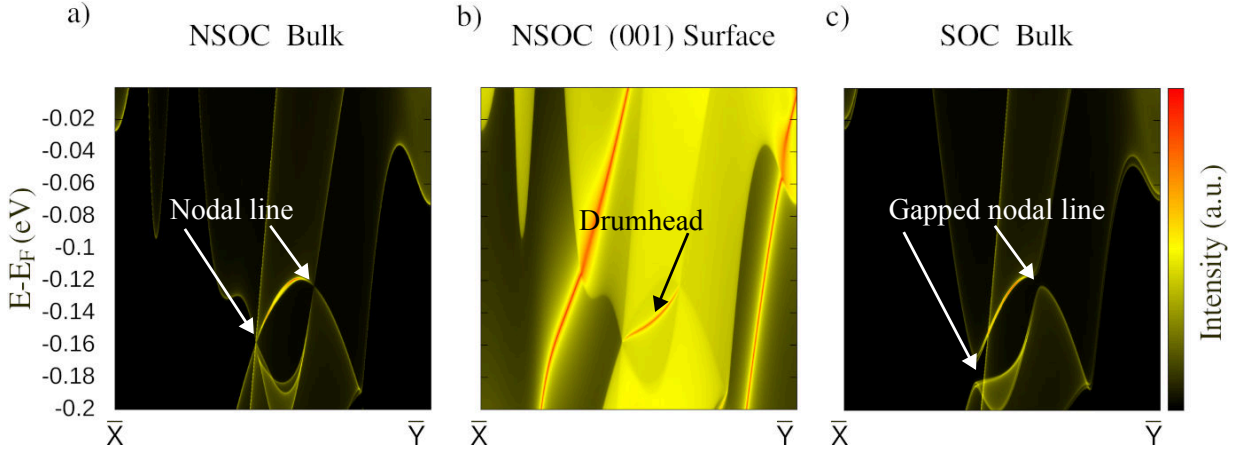


FIG. S1. a) Mn_2AlB_2 (BCSID 1.508) bulk bands projection on the (001) surface without SOC. We can clearly see the nodal line bandcrossing. b) Surface spectrum of a semi-infinite slab in the (001) direction. Drumhead states connect the projection of the nodal line crossings. c) Same calculation as in a) including SOC. The nodal line is gapped and the drumhead states are gapped as well.

1. Mn_2AlB_2 nodal line semimetal to mirror Chern insulator transition

Mn_2AlB_2 (BCSID 1.508) crystallizes in inversion symmetric SG Cmmm (65). When the magnetic moments of the Mn atoms are ordered, the resulting MSG 63.466 ($C_c mcm$). This MSG preserves inversion symmetry and m_z mirror; these determine the symmetry indicators of this MSG. In the absence of SOC, the system exhibits a mirror symmetry-protected nodal line in the $k_z = 0$ plane, formed by the crossing of 2 spin degenerate bands, so that the degeneracy at the nodal line is 4. The projection of the nodal line on the (001) surface and its corresponding drumhead states are displayed in Fig. S1a and S1b. If the SOC is included, the nodal line will open a gap as shown in Fig. S1c. We can then characterize its topology from symmetry indicators. Since inversion symmetry protects the η_{4I} symmetry indicator, it can be computed from inversion eigenvalues of the occupied set of bands [2],

$$\eta_{4I} = \sum_{K \in \text{TRIM}} \frac{n_K^- - n_K^+}{2} \bmod 4, \quad (\text{B1})$$

where K runs over the inversion symmetric momenta in the BZ and n_K^\pm are the number of positive/negative inversion eigenvalues of the occupied Bloch wavefunctions at point K . Notice that this indicator is equivalent to the one in Eq. A14. This index, when equal to 2, implies that the axion angle θ is non-trivial and it equals $\theta = \pi$. Thus, the system is an axion insulator. Moreover, this MSG has another symmetry indicator, δ_{2m} , and can be computed as follows:

$$\delta_{2m} = \sum_{K=Z,D,C,E} n_K^{\frac{1}{2},+i} - \sum_{K=\Gamma,A,B,Y} n_K^{\frac{1}{2},-i} \bmod 2, \quad (\text{B2})$$

where $n_K^{\frac{1}{2},\pm i}$ is the number of occupied states with C_2 eigenvalue $e^{-i\pi/2}$ and mirror eigenvalue $\pm i$. This indicator can be understood as the difference between the mirror Chern numbers in planes $k_z = 0, \pi$ modulo 2, i.e.,

$$\delta_{2m} = C_{k_z=\pi} - C_{k_z=0} \bmod 2. \quad (\text{B3})$$

We calculated the system's symmetry indicator and found that $\delta_{2m} = 1$, indicating that the system behaves as a mirror Chern insulator when spin-orbit coupling (SOC) is considered. The effect of SOC is, however, small. In particular, the nodal line gaps approximately ~ 8 meV (see Fig. S1), and makes it impossible to converge the Wilson loops. Moreover, there are many bulk states that project onto the surface, thus making it impossible to pinpoint the surface states associated with the mirror Chern number.

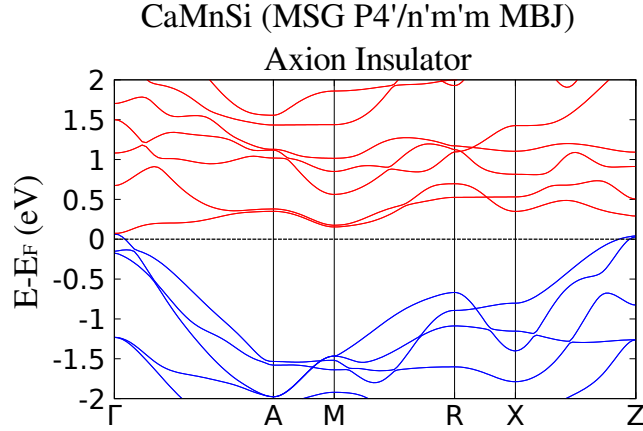


FIG. S2. **CaMnSi** bulk band calculation with MBJ functional. In the title, we show the chemical formula, magnetic space group and exchange correlation used (MBJ). The topological classification remains the same as with Hubbard+U.

2. CaMnSi Axion Insulator

CaMnSi (BCSID 0.599) crystallizes on tetragonal SG P4/nmm (129). When the magnetic ordering is also considered, the resulting MSG 129.416 ($P4'/n'm'm$) [42]. Notice that both materials with **BCSID 0.599** and **BCSID 0.600** are almost isostructural ($\sim 0.5\%$ difference on lattice parameter). The main difference between them is the experimentally measured magnetic moments and experimental temperature ($T_{0.599} = 2K$, $T_{0.600} = 300K$). Based on the results of Table S2 we observe that experimentally, $\mu_{0.599} = 3.27$ and $\mu_{0.600} = 1.96$. Our calculations show very good agreement for the 0.599 structure (0.8% error) while they show rather bad agreement with 0.600. Thus, we selected the 0.599 structure to explore its topological properties in depth.

The insulators in MSG 129.416 ($P4'/n'm'm$) exhibit the symmetry indicator z_2 . This symmetry indicator is protected by S_4 rotoinversion symmetry, and can be computed as follows:

$$z_2 = \sum_{K=\Gamma,M,Z,A} \frac{n_K^{\frac{1}{2}} - n_K^{-\frac{1}{2}}}{2} \bmod 2, \quad (\text{B4})$$

where $n_K^{\pm\frac{1}{2}}$ denotes the number of bands with eigenvalue $e^{\mp i\frac{\pi}{4}}$ under S_4 symmetry and Γ, M, Z, A represent the k-points invariants under S_4 . We computed the index for CaMnSi to be $z_2 = 1$.

Since the smallest direct gap computed with GGA functionals is small (it ranges from 15.3 meV for $U = 0$ eV to 2 meV with $U = 3$ eV), we performed additional DFT calculations with the modified Becke-Johnson functional (MBJ) [73]. The MBJ predicted gap remains small (6.1 meV) and the topological diagnosis is the same (see Fig. S2). The surface state calculation shows gapped surface states, as expected for an axion insulator (see Fig. 3b).

3. UAsS enforced semimetal

We studied a family of Uranium pnictide chalcogens (**UPSe (BCSID 0.593)**, **UAsS (BCSID 0.594)**, **UPTe (BCSID 0.595)** and **UAsTe (BCSID 0.596)**). We identified all of them as enforced semimetals. Among these, we selected **UAsS (BCSID 0.594)** for further investigation, because it displays the cleanest Fermi level (see Fig. 2c). **UAsS** crystallizes in SG P4/nmm (129), with the ferromagnetic ground state assigned to MSG 129.417 ($P4/nm'm'$). Our findings indicate that $U=0$ eV provides the best fit for the magnetic moment, with an average error of 24.9%.

Similar to other ferromagnetic semimetals, we find Weyl nodes close to the Fermi level, which can be split into three families; 2 pairs of 2 Weyl nodes on the $\Gamma - Z$ line ($W_1 = (0, 0, 0.25)\text{\AA}^{-1}$ and $W_2 = (0, 0, 0.33)\text{\AA}^{-1}$) and a family of 8 symmetry-related Weyl nodes ($W_3 = (0.43, 0.43, 0.26)\text{\AA}^{-1}$). We show their location in Fig. S3a. The topological charge for a member of each family is displayed in Fig. S3b. The Weyl nodes along the $\Gamma - Z$ direction lie below the Fermi level ($E_{W_1} = -0.08\text{eV}$, $E_{W_2} = -0.11\text{eV}$), in an energy window densely populated by bulk states, and are close to each other, making it challenging to identify their characteristic Fermi arcs. However, we did observe double Fermi arcs originating from the (100) surface projections of the other family of Weyl nodes ($E_{W_3} = -0.02\text{eV}$), which lie

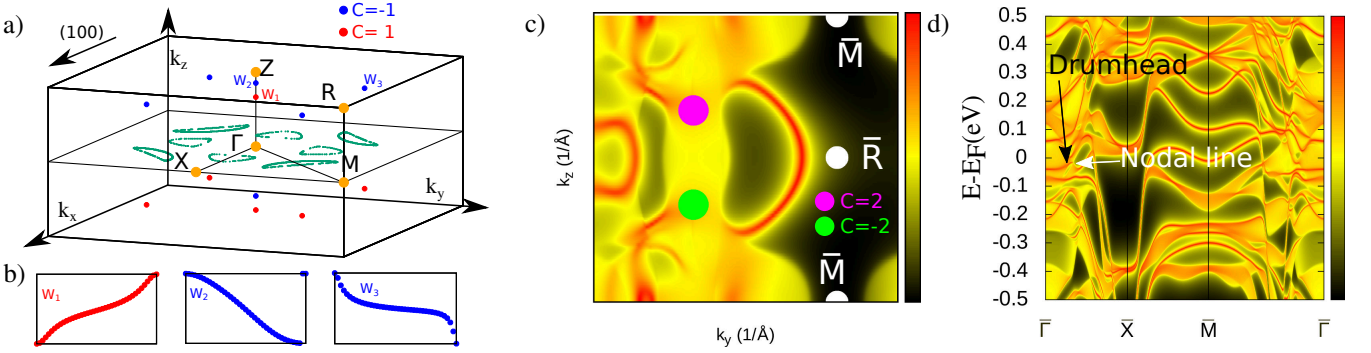


FIG. S3. a) BZ and the spatial distribution of Weyl nodes and nodal lines in **UAsS** (BCSID 0.594). In red (blue) Weyl nodes with charge +1 (-1). b) Wilson loop on a sphere surrounding the location of Weyl nodes \$W_1\$, \$W_2\$ and \$W_3\$ indicated in a). c) (100) surface termination Fermi surface showing double Fermi arcs stemming from the projection of same-charge Weyl nodes. Magenta (green) color stands for two +1 (-1) Weyls projected in the same point, effectively doubling the charge. d) Drumhead states emerging from the projection of the nodal lines onto the (001) surface termination.

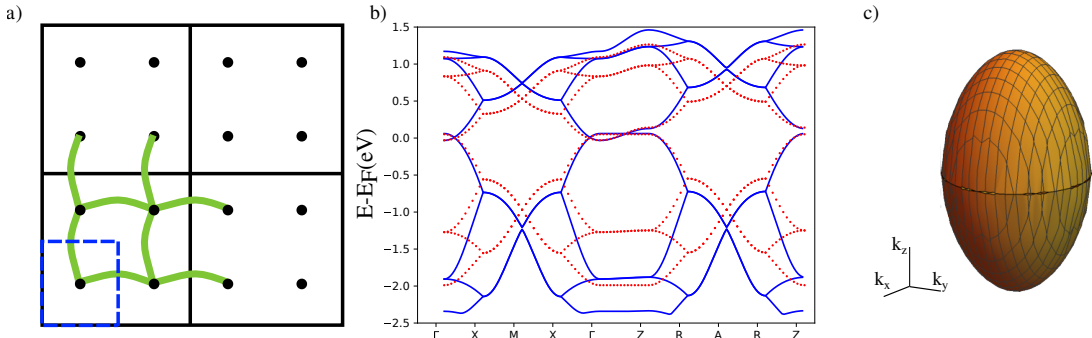


FIG. S4. (a) TB with nearest neighbor model hoppings of **CsMnF₄** (BCSID 0.327). In dashed blue lines, the ‘primitive’ unit cell of the unfolded model. (b) Comparison between the TB effective model band dispersion and DFT bands. We observe a good agreement close to the Fermi level. c) Nodal surface of the effective tight binding model. The shape matches with the nodal surface reported in Fig. 3d.

closer to the Fermi level. Double arcs arise because same-charge Weyl nodes’ projections coincide on that particular surface, as illustrated in Fig. S3c.

We also found a set of 8 nodal lines at the \$k_z = 0\$ plane protected by the \$\{m_z | \frac{1}{2}, \frac{1}{2}\}\$ glide plane. The (001) surface spectrum reveals that the outer part of the nodal line corresponds to the topologically non-trivial region, where drumhead states are anticipated. In Fig S3a we show the nodal lines in momentum space, located at \$k_z = 0\$ and the path used for the surface. Along the surface path \$\bar{\Gamma} - \bar{X}\$, we observe the projection of the bulk nodal line and the emergence of drumhead states stemming from it (refer to Fig. S3d).

4. CsMnF₄ nodal surface semimetal

CsMnF₄ (BCSID 0.327) crystallizes in the SG P4/nmm and its ferromagnetic phase is assigned to MSG 59.410 (*Pmm'm'*). Note that this is one of the experimentally reported structures for this compound [76]. It has been suggested that another structure could be the lowest energy state, potentially influenced by the Jahn-Teller effect [77]. The definitive structure, however, remains a subject of ongoing debate [92, 93]. In this work we study the structure in [76]. We selected the system with \$U=3\text{eV}\$, as it exhibits the smallest error in magnetization while still being a metal. We computed the orbital and atomic weight on the bands close to the Fermi level and found out they are formed exclusively from the d-orbitals originating from the Mn atoms at the 4c Wyckoff position. In total, four Mn atoms are present within the unit cell, each with 10 d-orbitals, thereby yielding a total of 40 bands. Owing to the magnetic order, the spin-up and spin-down bands are split. As the splitting is large in this case (\$\sim 3 - 4\text{eV}\$, depending on the value of Hubbard \$U\$), we can limit the current scope of research to the spin-up sector. Moreover, as the SOC is very small, we can discard it as a first approximation. Therefore, we studied the remaining 20 spin-polarized bands

crossing the Fermi level. Owing to the crystal field splitting, the $T_{2g}(d_{xy}, d_{xz}, d_{yz})$ and $E_g(d_{z^2}, d_{x^2-y^2})$ orbitals are separated by a gap. The T_{2g} orbitals are fully occupied, while the E_g are only half-occupied and, thus, lie at the Fermi level. Subsequently, to analyze the crossings at the Fermi level, we constructed a Wannier Hamiltonian based on the $E_g(d_{z^2}, d_{x^2+y^2})$ irrep. The resulting Wannier TB at nearest neighbors can then be expressed in blocks, with the sites $q_0 = (0, 0, 0)$, $q_1 = (\frac{1}{2}, 0, 0)$, $q_2 = (\frac{1}{2}, \frac{1}{2}, 0)$, $q_3 = (0, \frac{1}{2}, 0)$ and the basis $\mathcal{B} = \{d_{z^2}, d_{x^2-y^2}\} \otimes \{q_0, q_1, q_2, q_3\}$ (see Fig. S4a):

$$H_{NN} = \begin{pmatrix} \epsilon_{d_{z^2}} + t_{d_{z^2}} H_{d_{z^2}} + t_{d_{z^2}}^v H_{d_{z^2}}^v & t_{dd} H_{dd} \\ t_{dd} H_{dd}^\dagger & \epsilon_{d_{x^2-y^2}} + t_{d_{x^2-y^2}} H_{d_{x^2-y^2}} \end{pmatrix}, \quad (B5)$$

with $\epsilon_{d_{z^2}} = 0.582\text{eV}$ and $\epsilon_{d_{x^2-y^2}} = -1.004\text{eV}$ the on-site energies, $t_{d_{z^2}} = -0.140\text{eV}$, $t_{d_{z^2}}^v = -0.042\text{eV}$, $t_{dd} = 0.185\text{eV}$, $t_{d_{x^2-y^2}} = -0.255\text{eV}$ the nearest neighbors hoppings and the blocks:

$$H_{d_{z^2}}(k_x, k_y) = \begin{pmatrix} 0 & 2 \cos\left(\frac{k_x}{2}\right) & 0 & 2 \cos\left(\frac{k_y}{2}\right) \\ 2 \cos\left(\frac{k_x}{2}\right) & 0 & 2 \cos\left(\frac{k_y}{2}\right) & 0 \\ 0 & 2 \cos\left(\frac{k_y}{2}\right) & 0 & 2 \cos\left(\frac{k_x}{2}\right) \\ 2 \cos\left(\frac{k_y}{2}\right) & 0 & 2 \cos\left(\frac{k_x}{2}\right) & 0 \end{pmatrix} = H_{d_{x^2-y^2}}(k_x, k_y), \quad (B6)$$

$$H_{dd}(k_x, k_y) = \begin{pmatrix} 0 & 2e^{ik_x} \cos\left(\frac{k_x}{2}\right) & 0 & -2e^{ik_y} \cos\left(\frac{k_y}{2}\right) \\ 2e^{-ik_x} \cos\left(\frac{k_x}{2}\right) & 0 & -2e^{ik_y} \cos\left(\frac{k_y}{2}\right) & 0 \\ 0 & -2e^{-ik_y} \cos\left(\frac{k_y}{2}\right) & 0 & 2e^{-ik_x} \cos\left(\frac{k_x}{2}\right) \\ -2e^{-ik_y} \cos\left(\frac{k_y}{2}\right) & 0 & 2e^{ik_x} \cos\left(\frac{k_x}{2}\right) & 0 \end{pmatrix} \quad (B7)$$

and

$$H_{d_{z^2}}^v = 2 \cos(k_z) \mathbb{I}_{4 \times 4}. \quad (B8)$$

These blocks represent the nearest neighbor hoppings between d_{z^2} ($H_{d_{z^2}}$), $d_{x^2-y^2}$ ($H_{d_{x^2-y^2}}$) and $d_{z^2} - d_{x^2-y^2}$ (H_{dd}) orbitals. Notice that we added the (001) direction hopping for the d_{z^2} orbitals but neglected it for $d_{x^2-y^2}$, due to being very small ($t_{d_{x^2-y^2}}^v \approx 2.10^{-4}\text{eV}$). We can see a comparison between the DFT (blue solid lines) and the Wannier TB model (red dots) in Fig. S4b. MTQC formalism predicts this material to be an ES with a nodal degeneracy in the $k_x = 0$ plane. This is due to the interchange of mirror $\{m_x|0\}$ eigenvalues between the last valence and first conduction bands at $\Gamma = (0, 0, 0)$ and $Z = (0, 0, \frac{1}{2})$. In order to check that the model presents the same band inversion, we compute the eigenstates at Γ and Z of the last valence and first conduction bands:

$$\begin{aligned} |\Gamma, v\rangle &= \frac{1}{2}(1, 1, 1, 1, 0, 0, 0, 0, 0) \\ |\Gamma, c\rangle &= \frac{1}{2}(0, 0, 0, 0, -1, 1, -1, 1) \\ |Z, v\rangle &= \frac{1}{2}(0, 0, 0, 0, -1, 1, -1, 1) \\ |Z, c\rangle &= \frac{1}{2}(1, 1, 1, 1, 0, 0, 0, 0, 0), \end{aligned} \quad (B9)$$

where v, c stand for last valence and first conduction bands. The representation of the mirror $\{m_x|0\}$ in the basis \mathcal{B} is:

$$\sigma_0 \otimes \begin{pmatrix} 0 & 1 & 0 & 0 \\ 1 & 0 & 0 & 0 \\ 0 & 0 & 0 & 1 \\ 0 & 0 & 1 & 0 \end{pmatrix} \quad (B10)$$

where the σ_0 matrix acts on the orbital degree of freedom. From Eq. B9 and Eq. B10 we extract the mirror

eigenvalues:

$$\begin{aligned} m_x |\Gamma, v\rangle &= |\Gamma, v\rangle \\ m_x |\Gamma, c\rangle &= -|\Gamma, c\rangle \\ m_x |Z, v\rangle &= -|Z, v\rangle \\ m_x |Z, c\rangle &= |Z, c\rangle, \end{aligned} \quad (\text{B11})$$

which determines that the model reproduces the band inversion. As we explained in the main text, instead of a nodal line, we find in this system an approximate nodal surface. We can reproduce this analytically here. At first order in perturbation theory, we construct the low energy effective TB model close to Γ as follows:

$$H_{i,j}^{\text{eff}} = \langle i | H_{\text{NN}} | j \rangle = \begin{pmatrix} \epsilon_{d_{z^2}} + 2t_{d_{z^2}} \left(\cos\left(\frac{k_x}{2}\right) + \cos\left(\frac{k_y}{2}\right) \right) + 2t_{d_{z^2}}^v \cos(k_z) & 0 \\ 0 & \epsilon_{d_{x^2-y^2}} - 2t_{d_{x^2-y^2}} \left(\cos\left(\frac{k_x}{2}\right) + \cos\left(\frac{k_y}{2}\right) \right) \end{pmatrix}, \quad (\text{B12})$$

where $|i\rangle, |j\rangle = |\Gamma, v\rangle, |\Gamma, c\rangle$ following the notation of Eq. B11 and the constants are the same as in Eq. B5. Notice that at this order in perturbation theory, the effective tight binding does not depend on t_{dd} , which measures the hopping that mixes orbitals. The nodal surface will then be the set of (k_x, k_y, k_z) points that make this block Hamiltonian degenerate. After some manipulation, we conclude that the points forming the nodal surface satisfy the following equation:

$$\cos \frac{k_x}{2} + \cos \frac{k_y}{2} = f(k_z), \quad (\text{B13})$$

with

$$f(k_z) = \frac{\epsilon_{d_{x^2-y^2}} - \epsilon_{d_{z^2}}}{2(t_{d_{x^2-y^2}} + t_{d_{z^2}})} - \frac{t_{d_{z^2}}^v}{t_{d_{x^2-y^2}} + t_{d_{z^2}}} \cos(k_z) = 2.006 - 0.108 \cos(k_z) \quad (\text{B14})$$

where in the last step we introduced the numerical values of the Wannier TB. We can see a numerical rendering of the shape in Fig. S4c. We can also extract the energies of the nodal surface crossing by plugging Eq. B13 into any of the diagonal entries in H^{eff} , for instance, the lower one:

$$E_{\text{nodal}} = \epsilon_{d_{x^2-y^2}} - 2t_{d_{x^2-y^2}} f(k_z). \quad (\text{B15})$$

Interestingly, it only depends on k_z and it is symmetric under $k_z \rightarrow -k_z$, both properties that we can see in the nodal surface from the full Wannier TB in Fig. 3d.

Notice that the Wannier TB seems to have a unit cell that is 2×2 larger than it should, due to the intra-cell and inter-cell hoppings being equal. We can then construct a TB model in the ‘primitive’ unit cell, highlighted in dashed blue lines in Fig. S4a. This new primitive model does not present any crossing; the crossings in the Wannier TB come from band folding. Since the bands at the Fermi level come exclusively from Mn atoms, the corrections to the hoppings from the interaction with Cs and F atoms will be very small. Indeed, there is no difference in the numerical Wannier TB. We can however push the difference between the intra-cell and inter-cell hoppings to gap the nodal surface while keeping the nodal line at $k_x = 0$. In particular, we can add a term of the form:

$$H_{dd}^b = t_{dd}^b \begin{pmatrix} 0 & -e^{ik_x} & 0 & 0 \\ -e^{-ik_x} & 0 & 0 & 0 \\ 0 & 0 & 0 & e^{-ik_x} \\ 0 & 0 & e^{ik_x} & 0 \end{pmatrix}, \quad (\text{B16})$$

which introduces a modulation in the hopping in the (100) direction between the intra-cell and inter-cell hoppings that mix different orbitals, with the modulation being different for orbitals in $q_i^y = 0$ and $q_i^y = \frac{1}{2}$. Any finite value of t_{dd}^b will gap the nodal surface except at the $k_x = 0$ plane, thus giving rise to the predicted nodal line. The nodal surface degeneracy, which is exactly protected by band folding, is thus gapped away when taking into account all symmetry allowed terms. We can then say that, in the absence of interaction with the crystal environment, there is a ‘quasisymmetry’ protected nodal surface, similar to the recent results found in other materials systems [44, 45].

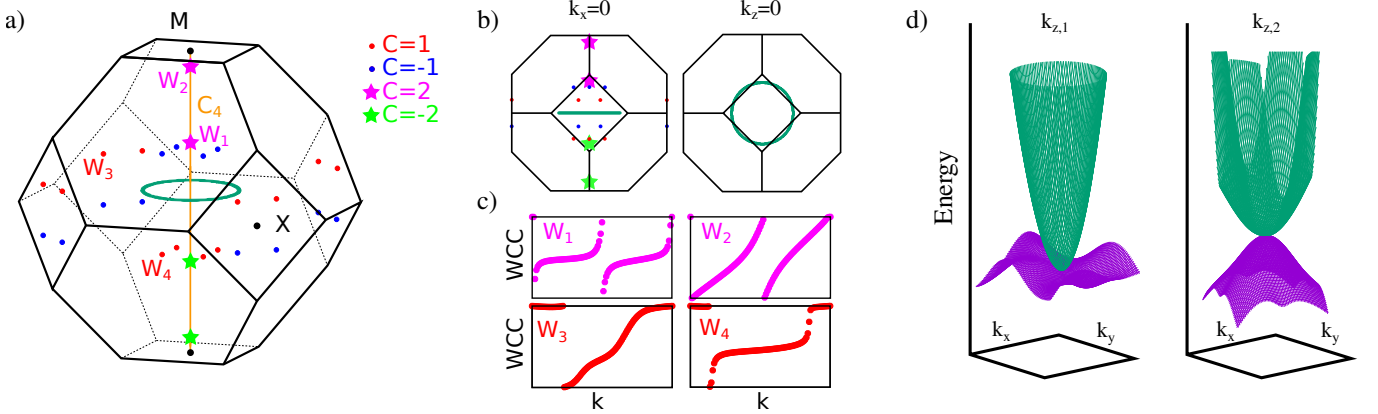


FIG. S5. a) Location of topological crossings in the Brillouin Zone of FeCr₂S₄ (BCSID 0.613). In red and magenta Weyl nodes with topological charge 1 and 2, respectively. In blue and green Weyl nodes with topological charge -1 and -2. Charge 2 Weyl nodes are represented by stars. In dark green, mirror-symmetry protected nodal line. b) Projection of crossing location. c) Wilson loop on a sphere surrounding the location of Weyl nodes W₁, W₂, W₃ and W₄ indicated in a). d) Fixed k_z plane dispersion of double Weyls. As expected, the dispersion is quadratic in the k_xk_y direction.

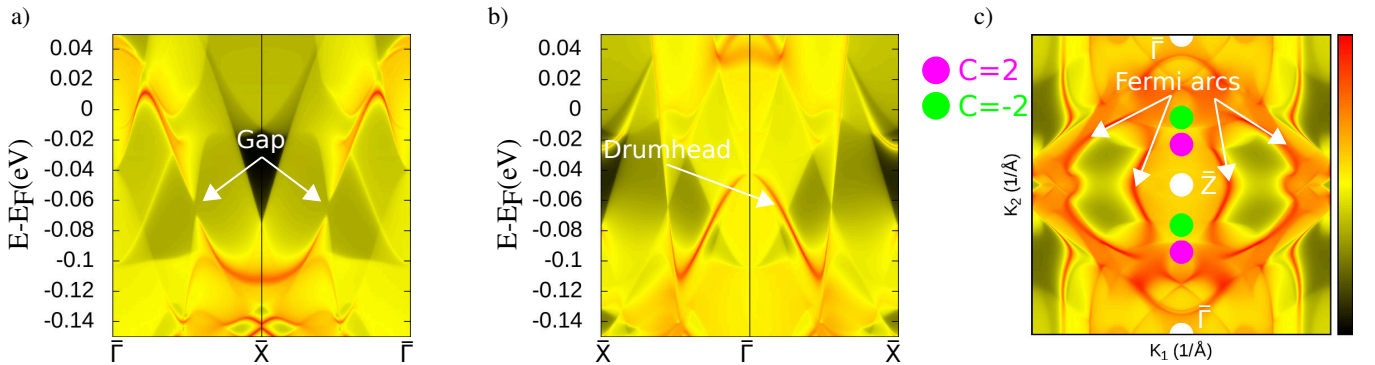


FIG. S6. Surface spectrum of FeCr₂S₄ (BCSID 0.613) for two different surface terminations, a) (100) and b) (001). Notice that the pre-existing nodal line is gapped in the (100) termination, and the surface states are not protected. In the (001) termination the drumhead states stem from the nodal line and are topologically protected. c) (100) surface termination Fermi surface. We see two Fermi arcs stemming from the projection of each of the bulk double Weyls.

5. FeCr₂S₄ enforced semimetal

FeCr₂S₄ (BCSID 0.613) crystallizes in the cubic SG Fd $\bar{3}$ m (227) and its anti-ferrimagnetic phase (with magnetic momenta aligned along the 'z' direction) is assigned to the tetragonal MSG 141.557 ($I4_1/am'd'$). To examine the electronic properties of the system, we initially fit the Hubbard U parameter values that best fit the experimental magnetic momentum, varying it independently for Fe and Cr, in a grid of values ranging from $U=0$ eV-4eV. We observed that the best values are $U_{\text{Fe}} = 4$ eV and $U_{\text{Cr}} = 0$ eV, with an error of 2.2% for Fe and 3.2% for Cr, and leaving the magnetic momenta of S as close as possible to 0.

As typical both for ferro- and ferri-magnetic materials, this system has several Weyl nodes with topological charge ± 1 ("single-Weyl" nodes), which are displayed in Fig. S5a. Owing to the presence of the C_4 symmetry (orange axis in Fig. S5a), this compound can also display double-Weyl nodes [46], doubling the usual charge. This follows from the C_4 symmetry constraining the local Weyl Hamiltonian to have quadratic dispersion in the momentum orthogonal to the symmetry axis. In this material, we find two pairs of double-Weyls located at $k_{z,1} = \pm 0.24511\text{\AA}^{-1}$ and $k_{z,2} = \pm 0.56557\text{\AA}^{-1}$, which are displayed in Fig. S5a, in magenta ($C = 2$) and green ($C = -2$). The band dispersion of the two Weyls in the $k_z = k_{z,1}$ and $k_z = k_{z,2}$ planes is illustrated in Fig. S5d showing the predicted quadratic dispersion. We further confirm their topological charge by computing the Wilson loops on a sphere surrounding the degeneracy points (see Fig. S5c). The rest of the Weyls have topological charge 1 (see Fig. S5c). Moreover, in the $k_z = 0$ plane there exists a symmetry protected nodal line, displayed in Fig. S5a and Fig. S5b.

The surface state calculations in the (100) and (001) surface terminations are displayed in Fig. S6. In Fig. S6a we can observe the surface spectrum for the (100) termination where the band dispersion of a pre-existing nodal line that has been gapped owing to the magnetic symmetry subduction can be observed. Fig. S6b shows the drumhead states originate from the projection of the remaining nodal line. Finally, the Fermi surface calculations on the (100) surface are displayed in Fig. S6c. Two Fermi arcs stem from the projection of each of the bulk double Weyls, getting in total 4 Fermi arcs.

Appendix C: Experimental magnetic momenta vs calculation

The experimentally determined magnetic momenta of nonequivalent atoms for all computed systems and those within DFT+U for various values of the Hubbard U parameter are presented herein in two tables. In Table S2, we consider the compounds with magnetic elements containing only d electrons. In Table S3, we consider compounds with only f electrons and in Table S4 we consider compounds with both d and f electrons. The first three columns contain the BCS ID of the material, the chemical formula and MSG. In the next columns, we display the experimental magnetic momenta vs the computed one, with the resulting error quantified as follows:

$$\text{Error}(\%) = \sum_j \left(\sum_{i=x}^z \left| \frac{\mu_i^{\text{exp}} - \mu_i^{\text{comp}}}{\mu_i^{\text{exp}}} \right| \right) \frac{100}{N_j^{\text{at}}}, \quad (\text{C1})$$

where i runs over the 3 components of the magnetic momenta and j runs over the magnetic elements. Missing entries correspond to cases where the numerical calculation failed to converge.

BCS ID	Formula	MSG	M.E.	μ_{exp}	U=0	U=1	U=2	U=3	U=4
0.229	Ba2 Mn1 Si2 O7	MSG 113.267 ($P\bar{4}2_1m$)	Mn	4.1	4.38	4.44	4.5	4.56	4.6
			Error(%)		6.9 %	8.41 %	9.8 %	11.1 %	12.29 %
0.230	K2 Co1 P2 O7	MSG 58.395 ($Pn'n'm$)	Mn	4.1	4.38	4.44	4.5	4.56	4.6
			Error(%)		6.9 %	8.41 %	9.8 %	11.1 %	12.29 %
0.234	Mn2 La1 Sb1 O6	MSG 13.69 ($P2'/c'$)	Co	3.03	2.57	2.62	2.66	2.7	2.74
			Error(%)		15.35 %	13.7 %	12.18 %	10.76 %	9.44 %
0.236	Ca1 Fe4 Al8	MSG 139.535 ($I4'/mmm'$)	Co	3.03	2.57	2.62	2.66	2.7	2.74
			Error(%)		5.12 %	4.57 %	4.06 %	3.59 %	3.15 %
0.239	Ca3 Li1 Ru1 O6	MSG 15.89 ($C2'/c'$)	Mn	4.8	4.39	4.46	4.52	4.57	4.62
			Error(%)		2.13 %	1.79 %	1.48 %	1.2 %	0.95 %
0.254	Cu1 O6 C4 H9 N3	MSG 33.144 ($Pna2_1$)	La	4.8	0.01	0.01	0.01	0.01	0.01
			Error(%)		25.07 %	25.06 %	25.06 %	25.05 %	25.05 %
0.258	Fe2 P3 O12 Li3	MSG 14.79 ($P2'_1/c'$)	Fe	0.71	3.07	3.23	3.28	3.3	3.34
			Error(%)		2121.6 %	1343.02 %	1155.86 %	1248.71 %	968.82 %
0.260	Cu1 Fe1 P1 O5	MSG 62.441 ($Pnma$)	Fe	0.71	3.14	3.24	3.31	3.34	3.38
			Error(%)		2180.36 %	1358.35 %	1170.89 %	1264.29 %	978.58 %
0.261	Ni1 Fe1 P1 O5	MSG 62.441 ($Pnma$)	Fe	0.71	3.05	3.21	3.27	3.28	3.3
			Error(%)		1055.69 %	673.3 %	577.23 %	621.46 %	478.76 %
0.262	Co1 Fe1 P1 O5	MSG 62.447 ($Pnm'a'$)	Ru	2.8	1.82	1.91	1.99	2.06	2.14
			Error(%)		35.18 %	31.96 %	29.11 %	26.36 %	23.54 %
0.263	Fe2 P1 O5	MSG 62.441 ($Pnma$)	Ru	2.8	1.82	1.91	1.99	2.06	2.14
			Error(%)		35.18 %	31.96 %	29.11 %	26.36 %	23.54 %
0.264	Cu1 O6 C4 H9 N3	MSG 33.144 ($Pna2_1$)	Cu	0.63	0.12	0.01	0.03	0.46	0.02
			Error(%)		118.41 %	99.84 %	105.24 %	173.49 %	103.65 %
0.265	Fe2 P3 O12 Li3	MSG 14.79 ($P2'_1/c'$)	Cu	0.63	0.12	0.01	0.04	0.46	0.03
			Error(%)		39.58 %	33.33 %	35.13 %	57.83 %	34.66 %
0.266	Cu1 Fe1 P1 O5	MSG 62.441 ($Pnma$)	Fe	4.7	4.03	4.11	4.19	4.26	4.33
			Error(%)		3.56 %	3.14 %	2.74 %	2.35 %	1.96 %
0.267	Fe2 P1 O5	MSG 62.441 ($Pnma$)	Fe	4.0	4.02	4.1	4.17	4.25	4.32
			Error(%)		0.13 %	0.62 %	1.08 %	1.54 %	1.99 %
0.268	Cu1 Fe1 P1 O5	MSG 62.441 ($Pnma$)	Cu	0.95	0.49	0.54	0.59	0.62	0.65
			Error(%)		48.74 %	42.74 %	38.32 %	34.74 %	31.58 %
0.269	Ni1 Fe1 P1 O5	MSG 62.441 ($Pnma$)	Cu	0.95	0.48	0.54	0.58	0.62	0.65
			Error(%)		16.42 %	14.35 %	12.84 %	11.65 %	10.56 %
0.270	Fe2 P3 O12 Li3	MSG 14.79 ($P2'_1/c'$)	Fe	4.28	3.83	3.97	4.08	4.17	4.25
			Error(%)		10.49 %	7.24 %	4.79 %	2.66 %	0.68 %
0.271	Cu1 Fe1 P1 O5	MSG 62.441 ($Pnma$)	Fe	4.28	3.84	3.97	4.08	4.17	4.25
			Error(%)		3.47 %	2.4 %	1.59 %	0.88 %	0.23 %
0.272	Ni1 Fe1 P1 O5	MSG 62.441 ($Pnma$)	Ni	2.03	1.48	1.55	1.61	1.66	1.7
			Error(%)		27.09 %	23.65 %	20.84 %	18.47 %	16.31 %
0.273	Fe2 P1 O5	MSG 62.441 ($Pnma$)	Ni	2.03	1.48	1.55	1.61	1.65	1.7
			Error(%)		9.08 %	7.91 %	6.98 %	6.17 %	5.45 %
0.274	Fe2 P3 O12 Li3	MSG 14.79 ($P2'_1/c'$)	Fe	4.09	3.83	3.96	4.06	4.16	4.24
			Error(%)		6.36 %	3.2 %	0.66 %	1.59 %	3.69 %
0.275	Cu1 Fe1 P1 O5	MSG 62.441 ($Pnma$)	Fe	4.09	3.83	3.96	4.06	4.16	4.24
			Error(%)		2.11 %	1.06 %	0.22 %	0.53 %	1.22 %
0.276	Co1 Fe1 P1 O5	MSG 62.447 ($Pnm'a'$)	Co	3.45	2.52	2.58	2.63	2.68	2.73
			Error(%)		100.73 %	114.09 %	103.25 %	97.86 %	86.6 %
0.277	Fe2 P1 O5	MSG 62.447 ($Pnm'a'$)	Co	3.45	2.52	2.58	2.63	2.68	2.73
			Error(%)		33.53 %	38.02 %	34.42 %	32.62 %	28.87 %
0.278	Fe2 P3 O12 Li3	MSG 14.79 ($P2'_1/c'$)	Fe	4.22	3.78	3.96	4.07	4.16	4.24
			Error(%)		10.47 %	6.14 %	3.63 %	1.45 %	0.57 %
0.279	Cu1 Fe1 P1 O5	MSG 62.441 ($Pnma$)	Fe	4.22	3.78	3.96	4.07	4.16	4.24
			Error(%)		3.52 %	2.04 %	1.21 %	0.48 %	0.19 %
0.280	Ni1 Fe1 P1 O5	MSG 62.441 ($Pnma$)	Fe	3.89	3.61	3.67	3.67	3.69	3.73
			Error(%)		7.1 %	5.78 %	5.78 %	5.24 %	4.22 %
0.281	Fe2 P1 O5	MSG 62.441 ($Pnma$)	Fe	3.89	3.63	3.67	3.67	3.69	3.73
			Error(%)		2.25 %	1.88 %	1.89 %	1.73 %	1.41 %
0.282	Fe2 P3 O12 Li3	MSG 14.79 ($P2'_1/c'$)	Fe	4.22	3.78	3.94	4.06	4.16	4.25
			Error(%)		10.43 %	6.75 %	3.89 %	1.49 %	0.62 %
0.283	Cu1 Fe1 P1 O5	MSG 62.441 ($Pnma$)	Fe	4.22	3.78	3.94	4.06	4.16	4.25
			Error(%)						

			Error(%)		3.48 %	2.23 %	1.28 %	0.49 %	0.21 %	
0.264	Fe3 P2 O8	MSG 14.78 ($P2_1/c'$)	Fe	4.31	3.57	3.63	3.67	3.72	3.76	
			Error(%)		17.1 %	15.89 %	14.78 %	13.76 %	12.78 %	
	Na2 Ba1 Mn1 V2 O8		Fe	4.31	3.57	3.63	3.67	3.72	3.76	
			Error(%)		5.7 %	5.3 %	4.93 %	4.59 %	4.26 %	
0.266	Na2 Ba1 Mn1 V2 O8	MSG 164.89 ($P\bar{3}m'1$)	Mn	2.2	4.29	4.37	4.44	4.5	4.56	
			Error(%)		95.18 %	98.73 %	101.86 %	104.77 %	107.41 %	
0.273	Mn3 Zn1 N1	MSG 166.97 ($R\bar{3}m$)	Mn	1.21	2.63	3.06	3.36	3.59	3.79	
			Error(%)		233.76 %	305.49 %	354.32 %	393.69 %	426.52 %	
			Mn	1.21	2.61	3.05	3.35	3.6	3.8	
0.275	Al1 Mn3 N1	MSG 166.101 ($R\bar{3}m'$)	Mn	1.21	2.9	3.37	3.67	3.88	4.05	
			Error(%)		278.39 %	355.96 %	405.49 %	441.12 %	469.16 %	
			Mn	1.21	1.12	1.67	3.16	3.32	3.52	
0.276	Al1 Mn3 N1	MSG 65.486 ($Cmm'm'$)	Mn	0.91	1.17	0.53	0.35	3.34	3.55	
			Error(%)		28.91 %	41.33 %	61.48 %	268.75 %	292.19 %	
0.277	Mg1 Mn1 O3	MSG 148.19 ($R\bar{3}'$)	Mn	1.9	1.24	2.53	3.18	3.36	3.56	
			Error(%)		69.48 %	66.87 %	135.97 %	154.18 %	175.6 %	
			Mn	2.53	2.69	2.78	2.87	2.96	3.06	
0.279	Mn3 As1	MSG 63.463 ($Cmc'm'$)	Error(%)		6.17 %	9.92 %	13.52 %	17.11 %	20.87 %	
			Mn	2.53	2.69	2.78	2.87	2.96	3.06	
			Error(%)		6.17 %	9.92 %	13.52 %	17.11 %	20.87 %	
0.280	Mn3 As1	MSG 63.464 ($Cm'cm'$)	Mn	3.0	3.34	3.67	3.91	4.09	4.22	
			Error(%)		22.44 %	44.83 %	60.59 %	72.38 %	81.67 %	
			Mn	3.0	3.35	3.69	3.93	4.11	4.25	
0.284	K1 Os1 O4	MSG 88.85 ($I4'_1/a'$)	Mn	3.0	3.34	3.68	3.92	4.1	4.24	
			Error(%)		11.1 %	22.59 %	30.61 %	36.52 %	41.13 %	
			Mn	5.2	3.34	3.68	3.93	4.11	4.26	
0.285	K1 Ru1 O4	MSG 88.85 ($I4'_1/a'$)	Error(%)		71.57 %	58.17 %	48.83 %	41.89 %	36.14 %	
			Mn	5.2	3.34	3.68	3.93	4.11	4.26	
			Error(%)		11.91 %	9.7 %	8.13 %	6.98 %	6.02 %	
0.286	Cu2 Cl1 O3	MSG 14.75 ($P2_1/c$)	Mn	5.2	3.34	3.68	3.93	4.11	4.26	
			Error(%)		35.74 %	29.09 %	24.39 %	20.94 %	18.06 %	
			Os	0.46	0.46	0.52	0.58	0.68	18.95	
0.287	Na1 Cr1 Ge2 O6	MSG 15.89 ($C2'/c'$)	Error(%)		0.87 %	12.17 %	25.65 %	47.39 %	4019.57 %	
			Os	0.46	0.46	0.52	0.58	0.68	21.4	
			Error(%)		0.87 %	12.17 %	25.65 %	47.39 %	4553.04 %	
0.288	Na2 Ba1 Fe1 V2 O8	MSG 15.89 ($C2'/c'$)	Ru	0.57	0.41	0.48	0.51	0.53	0.56	
			Error(%)		27.37 %	16.32 %	11.23 %	6.84 %	1.75 %	
			Ru	0.57	0.41	0.48	0.51	0.53	0.56	
0.289	Fe2 O3	MSG 33.147 ($Pna'2'_1$)	Error(%)		27.37 %	16.32 %	11.23 %	6.84 %	1.75 %	
			Ni	2.18	1.52	1.58	1.62	1.67	1.71	
			Error(%)		237.73 %	108.97 %	99.84 %	90.85 %	80.52 %	
0.290	Te2 Ni1 O5	MSG 62.441 ($Pnma$)	Ni	2.18	1.52	1.58	1.62	1.67	1.71	
			Error(%)		237.36 %	108.6 %	99.84 %	90.48 %	80.52 %	
			Ni	2.18	1.52	1.58	1.62	1.67	1.71	
0.291	Cu2 Cl1 O3	MSG 14.75 ($P2_1/c$)	Error(%)		39.56 %	18.1 %	16.64 %	15.14 %	13.42 %	
			Cu	0.58	0.19	0.18	0.16	0.13	0.06	
			Error(%)		197.65 %	220.27 %	187.48 %	208.15 %	261.26 %	
0.292	Na2 Ba1 Fe1 V2 O8	MSG 15.89 ($C2'/c'$)	Cu	0.58	0.19	0.18	0.16	0.13	0.06	
			Error(%)		28.06 %	31.23 %	26.69 %	29.65 %	37.32 %	
			Cr	1.85	2.82	2.87	2.92	2.96	3.0	
0.293	Na2 Ba1 Fe1 V2 O8	MSG 15.89 ($C2'/c'$)	Error(%)		52.68 %	55.23 %	57.62 %	59.94 %	62.12 %	
			Fe	4.74	3.54	3.59	3.63	3.68	3.72	
			Error(%)		75.88 %	74.94 %	73.26 %	70.48 %	66.83 %	
0.294	Fe2 O3	MSG 33.147 ($Pna'2'_1$)	Fe	4.74	3.54	3.59	3.63	3.68	3.72	
			Error(%)		77.72 %	74.88 %	73.22 %	70.63 %	66.9 %	
			Fe	3.1	3.52	3.76	3.91	4.03	4.14	
0.295	Fe2 O3	MSG 33.147 ($Pna'2'_1$)	Error(%)		3.39 %	5.28 %	6.56 %	7.52 %	8.37 %	
			Fe	3.1	3.53	3.75	3.9	4.03	4.13	
			Error(%)		3.46 %	5.27 %	6.46 %	7.47 %	8.3 %	

			Fe Error(%)	0.9 77.42 %	3.69 82.42 %	3.87 85.75 %	3.99 88.53 %	4.09 90.94 %
			Fe Error(%)	0.9 74.11 %	3.57 79.61 %	3.77 83.53 %	3.91 86.75 %	4.02 89.64 %
0.300	Fe2 O3	MSG 33.147 ($Pna'2'_1$)	Fe Error(%)	3.6 0.38 %	3.55 1.19 %	3.77 2.24 %	3.92 3.06 %	4.04 3.76 %
			Fe Error(%)	3.6 0.58 %	3.52 1.03 %	3.75 2.11 %	3.9 2.97 %	4.03 3.7 %
			Fe Error(%)	2.5 11.91 %	3.69 13.69 %	3.87 14.9 %	3.99 15.89 %	4.09 16.77 %
			Fe Error(%)	2.7 8.03 %	3.57 9.86 %	3.77 11.17 %	3.91 12.23 %	4.02 13.19 %
			Co Error(%)	2.1 36.15 %	2.5 45.73 %	2.57 54.24 %	2.63 62.71 %	2.68 69.84 %
0.301	Sr2 Co1 Te1 O6	MSG 14.75 ($P2_1/c$)	Co Error(%)	2.1 36.15 %	2.5 45.73 %	2.57 54.3 %	2.63 62.82 %	2.68 69.84 %
0.303	Ba1 F5 Cr1	MSG 19.27 ($P2'_12'_12_1$)	Cr Error(%)	1.0 177.1 %	2.77 180.5 %	2.81 183.5 %	2.84 186.3 %	2.86 188.9 %
			Cr Error(%)	1.0 59.03 %	2.77 60.17 %	2.81 61.17 %	2.84 62.1 %	2.86 62.97 %
0.307	Sc1 Cr1 O3	MSG 62.441 ($Pnma$)	Cr Error(%)	2.7 1.59 %	2.66 1.85 %	2.75 4.63 %	2.83 7.04 %	2.89 9.22 %
			Cr Error(%)	2.7 0.51 %	2.66 0.63 %	2.75 1.56 %	2.83 2.36 %	2.89 3.09 %
			Cr Error(%)	2.5 10.12 %	2.75 13.12 %	2.83 15.6 %	2.89 17.76 %	2.94 19.8 %
0.308	In1 Cr1 O3	MSG 62.441 ($Pnma$)	Cr Error(%)	2.5 3.39 %	2.75 4.39 %	2.83 5.2 %	2.89 5.93 %	2.94 6.6 %
			Mn Error(%)	4.7 2.13 %	4.4 1.52 %	4.49 1.02 %	4.56 0.62 %	4.61 0.28 %
			Fe Error(%)	4.34 8.09 %	3.99 5.74 %	4.09 3.59 %	4.18 1.61 %	4.27 0.28 %
0.310	Na1 Mn1 Fe1 F6	MSG 150.27 ($P32'_1$)	Fe Error(%)	4.42 3.54 %	4.11 2.66 %	4.18 1.84 %	4.26 1.04 %	4.33 0.23 %
			Co Error(%)	3.3 218.82 %	2.61 144.64 %	2.65 56.79 %	2.67 43.94 %	2.71 45.25 %
			Co Error(%)	3.3 219.73 %	2.61 144.97 %	2.65 56.79 %	2.67 43.94 %	2.71 45.25 %
0.311	Co1 Ge1 O3	MSG 61.435 ($Pb'ca$)	Co Error(%)	3.3 36.47 %	2.61 24.11 %	2.65 9.47 %	2.67 7.32 %	2.71 7.54 %
			Co Error(%)	4.03 197.44 %	2.56 159.34 %	2.62 111.01 %	2.66 109.46 %	2.71 101.04 %
			Co Error(%)	4.03 198.32 %	2.54 159.48 %	2.61 111.04 %	2.66 109.46 %	2.71 101.04 %
			Co Error(%)	4.03 32.91 %	2.56 26.56 %	2.62 18.5 %	2.66 18.24 %	2.71 16.84 %
			Mn Error(%)	4.29 4.3 %	4.39 7.74 %	4.46 10.58 %	4.52 12.96 %	4.57 15.24 %
			Mn Error(%)	4.29 1.43 %	4.39 2.58 %	4.46 3.53 %	4.52 4.32 %	4.57 5.08 %
0.313	Mn1 Ge1 O3	MSG 15.87 ($C2'/c$)	Mn Error(%)	4.05 13.41 %	4.43 55.94 %	4.49 15.25 %	4.55 20.43 %	4.6 23.52 %
			Mn Error(%)	4.05 13.41 %	4.43 55.94 %	4.49 15.25 %	4.55 20.43 %	4.6 23.52 %
			Mn Error(%)	4.05 0.96 %	4.43 4.0 %	4.49 1.09 %	4.55 1.46 %	4.6 1.68 %
			Mn Error(%)	4.68 2.37 %	4.46 1.81 %	4.51 1.28 %	4.56 0.8 %	4.61 0.35 %
0.315	Zr1 Mn2 Ge4 O12	MSG 125.367 ($P4'/nbm'$)	Mn Error(%)	4.68 2.37 %	4.46 1.79 %	4.51 1.28 %	4.56 0.8 %	4.61 0.35 %
			Mn Error(%)	4.68 2.37 %	4.46 1.79 %	4.51 1.28 %	4.56 0.8 %	4.61 0.35 %
			Cr Error(%)	2.51 4.46 %	2.62 8.84 %	2.73 12.23 %	2.82 15.14 %	2.89 17.73 %
0.323	La1 Cr1 O3	MSG 62.441 ($Pnma$)	Cr Error(%)	2.51 4.46 %	2.62 8.84 %	2.73 12.23 %	2.82 15.14 %	2.89 17.73 %

			Error(%)		1.5 %	2.95 %	4.08 %	5.05 %	5.91 %
0.327	Mn1 Cs1 F4	MSG 59.410 ($Pmm'n'$)	Mn Error(%)	4.0 2.04 %	3.67 1.67 %	3.73 1.37 %	3.78 1.14 %	3.82 0.91 %	3.85
0.328	Mn1 F4 K1	MSG 14.79 ($P2'_1/c'$)	Mn Error(%)	2.83	3.58 81.03 %	3.64 88.34 %	3.7 94.47 %	3.76 100.04 %	3.81 105.36 %
			Mn Error(%)	2.83	3.58 81.03 %	3.64 88.34 %	3.7 94.47 %	3.76 99.8 %	3.81 105.36 %
			Mn Error(%)	2.83	3.57 39.63 %	3.64 43.58 %	3.69 46.76 %	3.75 49.67 %	3.8 52.43 %
0.329	Mn1 F4 Rb1	MSG 2.4 ($P\bar{I}$)	Mn Error(%)	2.97	3.56 61.22 %	3.63 68.06 %	3.7 74.28 %	3.75 79.9 %	3.81 85.31 %
			Mn Error(%)	2.97	3.56 19.56 %	3.63 22.21 %	3.7 24.41 %	3.75 26.44 %	3.81 28.26 %
			Fe Error(%)	4.6	3.55 22.78 %	3.58 22.15 %	3.59 21.96 %	3.64 20.87 %	3.69 19.7 %
0.331	Fe2 Mo3 O8	MSG 186.205 ($P6'_3m'c$)	Fe Error(%)	4.6	3.55 7.59 %	3.58 7.38 %	3.59 7.32 %	3.64 6.96 %	3.69 6.57 %
			Co Error(%)	3.3	2.39 27.48 %	2.44 26.15 %	2.51 24.06 %	2.58 21.91 %	2.64 20.0 %
			Co Error(%)	3.3	2.39 9.16 %	2.44 8.72 %	2.51 8.02 %	2.58 7.3 %	2.64 6.67 %
0.333	Mn2 Mo3 O8	MSG 186.207 ($P6_3m'c'$)	Mn Error(%)	4.3	4.36 0.66 %	4.41 1.28 %	4.48 2.1 %	4.54 2.81 %	4.6 3.44 %
			Mn Error(%)	4.3	4.35 100.57 %	4.42 1.38 %	4.49 2.26 %	4.56 2.99 %	4.61 3.63 %
			Co Error(%)	3.21	2.85 11.25 %	3.01 6.2 %	3.11 3.27 %	3.18 0.87 %	3.25 1.31 %
0.334	Co1 F3	MSG 167.103 ($R\bar{3}c$)	Co Error(%)	3.21	2.85 11.09 %	3.01 6.2 %	3.11 3.27 %	3.18 0.87 %	3.25 1.34 %
			Fe Error(%)	2.6	4.05 55.65 %	4.14 59.08 %	4.21 61.88 %	4.27 64.35 %	4.33 66.58 %
			Fe Error(%)	2.6	4.05 55.65 %	4.14 59.08 %	4.21 61.88 %	4.27 64.35 %	4.33 66.58 %
0.338	Co2 Mo3 O8	MSG 186.205 ($P6'_3m'c$)	Co Error(%)	3.44	2.46 28.46 %	2.52 26.74 %	2.59 24.83 %	2.64 23.14 %	2.7 21.66 %
			Co Error(%)	3.44	2.46 28.46 %	2.52 26.74 %	2.59 24.83 %	2.64 23.14 %	2.7 21.66 %
			Co Error(%)	3.35	2.45 26.84 %	2.58 23.07 %	2.63 21.37 %	2.68 19.94 %	2.73 18.6 %
			Co Error(%)	3.35	2.45 26.84 %	2.58 23.07 %	2.63 21.37 %	2.68 19.94 %	2.73 18.6 %
			Cu Error(%)	0.93	0.48 47.96 %	0.52 44.62 %	0.54 41.94 %	0.56 39.46 %	0.58 37.2 %
0.348	Bi2 Cu1 O4	MSG 130.431 ($P4/n'c'c'$)	Cu Error(%)	0.93	0.49 15.88 %	0.52 14.77 %	0.54 13.91 %	0.57 13.08 %	0.59 12.33 %
			Fe Error(%)	2.85	3.59 148.76 %	3.7 207.35 %	3.79 241.07 %	3.88 230.64 %	3.89 453.72 %
			Fe Error(%)	2.85	3.59 49.05 %	3.7 69.03 %	3.79 80.35 %	3.88 76.88 %	3.89 151.2 %
0.357	Ca1 Fe5 O7	MSG 11.50 ($P2_1/m$)	Fe Error(%)	3.29	3.55 120.76 %	3.7 120.27 %	3.8 119.52 %	3.91 111.09 %	4.04 107.68 %
			Fe Error(%)	3.29	3.55 40.28 %	3.7 40.17 %	3.8 39.91 %	3.91 37.07 %	4.04 35.82 %
			Fe Error(%)	2.01	3.57 159.83 %	3.61 101.89 %	3.72 144.83 %	3.66 98.67 %	3.7 181.94 %
			Fe Error(%)	2.01	3.57 159.83 %	3.61 101.89 %	3.72 144.83 %	3.66 98.67 %	3.7 181.94 %
			Ru Error(%)	2.03	1.85 8.87 %	1.94 4.63 %	2.02 0.69 %	2.1 3.25 %	2.18 7.39 %
			Ru Error(%)	2.03	1.85 8.87 %	1.94 4.63 %	2.02 0.69 %	2.1 3.25 %	2.18 7.39 %
0.368	Co1 C4 N1 O6 H9	MSG 62.448 ($Pn'ma'$)	Co Error(%)	2.89	2.6 77.47 %	2.64 48.19 %	2.68 35.1 %	2.72 32.27 %	2.76 29.47 %

			Co Error(%)	2.89 25.82 %	2.6 16.06 %	2.64 11.7 %	2.68 10.76 %	2.72 9.82 %	2.76 9.82 %
0.369	N1 C4 O6 Co1 H9	MSG 14.79 ($P2_1'/c'$)	Co Error(%)	2.98 129.31 %	2.52 115.62 %	2.57 115.62 %	2.65 22.29 %	2.7 34.33 %	2.74 44.36 %
			Co Error(%)	2.98 136.24 %	2.52 121.03 %	2.57 121.03 %	2.65 27.09 %	2.7 42.91 %	2.74 44.36 %
			Co Error(%)	2.91 255.25 %	2.01 99.53 %	2.06 99.53 %	2.2 50.23 %	2.29 25.25 %	2.37 22.35 %
			Co Error(%)	2.42 10.09 %	2.49 19.39 %	2.57 19.39 %	2.6 30.96 %	2.65 28.06 %	2.7 33.8 %
0.375	La2 Co1 Ir1 O6	MSG 14.75 ($P2_1/c$)	Co Error(%)	2.42 10.38 %	2.49 19.79 %	2.57 19.79 %	2.6 32.71 %	2.65 26.25 %	2.7 33.01 %
			Mn Error(%)	3.1 7.77 %	3.58 12.27 %	3.86 12.27 %	4.03 14.92 %	4.15 16.98 %	4.26 18.69 %
0.395	Ga1 Mn1 Pt1	MSG 63.462 ($Cm'c'm$)	Mn Error(%)	2.69 147.56 %	3.58 132.64 %	3.84 132.64 %	4.02 80.26 %	4.15 95.72 %	4.26 117.28 %
			Mn Error(%)	2.69 148.44 %	3.59 133.18 %	3.85 133.18 %	4.03 80.56 %	4.16 96.02 %	4.26 117.6 %
0.399	Fe1 O2 H1	MSG 62.445 ($Pnma'$)	Fe Error(%)	4.45 16.99 %	3.69 12.31 %	3.9 12.31 %	4.02 9.62 %	4.11 7.64 %	4.18 6.0 %
			Fe Error(%)	4.45 5.66 %	3.69 4.1 %	3.9 4.1 %	4.02 3.21 %	4.11 2.55 %	4.18 2.0 %
0.414	Fe2 B2 Al1	MSG 65.486 ($Cmm'm'$)	Fe Error(%)	1.4 0.57 %	1.38 5.11 %	1.54 5.11 %	1.64 8.54 %	1.76 13.04 %	1.94 19.32 %
0.416	La1 Cr1 O3	MSG 167.103 ($R\bar{3}c$)	Cr Error(%)	1.67 52.46 %	2.55 58.44 %	2.65 58.44 %	2.72 62.87 %	2.78 66.53 %	2.83 69.58 %
			Cr Error(%)	1.67 52.46 %	2.55 58.44 %	2.65 58.44 %	2.72 62.87 %	2.78 66.53 %	2.83 69.58 %
0.433	K1 Mn1 F3	MSG 140.541 ($I4/mcm$)	Mn Error(%)	1.0 348.8 %	4.49 353.8 %	4.54 353.8 %	4.58 357.8 %	4.61 361.3 %	4.64 364.4 %
			Mn Error(%)	1.0 348.8 %	4.49 353.8 %	4.54 353.8 %	4.58 357.8 %	4.61 361.3 %	4.64 364.4 %
0.447	Ge1 Mn1 Co1	MSG 194.270 ($P6_3/mm'c'$)	Mn Error(%)	2.01 21.0 %	2.85 35.65 %	3.44 41.47 %	3.68 45.32 %	3.83 48.53 %	3.96 48.53 %
			Co Error(%)	0.72 21.25 %	0.41 7.29 %	0.62 7.29 %	0.77 3.75 %	0.86 9.58 %	0.94 15.07 %
0.464	Ba1 Mn2 P2	MSG 139.536 ($I4'/m'm'm'$)	Mn Error(%)	4.2 20.12 %	3.36 12.45 %	3.68 12.45 %	- - %	4.07 3.14 %	- - %
			Mn Error(%)	4.2 20.12 %	3.36 12.45 %	3.68 12.45 %	- - %	4.07 3.14 %	- - %
0.470	Ba1 Mn2 Sb2	MSG 139.536 ($I4'/m'm'm'$)	Mn Error(%)	3.83 1.7 %	3.77 4.07 %	3.99 4.07 %	- - %	- - %	- - %
			Mn Error(%)	3.83 1.7 %	3.77 4.07 %	3.99 4.07 %	- - %	- - %	- - %
0.471	Ba2 Mn3 Sb2 O2	MSG 139.536 ($I4'/m'm'm'$)	Mn Error(%)	3.45 - %	- 15.29 %	3.97 15.29 %	- - %	4.28 24.25 %	4.39 27.24 %
			Mn Error(%)	3.45 - %	- 15.29 %	3.97 15.29 %	- - %	4.28 24.25 %	4.39 27.24 %
0.473	La1 Mn2 Si2	MSG 44.231 ($Im'm2'$)	Mn Error(%)	2.44 34.89 %	2.83 59.7 %	3.3 59.7 %	3.61 87.66 %	3.84 110.51 %	4.02 129.24 %
			Mn Error(%)	2.44 35.17 %	2.84 59.8 %	3.3 59.8 %	3.61 87.75 %	3.85 110.56 %	4.02 129.35 %
0.482	Sr1 Mn2 As2	MSG 12.60 ($C2'/m$)	Mn Error(%)	3.6 7.42 %	3.87 13.22 %	4.08 13.22 %	4.22 17.28 %	4.33 20.36 %	4.42 22.83 %
			Mn Error(%)	3.6 7.42 %	3.87 13.22 %	4.08 13.22 %	4.22 17.28 %	4.33 20.36 %	4.42 22.83 %
0.495	La1 Mn2 Si2	MSG 44.231 ($Im'm2'$)	Mn Error(%)	1.92 107.74 %	2.82 154.31 %	3.29 154.31 %	3.61 196.38 %	3.84 234.07 %	4.02 268.37 %
			Mn Error(%)	1.92 107.95 %	2.82 154.42 %	3.29 154.42 %	3.6 196.31 %	3.84 234.07 %	4.02 268.36 %
0.496	La1 Mn2 Si2	MSG 44.231 ($Im'm2'$)	Mn Error(%)	2.74 29.1 %	2.77 41.7 %	3.25 41.7 %	3.58 53.19 %	3.82 73.92 %	4.0 90.39 %
			Mn Error(%)	2.74 29.1 %	2.77 41.7 %	3.25 41.7 %	3.58 53.19 %	3.81 73.92 %	4.0 90.39 %

			Error(%)		28.88 %	41.49 %	53.15 %	73.88 %	90.34 %	
0.497	La1 Mn2 Si2	MSG 44.231 ($Im'm2'$)	Mn	2.61	2.77	3.25	3.58	3.81	3.99	
			Error(%)		26.3 %	39.75 %	67.47 %	88.12 %	103.56 %	
	Mn3 As2		Mn	2.61	2.77	3.25	3.58	3.82	4.0	
			Error(%)		26.53 %	39.74 %	67.56 %	88.16 %	103.67 %	
0.512	Mn3 As2	MSG 12.58 ($C2/m$)	Mn	0.52	3.42	3.73	3.95	4.12	4.24	
			Error(%)		278.94 %	308.37 %	330.0 %	346.06 %	357.98 %	
			Mn	2.55	2.87	3.34	3.68	3.92	4.09	
			Error(%)		6.22 %	15.39 %	22.22 %	26.9 %	30.12 %	
0.513	Y1 Ru1 O3	MSG 62.448 ($Pn'ma'$)	Mn	1.69	3.67	3.92	4.11	4.24	4.35	
			Error(%)		117.34 %	132.13 %	143.14 %	151.18 %	157.34 %	
	Ca1 Mn2 Sb2		Mn	0.59	2.27	3.1	3.58	3.87	4.04	
			Error(%)		285.25 %	425.08 %	506.95 %	555.76 %	584.58 %	
0.513	Y1 Ru1 O3	MSG 62.448 ($Pn'ma'$)	Ru	0.33	0.01	0.45	0.68	0.71	0.73	
			Error(%)		98.18 %	34.24 %	59.7 %	96.06 %	114.55 %	
	Ca1 Mn2 Sb2		Ru	0.33	0.01	0.46	0.68	0.71	0.73	
			Error(%)		32.63 %	12.12 %	19.9 %	31.92 %	38.18 %	
0.523	Ca1 Mn2 Sb2	MSG 2.6 ($P\bar{I}'$)	Mn	3.38	-	4.14	4.27	4.38	4.46	
			Error(%)		- %	45.02 %	52.96 %	59.18 %	64.18 %	
	Mn1 P1 Se3		Mn	3.38	-	4.14	4.27	4.38	4.46	
			Error(%)		- %	45.02 %	52.96 %	59.22 %	64.18 %	
0.524	Mn1 P1 Se3	MSG 2.6 ($P\bar{I}'$)	Mn	3.83	-	4.3	4.38	4.45	4.51	
			Error(%)		- %	24.68 %	28.94 %	32.49 %	35.51 %	
	Mn4 Ta2 O9		Mn	3.83	-	4.3	4.38	4.45	4.51	
			Error(%)		- %	24.74 %	28.94 %	32.49 %	35.51 %	
0.526	Mn4 Ta2 O9	MSG 165.94 ($P\bar{3}'c'1$)	Mn	5.1	4.32	4.4	4.47	4.52	4.57	
			Error(%)		15.24 %	13.63 %	12.37 %	11.33 %	10.45 %	
			Mn	5.1	4.32	4.4	4.47	4.52	4.57	
			Error(%)		5.08 %	4.54 %	4.12 %	3.78 %	3.48 %	
0.528	Cr1 Sb1	MSG 194.268 ($P6'_3/m'm'c$)	Mn	4.8	4.36	4.43	4.49	4.54	4.58	
			Error(%)		9.25 %	7.67 %	6.44 %	5.42 %	4.54 %	
	Cr1 Sb1		Mn	4.8	4.36	4.43	4.49	4.54	4.58	
			Error(%)		3.08 %	2.56 %	2.15 %	1.81 %	1.51 %	
0.529	Co4 Nb2 O9	MSG 15.88 ($C2/c'$)	Cr	2.45	2.76	3.07	3.32	3.52	3.68	
			Error(%)		12.49 %	25.27 %	35.47 %	43.67 %	50.37 %	
			Cr	2.45	2.78	3.09	3.33	3.53	3.69	
			Error(%)		13.43 %	25.92 %	35.88 %	43.96 %	50.61 %	
0.532	Pb2 Mn1 O4	MSG 114.278 ($P\bar{4}'2_1c'$)	Co	2.82	-	2.58	2.65	2.69	2.75	
			Error(%)		- %	18.09 %	12.69 %	9.53 %	5.37 %	
	Pb2 Mn1 O4		Co	2.82	-	2.57	2.65	2.69	2.75	
			Error(%)		- %	12.04 %	8.86 %	9.93 %	4.63 %	
0.571	Co1 S1 O4	MSG 62.441 ($Pnma$)	Co	2.82	-	2.58	2.65	2.68	2.75	
			Error(%)		- %	17.77 %	12.68 %	11.25 %	5.34 %	
			Co	2.82	-	2.58	2.65	2.69	2.75	
			Error(%)		- %	2.57 %	1.79 %	1.75 %	1.02 %	
0.572	Na2 F7 Ni1 Cr1	MSG 74.558 ($Im'm'a$)	Mn	2.74	2.63	2.73	2.82	2.92	3.02	
			Error(%)		8.2 %	1.7 %	5.67 %	12.68 %	19.95 %	
			Mn	2.74	2.63	2.73	2.82	2.92	3.02	
			Error(%)		1.17 %	0.24 %	0.82 %	1.81 %	2.85 %	
0.572	Na2 F7 Ni1 Cr1	MSG 74.558 ($Im'm'a$)	Co	3.82	2.58	2.63	2.68	2.72	2.76	
			Error(%)		106.89 %	98.41 %	92.94 %	89.08 %	84.3 %	
			Co	3.82	2.58	2.63	2.68	2.72	2.76	
			Error(%)		106.9 %	98.39 %	92.86 %	89.04 %	84.26 %	
0.572	Na2 F7 Ni1 Cr1	MSG 74.558 ($Im'm'a$)	Co	3.82	2.57	2.63	2.68	2.72	2.76	
			Error(%)		53.47 %	49.21 %	46.48 %	44.56 %	42.18 %	
			Ni	1.64	1.65	1.69	1.73	1.76	1.78	
			Error(%)		565.67 %	126.91 %	90.93 %	108.89 %	132.13 %	
0.572	Na2 F7 Ni1 Cr1	MSG 74.558 ($Im'm'a$)	Ni	1.64	1.66	1.7	1.73	1.76	1.78	
			Error(%)		567.56 %	125.71 %	90.58 %	108.89 %	131.65 %	
			Cr	1.84	2.75	2.81	2.84	2.87	2.89	
			Error(%)		109.18 %	116.14 %	111.68 %	113.1 %	115.65 %	
0.572	Na2 F7 Ni1 Cr1	MSG 74.558 ($Im'm'a$)	Cr	1.84	2.76	2.81	2.84	2.87	2.89	
			Error(%)		110.05 %	116.47 %	111.9 %	113.26 %	115.76 %	

0.573	Na2 F7 Ni1 Cr1	MSG 74.558 ($Im'm'a$)	Ni Error(%)	1.75	1.65 117.84 %	1.69 36.96 %	1.73 30.68 %	1.76 34.5 %	1.78 41.95 %
			Ni Error(%)	1.75	1.66 117.31 %	1.7 36.24 %	1.73 30.38 %	1.76 34.26 %	1.78 41.95 %
			Cr Error(%)	2.22	2.76 37.61 %	2.81 43.02 %	2.84 37.79 %	2.87 52.39 %	2.89 46.76 %
			Cr Error(%)	2.22	2.77 38.15 %	2.81 43.29 %	2.84 37.97 %	2.87 52.52 %	2.89 46.89 %
0.574	Mn1 Fe1 F5 O2 H4	MSG 5.15 ($C2'$)	Mn Error(%)	4.94	- - %	4.47 68.49 %	4.55 37.47 %	4.6 25.09 %	4.64 21.65 %
			Mn Error(%)	4.94	- - %	4.47 68.49 %	4.55 37.47 %	4.6 25.02 %	4.64 21.65 %
			Fe Error(%)	3.43	- - %	4.14 55.71 %	4.21 50.95 %	4.28 51.11 %	4.34 53.66 %
			Fe Error(%)	3.43	- - %	4.14 55.71 %	4.21 50.95 %	4.28 51.11 %	4.34 53.66 %
0.575	Zn1 Fe1 F5 O2 H4	MSG 44.229 ($Imm2$)	Fe Error(%)	3.78	- - %	4.18 10.66 %	4.24 12.14 %	4.29 13.54 %	4.34 14.87 %
			Fe Error(%)	3.78	- - %	4.18 10.56 %	4.24 12.06 %	4.29 13.47 %	4.34 14.79 %
			Cr Error(%)	2.67	- - %	2.79 107.63 %	2.83 17.13 %	2.86 72.4 %	2.88 14.09 %
0.576	Cr2 F5	MSG 15.85 ($C2/c$)	Cr Error(%)	2.67	- - %	2.79 107.89 %	2.83 17.13 %	2.86 72.4 %	2.88 14.05 %
			Cr Error(%)	3.59	- - %	3.68 122.11 %	3.72 26.07 %	3.75 82.42 %	3.77 17.54 %
			Cr Error(%)	3.59	- - %	3.68 122.14 %	3.72 26.1 %	3.75 82.44 %	3.78 17.57 %
			Mn Error(%)	4.08	- - %	4.49 8.09 %	4.56 8.29 %	4.61 8.2 %	4.64 8.13 %
0.577	Ba1 Mn1 Fe1 F7	MSG 14.79 ($P2'_1/c'$)	Fe Error(%)	4.11	- - %	4.15 2.01 %	4.22 1.66 %	4.28 1.12 %	4.33 1.95 %
			Fe Error(%)	3.59	4.11 888.13 %	4.17 362.29 %	4.23 900.19 %	4.29 233.52 %	4.34 161.36 %
			Fe Error(%)	3.59	4.11 296.04 %	4.17 120.76 %	4.23 300.06 %	4.29 77.84 %	4.34 53.77 %
0.578	Fe2 Na1 Ba1 F9	MSG 14.75 ($P2_1/c$)	Fe Error(%)	3.61	4.11 69.24 %	4.18 36.4 %	4.24 72.76 %	4.29 43.59 %	4.34 51.95 %
			Fe Error(%)	3.61	4.11 23.08 %	4.18 12.13 %	4.24 24.25 %	4.29 14.53 %	4.34 17.32 %
			Ni Error(%)	0.97	1.47 102.0 %	1.55 104.92 %	1.62 124.57 %	1.68 132.71 %	1.73 112.29 %
			Ni Error(%)	0.97	1.52 111.09 %	1.59 111.82 %	1.65 126.8 %	1.7 136.61 %	1.74 114.94 %
0.579	Na2 Ni1 Fe1 F7	MSG 74.559 ($Imm'a$)	Fe Error(%)	4.34	4.06 3.23 %	4.15 2.14 %	4.22 1.36 %	4.28 0.67 %	4.34 0.05 %
			Ni Error(%)	1.36	- - %	1.57 117.98 %	1.64 50.39 %	1.69 31.01 %	1.73 32.09 %
			Ni Error(%)	1.36	- - %	1.6 120.7 %	1.66 51.09 %	1.71 33.64 %	1.74 32.09 %
0.580	Na2 Ni1 Fe1 F7	MSG 74.559 ($Imm'a$)	Fe Error(%)	4.93	- - %	4.16 7.8 %	4.23 7.12 %	4.29 6.52 %	4.34 5.98 %
			Fe Error(%)	4.45	- - %	4.14 7.01 %	4.21 5.37 %	4.28 3.93 %	4.33 2.63 %
			Fe Error(%)	4.45	- - %	4.14 7.01 %	4.21 5.37 %	4.28 3.93 %	4.33 2.63 %
0.581	Fe1 F3	MSG 15.89 ($C2'/c'$)	Fe Error(%)	3.98	- - %	4.11 3.14 %	4.21 5.68 %	4.28 7.44 %	4.34 8.94 %
			Fe Error(%)	3.98	- - %	4.1 3.09 %	4.21 5.65 %	4.28 7.41 %	4.34 8.94 %
			Fe Error(%)	3.87	- - %	3.82 60.94 %	3.81 30.39 %	3.75 10.88 %	3.72 17.01 %
0.583	Fe2 F5 O2 H4	MSG 74.559 ($Imm'a$)							

			Fe Error(%)	3.87 -	- % 60.9 %	3.82 30.26 %	3.81 10.4 %	3.76 16.44 %
			Fe Error(%)	2.8 -	- % 23.09 %	4.09 24.77 %	4.19 26.57 %	4.29 27.93 %
0.584	Fe2 F5 O2 H4	MSG 15.89 ($C2'/c'$)	Fe Error(%)	3.89 29.26 %	3.81 12.35 %	3.81 14.32 %	3.75 24.66 %	3.73 19.91 %
			Fe Error(%)	3.89 29.16 %	3.81 12.35 %	3.81 14.32 %	3.75 24.66 %	3.73 19.91 %
			Fe Error(%)	4.91 59.41 %	3.98 39.06 %	4.09 31.47 %	4.18 36.07 %	4.28 26.0 %
			Fe Error(%)	4.91 59.56 %	3.98 38.92 %	4.09 31.5 %	4.18 36.1 %	4.28 26.0 %
			Cr Error(%)	2.96 11.39 %	2.62 8.68 %	2.7 6.59 %	2.77 4.86 %	2.82 3.34 %
0.586	Y1 Cr1 O3	MSG 62.448 ($Pn'ma'$)	Cr Error(%)	2.96 3.78 %	2.62 2.88 %	2.7 2.77	2.82 2.18 %	2.86 1.62 %
			Cr Error(%)	0.92 35.36 %	1.4 84.63 %	2.08 122.57 %	2.6 122.57 %	3.01 152.29 %
0.598	Al1 Cr2	MSG 14.83 (P_{A21}/c)	Cr Error(%)	0.92 106.09 %	1.4 253.9 %	2.08 367.7 %	2.6 367.7 %	3.01 456.88 %
			Cr Error(%)	0.92 35.36 %	1.4 84.63 %	2.08 122.57 %	2.6 122.57 %	3.01 152.29 %
0.599	Mn1 Ca1 Si1	MSG 129.416 ($P4'/n'm'm$)	Mn Error(%)	3.27 1.59 %	3.32 11.71 %	3.65 18.93 %	3.89 24.43 %	4.07 - %
			Mn Error(%)	3.27 1.59 %	3.32 11.71 %	3.65 18.93 %	3.89 24.43 %	4.07 - %
0.600	Mn1 Ca1 Si1	MSG 129.416 ($P4'/n'm'm$)	Mn Error(%)	1.96 71.12 %	3.35 87.6 %	3.68 99.39 %	3.91 99.39 %	4.08 108.37 %
			Mn Error(%)	1.96 71.12 %	3.35 87.6 %	3.68 99.39 %	3.91 99.39 %	4.08 108.37 %
0.601	Mn1 Ca1 Ge1	MSG 11.53 (P_{21}/m')	Mn Error(%)	3.34 12.02 %	3.54 - %	- - %	4.19 50.4 %	- - %
			Mn Error(%)	3.34 12.05 %	3.54 - %	- - %	4.19 50.4 %	- - %
0.603	Ca1 Mn2 Ge2	MSG 139.536 ($I4'/m'm'm$)	Mn Error(%)	2.67 18.16 %	3.16 31.95 %	3.52 41.8 %	3.79 49.25 %	3.99 - %
			Mn Error(%)	2.67 18.16 %	3.16 31.95 %	3.52 41.8 %	3.79 49.25 %	3.99 - %
0.604	Ca1 Mn2 Ge2	MSG 139.536 ($I4'/m'm'm$)	Mn Error(%)	2.6 - %	- 34.58 %	3.5 44.85 %	3.77 52.62 %	3.97 - %
			Mn Error(%)	2.6 - %	- 34.58 %	3.5 44.85 %	3.77 52.62 %	3.97 - %
0.605	Ba1 Mn2 Ge2	MSG 139.536 ($I4'/m'm'm$)	Mn Error(%)	3.66 - %	- 4.62 %	3.83 10.08 %	4.03 14.32 %	4.18 - %
			Mn Error(%)	3.66 - %	- 4.62 %	3.83 10.08 %	4.03 14.32 %	4.18 - %
0.606	Ba1 Mn2 Ge2	MSG 139.536 ($I4'/m'm'm$)	Mn Error(%)	3.6 0.17 %	3.59 7.19 %	3.86 12.61 %	4.05 16.78 %	4.2 - %
			Mn Error(%)	3.6 0.17 %	3.59 7.19 %	3.86 12.61 %	4.05 16.78 %	4.2 - %
0.607	Ru1 O2	MSG 136.499 ($P4'_2/mnm'$)	Ru Error(%)	0.05 -	- % 18.0 %	0.04 90.0 %	0.0 90.0 %	0.01 78.0 %
			Ru Error(%)	0.05 -	- % 20.0 %	0.04 92.0 %	0.0 88.0 %	0.01 76.0 %
0.612	Cu2 S1 O5	MSG 12.58 ($C2/m$)	Cu Error(%)	0.86 154.19 %	0.47 110.43 %	0.57 85.31 %	0.63 68.87 %	0.67 55.49 %
			Cu Error(%)	0.86 154.41 %	0.46 110.35 %	0.57 84.97 %	0.63 68.77 %	0.67 55.21 %
			Cu Error(%)	0.86 19.01 %	0.53 15.41 %	0.6 12.97 %	0.64 10.87 %	0.67 9.01 %
0.613	Fe1 Cr2 S4	MSG 141.557 ($I4_1/am'd'$)	Fe Error(%)	3.52 -	- % 3.76 %	3.26 2.13 %	3.37 0.81 %	3.46 0.06 %
			Cr Error(%)	2.72 -	- % 1.33 %	2.87 2.19 %	2.96 2.93 %	3.04 3.14 %
			Mn	4.1	3.92	4.1	4.24	4.35
0.617	Mn1 K1 Sb1	MSG 129.416 ($P4'/n'm'm$)						4.44

			Error(%)		4.41 %	0.02 %	3.41 %	6.1 %	8.27 %
			Mn	4.1	3.92	4.1	4.24	4.35	4.44
			Error(%)		4.41 %	0.02 %	3.41 %	6.1 %	8.27 %
0.618	Mn1 K1 Bi1	MSG 129.416 ($P4'/n'm'm$)	Mn	4.5	3.98	4.15	4.28	4.39	4.48
			Error(%)		11.56 %	7.76 %	4.82 %	2.44 %	0.53 %
0.618	Mn1 K1 Bi1	MSG 129.416 ($P4'/n'm'm$)	Mn	4.5	3.98	4.15	4.28	4.39	4.48
			Error(%)		11.56 %	7.76 %	4.82 %	2.44 %	0.53 %
0.619	Mn1 La1 As1 O1	MSG 129.416 ($P4'/n'm'm$)	Mn	2.43	3.6	3.86	4.05	4.19	-
			Error(%)		47.94 %	58.72 %	66.5 %	72.43 %	- %
0.619	Mn1 La1 As1 O1	MSG 129.416 ($P4'/n'm'm$)	Mn	2.43	3.6	3.86	4.05	4.19	-
			Error(%)		47.94 %	58.72 %	66.5 %	72.43 %	- %
0.624	Mn1 La1 As1 O1	MSG 129.416 ($P4'/n'm'm$)	Mn	3.54	3.59	3.85	4.04	4.18	4.3
			Error(%)		1.3 %	8.76 %	14.12 %	18.22 %	21.47 %
0.624	Mn1 La1 As1 O1	MSG 129.416 ($P4'/n'm'm$)	Mn	3.54	3.59	3.85	4.04	4.19	4.3
			Error(%)		1.3 %	8.76 %	14.12 %	18.22 %	21.47 %
0.626	Na1 Mn1 P1	MSG 129.416 ($P4'/n'm'm$)	Mn	3.63	-	3.78	3.98	4.13	4.25
			Error(%)		- %	4.02 %	9.5 %	13.72 %	17.05 %
0.626	Na1 Mn1 P1	MSG 129.416 ($P4'/n'm'm$)	Mn	3.63	-	3.78	3.98	4.13	4.25
			Error(%)		- %	4.02 %	9.5 %	13.72 %	17.05 %
0.627	Na1 Mn1 P1	MSG 129.416 ($P4'/n'm'm$)	Mn	3.6	-	3.78	3.98	4.13	-
			Error(%)		- %	5.06 %	10.56 %	14.78 %	- %
0.627	Na1 Mn1 P1	MSG 129.416 ($P4'/n'm'm$)	Mn	3.6	-	3.78	3.98	4.13	-
			Error(%)		- %	5.06 %	10.56 %	14.78 %	- %
0.628	Mn1 Na1 P1	MSG 129.416 ($P4'/n'm'm$)	Mn	3.21	3.52	3.79	3.99	4.14	-
			Error(%)		9.66 %	18.16 %	24.27 %	28.94 %	- %
0.628	Mn1 Na1 P1	MSG 129.416 ($P4'/n'm'm$)	Mn	3.21	3.52	3.79	3.99	4.14	-
			Error(%)		9.66 %	18.16 %	24.27 %	28.94 %	- %
0.629	Mn1 Na1 As1	MSG 129.416 ($P4'/n'm'm$)	Mn	4.01	3.68	3.92	4.09	4.23	4.33
			Error(%)		8.13 %	2.24 %	2.07 %	5.41 %	8.08 %
0.629	Mn1 Na1 As1	MSG 129.416 ($P4'/n'm'm$)	Mn	4.01	3.68	3.92	4.09	4.23	4.33
			Error(%)		8.13 %	2.24 %	2.07 %	5.41 %	8.08 %
0.630	Mn1 Na1 As1	MSG 129.416 ($P4'/n'm'm$)	Mn	3.45	-	3.92	4.09	4.23	-
			Error(%)		- %	13.68 %	18.67 %	22.52 %	- %
0.630	Mn1 Na1 As1	MSG 129.416 ($P4'/n'm'm$)	Mn	3.45	-	3.92	4.09	4.23	-
			Error(%)		- %	13.68 %	18.67 %	22.52 %	- %
0.633	Fe1 K1 S2	MSG 15.87 ($C2'/c$)	Fe	1.97	-	3.18	3.36	3.51	3.63
			Error(%)		- %	123.12 %	141.75 %	156.56 %	168.79 %
0.633	Fe1 K1 S2	MSG 15.87 ($C2'/c$)	Fe	1.97	-	3.18	3.36	3.51	3.63
			Error(%)		- %	123.12 %	141.75 %	156.56 %	168.79 %
0.634	Mn1 Na1 Bi1	MSG 129.416 ($P4'/n'm'm$)	Mn	4.58	-	4.1	-	4.36	-
			Error(%)		- %	10.52 %	- %	4.87 %	- %
0.634	Mn1 Na1 Bi1	MSG 129.416 ($P4'/n'm'm$)	Mn	4.58	-	4.1	-	4.36	-
			Error(%)		- %	10.52 %	- %	4.87 %	- %
0.636	Fe1 Rb1 S2	MSG 15.87 ($C2'/c$)	Fe	1.72	2.91	3.16	3.35	3.49	3.61
			Error(%)		138.73 %	167.84 %	189.37 %	206.36 %	220.55 %
0.636	Fe1 Rb1 S2	MSG 15.87 ($C2'/c$)	Fe	1.72	2.91	3.16	3.35	3.49	3.61
			Error(%)		138.73 %	167.84 %	189.37 %	206.36 %	220.55 %
0.637	Fe1 K1 Se2	MSG 15.88 ($C2/c'$)	Fe	3.0	2.42	2.8	3.02	3.18	3.32
			Error(%)		19.43 %	6.73 %	0.63 %	6.13 %	10.67 %
0.637	Fe1 K1 Se2	MSG 15.88 ($C2/c'$)	Fe	3.0	2.42	2.8	3.02	3.18	3.32
			Error(%)		19.43 %	6.73 %	0.63 %	6.13 %	10.67 %
0.638	Fe1 Rb1 Se2	MSG 15.88 ($C2/c'$)	Fe	2.66	2.95	3.18	3.35	3.49	3.6
			Error(%)		11.02 %	19.62 %	25.98 %	31.05 %	35.3 %
0.638	Fe1 Rb1 Se2	MSG 15.88 ($C2/c'$)	Fe	2.66	2.95	3.18	3.35	3.49	3.6
			Error(%)		11.02 %	19.62 %	25.98 %	31.05 %	35.3 %
0.639	Au1 Mn2	MSG 71.535 ($Im'mm$)	Mn	4.3	-	3.88	4.06	4.2	4.31
			Error(%)		- %	9.79 %	5.58 %	2.33 %	0.28 %
0.639	Au1 Mn2	MSG 71.535 ($Im'mm$)	Mn	4.3	-	3.88	4.06	4.2	4.31
			Error(%)		- %	9.79 %	5.58 %	2.33 %	0.28 %
0.640	Au1 Mn2	MSG 71.535 ($Im'mm$)	Mn	4.0	3.62	3.87	4.05	4.19	4.3
			Error(%)		9.52 %	3.35 %	1.2 %	4.75 %	7.57 %
0.640	Au1 Mn2	MSG 71.535 ($Im'mm$)	Mn	4.0	3.62	3.87	4.05	4.19	4.3
			Error(%)		9.52 %	3.35 %	1.2 %	4.75 %	7.57 %

0.641	Ga1 Mn3	MSG 12.62 ($C2'/m'$)	Mn Error(%)	3.29	3.12 59.11 %	3.57 67.72 %	3.81 78.94 %	3.98 65.62 %	4.16 89.07 %
			Mn Error(%)	2.08	2.45 8.27 %	2.8 16.49 %	3.55 34.42 %	3.83 41.73 %	3.98 44.86 %
0.642	La1 Mn1 O3	MSG 62.448 ($Pn'ma'$)	Mn Error(%)	3.7	3.51 5.14 %	3.6 2.59 %	3.68 0.54 %	3.75 1.27 %	3.81 2.95 %
			Mn Error(%)	3.7	3.51 1.71 %	3.6 0.86 %	3.68 0.18 %	3.75 0.42 %	3.81 0.98 %
0.662	Mn3 Sn2	MSG 62.448 ($Pn'ma'$)	Mn Error(%)	0.83	3.07 33.75 %	3.51 40.35 %	3.74 43.77 %	3.93 46.69 %	4.08 45.66 %
			Mn Error(%)	1.53	2.75 19.85 %	3.21 27.52 %	3.51 32.34 %	3.76 36.5 %	3.95 39.53 %
0.663	Mn3 Sn2	MSG 62.448 ($Pn'ma'$)	Mn Error(%)	1.9	3.14 114.78 %	3.49 159.29 %	3.76 186.97 %	3.97 208.03 %	4.13 221.51 %
			Mn Error(%)	1.9	3.14 16.43 %	3.49 22.74 %	3.76 26.71 %	3.97 29.74 %	4.13 31.7 %
			Mn Error(%)	1.79	2.58 11.09 %	3.09 18.2 %	3.46 23.35 %	3.74 27.19 %	3.94 30.01 %
0.664	Mn3 Sn2	MSG 14.79 ($P2'_1/c'$)	Mn Error(%)	2.97	3.14 16.75 %	3.49 15.43 %	3.76 24.75 %	3.97 30.76 %	4.13 36.56 %
			Mn Error(%)	2.97	3.14 5.58 %	3.49 5.13 %	3.75 8.24 %	3.97 10.25 %	4.12 12.18 %
			Mn Error(%)	2.3	2.58 3.05 %	3.09 8.61 %	3.46 12.6 %	3.74 15.64 %	3.94 17.84 %
0.682	Ca2 Fe1 Os1 O6	MSG 14.79 ($P2'_1/c'$)	Fe Error(%)	2.58	- - %	3.88 25.27 %	4.01 27.62 %	4.1 29.42 %	4.18 30.93 %
			Os Error(%)	1.5	- - %	1.62 3.5 %	1.8 9.47 %	1.96 14.83 %	2.12 20.17 %
0.692	Ru3 Ba4 O10	MSG 64.471 ($Cm'ca$)	Ru Error(%)	1.0	0.89 188.8 %	1.2 19.1 %	1.4 35.2 %	1.54 52.9 %	1.63 62.3 %
			Ru Error(%)	1.0	0.89 62.93 %	1.2 6.37 %	1.4 11.73 %	1.54 17.63 %	1.63 20.77 %
0.693	Ru3 Ba4 O10	MSG 64.472 ($Cmc'a$)	Ru Error(%)	0.89	0.89 200.34 %	1.19 33.82 %	1.39 55.73 %	1.53 72.25 %	1.63 83.03 %
			Ru Error(%)	0.89	0.9 66.89 %	1.19 11.24 %	1.39 18.58 %	1.53 24.08 %	1.63 27.68 %
0.694	Bi2 Cu1 O4	MSG 130.431 ($P4/n'c'c'$)	Cu Error(%)	0.45	0.43 5.33 %	0.47 4.89 %	0.5 12.0 %	0.53 18.0 %	0.56 24.22 %
			Cu Error(%)	0.45	0.43 1.7 %	0.48 1.85 %	0.51 4.22 %	0.53 6.22 %	0.56 8.3 %
0.695	Bi2 Cu1 O4	MSG 56.367 ($Pc'cn$)	Cu Error(%)	0.85	0.52 39.06 %	0.55 35.18 %	0.58 32.0 %	0.6 29.06 %	0.63 26.0 %
			Cu Error(%)	0.85	0.52 12.98 %	0.55 11.73 %	0.58 10.67 %	0.6 9.65 %	0.63 8.67 %
0.699	Mn6 Sn6 Li1	MSG 65.486 ($Cmm'm'$)	Mn Error(%)	2.58	2.54 0.25 %	3.08 3.2 %	3.54 6.23 %	3.83 8.05 %	4.0 9.15 %
0.708	Nb4 Cr1 S8	MSG 194.268 ($P6'_3/m'm'c$)	Cr Error(%)	1.5	2.53 68.87 %	2.76 83.67 %	2.92 95.0 %	3.07 104.4 %	3.19 112.8 %
			Cr Error(%)	1.5	2.54 69.33 %	2.76 84.07 %	2.93 95.33 %	3.07 104.73 %	3.2 113.13 %
0.709	Nb4 Mn1 S8	MSG 63.463 ($Cmc'm'$)	Mn Error(%)	3.4	3.74 10.06 %	3.97 16.66 %	4.13 21.36 %	4.25 24.89 %	4.34 27.67 %
0.711	Ta4 Mn1 S8	MSG 63.463 ($Cmc'm'$)	Mn Error(%)	4.2	3.84 8.68 %	4.03 4.06 %	4.17 0.77 %	4.28 1.8 %	4.36 3.87 %
0.712	Nb3 V1 S6	MSG 20.33 ($C2'2'2_1$)	V Error(%)	1.5	1.75 16.53 %	1.84 22.53 %	1.91 27.6 %	1.98 31.87 %	2.03 35.47 %
			V Error(%)	1.5	1.75 16.47 %	1.84 22.53 %	1.91 27.6 %	1.98 31.87 %	2.03 35.4 %
0.714	Ni1 Li2 S2 O8	MSG 14.75 ($P2_1/c$)	Ni Error(%)	2.29	1.63 29.04 %	1.66 27.34 %	1.7 25.76 %	1.73 24.37 %	1.76 23.1 %
			Ni Error(%)	2.29	1.63 29.04 %	1.66 27.34 %	1.7 25.76 %	1.73 24.37 %	1.76 23.06 %

0.722	Mn4 Nb2 O9	MSG 9.37 (<i>Cc</i>)	Mn Error(%)	2.68	4.12 111.22 %	4.25 119.16 %	4.34 125.01 %	4.41 129.31 %	4.48 133.9 %
			Mn Error(%)	2.68	4.11 15.76 %	4.24 16.9 %	4.34 17.84 %	4.41 18.46 %	4.47 19.12 %
0.724	Ba1 Co1 Si1 O4	MSG 173.129 (<i>P6₃</i>)	Co Error(%)	2.71	2.5 7.79 %	- - %	- - %	- - %	2.71 0.15 %
			Co Error(%)	2.71	2.5 15.74 %	- - %	- - %	- - %	2.71 1.47 %
			Co Error(%)	2.71	2.5 15.19 %	- - %	- - %	- - %	2.71 1.47 %
			Co Error(%)	2.71	2.5 7.79 %	- - %	- - %	- - %	2.71 0.15 %
			Co Error(%)	2.71	2.5 7.84 %	- - %	- - %	- - %	2.71 0.73 %
0.726	Mn2 Cs1 F6	MSG 62.447 (<i>Pnm'm'a'</i>)	Mn Error(%)	3.25	3.64 266.66 %	- - %	- - %	3.76 281.34 %	3.79 134.74 %
			Mn Error(%)	3.25	3.64 88.89 %	- - %	- - %	3.76 93.78 %	3.79 44.91 %
			Mn Error(%)	0.6	4.47 1227.34 %	- - %	- - %	4.62 1307.5 %	4.65 1334.5 %
			Mn Error(%)	0.6	4.47 409.11 %	- - %	- - %	4.62 435.83 %	4.65 444.83 %
0.732	Sr1 Ru1 O3	MSG 62.446 (<i>Pn'm'a'</i>)	Ru Error(%)	1.63	1.24 5.98 %	1.4 3.63 %	1.42 3.28 %	1.44 2.99 %	1.47 2.42 %
0.733	Ru1 Ag1 O3	MSG 167.106 (<i>R3'c'</i>)	Ru Error(%)	1.85	1.18 36.0 %	1.57 15.19 %	1.76 4.97 %	1.89 2.32 %	2.01 8.81 %
			Ru Error(%)	1.85	1.18 12.02 %	1.57 5.08 %	1.76 1.68 %	1.89 0.77 %	2.01 2.94 %
0.735	La1 Ba1 Mn2 O5	MSG 129.417 (<i>P4/nm'm'</i>)	Mn Error(%)	2.7	3.09 7.17 %	3.24 10.04 %	3.37 12.35 %	3.47 14.31 %	3.57 16.07 %
			Mn Error(%)	3.2	4.04 13.06 %	4.18 15.25 %	4.28 16.92 %	4.37 18.25 %	4.44 19.38 %
			Mn Error(%)	2.88	3.14 4.58 %	3.24 6.32 %	3.34 8.02 %	3.45 9.92 %	3.56 11.79 %
0.737	La1 Ba1 Mn2 O6	MSG 123.345 (<i>P4/mm'm'</i>)	Mn Error(%)	1.29	3.15 72.3 %	3.25 76.18 %	3.35 80.07 %	3.46 84.34 %	3.57 88.58 %
0.739	Y1 Ba1 Mn2 O5	MSG 129.417 (<i>P4/nm'm'</i>)	Mn Error(%)	2.9	3.12 3.72 %	3.26 6.29 %	3.38 8.34 %	3.48 10.09 %	3.58 11.64 %
			Mn Error(%)	3.9	4.04 1.81 %	4.18 3.59 %	4.28 4.94 %	4.37 6.03 %	4.44 6.92 %
			Co Error(%)	2.45	2.66 3408.57 %	2.77 25511.02 %	2.84 37311.71 %	2.9 48961.06 %	2.81 90262.49 %
0.747	Ba3 Co1 Ir2 O9	MSG 15.85 (<i>C2/c</i>)	Co Error(%)	2.45	2.61 3356.53 %	2.72 25009.1 %	2.81 36760.41 %	2.87 48460.12 %	2.79 89712.98 %
			Ir Error(%)	0.57	0.57 0.53 %	0.69 18.6 %	0.74 23.86 %	0.76 25.09 %	1.0 40.88 %
			Ir Error(%)	0.57	0.57 0.23 %	0.69 6.32 %	0.74 8.36 %	0.77 8.95 %	1.01 14.15 %
			Ni Error(%)	1.7	1.65 2.94 %	1.68 1.47 %	1.7 0.06 %	1.72 1.12 %	1.74 2.47 %
			Ni Error(%)	1.7	1.65 3.0 %	1.68 1.47 %	1.7 0.12 %	1.72 1.12 %	1.74 2.47 %
0.748	Ba3 Ni1 Ru2 O9	MSG 194.268 (<i>P6'_3/m'm'c</i>)	Ru Error(%)	1.5	1.68 12.0 %	1.82 21.0 %	1.91 27.6 %	2.0 33.53 %	2.09 39.33 %
			Ru Error(%)	1.5	1.68 3.98 %	1.81 6.98 %	1.91 9.2 %	2.0 11.18 %	2.09 13.11 %
			Mn Error(%)	4.34	4.5 3.59 %	- - %	- - %	- - %	4.65 7.05 %
			Mn Error(%)	4.34	4.5 0.51 %	- - %	- - %	- - %	4.65 1.01 %
0.755	Mn2 Se1 F2 O3	MSG 62.448 (<i>Pn'ma'</i>)	V Error(%)	0.23	0.03 113.91 %	1.3 463.04 %	1.37 495.65 %	1.67 623.91 %	1.77 668.26 %
			V Error(%)	0.23	0.03 113.91 %	1.3 463.04 %	1.37 495.65 %	1.67 623.91 %	1.77 668.26 %
0.756	Ga1 V4 S8	MSG 160.67 (<i>R3m'</i>)							

			V Error(%)	0.22 117.67 %	0.14 128.92 %	0.3 866.25 %	1.31 1630.76 %	1.74 1214.71 %
			V Error(%)	0.22 71.44 %	0.15 93.17 %	0.3 770.16 %	1.31 1222.34 %	1.74 1107.79 %
			V Error(%)	0.22 120.12 %	0.14 129.44 %	0.3 865.03 %	1.31 1622.08 %	1.74 1212.02 %
0.760	Fe1 S1 O5 H1	MSG 15.89 ($C2'/c'$)	Fe Error(%)	4.09 3.55 %	3.95 0.83 %	4.06 1.08 %	4.13 2.69 %	4.2 4.16 %
0.760	Fe1 S1 O5 H1	MSG 15.89 ($C2'/c'$)	Fe Error(%)	4.09 3.55 %	3.95 0.83 %	4.06 1.08 %	4.13 2.69 %	4.2 4.16 %
0.761	Sr1 Fe2 Se2 O1	MSG 59.411 ($Pm'm'n'$)	Fe Error(%)	3.46 106.43 %	3.0 101.91 %	3.18 96.79 %	3.3 91.45 %	3.4 90.37 %
0.761	Sr1 Fe2 Se2 O1	MSG 59.411 ($Pm'm'n'$)	Fe Error(%)	3.46 102.4 %	3.01 98.88 %	3.18 94.79 %	3.3 89.95 %	3.4 89.34 %
0.761	Sr1 Fe2 Se2 O1	MSG 59.411 ($Pm'm'n'$)	Fe Error(%)	3.46 51.2 %	3.01 49.44 %	3.18 47.39 %	3.3 44.97 %	3.4 44.67 %
0.762	Sr1 Fe2 S2 O1	MSG 59.411 ($Pm'm'n'$)	Fe Error(%)	3.31 108.73 %	2.95 102.33 %	3.14 96.27 %	3.27 95.85 %	3.37 96.36 %
0.762	Sr1 Fe2 S2 O1	MSG 59.411 ($Pm'm'n'$)	Fe Error(%)	3.31 105.97 %	2.95 100.61 %	3.14 94.91 %	3.27 94.85 %	3.37 95.36 %
0.762	Sr1 Fe2 S2 O1	MSG 59.411 ($Pm'm'n'$)	Fe Error(%)	3.31 52.98 %	2.95 50.3 %	3.14 47.45 %	3.27 47.42 %	3.37 47.68 %
0.768	Sr1 Mn1 Sb2	MSG 33.148 ($Pn'a'2_1$)	Mn Error(%)	3.78 100.08 %	3.77 105.78 %	3.99 110.63 %	4.15 114.05 %	4.28 117.26 %
0.768	Sr1 Mn1 Sb2	MSG 33.148 ($Pn'a'2_1$)	Mn Error(%)	3.78 33.03 %	3.77 34.93 %	3.99 36.54 %	4.15 37.68 %	4.28 38.59 %
0.778	La1 Mn1 Si2	MSG 63.464 ($Cm'cm'$)	Mn Error(%)	2.07 0.24 %	2.08 14.4 %	2.67 35.75 %	3.55 41.33 %	3.78 12.75 %
0.779	La1 Mn1 Si2	MSG 63.464 ($Cm'cm'$)	Mn Error(%)	2.03 1.23 %	2.08 14.78 %	2.63 23.45 %	2.98 43.13 %	3.78 47.91 %
0.780	La1 Mn1 Si2	MSG 63.464 ($Cm'cm'$)	Mn Error(%)	1.77 8.76 %	2.08 29.6 %	2.82 24.15 %	2.63 56.81 %	3.78 62.29 %
0.787	Y1 V1 O3	MSG 62.446 ($Pn'm'a$)	V Error(%)	1.72 8.6 %	1.57 2.67 %	1.67 1.51 %	1.75 4.42 %	1.8 6.69 %
0.787	Y1 V1 O3	MSG 62.446 ($Pn'm'a$)	V Error(%)	1.72 2.93 %	1.57 0.85 %	1.68 0.5 %	1.75 1.47 %	1.8 2.23 %
0.788	Y1 V1 O3	MSG 2.4 ($P\bar{I}$)	V Error(%)	1.06 208.76 %	1.64 238.69 %	1.72 216.75 %	1.78 171.53 %	1.82 215.28 %
0.788	Y1 V1 O3	MSG 2.4 ($P\bar{I}$)	V Error(%)	1.06 95.08 %	1.64 91.97 %	1.72 72.03 %	1.78 53.22 %	1.82 73.68 %
0.795	Sr2 Y1 Ru1 O6	MSG 14.75 ($P2_1/c$)	Ru Error(%)	2.2 28.21 %	1.88 19.86 %	1.97 13.0 %	2.05 5.99 %	2.13 1.07 %
0.795	Sr2 Y1 Ru1 O6	MSG 14.75 ($P2_1/c$)	Ru Error(%)	2.2 28.16 %	1.88 19.86 %	1.97 13.0 %	2.05 5.99 %	2.13 1.07 %
0.796	Ca2 Ni1 Os1 O6	MSG 14.79 ($P2'_1/c'$)	Ni Error(%)	2.6 76.21 %	1.37 44.13 %	1.48 20.48 %	1.57 19.25 %	1.63 18.04 %
0.796	Ca2 Ni1 Os1 O6	MSG 14.79 ($P2'_1/c'$)	Os Error(%)	1.41 81.7 %	0.92 21.7 %	1.07 9.65 %	1.14 7.45 %	1.23 3.76 %
0.798	Mn1 Pd2	MSG 62.445 ($Pnma'$)	Mn Error(%)	4.0 5.87 %	3.76 0.42 %	3.98 3.55 %	4.14 6.6 %	4.26 9.02 %
0.798	Mn1 Pd2	MSG 62.445 ($Pnma'$)	Mn Error(%)	4.0 1.96 %	3.77 0.15 %	3.98 1.18 %	4.14 2.19 %	4.26 3.01 %
0.799	Sr2 Co2 O5	MSG 30.122 ($P_{I}nc2$)	Co Error(%)	3.12 29.65 %	2.2 17.56 %	2.57 11.38 %	2.77 8.04 %	2.87 5.38 %
0.799	Sr2 Co2 O5	MSG 30.122 ($P_{I}nc2$)	Co Error(%)	3.12 9.88 %	2.2 5.84 %	2.57 3.79 %	2.77 2.68 %	2.87 1.79 %
0.799	Sr2 Co2 O5	MSG 30.122 ($P_{I}nc2$)	Co Error(%)	2.88 8.54 %	2.39 5.42 %	2.57 2.95 %	2.71 1.23 %	2.81 0.26 %
0.799	Sr2 Co2 O5	MSG 30.122 ($P_{I}nc2$)	Co Error(%)	2.88 8.54 %	2.39 5.42 %	2.57 2.95 %	2.71 1.23 %	2.81 0.26 %
0.800	Mn1 Te1	MSG 63.457 ($Cmcm$)	Mn Error(%)	4.6 22.62 %	4.08 16.61 %	4.22 12.02 %	4.32 8.37 %	4.41 5.29 %
0.800	Mn1 Te1	MSG 63.457 ($Cmcm$)	Mn Error(%)	4.6 22.62 %	4.09 16.61 %	4.23 12.02 %	4.34 8.37 %	4.42 5.29 %

			Error(%)		22.14 %	16.03 %	11.51 %	7.88 %	4.83 %	
0.801	Ti3 Fe2 S4	MSG 62.445 ($Pnma'$)	Fe	1.52	-	3.09	3.26	3.39	3.49	
			Error(%)		- %	103.49 %	114.61 %	123.22 %	129.67 %	
	Cu1 Fe1 S2		Fe	1.52	-	3.09	3.27	3.4	3.5	
			Error(%)		- %	14.78 %	16.45 %	17.71 %	18.64 %	
0.802	Cul Fe1 S2	MSG 122.333 ($I\bar{4}2d$)	Fe	3.85	3.08	3.3	3.46	3.58	3.69	
			Error(%)		20.03 %	14.31 %	10.23 %	6.96 %	4.18 %	
	Mo1 P3 Si1 O11		Fe	3.85	3.08	3.3	3.46	3.58	3.69	
			Error(%)		20.0 %	14.29 %	10.21 %	6.94 %	4.18 %	
0.803	Mn1 Nb1 P1	MSG 31.125 ($Pm'n2'_1$)	Mn	1.21	1.54	2.08	2.61	3.06	3.37	
			Error(%)		174.9 %	236.71 %	296.74 %	298.89 %	355.14 %	
			Mn	1.21	1.54	2.08	2.61	3.06	3.37	
	Mo1 P3 Si1 O11		Error(%)		174.9 %	236.71 %	296.74 %	298.89 %	355.14 %	
			Mn	1.21	1.54	2.08	2.61	3.07	3.37	
			Error(%)		87.27 %	118.36 %	148.25 %	149.92 %	177.62 %	
0.804	Mo1 P3 Si1 O11	MSG 15.88 ($C2/c'$)	Mo	2.63	2.36	2.49	2.6	2.67	2.74	
			Error(%)		10.4 %	5.32 %	1.33 %	1.52 %	3.87 %	
			Mo	2.63	2.36	2.49	2.6	2.67	2.74	
			Error(%)		3.45 %	1.77 %	0.44 %	0.51 %	1.29 %	
0.809	Fe2 O6 W1	MSG 14.78 ($P2_1/c'$)	Fe	4.07	0.01	3.92	4.02	4.11	4.18	
			Error(%)		299.3 %	31.11 %	33.87 %	21.31 %	28.09 %	
			Fe	4.07	0.01	3.92	4.02	4.11	4.18	
			Error(%)		299.49 %	31.11 %	33.84 %	21.18 %	27.96 %	
			Fe	4.07	0.01	3.92	4.02	4.11	4.18	
			Error(%)		149.52 %	15.6 %	16.9 %	10.65 %	14.05 %	
0.810	Fe2 W1 O6	MSG 60.423 ($Pbc'n'$)	Fe	3.73	0.0	3.81	3.95	4.05	4.13	
			Error(%)		300.89 %	36.17 %	47.95 %	43.86 %	53.86 %	
			Fe	3.73	0.0	3.81	3.95	4.05	4.13	
			Error(%)		300.85 %	36.2 %	47.95 %	43.86 %	53.86 %	
0.811	Fe2 W1 O6	MSG 60.423 ($Pbc'n'$)	Fe	3.73	0.0	3.81	3.95	4.05	4.13	
			Error(%)		149.67 %	18.12 %	24.0 %	21.93 %	27.05 %	
			Fe	2.81	3.88	4.0	4.08	4.15	4.22	
			Error(%)		72.68 %	62.81 %	74.44 %	82.14 %	88.25 %	
0.812	Fe2 W1 O6	MSG 30.113 ($Pn'c2'$)	Fe	2.81	3.85	3.98	4.07	4.15	4.21	
			Error(%)		23.42 %	20.4 %	24.5 %	27.21 %	29.37 %	
			Fe	1.96	3.58	3.83	3.97	4.08	4.16	
			Error(%)		82.24 %	94.9 %	102.35 %	107.55 %	111.79 %	
0.813	Fe2 W1 O6	MSG 60.423 ($Pbc'n'$)	Fe	1.96	3.64	3.85	3.99	4.09	4.17	
			Error(%)		28.33 %	32.06 %	34.37 %	36.04 %	37.41 %	
			Fe	2.55	3.88	4.0	4.08	4.15	4.22	
			Error(%)		52.24 %	56.78 %	60.04 %	62.82 %	65.33 %	
0.814	Fe2 W1 O6	MSG 60.419 ($Pb'cn$)	Fe	2.55	3.85	3.98	4.07	4.15	4.21	
			Error(%)		17.02 %	18.65 %	19.87 %	20.86 %	21.75 %	
			Fe	2.15	3.58	3.83	3.97	4.08	4.16	
			Error(%)		66.6 %	78.0 %	84.74 %	89.53 %	93.35 %	
0.814	Fe2 W1 O6	MSG 60.419 ($Pb'cn$)	Fe	2.15	3.64	3.85	3.99	4.09	4.17	
			Error(%)		23.05 %	26.4 %	28.5 %	30.02 %	31.27 %	
			Fe	3.4	3.87	3.98	4.07	4.15	4.21	
			Error(%)		25.09 %	33.95 %	45.37 %	47.74 %	50.0 %	
0.812	Fe2 W1 O6	MSG 30.113 ($Pn'c2'$)	Fe	3.4	3.87	3.98	4.07	4.15	4.21	
			Error(%)		24.64 %	34.0 %	45.38 %	47.78 %	50.04 %	
			Fe	3.4	3.87	3.98	4.07	4.15	4.21	
			Error(%)		3.89 %	5.74 %	7.38 %	7.79 %	8.19 %	
0.813	Fe2 W1 O6	MSG 60.423 ($Pbc'n'$)	Fe	3.6	-	3.99	4.07	4.14	4.21	
			Error(%)		- %	10.83 %	13.14 %	15.11 %	16.89 %	
			Fe	3.6	-	3.97	4.06	4.14	4.21	
			Error(%)		- %	3.41 %	4.26 %	4.97 %	5.6 %	
0.813	Fe2 W1 O6	MSG 60.423 ($Pbc'n'$)	Fe	4.5	-	3.81	3.96	4.06	4.14	
			Error(%)		- %	15.24 %	12.07 %	9.76 %	7.89 %	
			Fe	4.5	-	3.84	3.97	4.07	4.15	
			Error(%)		- %	4.91 %	3.91 %	3.17 %	2.56 %	
			Fe	3.6	3.82	3.96	4.05	4.13	4.2	
			Error(%)		6.22 %	9.94 %	12.56 %	14.72 %	16.64 %	

			Fe Error(%)	3.6 2.11 %	3.83 3.31 %	3.96 4.19 %	4.05 4.91 %	4.13 5.55 %	4.2 5.55 %
			Fe Error(%)	4.5 19.96 %	3.6 14.98 %	3.83 11.91 %	3.96 9.64 %	4.07 7.82 %	4.15 7.82 %
			Fe Error(%)	4.5 6.64 %	3.6 5.0 %	3.83 3.98 %	3.96 3.22 %	4.07 2.61 %	4.15 2.61 %
0.815	Mn1 Nb2 O6	MSG 60.419 ($Pb'cn$)	Mn Error(%)	4.0 5.14 %	4.41 5.85 %	4.47 6.47 %	4.52 7.0 %	4.56 7.47 %	4.6 7.47 %
0.816	Mn1 Ta2 O6	MSG 60.419 ($Pb'cn$)	Mn Error(%)	4.0 5.14 %	4.41 5.86 %	4.47 6.47 %	4.52 7.01 %	4.56 7.49 %	4.6 7.49 %
0.818	Mn1 Ta2 O6	MSG 60.419 ($Pb'cn$)	Mn Error(%)	4.24 7.55 %	4.41 10.4 %	4.47 12.8 %	4.52 14.88 %	4.56 16.72 %	4.6 16.72 %
0.819	Mn1 Nb2 O6	MSG 60.419 ($Pb'cn$)	Mn Error(%)	4.24 7.62 %	4.41 10.43 %	4.47 12.84 %	4.52 14.92 %	4.56 16.72 %	4.6 16.72 %
0.823	Mn1 Sr2 Ga1 O5	MSG 46.243 ($Im'a2'$)	Mn Error(%)	3.16 7.69 %	3.4 11.11 %	3.51 13.92 %	3.6 16.39 %	3.68 18.7 %	3.75 18.7 %
0.825	Ca2 Mn1 Ga1 O5	MSG 62.447 ($Pnm'a'$)	Mn Error(%)	3.16 7.72 %	3.4 11.11 %	3.51 13.92 %	3.6 16.42 %	3.68 18.7 %	3.75 18.7 %
0.834	Cr1 Sb1 Se3	MSG 62.447 ($Pnm'a'$)	Cr Error(%)	3.06 0.96 %	2.94 0.2 %	3.04 0.52 %	3.12 1.23 %	3.21 1.9 %	3.29 1.9 %
0.855	Mn2 Sb1	MSG 129.417 ($P4/nm'm'$)	Mn Error(%)	2.1 15.43 %	2.75 27.17 %	3.24 33.74 %	3.52 38.33 %	3.71 42.12 %	3.87 42.12 %
0.859	Y1 Co3	MSG 166.101 ($R\bar{3}m'$)	Mn Error(%)	3.9 2.38 %	3.71 1.1 %	3.99 4.17	4.17 4.31	4.31 5.23 %	4.42 6.69 %
0.860	Sn2 Co3 S2	MSG 166.101 ($R\bar{3}m'$)	Co Error(%)	0.88 227.84 %	1.13 111.7 %	0.1 62.05 %	1.43 63.07 %	1.44 83.86 %	1.62 83.86 %
0.861	Sn2 Co3 S2	MSG 166.101 ($R\bar{3}m'$)	Co Error(%)	0.11 365.91 %	0.7 33.18 %	0.04 830.45 %	1.72 880.45 %	1.83 878.64 %	1.82 878.64 %
0.881	Mn1 Cu1 As1	MSG 59.407 ($Pm'mn$)	Co Error(%)	0.79 36.69 %	0.95 16.29 %	0.02 16.98 %	1.6 18.42 %	1.66 20.97 %	1.78 20.97 %
0.891	Cu1 Cr2 O4	MSG 15.89 ($C2'/c'$)	Co Error(%)	0.39 17.26 %	0.19 11.88 %	0.25 7.86 %	0.3 1.11 %	0.41 67.26 %	1.2 67.26 %
0.892	Ni1 Cr2 O4	MSG 70.530 ($Fd'd'd$)	Co Error(%)	0.22 4.7 %	0.19 4.85 %	0.25 11.97 %	0.3 28.18 %	0.41 110.0 %	1.21 110.0 %
			Mn Error(%)	3.73 1.98 %	3.66 5.01 %	3.92 10.13 %	4.11 14.02 %	4.25 16.97 %	4.36 16.97 %
			Mn Error(%)	3.73 1.98 %	3.66 5.01 %	3.92 10.13 %	4.11 14.02 %	4.25 16.97 %	4.36 16.97 %
			Cu Error(%)	0.85 41.65 %	0.14 25.76 %	0.41 18.53 %	0.54 13.47 %	0.62 9.88 %	0.68 9.88 %
			Cr Error(%)	2.62 97.35 %	2.48 38.39 %	2.65 9.14 %	2.76 15.97 %	2.84 20.52 %	2.89 20.52 %
			Cr Error(%)	2.62 32.49 %	2.48 12.8 %	2.65 3.03 %	2.76 5.34 %	2.84 6.84 %	2.89 6.84 %
			Ni Error(%)	1.69 53.55 %	0.12 63.08 %	0.44 55.98 %	0.2 100.59 %	1.71 100.59 %	1.67 100.59 %
			Cr Error(%)	0.84 0.15	0.15 2.74	0.15 3.03 %	2.84 5.34 %	2.95 6.84 %	2.93 6.84 %

			Error(%)		26.22 %	53.07 %	59.52 %	62.74 %	62.17 %
0.893	Ni1 Cr2 O4	MSG 70.530 ($Fd'd'd$)	Ni	1.83	1.31	0.43	0.25	0.2	1.67
			Error(%)		14.32 %	61.78 %	56.72 %	55.49 %	4.26 %
			Cr	0.89	2.7	2.75	2.83	2.9	2.93
			Error(%)		50.7 %	52.05 %	54.44 %	56.04 %	57.28 %
0.896	Ni1 Cr1 O4	MSG 63.457 ($Cmcm$)	Ni	0.64	1.38	1.47	1.54	1.6	1.65
			Error(%)		116.09 %	129.53 %	140.47 %	149.69 %	157.5 %
			Ni	0.64	1.38	1.47	1.54	1.6	1.65
			Error(%)		116.25 %	129.69 %	140.47 %	149.69 %	157.66 %
0.898	Mn3 Ir1 Si1	MSG 198.9 ($P_{21}3$)	Mn	2.99	2.99	3.42	3.7	3.91	4.08
			Error(%)		50.59 %	79.21 %	95.25 %	106.04 %	120.69 %
			Mn	2.99	3.02	3.44	3.73	3.93	4.1
			Error(%)		51.88 %	80.61 %	97.68 %	107.84 %	122.1 %
			Mn	2.99	3.01	3.43	3.72	3.93	4.09
			Error(%)		25.76 %	40.1 %	48.33 %	53.62 %	60.81 %
			Mn	2.99	3.04	3.46	3.74	3.95	4.11
			Error(%)		54.81 %	83.18 %	99.89 %	109.86 %	124.04 %
			Mn	2.99	3.03	3.46	3.74	3.95	4.11
			Error(%)		56.13 %	84.24 %	100.15 %	110.5 %	124.55 %
0.899	Mn3 Ir1 Ge1	MSG 198.9 ($P_{21}3$)	Mn	2.99	3.03	3.45	3.73	3.94	4.1
			Error(%)		27.59 %	41.69 %	49.55 %	54.71 %	61.8 %
			Mn	2.99	3.05	3.46	3.74	3.95	4.11
			Error(%)		55.36 %	83.6 %	100.17 %	110.42 %	124.61 %
			Mn	2.99	3.04	3.46	3.73	3.94	4.1
			Error(%)		55.99 %	84.11 %	99.74 %	109.75 %	124.05 %
			Mn	2.99	3.05	3.46	3.74	3.95	4.11
			Error(%)		27.51 %	41.44 %	49.83 %	55.0 %	62.1 %
			Mn	3.42	3.19	3.57	3.82	4.01	4.16
			Error(%)		24.57 %	20.74 %	36.11 %	50.6 %	63.36 %
0.900	Mn3 Co1 Ge1	MSG 198.9 ($P_{21}3$)	Mn	3.42	3.22	3.59	3.84	4.03	4.18
			Error(%)		23.57 %	21.76 %	38.15 %	52.12 %	64.46 %
			Mn	3.42	3.21	3.58	3.83	4.02	4.17
			Error(%)		12.17 %	10.81 %	18.79 %	25.89 %	32.11 %
			Mn	3.42	3.23	3.6	3.85	4.04	4.18
			Error(%)		25.0 %	23.16 %	39.18 %	53.15 %	65.51 %
			Mn	3.42	3.23	3.6	3.85	4.04	4.19
			Error(%)		25.43 %	24.22 %	39.47 %	53.67 %	66.02 %
			Mn	3.42	3.22	3.59	3.84	4.03	4.18
			Error(%)		12.06 %	11.67 %	19.24 %	26.4 %	32.61 %
0.916	Cd2 Os2 O7	MSG 227.131 ($Fd\bar{3}m'$)	Mn	3.42	3.24	3.61	3.85	4.04	4.19
			Error(%)		23.15 %	23.56 %	39.68 %	53.72 %	66.03 %
			Mn	3.42	3.23	3.6	3.85	4.03	4.18
			Error(%)		24.87 %	24.31 %	39.35 %	53.36 %	65.6 %
			Mn	3.42	3.24	3.6	3.85	4.04	4.19
			Error(%)		11.29 %	11.37 %	19.7 %	26.82 %	33.02 %
			Mn	2.38	2.89	3.35	3.65	3.88	4.05
			Error(%)		67.19 %	124.02 %	159.27 %	177.87 %	201.82 %
0.916	Cd2 Os2 O7	MSG 227.131 ($Fd\bar{3}m'$)	Mn	2.38	2.92	3.37	3.67	3.89	4.06
			Error(%)		70.72 %	127.1 %	161.79 %	179.34 %	202.84 %
			Mn	2.38	2.9	3.36	3.66	3.88	4.05
			Error(%)		34.74 %	63.07 %	80.38 %	89.28 %	101.15 %
			Mn	2.38	2.94	3.39	3.69	3.9	4.07
			Error(%)		73.84 %	129.99 %	164.13 %	181.62 %	205.08 %
			Mn	2.38	2.92	3.38	3.69	3.91	4.08
			Error(%)		72.07 %	129.4 %	164.48 %	182.44 %	206.13 %
0.916	Cd2 Os2 O7	MSG 227.131 ($Fd\bar{3}m'$)	Mn	2.38	2.92	3.38	3.68	3.9	4.06
			Error(%)		36.04 %	64.21 %	81.46 %	90.29 %	102.07 %
			Mn	2.38	2.92	3.38	3.68	3.9	4.06
			Error(%)		71.64 %	128.39 %	163.15 %	180.83 %	204.45 %
			Mn	2.38	2.92	3.37	3.67	3.89	4.06
			Error(%)		24.03 %	42.8 %	54.31 %	60.33 %	68.21 %
			Os	0.68	0.07	1.25	1.61	1.86	2.08
			Error(%)		267.44 %	256.92 %	415.9 %	527.18 %	623.85 %

			Os Error(%)	0.68 267.69 %	0.07 248.46 %	1.24 410.26 %	1.6 523.85 %	1.86 622.05 %
			Os Error(%)	0.68 133.21 %	0.08 132.69 %	1.27 210.77 %	1.62 265.13 %	1.87 312.56 %
0.917	Sr2 Os1 Sc1 O6	MSG 14.75 (P_{21}/c)	Os Error(%)	1.6 4.75 %	1.52 12.12 %	1.8 22.06 %	1.95 30.81 %	2.09 39.94 %
0.917	Sr2 Os1 Sc1 O6	MSG 14.75 (P_{21}/c)	Os Error(%)	1.6 4.69 %	1.53 12.19 %	1.8 22.12 %	1.95 30.87 %	2.09 40.0 %
0.918	Ag2 Ru1 O4	MSG 62.444 ($Pnm'a$)	Ru Error(%)	1.64 101.19 %	0.9 93.98 %	1.01 91.76 %	1.08 86.89 %	1.14 68.38 %
0.918	Ag2 Ru1 O4	MSG 62.444 ($Pnm'a$)	Ru Error(%)	1.64 33.73 %	0.9 31.33 %	1.01 30.59 %	1.08 28.96 %	1.14 22.79 %
0.924	Rb1 Ru1 O4	MSG 62.449 ($Pn'm'a'$)	Ru Error(%)	0.8 73.94 %	0.44 99.31 %	0.49 57.06 %	0.52 88.1 %	0.53 97.23 %
0.924	Rb1 Ru1 O4	MSG 62.449 ($Pn'm'a'$)	Ru Error(%)	0.8 66.97 %	0.45 93.42 %	0.5 51.77 %	0.53 84.76 %	0.54 94.5 %
0.924	Rb1 Ru1 O4	MSG 62.449 ($Pn'm'a'$)	Ru Error(%)	0.8 36.97 %	0.44 49.65 %	0.49 28.53 %	0.52 44.05 %	0.53 48.61 %
0.933	Ru1 Na2 O4	MSG 14.78 (P_{21}/c')	Ru Error(%)	1.65 74.12 %	1.05 64.44 %	1.13 56.88 %	1.19 49.5 %	1.25 42.08 %
0.933	Ru1 Na2 O4	MSG 14.78 (P_{21}/c')	Ru Error(%)	1.65 10.59 %	1.05 9.21 %	1.13 8.13 %	1.19 7.07 %	1.25 6.01 %
0.934	Sr2 O6 Ni1 Te1	MSG 14.75 (P_{21}/c)	Ni Error(%)	1.79 30.68 %	1.51 23.07 %	1.58 17.08 %	1.63 12.07 %	1.68 7.78 %
0.934	Sr2 O6 Ni1 Te1	MSG 14.75 (P_{21}/c)	Ni Error(%)	1.79 30.68 %	1.51 23.07 %	1.58 17.08 %	1.63 12.07 %	1.68 7.78 %
0.936	Sr2 O6 Mn1 Te1	MSG 14.75 (P_{21}/c)	Mn Error(%)	4.55 4.42 %	4.35 2.86 %	4.42 1.56 %	4.48 0.46 %	4.53 0.48 %
0.936	Sr2 O6 Mn1 Te1	MSG 14.75 (P_{21}/c)	Mn Error(%)	4.55 4.42 %	4.35 2.86 %	4.42 1.56 %	4.48 0.46 %	4.53 0.48 %
0.937	Sr2 O6 Co1 Te1	MSG 14.75 (P_{21}/c)	Co Error(%)	2.24 25.48 %	2.52 31.47 %	2.59 36.12 %	2.65 41.46 %	2.69 46.56 %
0.937	Sr2 O6 Co1 Te1	MSG 14.75 (P_{21}/c)	Co Error(%)	2.24 25.48 %	2.52 31.47 %	2.59 36.12 %	2.65 41.46 %	2.69 46.56 %
0.947	Cr1 Y1 O3	MSG 62.448 ($Pn'ma'$)	Cr Error(%)	2.45 6.86 %	2.62 10.16 %	2.7 12.69 %	2.76 14.82 %	2.81 16.61 %
0.947	Cr1 Y1 O3	MSG 62.448 ($Pn'ma'$)	Cr Error(%)	2.45 2.3 %	2.62 3.39 %	2.7 4.23 %	2.76 4.94 %	2.81 5.55 %
0.948	Ca1 Ni3 P4 O14	MSG 14.75 (P_{21}/c)	Ni Error(%)	1.98 58.79 %	1.64 50.97 %	1.67 44.18 %	1.7 38.12 %	1.74 33.69 %
0.948	Ca1 Ni3 P4 O14	MSG 14.75 (P_{21}/c)	Ni Error(%)	1.98 19.6 %	1.64 16.99 %	1.67 14.73 %	1.7 12.71 %	1.74 11.23 %
0.948	Ca1 Ni3 P4 O14	MSG 14.75 (P_{21}/c)	Ni Error(%)	1.96 56.96 %	1.62 50.2 %	1.66 44.14 %	1.69 38.35 %	1.72 34.05 %
0.948	Ca1 Ni3 P4 O14	MSG 14.75 (P_{21}/c)	Ni Error(%)	1.96 57.13 %	1.62 50.25 %	1.65 44.3 %	1.69 38.35 %	1.72 34.05 %
0.959	Cr2 Te1 O6	MSG 58.395 ($Pn'nm$)	Cr Error(%)	1.24 115.08 %	2.67 121.13 %	2.74 125.56 %	2.8 129.19 %	2.84 132.26 %
0.959	Cr2 Te1 O6	MSG 58.395 ($Pn'nm$)	Cr Error(%)	1.24 38.39 %	2.67 40.38 %	2.74 41.88 %	2.8 43.06 %	2.84 44.09 %
0.960	Fe2 Te1 O6	MSG 136.503 ($P4_2/m'n'm'$)	Fe Error(%)	2.36 29.58 %	3.76 33.81 %	3.96 35.97 %	4.06 37.65 %	4.14 39.07 %
0.960	Fe2 Te1 O6	MSG 136.503 ($P4_2/m'n'm'$)	Fe Error(%)	2.36 30.11 %	3.78 34.15 %	3.97 36.27 %	4.07 37.9 %	4.15 39.32 %
0.961	Li1 Cr1 Ge2 O6	MSG 14.77 ($P2'_1/c$)	Cr Error(%)	2.17 53.46 %	2.76 57.43 %	2.8 61.0 %	2.84 64.08 %	2.87 66.97 %
0.961	Li1 Cr1 Ge2 O6	MSG 14.77 ($P2'_1/c$)	Cr Error(%)	2.17 17.82 %	2.76 19.14 %	2.8 20.33 %	2.84 21.36 %	2.87 22.32 %
0.962	Li1 Cr1 Ge2 O6	MSG 14.77 ($P2'_1/c$)	Cr Error(%)	2.1 62.53 %	2.76 66.63 %	2.8 70.27 %	2.84 73.54 %	2.87 76.41 %
0.962	Li1 Cr1 Ge2 O6	MSG 14.77 ($P2'_1/c$)	Cr Error(%)	2.1 20.84 %	2.76 22.21 %	2.8 23.42 %	2.84 24.51 %	2.87 25.47 %
0.963	Li1 Cr1 Ge2 O6	MSG 14.77 ($P2'_1/c$)	Cr	2.34	2.75	2.8	2.84	2.87

			Error(%)		35.37 %	39.13 %	42.39 %	45.28 %	47.9 %
			Cr	2.34	2.75	2.8	2.84	2.87	2.9
			Error(%)		11.79 %	13.04 %	14.13 %	15.09 %	15.97 %
0.964	Li1 Cr1 Ge2 O6	MSG 14.77 ($P2_1'/c$)	Cr	2.08	2.75	2.8	2.84	2.87	2.9
			Error(%)		64.5 %	68.68 %	72.34 %	75.62 %	78.55 %
0.964	Li1 Cr1 Ge2 O6	MSG 14.77 ($P2_1'/c$)	Cr	2.08	2.75	2.8	2.84	2.87	2.9
			Error(%)		21.5 %	22.89 %	24.11 %	25.21 %	26.18 %
0.965	Lu1 Fe2 O4	MSG 1.3 (P_s1)	Fe	4.8	3.63	3.7	3.73	3.73	3.71
			Error(%)		24.34 %	22.93 %	22.24 %	22.3 %	22.76 %
0.965	Lu1 Fe2 O4	MSG 1.3 (P_s1)	Fe	4.8	3.63	3.7	3.73	3.73	3.71
			Error(%)		3.48 %	3.28 %	3.18 %	3.19 %	3.25 %
0.966	W1 V2 O6	MSG 58.395 ($Pn'nm$)	V	0.9	-	1.69	1.77	1.83	1.87
			Error(%)		- %	43.83 %	48.39 %	51.5 %	53.72 %
0.966	W1 V2 O6	MSG 58.395 ($Pn'nm$)	V	0.9	-	1.69	1.77	1.83	1.87
			Error(%)		- %	43.83 %	48.39 %	51.5 %	53.72 %
0.968	Fe2 Ca1 O4	MSG 62.448 ($Pn'ma'$)	Fe	4.26	3.75	3.95	4.05	4.12	4.18
			Error(%)		2.99 %	1.85 %	1.26 %	0.82 %	0.45 %
0.968	Fe2 Ca1 O4	MSG 62.448 ($Pn'ma'$)	Fe	4.26	3.7	3.94	4.05	4.13	4.19
			Error(%)		3.27 %	1.86 %	1.23 %	0.77 %	0.4 %
0.969	Fe2 Ca1 O4	MSG 62.445 ($Pnma'$)	Fe	4.26	3.66	4.0	4.11	4.17	4.23
			Error(%)		14.01 %	6.13 %	3.52 %	2.02 %	0.7 %
0.969	Fe2 Ca1 O4	MSG 62.445 ($Pnma'$)	Fe	4.26	3.66	4.0	4.11	4.18	4.23
			Error(%)		2.0 %	0.88 %	0.5 %	0.29 %	0.1 %
0.984	V1 Lu1 O3	MSG 62.446 ($Pn'm'a$)	V	1.2	1.6	1.68	1.75	1.8	1.84
			Error(%)		33.58 %	40.17 %	45.92 %	49.83 %	53.08 %
0.984	V1 Lu1 O3	MSG 62.446 ($Pn'm'a$)	V	1.2	1.59	1.68	1.75	1.8	1.84
			Error(%)		10.83 %	13.44 %	15.28 %	16.61 %	17.67 %
1.277	Li1 Fe1 Cr4 O8	MSG 119.319 ($I\bar{4}m'2'$)	Fe	2.54	3.66	3.76	3.85	3.94	4.02
			Error(%)		44.09 %	48.03 %	51.65 %	55.04 %	58.31 %
1.277	Li1 Fe1 Cr4 O8	MSG 119.319 ($I\bar{4}m'2'$)	Cr	0.28	2.74	2.76	2.77	2.78	2.79
			Error(%)		219.64 %	220.98 %	222.14 %	223.04 %	223.93 %
1.278	Cu1 C2 N2 S2	MSG 2.7 ($P_s\bar{1}$)	Cu	0.3	0.37	0.41	0.44	0.46	0.48
			Error(%)		73.81 %	108.05 %	136.14 %	159.49 %	182.86 %
1.278	Cu1 C2 N2 S2	MSG 2.7 ($P_s\bar{1}$)	Cu	0.3	0.37	0.41	0.44	0.46	0.48
			Error(%)		73.81 %	108.05 %	135.48 %	160.15 %	182.86 %
1.281	Y1 Ba1 Fe1 Cu1 O5	MSG 42.223 ($F_{Smm}2$)	Fe	2.51	3.64	3.77	3.87	3.96	4.03
			Error(%)		44.94 %	50.08 %	54.26 %	57.61 %	60.56 %
1.281	Y1 Ba1 Fe1 Cu1 O5	MSG 42.223 ($F_{Smm}2$)	Fe	2.51	3.64	3.77	3.87	3.96	4.03
			Error(%)		44.94 %	50.08 %	54.26 %	57.61 %	60.56 %
1.286	Fe1 C3 O8 H4	MSG 2.7 ($P_s\bar{1}$)	Fe	4.15	1.3	3.15	3.32	3.45	3.97
			Error(%)		104.34 %	31.07 %	25.77 %	22.59 %	6.53 %
1.286	Fe1 C3 O8 H4	MSG 2.7 ($P_s\bar{1}$)	Fe	4.15	1.3	3.15	3.32	3.45	3.97
			Error(%)		104.02 %	31.16 %	25.72 %	22.53 %	6.53 %
1.287	V2 O3	MSG 14.84 (P_C2_1/c)	V	1.15	1.55	1.74	1.85	1.91	1.96
			Error(%)		69.32 %	102.93 %	120.81 %	132.02 %	140.08 %
1.287	V2 O3	MSG 14.84 (P_C2_1/c)	V	1.15	1.54	1.72	1.84	1.91	1.95
			Error(%)		9.68 %	14.3 %	17.09 %	18.76 %	19.97 %
1.304	Mg1 Mn1 O3	MSG 2.7 ($P_s\bar{1}$)	Mn	1.99	2.7	2.79	2.88	2.97	3.06
			Error(%)		53.79 %	60.65 %	67.29 %	74.11 %	81.12 %
1.304	Mg1 Mn1 O3	MSG 2.7 ($P_s\bar{1}$)	Mn	1.99	2.7	2.79	2.88	2.97	3.06
			Error(%)		53.79 %	60.62 %	67.35 %	74.02 %	81.09 %
1.305	Mn5 Si3	MSG 60.431 (P_Cbcn)	Mn	1.48	2.67	3.19	3.53	3.77	3.97
			Error(%)		80.61 %	115.81 %	138.65 %	155.0 %	167.97 %
1.305	Mn5 Si3	MSG 60.431 (P_Cbcn)	Mn	1.48	2.67	3.19	3.53	3.78	3.97
			Error(%)		11.51 %	16.53 %	19.8 %	22.15 %	24.01 %
1.308	Mn1 Bi2 Te4	MSG 167.108 ($R_I\bar{3}c$)	Mn	4.04	4.2	4.31	4.39	4.47	4.53
			Error(%)		4.06 %	6.61 %	8.74 %	10.57 %	12.1 %
1.308	Mn1 Bi2 Te4	MSG 167.108 ($R_I\bar{3}c$)	Mn	4.04	4.2	4.31	4.39	4.47	4.53
			Error(%)		4.06 %	6.61 %	8.74 %	10.57 %	12.1 %
1.311	Ba1 Mo1 P2 O8	MSG 2.7 ($P_s\bar{1}$)	Mo	1.31	1.67	1.72	1.76	1.81	1.85
			Error(%)		70.03 %	64.64 %	73.33 %	74.79 %	83.44 %
1.311	Ba1 Mo1 P2 O8	MSG 2.7 ($P_s\bar{1}$)	Mo	1.31	1.67	1.72	1.76	1.81	1.85
			Error(%)		70.03 %	64.64 %	73.33 %	74.69 %	83.44 %

1.314	Na1 Fe1 Si2 O6	MSG 14.84 ($P_{C21/c}$)	Fe	2.36	4.03	4.1	4.17	4.24	4.31
			Error(%)		141.18 %	147.17 %	153.02 %	158.88 %	164.78 %
1.319	Sr2 Ru1 O4	MSG 63.466 (C_{cmcm})	Fe	2.36	4.03	4.1	4.17	4.24	4.31
			Error(%)		47.06 %	49.07 %	51.01 %	52.96 %	54.93 %
1.321	Ba2 Fe1 W1 O6	MSG 2.7 ($P_{S\bar{I}}$)	Ru	0.4	0.71	1.08	1.32	1.47	1.57
			Error(%)		77.5 %	170.25 %	229.75 %	268.0 %	291.75 %
1.323	Co1 Ge1 O3	MSG 14.84 ($P_{C21/c}$)	Fe	3.43	3.63	3.71	3.76	3.69	3.71
			Error(%)		17.91 %	25.07 %	31.74 %	20.4 %	24.1 %
1.323	Co1 Ge1 O3	MSG 14.84 ($P_{C21/c}$)	Fe	3.43	3.63	3.71	3.76	3.69	3.71
			Error(%)		17.91 %	25.18 %	34.1 %	21.41 %	24.08 %
1.345	Na1 Mn1 F4	MSG 14.80 ($P_{a21/c}$)	Co	2.88	2.59	2.62	2.66	2.7	2.74
			Error(%)		86.96 %	22.6 %	13.87 %	11.24 %	8.37 %
1.345	Na1 Mn1 F4	MSG 14.80 ($P_{a21/c}$)	Co	2.88	2.59	2.62	2.66	2.7	2.74
			Error(%)		29.05 %	7.52 %	4.64 %	3.75 %	2.79 %
1.347	Cu1 Fe1 O2	MSG 15.91 ($C_{a2/c}$)	Co	4.32	2.56	2.62	2.67	2.71	2.75
			Error(%)		150.64 %	94.01 %	83.22 %	78.22 %	77.65 %
1.347	Cu1 Fe1 O2	MSG 15.91 ($C_{a2/c}$)	Co	4.32	2.55	2.62	2.67	2.71	2.75
			Error(%)		50.26 %	31.38 %	27.74 %	26.07 %	25.88 %
1.351	Ba2 Co2 Cl1 F7	MSG 11.55 ($P_{a21/m}$)	Mn	3.53	3.58	3.64	3.7	3.75	3.8
			Error(%)		6.76 %	12.91 %	18.7 %	23.06 %	27.35 %
1.351	Ba2 Co2 Cl1 F7	MSG 11.55 ($P_{a21/m}$)	Mn	3.53	3.58	3.65	3.7	3.76	3.81
			Error(%)		6.96 %	12.86 %	18.62 %	23.24 %	27.49 %
1.370	Li2 Cu1 O2	MSG 58.404 (P_{Innm})	Mn	3.53	3.58	3.64	3.7	3.75	3.8
			Error(%)		3.66 %	6.33 %	9.35 %	11.53 %	13.69 %
1.383	Fe1 Ca2 O3 Br1	MSG 113.273 ($P_{C\bar{4}21m}$)	Fe	4.0	0.02	0.02	0.02	0.02	0.02
			Error(%)		100.57 %	100.55 %	100.5 %	100.48 %	100.48 %
1.383	Fe1 Ca2 O3 Br1	MSG 113.273 ($P_{C\bar{4}21m}$)	Fe	4.0	0.02	0.02	0.02	0.02	0.02
			Error(%)		33.52 %	33.52 %	33.5 %	33.49 %	33.49 %
1.395	Y1 Mn2 Si2	MSG 126.386 ($P_{I4/nnc}$)	Co	3.79	2.58	2.63	2.68	2.73	2.76
			Error(%)		16.03 %	15.28 %	14.58 %	14.04 %	13.54 %
1.395	Y1 Mn2 Si2	MSG 126.386 ($P_{I4/nnc}$)	Co	3.79	2.57	2.64	2.68	2.73	2.76
			Error(%)		5.35 %	5.07 %	4.86 %	4.67 %	4.51 %
1.396	Y1 Mn2 Ge2	MSG 126.386 ($P_{I4/nnc}$)	Cu	0.96	0.54	0.55	0.57	0.59	0.6
			Error(%)		44.27 %	42.5 %	40.73 %	38.96 %	37.19 %
1.396	Y1 Mn2 Ge2	MSG 126.386 ($P_{I4/nnc}$)	Cu	0.96	0.54	0.55	0.57	0.59	0.6
			Error(%)		44.27 %	42.5 %	40.73 %	38.96 %	37.19 %
1.498	Cu1 Si1 O4 H2	MSG 148.20 ($R_I\bar{3}$)	Fe	3.49	3.56	3.74	3.88	4.0	4.1
			Error(%)		4.18 %	14.81 %	22.68 %	29.25 %	35.21 %
1.498	Cu1 Si1 O4 H2	MSG 148.20 ($R_I\bar{3}$)	Fe	3.49	3.56	3.74	3.88	4.0	4.1
			Error(%)		1.39 %	4.92 %	7.57 %	9.76 %	11.74 %
1.495	Y1 Mn2 Si2	MSG 126.386 ($P_{I4/nnc}$)	Mn	2.4	1.9	2.17	2.43	3.39	3.65
			Error(%)		10.33 %	4.73 %	0.63 %	20.65 %	26.04 %
1.495	Y1 Mn2 Si2	MSG 126.386 ($P_{I4/nnc}$)	Mn	2.4	1.9	2.17	2.43	3.39	3.65
			Error(%)		10.33 %	4.73 %	0.63 %	20.65 %	26.04 %
1.496	Y1 Mn2 Ge2	MSG 126.386 ($P_{I4/nnc}$)	Mn	2.95	2.34	2.68	3.64	3.91	4.05
			Error(%)		10.36 %	4.58 %	11.75 %	16.19 %	18.63 %
1.496	Y1 Mn2 Ge2	MSG 126.386 ($P_{I4/nnc}$)	Mn	2.95	2.34	2.68	3.64	3.91	4.05
			Error(%)		10.36 %	4.58 %	11.75 %	16.19 %	18.63 %
1.498	Cu1 Si1 O4 H2	MSG 148.20 ($R_I\bar{3}$)	Cu	0.65	-	0.65	0.68	0.71	0.73
			Error(%)		- %	161.05 %	69.84 %	17.79 %	17.15 %
1.498	Cu1 Si1 O4 H2	MSG 148.20 ($R_I\bar{3}$)	Cu	0.65	-	0.65	0.68	0.71	0.73
			Error(%)		- %	160.16 %	75.77 %	22.17 %	21.69 %
1.498	Cu1 Si1 O4 H2	MSG 148.20 ($R_I\bar{3}$)	Cu	0.65	-	0.65	0.68	0.71	0.73
			Error(%)		- %	160.16 %	75.77 %	25.87 %	21.69 %
1.498	Cu1 Si1 O4 H2	MSG 148.20 ($R_I\bar{3}$)	Cu	0.65	-	0.65	0.68	0.71	0.73
			Error(%)		- %	40.27 %	17.94 %	5.14 %	4.33 %

			Fe	4.01	- %	4.07	4.14	4.2	4.26
			Error(%)		- %	2.95 %	6.43 %	9.59 %	12.53 %
			Fe	4.01	- %	4.07	4.14	4.2	4.26
			Error(%)		- %	2.74 %	6.32 %	9.58 %	12.54 %
			Fe	4.01	- %	4.07	4.14	4.2	4.26
			Error(%)		- %	1.4 %	3.19 %	4.79 %	6.26 %
			Fe	4.01	- %	4.07	4.14	4.2	4.26
			Error(%)		- %	2.92 %	6.41 %	9.62 %	12.53 %
			Fe	4.01	- %	4.07	4.14	4.2	4.26
			Error(%)		- %	2.74 %	6.37 %	9.55 %	12.59 %
			Fe	4.01	- %	4.07	4.14	4.2	4.26
			Error(%)		- %	1.4 %	3.19 %	4.79 %	6.28 %
1.499	Cs1 Fe1 Mo2 O8	MSG 143.3 (P_c3)	Co	3.81	- %	0.05	0.31	0.46	0.58
			Error(%)		- %	304.01 %	324.71 %	336.23 %	345.64 %
1.500	Co1 Cu2 S2 Sr2 O2	MSG 2.7 ($P_{S\bar{1}}$)	Co	3.81	- %	0.05	0.31	0.46	0.58
			Error(%)		- %	304.01 %	324.71 %	336.27 %	345.64 %
1.508	Al1 B2 Mn2	MSG 63.466 ($C_c mcm$)	Mn	0.71	0.8	1.28	-	-	3.23
			Error(%)		12.54 %	79.58 %	- %	- %	354.65 %
			Mn	0.71	0.8	1.28	-	-	3.23
			Error(%)		4.18 %	26.53 %	- %	- %	118.22 %
1.519	Co1 S1 O4	MSG 60.431 ($P_C bcn$)	Co	3.3	2.57	2.63	2.68	2.72	2.76
			Error(%)		114.3 %	48.59 %	82.26 %	44.0 %	35.82 %
			Co	3.3	2.57	2.63	2.68	2.72	2.76
			Error(%)		114.33 %	48.59 %	82.26 %	44.0 %	35.82 %
			Co	3.3	2.57	2.63	2.68	2.72	2.76
			Error(%)		57.17 %	24.3 %	41.13 %	22.0 %	17.91 %
1.520	Ni1 S1 O4	MSG 60.431 ($P_C bcn$)	Ni	2.1	- %	1.61	1.65	1.69	1.72
			Error(%)		- %	23.48 %	21.43 %	19.62 %	18.0 %
			Ni	2.1	- %	1.61	1.65	1.69	1.72
			Error(%)		- %	7.84 %	7.14 %	6.54 %	6.0 %
1.521	Fe1 S1 O4	MSG 60.431 ($P_C bcn$)	Fe	4.1	- %	3.64	3.68	3.71	3.74
			Error(%)		- %	11.17 %	10.32 %	9.56 %	8.9 %
			Fe	4.1	- %	3.64	3.68	3.71	3.74
			Error(%)		- %	3.72 %	3.44 %	3.19 %	2.96 %
1.522	Cr1 V1 O4	MSG 2.4 ($P\bar{1}$)	Cr	2.11	2.73	2.8	2.85	2.89	2.92
			Error(%)		88.19 %	97.52 %	104.64 %	111.1 %	116.27 %
			Cr	2.11	2.73	2.8	2.85	2.89	2.92
			Error(%)		87.5 %	96.42 %	104.58 %	109.56 %	114.72 %
1.523	V1 P1 O4	MSG 62.452 ($P_c nma$)	V	0.8	- %	1.84	1.87	1.89	1.91
			Error(%)		- %	130.12 %	133.5 %	136.25 %	138.62 %
			V	0.8	- %	1.84	1.87	1.89	1.91
			Error(%)		- %	18.59 %	19.07 %	19.46 %	19.8 %
1.524	In1 Mn1 O3	MSG 159.64 (P_c31c)	Mn	3.25	3.4	3.51	3.6	3.68	3.76
			Error(%)		4.62 %	8.03 %	10.86 %	13.32 %	15.6 %
			Mn	3.25	3.4	3.51	3.6	3.68	3.76
			Error(%)		9.43 %	16.16 %	21.76 %	26.77 %	31.23 %
			Mn	3.25	3.4	3.51	3.6	3.68	3.76
			Error(%)		9.19 %	16.08 %	21.69 %	26.64 %	31.13 %
			Mn	3.25	3.4	3.51	3.6	3.68	3.76
			Error(%)		9.3 %	16.13 %	21.7 %	26.71 %	31.16 %
			Mn	3.25	3.4	3.51	3.6	3.68	3.76
			Error(%)		0.58 %	1.0 %	1.36 %	1.67 %	1.95 %
1.528	Fe4 Bi2 O9	MSG 12.64 (C_a2/m)	Fe	3.52	3.45	3.66	3.8	3.91	4.01
			Error(%)		6.0 %	5.02 %	12.15 %	18.25 %	24.61 %
			Fe	3.52	3.45	3.66	3.8	3.91	4.01
			Error(%)		2.0 %	1.67 %	4.05 %	6.08 %	8.2 %
			Fe	3.52	3.45	3.66	3.8	3.91	4.01
			Error(%)		4.24 %	13.38 %	18.24 %	23.88 %	27.75 %
			Fe	3.52	3.45	3.66	3.8	3.91	4.01
			Error(%)		1.41 %	4.46 %	6.08 %	7.96 %	9.25 %
			Fe	3.73	3.78	3.92	4.02	4.1	4.17
			Error(%)		3.01 %	11.13 %	16.12 %	19.6 %	22.78 %
			Fe	3.73	3.78	3.92	4.02	4.1	4.17

			Error(%)		0.97 %	3.67 %	5.37 %	6.53 %	7.59 %
			Fe	3.73	3.78	3.92	4.02	4.1	4.17
			Error(%)		3.71 %	10.93 %	16.1 %	19.78 %	22.95 %
			Fe	3.73	3.78	3.92	4.02	4.1	4.17
			Error(%)		1.27 %	3.64 %	5.4 %	6.59 %	7.65 %
1.538	Mn1 Ba2 Te1 O6	MSG 14.83 ($P_{A21/c}$)	Mn	4.5	4.37	4.44	4.49	4.54	4.58
			Error(%)		8.21 %	3.84 %	0.16 %	2.97 %	5.75 %
			Mn	4.5	4.37	4.44	4.49	4.54	4.58
			Error(%)		8.27 %	3.78 %	0.16 %	2.97 %	5.75 %
1.542	Mn1 Rb1 P1	MSG 138.528 (P_c4_2/ncm)	Mn	3.21	3.84	-	-	4.3	-
			Error(%)		9.78 %	- %	- %	17.04 %	- %
			Mn	3.21	3.84	-	-	4.3	-
			Error(%)		9.78 %	- %	- %	17.04 %	- %
1.544	Mn1 Rb1 As1	MSG 138.528 (P_c4_2/ncm)	Mn	3.29	3.98	4.15	4.28	-	-
			Error(%)		10.46 %	13.09 %	15.06 %	- %	- %
			Mn	3.29	3.98	4.15	4.28	-	-
			Error(%)		10.46 %	13.09 %	15.06 %	- %	- %
1.545	Mn1 Rb1 Bi1	MSG 138.528 (P_c4_2/ncm)	Mn	4.24	3.99	4.16	4.29	4.39	4.48
			Error(%)		2.96 %	0.98 %	0.57 %	1.8 %	2.81 %
			Mn	4.24	3.99	4.16	4.29	4.39	4.48
			Error(%)		2.96 %	0.98 %	0.57 %	1.8 %	2.81 %
1.546	Mn1 Cs1 Bi1	MSG 138.528 (P_c4_2/ncm)	Mn	4.33	4.04	4.2	4.33	4.43	4.51
			Error(%)		3.3 %	1.47 %	0.05 %	1.11 %	2.03 %
			Mn	4.33	4.04	4.2	4.33	4.43	4.51
			Error(%)		3.3 %	1.47 %	0.05 %	1.11 %	2.03 %
1.547	Mn1 Cs1 P1	MSG 138.528 (P_c4_2/ncm)	Mn	3.55	3.67	3.91	4.09	4.22	4.33
			Error(%)		1.75 %	5.13 %	7.56 %	9.44 %	10.93 %
			Mn	3.55	3.67	3.91	4.09	4.22	4.33
			Error(%)		1.75 %	5.13 %	7.56 %	9.44 %	10.93 %
1.548	Mn1 Cs1 P1	MSG 138.528 (P_c4_2/ncm)	Mn	2.86	-	4.01	-	4.29	-
			Error(%)		- %	20.16 %	- %	24.97 %	- %
			Mn	2.86	-	4.01	-	4.29	-
			Error(%)		- %	20.16 %	- %	24.97 %	- %
1.550	Mn1 Li1 As1	MSG 138.528 (P_c4_2/ncm)	Mn	3.75	3.8	4.01	-	4.29	4.38
			Error(%)		0.71 %	3.52 %	- %	7.17 %	8.44 %
			Mn	3.75	3.8	4.01	-	4.29	4.38
			Error(%)		0.71 %	3.52 %	- %	7.17 %	8.44 %
1.553	Mn1 K1 As1	MSG 138.528 (P_c4_2/ncm)	Mn	4.03	3.86	4.05	-	4.32	4.41
			Error(%)		2.13 %	0.3 %	- %	3.54 %	4.68 %
			Mn	4.03	3.86	4.05	-	4.32	4.41
			Error(%)		2.13 %	0.3 %	- %	3.54 %	4.68 %
1.554	Mn1 K1 As1	MSG 138.528 (P_c4_2/ncm)	Mn	2.93	-	4.07	4.21	-	4.41
			Error(%)		- %	19.37 %	21.83 %	- %	25.31 %
			Mn	2.93	-	4.07	4.21	-	4.41
			Error(%)		- %	19.37 %	21.83 %	- %	25.31 %
1.555	Mn3 B4	MSG 58.404 (P_{Innm})	Mn	2.92	-	0.01	2.62	1.12	3.56
			Error(%)		- %	100.31 %	10.41 %	61.71 %	21.95 %
			Mn	2.92	-	0.01	2.62	1.12	3.56
			Error(%)		- %	100.31 %	10.41 %	61.71 %	21.95 %
			Mn	0.44	-	0.02	1.19	0.14	1.81
			Error(%)		- %	52.61 %	85.45 %	65.57 %	156.02 %
			Mn	0.44	-	0.03	1.19	0.15	1.81
			Error(%)		- %	53.18 %	85.34 %	66.7 %	156.02 %
1.556	Fe1 Sn2	MSG 60.432 (P_{Ibcn})	Fe	1.15	1.88	2.21	2.48	2.69	2.82
			Error(%)		63.39 %	91.83 %	116.09 %	133.57 %	145.48 %
			Fe	1.15	1.88	2.2	2.48	2.69	2.82
			Error(%)		21.04 %	30.55 %	38.67 %	44.52 %	48.52 %
1.557	Fe1 Ge2	MSG 60.432 (P_{Ibcn})	Fe	1.2	1.51	1.83	2.11	2.37	2.59
			Error(%)		25.5 %	52.25 %	76.08 %	97.67 %	115.75 %
			Fe	1.2	1.5	1.83	2.11	2.37	2.59
			Error(%)		8.44 %	17.36 %	25.31 %	32.53 %	38.58 %
1.558	Mn1 Sn2	MSG 68.520 (C_{Acca})	Mn	2.36	2.65	3.11	3.49	3.79	3.99
			Error(%)		24.07 %	63.11 %	95.21 %	120.78 %	138.2 %

			Mn Error(%)	2.36 8.02 %	2.65 21.0 %	3.11	3.48 31.7 %	3.79 40.22 %	3.99 46.01 %
1.559	Mn1 Sn2	MSG 66.498 ($C_c ccm$)	Mn Error(%)	2.33 18.85 %	2.55 - %	-	3.48 98.36 %	3.8 125.27 %	4.0 142.79 %
			Mn Error(%)	2.33 2.72 %	2.56 - %	-	3.49 14.14 %	3.8 17.98 %	4.01 20.47 %
			Ni Error(%)	1.3 9.4 %	1.55 18.8 %	1.59 22.5 %	1.63 25.65 %	1.67 28.42 %	1.7 31.03 %
1.560	Ge1 Ni2 O4	MSG 12.63 ($C_c 2/m$)	Ni Error(%)	1.3 9.4 %	1.55 9.4 %	1.59 11.22 %	1.63 12.8 %	1.67 14.21 %	1.7 15.52 %
			Ni Error(%)	1.8 3.71 %	1.56 25.98 %	1.61 21.26 %	1.64 17.09 %	1.68 13.23 %	1.71 9.61 %
			Ni Error(%)	1.8 3.71 %	1.56 3.04 %	1.61 2.44 %	1.64 2.44 %	1.68 1.89 %	1.71 1.37 %
1.562	Ge1 Ni2 O4	MSG 5.16 ($C_c 2$)	Ni Error(%)	1.3 61.33 %	1.56 71.07 %	1.61 79.73 %	1.64 79.73 %	1.68 87.87 %	1.71 95.2 %
			Ni Error(%)	1.3 61.47 %	1.57 71.07 %	1.61 79.73 %	1.64 79.73 %	1.68 87.87 %	1.71 95.2 %
			Ni Error(%)	2.0 22.61 %	1.55 20.35 %	1.59 18.3 %	1.63 18.3 %	1.67 16.54 %	1.7 14.84 %
			Ni Error(%)	2.0 11.31 %	1.55 10.18 %	1.59 9.15 %	1.63 9.15 %	1.67 8.27 %	1.7 7.42 %
1.563	Ge1 Ni2 O4	MSG 8.35 ($C_c m$)	Ni Error(%)	1.1 83.85 %	1.57 91.67 %	1.61 98.72 %	1.65 98.72 %	1.68 105.13 %	1.72 111.03 %
			Ni Error(%)	1.1 83.85 %	1.57 91.67 %	1.61 98.72 %	1.65 98.72 %	1.68 105.13 %	1.72 111.03 %
			Ni Error(%)	2.29 32.25 %	1.55 30.25 %	1.6 28.46 %	1.64 28.46 %	1.68 26.85 %	1.71 25.34 %
			Ni Error(%)	2.29 16.13 %	1.55 15.12 %	1.6 14.23 %	1.64 14.23 %	1.68 13.43 %	1.71 12.67 %
1.569	Sr1 Ru2 O6	MSG 162.78 ($P_c \bar{3}1m$)	Ru Error(%)	1.42 5.12 %	1.35 15.65 %	1.65 28.0 %	1.82 37.4 %	1.96 45.47 %	2.07
			Ru Error(%)	1.42 1.73 %	1.35 5.24 %	1.65 9.36 %	1.83 9.36 %	1.96 12.49 %	2.07 15.18 %
			Ni Error(%)	1.46 2.43 %	1.53 4.08 %	1.58 5.58 %	1.62 5.58 %	1.66 6.95 %	1.7 8.18 %
1.580	Ni1 Ti1 O3	MSG 2.7 ($P_S \bar{1}$)	Ni Error(%)	1.46 2.4 %	1.53 4.08 %	1.58 5.58 %	1.62 5.58 %	1.66 6.95 %	1.7 8.18 %
			Co Error(%)	3.02 15.71 %	2.07 - %	- - %	- - %	- - %	2.54 7.86 %
			Co Error(%)	3.02 5.21 %	2.07 - %	- - %	- - %	- - %	2.54 2.62 %
1.594	Ba1 Co1 S1 O1	MSG 57.386 ($P_a bcm$)	Co Error(%)	2.75 12.62 %	2.06 - %	- - %	- - %	- - %	2.54 3.87 %
			Co Error(%)	2.75 4.19 %	2.06 - %	- - %	- - %	- - %	2.54 1.29 %
			Fe Error(%)	4.21 9.7 %	3.93 - %	- - %	- - %	- - %	4.23 0.81 %
1.617	Mo2 Fe1 Li1 O8	MSG 2.7 ($P_S \bar{1}$)	Fe Error(%)	4.21 9.7 %	3.93 - %	- - %	- - %	- - %	4.23 0.77 %
			Mn Error(%)	4.4 9.26 %	4.19 4.5 %	4.3 0.84 %	4.38 0.84 %	4.45 2.25 %	4.5 4.82 %
			Mn Error(%)	4.4 9.32 %	4.19 4.57 %	4.3 0.84 %	4.38 0.84 %	4.45 2.25 %	4.5 4.82 %
1.625	Sr2 Fe3 S2 O3	MSG 62.451 ($P_b nma$)	Fe Error(%)	3.21 2.43 %	3.29 - %	- - %	- - %	- - %	3.58 11.65 %
			Fe Error(%)	3.21 0.36 %	3.29 - %	- - %	- - %	- - %	3.58 1.66 %
			Fe Error(%)	1.67 2.57 %	1.54 7.01 %	2.02 13.73 %	2.36 13.73 %	2.6 18.54 %	2.77 22.04 %
1.629	Fe1 Ge1	MSG 192.252 ($P_c 6/mcc$)	Fe Error(%)	1.67 4.67 %	1.44 6.59 %	2.0 13.61 %	2.35 13.61 %	2.56 17.82 %	2.72 21.04 %
			Mn	1.33	2.52	3.17	3.64	3.86	4.02
1.630	Lu1 Mn6 Sn6	MSG 63.466 ($C_c mcm$)							

			Error(%)		178.71 %	276.73 %	348.86 %	381.68 %	404.29 %
			Mn	1.33	2.51	3.16	3.64	3.86	4.01
			Error(%)		16.12 %	25.08 %	31.67 %	34.67 %	36.74 %
1.641	Ba2 Fe1 Si2 O7	MSG 36.177 (C_cmc2_1)	Fe	2.95	3.5	3.55	3.59	3.63	3.67
			Error(%)		37.7 %	40.91 %	43.79 %	46.38 %	48.82 %
			Fe	2.95	3.51	3.55	3.59	3.63	3.67
			Error(%)		12.58 %	13.64 %	14.58 %	15.46 %	16.27 %
1.649	Sr3 Zn1 O6 Ir1	MSG 13.74 ($Pc2/c$)	Ir	0.86	0.0	0.23	0.22	0.23	0.24
			Error(%)		298.74 %	231.89 %	219.83 %	213.49 %	205.59 %
			Ir	0.86	0.0	0.23	0.22	0.23	0.24
			Error(%)		298.74 %	231.89 %	219.83 %	213.49 %	205.59 %
1.653	Fe1 W1 O4	MSG 13.70 (P_a2/c)	Ir	0.86	0.0	0.23	0.22	0.23	0.24
			Error(%)		149.45 %	115.94 %	109.92 %	106.74 %	102.8 %
			Fe	2.19	3.54	3.59	3.62	3.66	3.69
			Error(%)		122.46 %	127.57 %	132.22 %	137.28 %	142.86 %
1.661	La2 Ni1 Ir1 O6	MSG 2.7 ($P_S\bar{1}$)	Fe	2.19	3.54	3.59	3.62	3.66	3.69
			Error(%)		40.77 %	42.52 %	44.07 %	45.79 %	47.62 %
			Ni	1.49	1.42	1.51	1.58	1.63	1.68
			Error(%)		10.4 %	8.47 %	11.63 %	18.78 %	24.99 %
1.662	La2 Ni1 Ir1 O6	MSG 2.7 ($P_S\bar{1}$)	Ni	1.49	1.42	1.51	1.58	1.63	1.68
			Error(%)		9.05 %	8.66 %	12.09 %	19.06 %	25.02 %
			Ni	1.49	1.43	1.52	1.58	1.63	1.68
			Error(%)		10.15 %	9.77 %	12.1 %	19.3 %	25.61 %
1.678	Cr1 N1	MSG 62.450 (P_anma)	Ni	1.49	1.43	1.52	1.58	1.63	1.68
			Error(%)		10.74 %	9.49 %	11.89 %	19.27 %	25.48 %
			Ir	0.18	0.19	0.31	0.35	0.39	0.41
			Error(%)		323.27 %	391.73 %	414.94 %	433.21 %	445.32 %
1.689	Lu1 Mn2 Ge2	MSG 126.386 (P_I4/nnc)	Ir	0.18	0.19	0.31	0.35	0.39	0.41
			Error(%)		108.29 %	130.58 %	138.29 %	144.89 %	148.74 %
			Ni	1.39	1.44	1.53	1.6	1.65	1.7
			Error(%)		53.61 %	70.42 %	32.02 %	31.85 %	44.17 %
1.691	Mn2 Y1 Ge2	MSG 126.386 (P_I4/nnc)	Ni	1.39	1.44	1.53	1.6	1.65	1.7
			Error(%)		13.9 %	22.47 %	8.43 %	14.65 %	15.97 %
			Ir	0.38	0.12	0.21	0.22	0.22	0.25
			Error(%)		184.38 %	172.23 %	189.69 %	192.63 %	205.94 %
1.692	Mn2 Y1 Ge2	MSG 126.386 (P_I4/nnc)	Ir	0.38	0.11	0.21	0.21	0.22	0.25
			Error(%)		63.23 %	57.44 %	64.14 %	64.9 %	64.9 %
			Cr	2.35	2.42	2.6	2.72	2.81	2.88
			Error(%)		2.85 %	10.85 %	15.87 %	19.53 %	22.43 %
1.698	Lu1 Mn2 Ge2	MSG 126.386 (P_I4/nnc)	Cr	2.35	2.42	2.6	2.72	2.81	2.88
			Error(%)		0.95 %	3.62 %	5.29 %	6.51 %	7.48 %
			Mn	2.32	2.26	2.55	3.49	3.8	4.0
			Error(%)		1.23 %	4.87 %	25.11 %	31.94 %	36.16 %
1.702	Ba1 Y1 Co2 O5	MSG 65.489 (C_ammm)	Mn	2.32	2.26	2.55	3.49	3.8	4.0
			Error(%)		1.23 %	4.87 %	25.11 %	31.94 %	36.16 %
			Mn	1.96	2.26	2.57	3.55	3.85	4.02
			Error(%)		7.58 %	15.59 %	40.64 %	48.24 %	52.55 %
1.703	Ba1 Y1 Co2 O5	MSG 53.330 (P_amna)	Mn	1.96	2.26	2.57	3.55	3.85	4.02
			Error(%)		7.58 %	15.59 %	40.64 %	48.24 %	52.55 %
			Mn	2.23	2.31	2.63	3.6	3.89	4.04
			Error(%)		1.7 %	8.95 %	30.81 %	37.13 %	40.54 %
1.702	Ba1 Y1 Co2 O5	MSG 65.489 (C_ammm)	Mn	2.23	2.31	2.63	3.6	3.89	4.04
			Error(%)		1.7 %	8.95 %	30.81 %	37.13 %	40.54 %
			Co	2.1	1.87	2.15	2.37	2.48	2.54
			Error(%)		10.76 %	2.19 %	12.95 %	18.1 %	21.05 %
1.703	Ba1 Y1 Co2 O5	MSG 53.330 (P_amna)	Co	2.1	1.88	2.15	2.38	2.49	2.55
			Error(%)		3.52 %	0.81 %	4.44 %	6.11 %	7.06 %
			Co	2.7	2.0	2.29	2.39	2.48	2.55
			Error(%)		26.04 %	15.3 %	11.63 %	8.3 %	5.48 %
1.703	Ba1 Y1 Co2 O5	MSG 53.330 (P_amna)	Co	2.7	2.0	2.29	2.39	2.48	2.55
			Error(%)		8.68 %	5.1 %	3.88 %	2.77 %	1.83 %
			Co	4.2	1.92	2.43	2.66	2.8	2.91
			Error(%)		54.26 %	42.12 %	36.57 %	33.24 %	30.69 %

			Co Error(%)	4.2 18.09 %	1.92 14.04 %	2.43 12.19 %	2.66 11.08 %	2.8 10.23 %	2.91	
1.706	Ba2 Mn1 Te1 O6	MSG 64.480 (C_{Amca})	Mn Error(%)	4.34	4.35 0.23 %	4.42 1.91 %	4.48	4.53	4.58	
			Mn Error(%)	4.34	4.35 0.23 %	4.42 1.91 %	4.48	4.53	4.58	
	Cr1 P1 S4		Cr Error(%)	2.86	2.82 3.17 %	2.91 3.03 %	2.99	3.07	3.14	
			Cr Error(%)	2.86	2.82 1.06 %	2.91 1.01 %	2.99	3.07	3.14	
1.709	Cs1 Cr1 F4	MSG 46.247 ($I_a ma2$)	Cr Error(%)	1.5	2.75 83.53 %	2.79 86.13 %	2.82	2.86	2.88	
			Cr Error(%)	1.5	2.75 167.13 %	2.79 172.28 %	2.83	2.85	2.88	
			Cr Error(%)	1.5	2.75 167.13 %	2.79 172.28 %	2.83	2.85	2.88	
			Cr Error(%)	1.5	2.75 27.84 %	2.79 28.71 %	2.82	2.86	2.88	
	Sr2 Co1 W1 O6		Co Error(%)	2.35	2.54 16.69 %	2.59 20.36 %	2.65	2.69	2.74	
			Co Error(%)	2.35	2.54 5.56 %	2.6 6.99 %	2.65	2.69	2.74	
			Mn Error(%)	4.17	4.2 2.19 %	4.32 11.11 %	4.41	4.48	-	
			Mn Error(%)	4.17	4.2 2.19 %	4.32 11.11 %	4.41	4.48	-	
1.717	Sr2 Mn1 W1 O6	MSG 14.80 ($P_{a21/c}$)	Mn Error(%)	4.17	4.2 1.13 %	4.32 5.55 %	4.41	4.48	-	
			Mn Error(%)	4.17	4.2 1.13 %	4.32 5.55 %	4.41	4.48	-	
			Mn Error(%)	4.17	4.2 7.67 %	4.32 5.0 %	4.41	4.48	-	
			Mn Error(%)	4.17	4.2 7.67 %	4.32 5.0 %	4.41	4.48	-	
	Ca2 Mn1 W1 O6		Mn Error(%)	4.91	4.31 36.61 %	4.39 31.63 %	4.46	4.51	-	
			Mn Error(%)	4.91	4.31 12.19 %	4.39 10.54 %	4.46	4.51	-	
			Mn Error(%)	4.91	4.31 12.19 %	4.39 10.54 %	4.46	4.51	-	
			Mn Error(%)	4.91	4.31 12.19 %	4.39 10.54 %	4.46	4.51	-	
1.719	Ca2 Mn1 W1 O6	MSG 2.7 ($P_{S\bar{I}}$)	Mn Error(%)	3.5	4.31 69.37 %	4.39 76.19 %	4.46	4.51	4.56	
			Mn Error(%)	3.5	4.31 23.08 %	4.39 25.39 %	4.45	4.51	4.56	
	Ba2 Ni1 Te1 O6		Ni Error(%)	1.88	1.51 19.95 %	1.56 16.97 %	1.61	1.65	1.69	
			Ni Error(%)	1.88	1.51 6.65 %	1.56 5.66 %	1.61	1.65	1.69	
1.726	Ru1 Cl3	MSG 5.16 (C_c2)	Ru Error(%)	0.5	0.69 38.12 %	0.75 50.49 %	0.76	0.8	0.86	
			Ru Error(%)	0.5	0.69 7.79 %	0.75 10.06 %	0.76	0.8	0.86	
	Cu2 Mn1 Si1 S4		Mn Error(%)	4.02	4.17 10.68 %	4.28 18.61 %	4.36	4.44	4.5	
			Mn Error(%)	4.02	4.17 10.71 %	4.28 18.64 %	4.36	4.44	4.5	
1.731	Cu2 Fe1 Si1 S4	MSG 7.27 (P_{ac})	Mn Error(%)	4.02	4.17 5.36 %	4.28 9.32 %	4.36	4.44	4.5	
			Fe Error(%)	2.98	3.16 16.78 %	3.27 28.44 %	3.37	3.45	3.53	
			Fe Error(%)	2.98	3.15 15.99 %	3.27 28.62 %	3.37	3.46	3.53	
	Fe1 Cu2 Si1 S4		Fe Error(%)	2.98	3.16 8.37 %	3.27 14.22 %	3.37	3.45	3.53	
			Mn	4.33	4.11	4.22	4.32	4.4	4.46	
			Mn	4.33	4.11	4.22	4.32	4.4	4.46	

1.732 Mn1 Sn1 Cu2 S4

MSG 5.16 (C_c2)

			Error(%)		10.26 %	4.95 %	0.56 %	3.11 %	6.23 %
			Mn	4.33	4.11	4.22	4.32	4.4	4.46
			Error(%)		10.26 %	4.95 %	0.56 %	3.11 %	6.23 %
1.733	Ge1 Mn1 Cu2 S4	MSG 7.27 (P_{ac})	Mn	4.3	3.95	4.09	4.21	4.3	4.38
			Error(%)		24.57 %	14.47 %	6.44 %	0.16 %	5.78 %
			Mn	4.3	3.95	4.09	4.21	4.3	4.38
1.734	Fe1 Ge1 Cu2 S4	MSG 1.3 (P_{S1})	Error(%)		24.57 %	14.47 %	6.44 %	0.16 %	5.67 %
			Mn	4.3	3.95	4.09	4.21	4.3	4.38
			Error(%)		12.28 %	7.24 %	3.27 %	0.08 %	2.89 %
1.736	Co1 S2 O8 N4 H10	MSG 2.7 ($P_{S\bar{1}}$)	Fe	3.54	3.13	3.25	3.35	3.44	3.51
			Error(%)		22.8 %	16.0 %	10.43 %	5.54 %	1.29 %
			Fe	3.54	3.13	3.25	3.35	3.44	3.51
1.741	Ni1 K1 As1 O4	MSG 2.7 ($P_{S\bar{1}}$)	Error(%)		190.44 %	332.52 %	97.19 %	335.99 %	538.61 %
			Co	3.2	0.07	2.16	0.81	2.4	2.39
			Error(%)		198.17 %	336.74 %	245.53 %	352.06 %	336.6 %
1.742	Ni1 K1 As1 O4	MSG 2.7 ($P_{S\bar{1}}$)	Ni	1.72	1.59	1.63	1.67	1.7	1.73
			Error(%)		7.32 %	5.14 %	3.11 %	1.19 %	0.59 %
			Ni	1.72	1.59	1.63	1.67	1.7	1.73
1.745	Co3 La2	MSG 61.439 ($P_C bca$)	Error(%)		21.97 %	18.48 %	15.35 %	12.58 %	9.85 %
			Ni	1.85	1.58	1.62	1.66	1.69	1.73
			Error(%)		21.97 %	18.48 %	15.35 %	12.58 %	9.85 %
1.746	Mn2 Y1	MSG 4.12 ($P_C 2_1$)	Co	0.35	0.98	1.26	1.54	1.71	1.79
			Error(%)		90.29 %	129.71 %	170.14 %	194.0 %	205.0 %
			Co	0.35	0.98	1.26	1.55	1.72	1.79
1.752	Cs1 Co2 Mo2 O9 H1	MSG 11.55 ($P_a 2_1/m$)	Error(%)		89.71 %	130.29 %	171.57 %	195.14 %	205.71 %
			Co	0.92	1.08	1.3	1.46	1.56	1.66
			Error(%)		127.53 %	152.65 %	170.41 %	182.06 %	193.29 %
2.31	Mn3 Zn1 N1	MSG 60.432 ($P_I bcn$)	Co	0.92	1.05	1.28	1.45	1.56	1.67
			Error(%)		124.82 %	151.35 %	170.06 %	182.59 %	194.59 %
			Co	0.92	1.08	1.29	1.45	1.56	1.66
2.35	Cr1 Se1	MSG 157.55 ($P31m'$)	Error(%)		21.15 %	25.25 %	28.21 %	30.21 %	32.18 %
			Mn	0.61	2.38	3.18	3.42	3.61	3.8
			Error(%)		289.02 %	420.66 %	460.82 %	492.46 %	522.95 %
			Mn	0.61	2.38	3.18	3.42	3.61	3.8
			Error(%)		41.29 %	60.09 %	65.83 %	70.35 %	74.71 %
			Mn	1.03	2.6	3.05	3.37	3.6	3.79
			Error(%)		152.14 %	196.5 %	226.99 %	249.03 %	267.77 %
			Mn	1.03	2.6	3.06	3.37	3.6	3.79
			Error(%)		50.74 %	65.57 %	75.7 %	83.04 %	89.26 %
			Cr	3.49	2.37	3.52	3.64	3.74	3.82
			Error(%)		96.63 %	261.28 %	270.24 %	230.1 %	285.51 %
			Cr	3.49	2.37	3.52	3.64	3.74	3.82
			Error(%)		96.4 %	181.0 %	183.79 %	158.72 %	189.02 %
			Fe	4.3	-	4.11	4.19	4.28	4.34
			Error(%)		- %	389.12 %	151.77 %	119.77 %	89.66 %

			Fe Error(%)	4.3 - %	4.11 389.83 %	4.19 151.77 %	4.28 119.7 %	4.34 89.66 %
			Fe Error(%)	4.3 - %	4.11 185.8 %	4.19 71.96 %	4.28 57.27 %	4.34 43.38 %
			Fe Error(%)	3.96 - %	3.84 20.42 %	3.83 6.69 %	3.78 9.11 %	3.77 9.83 %
			Fe Error(%)	3.96 - %	3.84 14.78 %	3.83 6.58 %	3.78 8.98 %	3.77 9.78 %
2.66	<chem>Fe1 Sn2</chem>	MSG 68.513 ($Cc'ca$)	Fe Error(%)	1.64 88.3 %	2.2 117.05 %	2.48 157.57 %	- % - %	2.82 206.65 %
			Fe Error(%)	1.64 88.63 %	2.21 117.86 %	2.49 157.98 %	- % - %	2.82 206.65 %
			Fe Error(%)	1.64 88.3 %	2.2 117.05 %	2.48 157.57 %	- % - %	2.82 206.65 %
			Fe Error(%)	1.64 88.63 %	2.21 117.86 %	2.49 157.98 %	- % - %	2.82 206.65 %
			Fe Error(%)	0.73 349.65 %	1.8 425.3 %	2.09 492.91 %	2.34 554.14 %	2.56 606.15 %
2.68	<chem>Ge2 Fe1</chem>	MSG 56.367 ($Pc'cn$)	Fe Error(%)	0.73 350.12 %	1.8 426.0 %	2.09 493.14 %	2.35 554.37 %	2.56 606.15 %
			Fe Error(%)	0.73 174.82 %	1.8 212.65 %	2.09 246.45 %	2.34 277.07 %	2.56 303.07 %
			Co Error(%)	1.2 238.46 %	2.5 163.87 %	2.58 213.62 %	2.64 219.15 %	2.7 237.15 %
2.93	<chem>Co1 Cr1 O4</chem>	MSG 60.417 ($Pbcn$)	Co Error(%)	1.2 240.3 %	2.51 164.53 %	2.58 213.82 %	2.64 219.25 %	2.7 237.15 %
			Co Error(%)	1.2 120.15 %	2.51 82.16 %	2.58 106.91 %	2.64 109.62 %	2.7 118.58 %
			Fe Error(%)	3.78 7.04 %	3.56 5.77 %	3.6 4.71 %	3.64 3.7 %	3.68 2.75 %
3.24	<chem>Ca1 Fe3 Ti4 O12</chem>	MSG 148.17 ($R\bar{3}$)	Fe Error(%)	3.78 7.09 %	3.56 5.82 %	3.6 4.74 %	3.64 3.7 %	3.68 2.75 %
			Fe Error(%)	3.78 1.73 %	3.56 1.44 %	3.6 1.18 %	3.64 0.93 %	3.68 0.69 %
			Fe Error(%)	3.78 7.04 %	3.56 5.77 %	3.6 4.71 %	3.64 3.7 %	3.68 2.75 %
			Fe Error(%)	3.78 7.09 %	3.56 5.82 %	3.6 4.74 %	3.64 3.7 %	3.68 2.75 %
			Fe Error(%)	3.78 1.74 %	3.56 1.44 %	3.6 1.18 %	3.64 0.92 %	3.68 0.69 %

TAB. S2: Magnetic momenta prediction of materials with only d electrons. In the first, second and third columns, we list the BCSID, chemical formula and MSG of each compound. In columns 4 and 5, we show the label of each magnetic atom in the structure and the experimentally measured magnetic momenta. In columns 6-10, we list the computed magnetizations per independent atom and the relative error (see Eq. C1 as function of the Hubbard U parameter).

BCS ID	Formula	MSG	M.E.	μ_{exp}	U=0	U=2	U=4	U=6	
0.237	Er2 Sn2 O7	MSG 141.555 ($I4'_1/amd'$)	Er	4.38	2.76	2.81	2.84	2.91	
			Error(%)		74.16 %	71.87 %	70.45 %	67.16 %	
	Er2 Sn2 O7		Er	4.38	2.74	2.8	2.84	2.91	
			Error(%)		24.96 %	24.09 %	23.55 %	22.44 %	
0.238	Er2 Sn2 O7	MSG 141.555 ($I4'_1/amd'$)	Er	4.81	2.76	2.81	2.84	2.91	
			Error(%)		85.03 %	83.09 %	81.82 %	78.82 %	
	U2 Pd2 In1	MSG 127.394 ($P4'/m'bm'$)	Er	4.81	2.75	2.8	2.84	2.91	
			Error(%)		28.54 %	27.8 %	27.33 %	26.32 %	
0.320	U2 Sn1 Pd2	MSG 127.394 ($P4'/m'bm'$)	U	1.55	1.61	2.11	-	-	
			Error(%)		7.4 %	72.33 %	- %	- %	
	U2 Sn1 Pd2		U	1.55	1.61	2.11	-	-	
			Error(%)		2.47 %	24.11 %	- %	- %	
0.321	U2 Sn1 Pd2	MSG 127.394 ($P4'/m'bm'$)	U	2.2	1.67	2.42	-	-	
			Error(%)		47.91 %	20.06 %	- %	- %	
	Cd1 Yb2 S4	MSG 141.551 ($I4_1/amd$)	U	2.2	1.67	2.42	-	-	
			Error(%)		15.97 %	6.69 %	- %	- %	
0.324	Cd1 Yb2 S4	MSG 141.551 ($I4_1/amd$)	Yb	0.77	0.02	0.13	-	0.51	
			Error(%)		206.24 %	200.37 %	- %	68.26 %	
	Cd1 Yb2 S4		Yb	0.77	0.03	0.13	-	0.5	
			Error(%)		68.87 %	66.79 %	- %	23.12 %	
0.326	Nd2 Sn2 O7	MSG 227.131 ($Fd\bar{3}m'$)	Nd	1.71	2.93	2.94	-	-	
			Error(%)		214.91 %	215.72 %	- %	- %	
			Nd	1.71	2.93	2.94	-	-	
			Error(%)		215.11 %	215.72 %	- %	- %	
0.330	Er1 Ge3	MSG 11.53 ($P2_1/m'$)	Nd	1.71	2.93	2.94	-	-	
			Error(%)		107.4 %	107.86 %	- %	- %	
	Er1 Ge3		Er	8.4	2.49	2.78	-	-	
			Error(%)		142.94 %	131.54 %	- %	- %	
0.339	Nd2 Hf2 O7	MSG 227.131 ($Fd\bar{3}m'$)	Er	8.4	2.49	2.78	-	-	
			Error(%)		142.94 %	131.54 %	- %	- %	
			Nd	0.62	2.94	2.93	-	-	
			Error(%)		1112.78 %	1108.61 %	- %	- %	
0.340	Nd2 Zr2 O7	MSG 227.131 ($Fd\bar{3}m'$)	Nd	0.62	2.94	2.93	-	-	
			Error(%)		1113.06 %	1108.61 %	- %	- %	
			Nd	0.62	2.94	2.93	-	-	
			Error(%)		556.11 %	554.03 %	- %	- %	
0.343	Tb1 Ge2	MSG 65.483 ($Cm'mm$)	Nd	1.26	2.93	2.93	-	-	
			Error(%)		396.03 %	394.79 %	- %	- %	
			Nd	1.26	2.93	2.93	-	-	
			Error(%)		396.3 %	394.79 %	- %	- %	
0.350	Tb1 Al1 O3	MSG 62.449 ($Pn'm'a'$)	Nd	1.26	2.93	2.93	-	-	
			Error(%)		197.81 %	197.4 %	- %	- %	
			Tb	9.45	5.83	5.92	5.98	6.04	
			Error(%)		38.33 %	37.32 %	36.76 %	36.14 %	
0.350	Tb1 Al1 O3	MSG 62.449 ($Pn'm'a'$)	Tb	9.45	5.83	5.92	5.98	6.04	
			Error(%)		38.33 %	37.32 %	36.76 %	36.14 %	
			Tb	7.55	5.75	5.87	5.96	6.03	
			Error(%)		23.85 %	22.2 %	21.13 %	20.15 %	
0.350	Tb1 Al1 O3	MSG 62.449 ($Pn'm'a'$)	Tb	7.55	5.75	5.87	5.96	6.03	
			Error(%)		23.85 %	22.2 %	21.13 %	20.15 %	
			Tb	8.29	5.81	5.95	-	-	
			Error(%)		61.73 %	56.78 %	- %	- %	
0.410	Gd1 Al1 O3	MSG 62.449 ($Pn'm'a'$)	Tb	8.29	5.79	5.95	-	-	
			Error(%)		62.09 %	56.8 %	- %	- %	
			Tb	8.29	5.81	5.95	-	-	
			Error(%)		30.82 %	28.39 %	- %	- %	
0.410	Gd1 Al1 O3	MSG 62.449 ($Pn'm'a'$)	Gd	6.1	0.0	0.0	0.0	0.0	
			Error(%)		50.0 %	50.0 %	50.0 %	50.0 %	
			Gd	6.1	0.0	0.0	0.0	0.0	
			Error(%)		50.0 %	50.0 %	50.0 %	50.0 %	
		Ce1 Na1 O2	Ce	0.57	0.83	0.94	0.95	0.87	
0.525		MSG 141.556 ($I4'_1/a'm'd$)							

			Error(%)		44.74 %	64.74 %	66.67 %	51.75 %
			Ce	0.57	0.83	0.94	0.95	0.87
			Error(%)		44.74 %	64.74 %	66.67 %	51.75 %
0.527	Er2 Si2 O7	MSG 12.60 ($C2'/m$)	Er	6.61	2.78	2.82	2.89	2.91
			Error(%)		113.06 %	110.68 %	112.83 %	111.53 %
0.593	U1 Se1 P1	MSG 129.417 ($P4/nm'm'$)	U	1.35	1.72	2.03	1.97	2.33
			Error(%)		13.74 %	25.11 %	23.0 %	36.3 %
0.594	U1 S1 As1	MSG 129.417 ($P4/nm'm'$)	U	1.24	1.86	2.17	2.37	2.37
			Error(%)		24.88 %	37.34 %	45.4 %	45.73 %
0.595	U1 Te1 P1	MSG 139.537 ($I4/mm'm'$)	U	1.44	-	1.72	1.68	2.26
			Error(%)		- %	9.79 %	8.4 %	28.58 %
0.596	U1 Te1 As1	MSG 139.537 ($I4/mm'm'$)	U	1.44	-	1.9	1.82	2.38
			Error(%)		- %	15.9 %	13.09 %	32.53 %
0.616	Hol B2	MSG 12.62 ($C2'/m'$)	Ho	6.75	3.7	3.8	3.93	3.98
			Error(%)		205.36 %	130.14 %	126.55 %	124.63 %
0.625	U2 In1 Pd2	MSG 127.394 ($P4'/m'bm'$)	U	1.73	-	1.81	2.42	2.61
			Error(%)		- %	9.75 %	80.82 %	102.46 %
0.650	Er2 Si2 O7	MSG 12.60 ($C2'/m$)	U	1.73	-	1.81	2.42	2.61
			Error(%)		- %	3.25 %	26.94 %	34.15 %
0.681	Sb3 Ce4	MSG 122.336 ($I\bar{4}'2d'$)	Er	6.69	2.78	2.82	2.89	2.91
			Error(%)		114.57 %	111.23 %	113.92 %	112.02 %
0.684	Pt1 Tb1	MSG 62.446 ($Pn'm'a$)	Er	6.69	2.78	2.82	2.89	2.91
			Error(%)		114.57 %	111.23 %	113.92 %	112.02 %
0.685	Er1 Pt1	MSG 62.447 ($Pnm'a'$)	Ce	1.24	0.8	0.97	0.9	-
			Error(%)		17.86 %	12.98 %	21.41 %	- %
0.686	Ho1 Pt1	MSG 62.447 ($Pnm'a'$)	Ce	1.24	0.79	0.97	0.9	-
			Error(%)		6.03 %	4.29 %	7.11 %	- %
0.687	Dy1 Pt1	MSG 62.446 ($Pn'm'a$)	Tb	8.1	5.82	5.87	5.99	6.05
			Error(%)		56.92 %	55.16 %	52.32 %	50.84 %
0.688	Tm1 Pt1	MSG 62.447 ($Pnm'a'$)	Tb	8.1	5.8	5.89	6.0	6.06
			Error(%)		19.13 %	18.24 %	17.37 %	16.88 %
0.689	Pt1 Pr1	MSG 63.462 ($Cm'c'm$)	Er	8.1	2.53	2.62	2.75	2.92
			Error(%)		135.21 %	134.77 %	133.86 %	129.03 %
0.690	Nd1 Pt1	MSG 15.89 ($C2'/c'$)	Er	8.1	2.54	2.62	2.75	2.91
			Error(%)		45.04 %	44.88 %	44.64 %	43.0 %
0.743	Ho3 Al5 O12	MSG 230.148 ($Ia\bar{3}d'$)	Ho	8.2	3.6	3.63	3.75	3.94
			Error(%)		113.1 %	105.3 %	101.07 %	100.07 %
			Ho	8.2	3.59	3.62	3.74	3.93
			Error(%)		37.77 %	35.2 %	33.8 %	33.41 %
			Dy	7.1	4.66	4.62	4.8	4.98
			Error(%)		68.69 %	69.77 %	64.97 %	59.78 %
			Dy	7.1	4.65	4.61	4.8	4.99
			Error(%)		23.05 %	23.35 %	21.6 %	19.83 %
			Tm	4.5	1.36	1.49	1.54	1.66
			Error(%)		139.51 %	134.83 %	131.98 %	127.14 %
			Tm	4.5	1.36	1.48	1.53	1.65
			Error(%)		46.48 %	45.07 %	44.15 %	42.51 %
			Pr	2.2	2.04	2.11	1.99	2.28
			Error(%)		3.59 %	2.07 %	4.77 %	1.77 %
			Nd	2.34	3.19	3.08	3.04	3.01
			Error(%)		35.46 %	35.11 %	36.85 %	43.37 %
			Ho	5.2	3.76	-	3.9	-
			Error(%)		27.6 %	- %	25.1 %	- %
			Ho	5.2	3.76	-	3.9	-
			Error(%)		27.6 %	- %	25.1 %	- %
			Ho	5.2	3.76	-	3.9	-
			Error(%)		27.6 %	- %	25.1 %	- %
			Ho	5.2	3.76	-	3.9	-
			Error(%)		27.6 %	- %	25.1 %	- %

			Ho Error(%)	5.2 3.94 %	3.76 - %	-	3.9 3.59 %	-
0.782	Nd1 Sc1 O3	MSG 62.444 ($Pnm'a$)	Nd Error(%)	2.07 111.36 %	2.91 92.71 %	2.93 89.42 %	2.94 91.87 %	2.96
			Nd Error(%)	2.07 37.12 %	2.91 30.92 %	2.93 29.81 %	2.94 30.62 %	2.96
			Nd Error(%)	2.85 19.86 %	2.93 15.05 %	2.94 23.67 %	2.94 11.01 %	2.93
0.783	Nd1 In1 O3	MSG 62.444 ($Pnm'a$)	Nd Error(%)	2.85 6.62 %	2.93 5.02 %	2.94 7.89 %	2.94 3.67 %	2.93
			Gd Error(%)	6.8 100.0 %	0.0 100.0 %	0.0 100.0 %	0.0 100.0 %	0.0
			Gd Error(%)	6.8 33.33 %	0.0 33.33 %	0.0 33.33 %	0.0 33.33 %	0.0
0.821	Sr1 Gd2 O4	MSG 62.445 ($Pnma'$)	Gd Error(%)	4.59 100.0 %	0.0 100.0 %	0.0 100.0 %	0.0 100.0 %	0.0
			Gd Error(%)	4.59 33.33 %	0.0 33.33 %	0.0 33.33 %	0.0 33.33 %	0.0
			Ce Error(%)	1.06 13.82 %	0.77 5.61 %	0.94 4.95 %	0.96 4.81 %	0.96
			Dy Error(%)	8.54 88.65 %	4.78 106.96 %	4.86 85.82 %	4.9 83.25 %	4.98
0.842	Dy1 Al1 O3	MSG 62.449 ($Pn'm'a'$)	Dy Error(%)	8.54 88.54 %	4.78 106.96 %	4.86 85.82 %	4.9 83.25 %	4.98
			Dy Error(%)	8.54 44.32 %	4.78 53.48 %	4.86 42.91 %	4.9 41.62 %	4.98
			Gd Error(%)	6.76 200.0 %	0.0 200.0 %	0.0 200.0 %	0.0 200.0 %	0.0
0.854	Gd2 Pt2 O7	MSG 141.555 ($I4'_1/amd'$)	Gd Error(%)	6.76 66.67 %	0.0 66.67 %	0.0 66.67 %	0.0 66.67 %	0.0
			Eu Error(%)	6.45 14.94 %	6.77 18.24 %	6.84 20.56 %	6.89 22.1 %	6.93
0.941	Er2 O3	MSG 206.37 ($Ia\bar{3}$)	Er Error(%)	6.06 165.8 %	2.71 161.31 %	2.8 158.91 %	2.85 157.37 %	2.88
			Er Error(%)	6.06 165.6 %	2.72 161.23 %	2.8 158.91 %	2.85 157.37 %	2.88
			Er Error(%)	6.06 82.89 %	2.71 80.61 %	2.8 79.46 %	2.85 78.69 %	2.88
			Er Error(%)	5.36 48.75 %	2.75 47.43 %	2.82 46.38 %	2.87 46.59 %	2.86
			Er Error(%)	5.36 48.77 %	2.75 47.43 %	2.82 46.38 %	2.87 46.59 %	2.86
			Er Error(%)	5.36 48.75 %	2.75 47.43 %	2.82 46.38 %	2.87 46.59 %	2.86
			Er Error(%)	5.36 48.77 %	2.75 47.43 %	2.82 46.38 %	2.87 46.59 %	2.86
			Er Error(%)	5.36 48.75 %	2.75 47.43 %	2.82 46.38 %	2.87 46.59 %	2.86
			Er Error(%)	5.36 6.96 %	2.75 6.78 %	2.82 6.63 %	2.87 6.66 %	2.86
			Er Error(%)	6.78 162.03 %	2.76 159.4 %	2.81 169.91 %	2.85 177.92 %	2.91
0.950	Er1 La1 O3	MSG 62.441 ($Pnma$)	Er Error(%)	6.78 161.86 %	2.76 159.4 %	2.81 169.93 %	2.85 177.89 %	2.91
			Er Error(%)	6.78 81.02 %	2.76 79.7 %	2.81 84.96 %	2.85 88.96 %	2.91
			Yb Error(%)	0.69 199.62 %	0.01 189.07 %	0.04 199.07 %	0.0 199.62 %	0.0
0.952	Yb1 Pd1 Si1	MSG 59.409 ($Pm'm'n$)	Yb Error(%)	0.69 66.98 %	0.0 63.41 %	0.04 66.69 %	0.0 66.79 %	0.0
			Yb Error(%)	1.3 50.27 %	0.01 44.77 %	0.14 50.0 %	0.0 50.0 %	0.0
			Yb Error(%)	0.15 0.0	0.0 0.0	0.0 0.0	0.0 0.0	0.0

			Error(%)		50.0 %	49.0 %	50.0 %	50.0 %
0.972	Ho1 Pd1 In1	MSG 189.225 ($P\bar{6}2'm'$)	Ho Error(%)	8.1 18.74 %	3.55 18.37 %	3.64 17.8 %	3.78 17.09 %	3.95
0.973	Ho1 Pd1 In1	MSG 189.225 ($P\bar{6}2'm'$)	Ho Error(%)	7.0 16.3 %	3.58 15.91 %	3.66 15.34 %	3.78 14.82 %	3.89
0.974	Er1 Pd1 In1	MSG 189.225 ($P\bar{6}2'm'$)	Er Error(%)	6.6 21.06 %	2.43 20.4 %	2.56 19.91 %	2.66 19.02 %	2.84
0.975	Er1 Pd1 In1	MSG 189.225 ($P\bar{6}2'm'$)	Er Error(%)	3.8 12.02 %	2.43 10.82 %	2.57 9.96 %	2.66 8.36 %	2.85
0.976	Nd1 Pd1 In1	MSG 38.191 ($Am'm'2$)	Nd Error(%)	1.8 53.49 %	3.21 46.88 %	3.12 44.72 %	3.08 60.27 %	3.57
0.977	Nd1 Pd1 In1	MSG 8.34 (Cm')	Nd Error(%)	1.5 115.0 %	3.22 102.54 %	3.12 103.91 %	3.04 101.95 %	3.02
0.985	Eu1 Pd3 Si2	MSG 74.559 ($Imm'a'$)	Eu Error(%)	8.0 7.94 %	6.73 7.31 %	6.83 6.77 %	6.92 6.49 %	6.96
1.288	Ce1 Pd2 Si2	MSG 66.500 (C_Accm)	Ce Error(%)	0.66 77.87 %	0.41 188.09 %	0.04 285.32 %	0.28 230.85 %	0.1
			Ce Error(%)	0.66 77.87 %	0.41 189.36 %	0.04 285.74 %	0.28 230.85 %	0.1
1.290	Ce1 Rh2 Si2	MSG 64.480 (C_Amca)	Ce Error(%)	1.28 81.33 %	0.24 128.98 %	0.37 - %	- - %	- - %
			Ce Error(%)	1.28 81.33 %	0.24 128.98 %	0.37 - %	- - %	- - %
1.291	Au2 Ce1 Si2	MSG 128.410 (P_I4/mnc)	Ce Error(%)	1.29 50.62 %	0.64 31.86 %	0.88 - %	- - %	- - %
			Ce Error(%)	1.29 50.62 %	0.64 31.86 %	0.88 - %	- - %	- - %
1.334	Pr2 Pd2 In1	MSG 62.451 (P_bnma)	Pr Error(%)	1.8 11.94 %	2.02 7.22 %	1.93 2.28 %	1.84 1.94 %	1.76
			Pr Error(%)	1.8 11.66 %	2.01 1.04 %	1.93 0.33 %	1.84 0.29 %	1.76
1.339	Eu1 As3	MSG 12.63 (C_c2/m)	Eu Error(%)	5.74 8.55 %	6.72 9.37 %	6.82 9.97 %	6.88 10.36 %	6.93
			Eu Error(%)	5.74 8.52 %	6.72 9.36 %	6.81 9.97 %	6.88 10.36 %	6.93
1.361	Dy1 Ge1	MSG 15.90 (C_c2/c)	Dy Error(%)	9.0 49.56 %	4.54 45.66 %	4.89 - %	- - %	- - %
			Dy Error(%)	9.0 16.52 %	4.54 15.23 %	4.89 - %	- - %	- - %
1.367	Pu2 O3	MSG 15.90 (C_c2/c)	Pu Error(%)	0.6 645.17 %	4.47 675.33 %	4.65 681.17 %	4.69 696.0 %	4.78
			Pu Error(%)	0.6 215.06 %	4.47 225.11 %	4.65 227.06 %	4.69 232.0 %	4.78
1.486	Ce1 Rh1 Al4 Si2	MSG 124.360 (P_c4/mcc)	Ce Error(%)	1.14 - %	- 107.72 %	0.09 32.81 %	0.77 184.12 %	0.96
			Ce Error(%)	1.14 - %	- 107.72 %	0.09 32.72 %	0.77 184.12 %	0.96
1.497	Eu1 Bi2 Mg2	MSG 12.63 (C_c2/m)	Eu Error(%)	5.3 28.62 %	6.82 29.91 %	6.88 30.57 %	6.92 31.06 %	6.95
			Eu Error(%)	5.3 28.62 %	6.82 29.91 %	6.88 30.57 %	6.92 31.06 %	6.95
1.505	Gd1 Ag1 Sn1	MSG 33.154 (P_Cna2_1)	Gd Error(%)	7.2 49.97 %	0.0 49.97 %	0.0 49.97 %	0.0 49.97 %	0.0
			Gd Error(%)	7.2 50.03 %	0.0 50.03 %	0.0 50.03 %	0.0 50.03 %	0.0
1.507	Al2 Pd5 Nd1	MSG 62.450 (P_anma)	Nd Error(%)	2.7 13.11 %	3.05 16.11 %	3.14 10.15 %	2.97 10.0 %	2.97
			Nd Error(%)	2.7 4.37 %	3.05 5.36 %	3.13 3.4 %	2.98 3.33 %	2.97
1.530	Ce1 C2	MSG 128.410 (P_I4/mnc)	Ce Error(%)	1.74 71.9 %	0.49 60.86 %	0.68 45.86 %	0.94 44.94 %	0.96
			Ce Error(%)	1.74 71.9 %	0.49 60.86 %	0.68 45.86 %	0.94 44.94 %	0.96

1.531	Pr1 C2	MSG 128.410 (P_{I4}/mnc)	Pr Error(%)	1.14	1.95 70.7 %	1.98 73.51 %	1.98 73.42 %	1.93 69.56 %
			Pr Error(%)	1.14	1.95 70.7 %	1.98 73.51 %	1.98 73.42 %	1.93 69.56 %
1.532	Nd1 C2	MSG 128.410 (P_{I4}/mnc)	Nd Error(%)	2.95	3.08 4.44 %	3.05 3.25 %	3.01 1.9 %	3.0 1.56 %
			Nd Error(%)	2.95	3.08 4.44 %	3.05 3.25 %	3.01 1.9 %	3.0 1.56 %
1.536	U1 Pd2 Si2	MSG 128.410 (P_{I4}/mnc)	U Error(%)	2.4	- - %	1.8 25.17 %	1.43 40.37 %	1.27 47.25 %
			U Error(%)	2.4	- - %	1.8 25.17 %	1.43 40.37 %	1.27 47.25 %
1.574	Nd1 Bi1 Pt1	MSG 118.314 ($P_{I\bar{4}n2}$)	Nd Error(%)	1.78	3.11 74.49 %	3.05 71.07 %	2.99 67.92 %	2.99 67.98 %
			Nd Error(%)	1.78	3.1 74.1 %	3.04 70.51 %	2.99 67.87 %	2.99 67.98 %
1.576	O2 S1 Yb2	MSG 12.63 (C_{c2}/m)	Yb Error(%)	2.0	0.31 42.4 %	0.55 36.18 %	0.63 34.25 %	0.71 32.3 %
			Yb Error(%)	2.0	0.34 41.7 %	0.56 36.0 %	0.63 34.15 %	0.71 32.25 %
1.578	K1 Er1 Se2	MSG 12.63 (C_{c2}/m)	Er Error(%)	3.06	2.58 31.28 %	2.74 20.77 %	2.82 15.69 %	2.87 12.68 %
			Er Error(%)	3.06	2.63 28.33 %	2.74 20.77 %	2.82 15.69 %	2.87 12.68 %
1.623	Bi2 Eu1 Mg2	MSG 12.63 (C_{c2}/m)	Eu Error(%)	6.61	6.82 3.13 %	6.88 4.16 %	6.92 4.69 %	6.95 5.08 %
			Eu Error(%)	6.61	6.82 3.13 %	6.88 4.16 %	6.92 4.69 %	6.95 5.08 %
1.627	Ce1 K1 S2	MSG 15.90 (C_{c2}/c)	Ce Error(%)	0.32	1.05 569.93 %	1.02 1985.94 %	0.99 1403.77 %	0.3 860.14 %
			Ce Error(%)	0.32	1.05 569.93 %	1.02 1986.26 %	0.99 1400.23 %	0.3 856.91 %
1.643	Cl1 Dy1 O1	MSG 62.450 ($P_{a}nma$)	Dy Error(%)	10.1	4.84 52.06 %	4.82 52.29 %	4.89 51.55 %	4.96 50.84 %
			Dy Error(%)	10.1	4.84 17.35 %	4.82 17.43 %	4.89 17.18 %	4.96 16.95 %
1.648	Nd2 O3	MSG 12.63 (C_{c2}/m)	Nd Error(%)	1.87	- - %	2.92 56.27 %	2.93 56.67 %	2.93 56.61 %
			Nd Error(%)	1.87	- - %	2.92 56.37 %	2.93 56.75 %	2.93 56.58 %
1.658	Dy1 Ga3	MSG 15.90 (C_{c2}/c)	Dy Error(%)	5.72	4.63 38.13 %	4.75 34.24 %	4.93 27.61 %	4.99 25.44 %
			Dy Error(%)	5.72	4.63 5.45 %	4.75 4.83 %	4.93 3.99 %	4.99 3.59 %
1.667	U1 Pd1 Ga5	MSG 67.509 ($C_{a}mma$)	U Error(%)	0.32	1.36 325.0 %	2.13 564.69 %	2.42 654.69 %	2.6 713.75 %
			U Error(%)	0.32	1.36 325.0 %	2.13 564.69 %	2.42 654.69 %	2.6 713.75 %
1.672	Eu1 Zn2 As2	MSG 12.63 (C_{c2}/m)	Eu Error(%)	7.33	6.76 7.76 %	6.84 6.67 %	6.9 5.91 %	6.93 5.42 %
			Eu Error(%)	7.33	6.76 7.76 %	6.84 6.67 %	6.9 5.91 %	6.93 5.42 %
1.714	Ce1 Bi2 Au1	MSG 130.432 (P_{c4}/ncc)	Ce Error(%)	2.3	0.69 70.0 %	0.91 60.57 %	0.92 60.04 %	0.93 59.74 %
			Ce Error(%)	2.3	0.69 23.33 %	0.91 20.19 %	0.92 20.01 %	0.93 19.91 %
1.740	Ce1 Au1 Sb2	MSG 39.201 ($A_{b}bm2$)	Ce Error(%)	1.15	0.53 73.09 %	0.88 14.09 %	0.91 10.39 %	0.92 10.09 %
			Ce Error(%)	1.15	0.53 73.04 %	0.88 14.22 %	0.91 10.43 %	0.92 10.09 %
1.744	Pr1 Pd1 Sn1	MSG 14.80 (P_{a21}/c)	Pr Error(%)	3.38	2.05 39.26 %	2.03 40.03 %	2.0 40.77 %	2.0 40.86 %

			Pr Error(%)	3.38 5.63 %	2.05 5.73 %	2.03 5.82 %	2.0 5.84 %
1.747	Er1 In1 Au1	MSG 174.136 ($P_c\bar{6}$)	Er Error(%)	2.5 8.81 %	2.46 1.56 %	2.58 2.32 %	2.61 4.12 %
			Er Error(%)	2.5 8.84 %	2.46 8.54 %	2.58 29.52 %	2.77 10.37 %
			Er Error(%)	2.5 8.84 %	2.47 8.54 %	2.58 29.65 %	2.77 7.11 %
			Er Error(%)	2.5 8.82 %	2.46 0.82 %	2.58 1.22 %	2.77 2.18 %
			Ho Error(%)	4.99 14.12 %	3.58 13.13 %	3.68 11.5 %	3.84 11.45 %
			Ho Error(%)	4.99 14.15 %	3.57 13.08 %	3.68 11.46 %	3.84 11.39 %
1.753	Ho1 Bi1	MSG 15.90 (C_c2/c)	Ho Error(%)	10.3 65.58 %	3.55 64.85 %	3.62 63.79 %	3.87 62.48 %
			Ho Error(%)	10.3 65.85 %	3.52 64.85 %	3.62 64.75 %	3.78 63.33 %
1.755	K1 Er1 Se2	MSG 12.63 (C_c2/m)	Er Error(%)	9.58 145.18 %	2.63 142.75 %	2.74 140.89 %	2.9 139.5 %
			Er Error(%)	9.58 145.1 %	2.63 142.72 %	2.74 140.96 %	2.9 139.5 %
			Ho Error(%)	9.16 116.41 %	3.64 118.75 %	3.73 114.83 %	3.89 118.64 %
2.100	Ho1 P1	MSG 15.89 ($C2'/c'$)	Ho Error(%)	9.16 115.85 %	3.64 118.75 %	3.73 114.83 %	3.89 118.65 %
			Eu Error(%)	5.08 16.66 %	6.77 17.42 %	6.85 17.95 %	6.9 18.3 %
2.103	Eu3 Pb1 O1	MSG 47.252 ($Pm'm'm$)	Eu Error(%)	5.08 8.42 %	6.79 8.87 %	6.88 9.14 %	6.94 9.32 %
			Ho Error(%)	5.2 89.2 %	3.65 89.57 %	3.79 81.2 %	3.82 79.37 %
2.71	Ho1 Rh1	MSG 11.57 (P_C2_1/m)	Ho Error(%)	5.2 44.53 %	3.65 40.5 %	3.79 40.5 %	3.82 41.32 %
			Tm Error(%)	5.99 238.15 %	1.24 236.88 %	1.26 232.46 %	1.35 226.65 %
			Tm Error(%)	5.99 239.42 %	1.21 237.46 %	1.25 233.5 %	1.33 227.77 %
3.21	Ga3 Tm1	MSG 229.143 ($Im\bar{3}m'$)	Tm Error(%)	5.99 119.15 %	1.23 118.45 %	1.26 116.52 %	1.34 113.58 %
			Eu Error(%)	6.45 2.43 %	6.76 3.12 %	6.85 3.53 %	6.91 3.82 %
			Eu Error(%)	6.45 0.51 %	6.78 0.65 %	6.87 0.74 %	6.96 0.8 %
3.23	Eu3 Pb1 O1	MSG 123.345 ($P4/mm'm'$)	Eu Error(%)	6.45 2.43 %	6.76 3.12 %	6.85 3.53 %	6.91 3.82 %
			Eu Error(%)	6.45 0.51 %	6.78 0.65 %	6.87 0.74 %	6.96 0.8 %

TAB. S3: Magnetic momenta prediction of materials with only f electrons. In the first, second and third columns, we list the BCSID, chemical formula and MSG of each compound. In columns 4 and 5, we show the label of each magnetic atom in the structure and the experimentally measured magnetic momenta. In columns 6-9, we list the computed magnetizations per independent atom and the relative error (see Eq. C1 as function of the Hubbard U parameter).

BCS ID	Formula	MSG	M.E.	μ_{exp}	U=0	U=2	U=4	U=6
0.231	Tm1 Mn3 O6	MSG 59.410 ($Pmm'm'n'$)	Tm	0.77	1.56	1.69	-	-
			Error(%)		151.49 %	159.55 %	- %	- %
			Tm	3.7	1.59	1.72	-	-
			Error(%)		71.5 %	26.81 %	- %	- %
			Mn	2.0	3.8	3.81	-	-
			Error(%)		44.91 %	45.11 %	- %	- %
0.232	Tm1 Mn3 O6	MSG 59.409 ($Pm'm'n$)	Mn	3.17	4.42	4.44	-	-
			Error(%)		19.78 %	19.98 %	- %	- %
			Mn	1.91	3.68	3.73	-	-
			Error(%)		23.14 %	23.81 %	- %	- %
0.235	Mn2 Pr1 Sb1 O6	MSG 86.67 ($P4_2/n$)	Mn	1.59	3.25	3.32	-	-
			Error(%)		26.02 %	27.23 %	- %	- %
			Mn	1.96	3.8	3.81	-	-
			Error(%)		47.14 %	47.34 %	- %	- %
0.289	Nd1 Mn1 O3	MSG 62.448 ($Pn'ma'$)	Mn	3.1	4.43	4.44	-	-
			Error(%)		21.45 %	21.69 %	- %	- %
			Mn	1.89	3.66	3.72	-	-
			Error(%)		23.44 %	24.26 %	- %	- %
0.290	Ce1 Cu2	MSG 74.560 ($Im'm'a'$)	Mn	1.58	3.24	3.32	-	-
			Error(%)		26.2 %	27.56 %	- %	- %
			Ce	0.33	0.44	0.02	-	-
			Error(%)		233.64 %	99.09 %	- %	- %
0.318	Tm2 Co1 Mn1 O6	MSG 14.79 ($P2'_1/c'$)	Ce	0.33	0.44	0.03	-	-
			Error(%)		233.64 %	103.64 %	- %	- %
			Tm	2.18	1.57	1.72	1.78	1.81
			Error(%)		56.03 %	72.23 %	31.05 %	22.63 %
0.319	Tm2 Co1 Mn1 O6	MSG 14.79 ($P2'_1/c'$)	Tm	2.18	1.58	1.72	1.78	1.81
			Error(%)		56.24 %	66.4 %	32.33 %	21.98 %
			Co	2.83	0.14	0.16	1.41	0.18
			Error(%)		47.69 %	47.39 %	24.4 %	46.99 %
0.367	Eu1 Cr2 As2	MSG 119.319 ($I\bar{4}m'2'$)	Tm	0.78	1.58	1.73	1.78	1.81
			Error(%)		50.9 %	54.79 %	59.86 %	65.21 %
			Co	2.56	0.16	0.15	1.8	0.18
			Error(%)		47.68 %	47.3 %	13.12 %	46.93 %
0.372	Dy1 Cr1 O4	MSG 15.87 ($C2'/c$)	Eu	6.2	6.7	6.88	-	-
			Error(%)		8.1 %	10.92 %	- %	- %
			Cr	1.7	3.28	3.25	-	-
			Error(%)		92.71 %	91.18 %	- %	- %
0.374	Tb1 Ni4 Si1	MSG 65.486 ($Cmm'm'$)	Cr	1.7	3.41	3.39	-	-
			Error(%)		100.53 %	99.35 %	- %	- %
			Dy	9.67	4.72	4.85	4.92	5.0
			Error(%)		51.18 %	51.54 %	49.32 %	64.41 %
			Dy	9.67	4.72	4.85	4.92	5.0
			Error(%)		51.18 %	51.54 %	49.31 %	64.41 %
			Cr	0.99	0.76	0.94	0.04	0.37
			Error(%)		23.13 %	5.35 %	100.91 %	133.54 %
			Cr	0.99	0.76	0.94	0.03	0.37
			Error(%)		23.13 %	5.35 %	100.91 %	133.54 %
			Tb	8.66	0.07	5.97	-	-

			Error(%)		99.3 %	31.05 %	- %	- %
0.406	Gd1 Ni1 Si3	MSG 65.484 ($Cmmm'$)	Gd	1.0	0.0	0.0	0.0	0.0
			Error(%)		100.0 %	100.0 %	100.0 %	100.0 %
			Gd	1.0	0.0	0.0	0.0	0.0
			Error(%)		100.0 %	100.0 %	100.0 %	100.0 %
0.519	Ho1 Cr2 Si2	MSG 139.536 ($I4'/m'm'm$)	Cr	1.6	0.01	-	0.09	-
			Error(%)		99.88 %	- %	105.75 %	- %
			Cr	1.6	0.01	-	0.1	-
			Error(%)		99.88 %	- %	106.0 %	- %
0.561	Ni1 Nd1 Ge2	MSG 63.462 ($Cm'c'm$)	Nd	2.32	-	3.07	3.02	2.98
			Error(%)		- %	16.25 %	15.06 %	14.16 %
0.566	Ge2 Ni1 Tb1	MSG 63.459 ($Cm'cm$)	Tb	8.8	5.76	5.83	5.96	6.01
			Error(%)		34.55 %	33.78 %	32.33 %	31.66 %
			Tb	8.8	5.76	5.83	5.96	6.01
			Error(%)		34.55 %	33.78 %	32.33 %	31.66 %
0.587	Tm1 Cr1 O3	MSG 62.448 ($Pn'ma'$)	Cr	2.58	2.45	-	2.78	-
			Error(%)		5.35 %	- %	5.23 %	- %
			Cr	2.58	2.45	-	2.78	-
			Error(%)		1.77 %	- %	1.74 %	- %
0.590	Er1 Cr1 O3	MSG 11.50 ($P2_1/m$)	Er	5.2	-	-	2.85	2.86
			Error(%)		- %	- %	22.63 %	22.5 %
			Er	5.2	-	-	2.83	2.86
			Error(%)		- %	- %	22.75 %	22.5 %
0.620	Mn1 Nd1 As1 O1	MSG 129.416 ($P4'/n'm'm$)	Cr	2.9	-	-	2.76	2.76
			Error(%)		- %	- %	9.07 %	9.11 %
			Cr	2.9	-	-	2.76	2.76
			Error(%)		- %	- %	3.01 %	3.02 %
0.621	Mn1 Nd1 As1 O1	MSG 59.407 ($Pm'mn$)	Mn	2.35	0.01	-	0.12	4.0
			Error(%)		100.09 %	- %	94.98 %	70.21 %
			Mn	2.35	0.01	-	0.12	4.0
			Error(%)		100.09 %	- %	94.98 %	70.21 %
0.622	Mn1 Nd1 As1 O1	MSG 59.407 ($Pm'mn$)	Mn	3.33	0.34	4.0	0.16	4.01
			Error(%)		110.24 %	20.24 %	104.86 %	20.3 %
			Mn	3.33	0.34	4.0	0.16	4.01
			Error(%)		110.24 %	20.24 %	104.86 %	20.3 %
0.623	Mn1 Nd1 As1 O1	MSG 129.416 ($P4'/n'm'm$)	Nd	1.93	2.99	2.95	2.94	2.96
			Error(%)		54.77 %	52.59 %	52.54 %	53.32 %
			Nd	1.93	2.99	2.95	2.94	2.96
			Error(%)		54.77 %	52.59 %	52.54 %	53.32 %
0.656	Nd1 Mn2 Ge2	MSG 44.231 ($Im'm2'$)	Mn	3.72	3.46	3.98	3.99	-
			Error(%)		6.99 %	6.88 %	7.34 %	- %
			Mn	3.72	3.46	3.98	3.99	-
			Error(%)		6.99 %	6.88 %	7.34 %	- %
0.657	Pr1 Mn2 Ge2	MSG 44.231 ($Im'm2'$)	Nd	1.94	2.98	3.01	2.94	-
			Error(%)		53.71 %	55.05 %	51.65 %	- %
			Nd	1.94	2.98	3.01	2.94	-
			Error(%)		53.71 %	55.05 %	51.65 %	- %
0.666	Ce1 Mn1 Sb1 O1	MSG 59.407 ($Pm'mn$)	Mn	2.41	0.01	-	0.14	3.99
			Error(%)		99.96 %	- %	94.11 %	65.56 %
			Mn	2.41	0.01	-	0.14	3.99
			Error(%)		99.96 %	- %	94.11 %	65.56 %
0.656	Nd1 Mn2 Ge2	MSG 44.231 ($Im'm2'$)	Mn	1.86	0.07	3.77	0.24	3.75
			Error(%)		203.69 %	212.32 %	227.25 %	223.09 %
			Mn	1.86	0.06	3.77	0.25	3.75
			Error(%)		203.49 %	212.35 %	227.73 %	223.11 %
0.657	Pr1 Mn2 Ge2	MSG 44.231 ($Im'm2'$)	Mn	2.43	3.06	3.72	3.72	3.71
			Error(%)		90.5 %	133.47 %	131.29 %	145.31 %
			Mn	2.43	3.06	3.73	3.72	3.72
			Error(%)		90.45 %	133.65 %	131.14 %	145.31 %
0.666	Ce1 Mn1 Sb1 O1	MSG 59.407 ($Pm'mn$)	Ce	1.02	0.62	0.79	0.36	0.25
			Error(%)		39.22 %	22.45 %	64.51 %	75.88 %
			Ce	1.02	0.62	0.79	0.36	0.25
			Error(%)		39.22 %	22.45 %	64.51 %	75.88 %

			Mn Error(%)	3.92 8.57 %	3.58 3.62 %	4.06 3.8 %	4.07 3.8 %	4.07 3.8 %
			Mn Error(%)	3.92 8.57 %	3.58 3.62 %	4.06 3.8 %	4.07 3.8 %	4.07 3.8 %
0.668	Pr1 Mn1 Sb1 O1	MSG 59.407 ($Pm'mn$)	Pr Error(%)	2.96 35.88 %	1.9 34.39 %	1.94 40.07 %	1.77 40.1 %	1.77 40.1 %
			Pr Error(%)	2.96 35.88 %	1.9 34.39 %	1.94 40.07 %	1.77 40.1 %	1.77 40.1 %
			Mn Error(%)	3.69 100.98 %	0.04 100.98 %	1.2 132.44 %	4.07 10.38 %	4.07 10.38 %
			Mn Error(%)	3.69 100.98 %	0.04 100.98 %	1.2 132.44 %	4.07 10.38 %	4.07 10.38 %
			Tm Error(%)	1.4 7789.79 %	1.64 15489.21 %	1.73 13871.5 %	1.8 13698.07 %	1.82 13698.07 %
0.671	Sr2 Tm1 Ru1 O6	MSG 14.75 (P_{21}/c)	Tm Error(%)	1.4 7814.79 %	1.64 15489.21 %	1.73 13871.5 %	1.8 13698.07 %	1.82 13698.07 %
			Ru Error(%)	1.5 9413.2 %	1.74 8458.8 %	2.04 2636.27 %	2.05 2636.27 %	2.05 4611.07 %
			Ru Error(%)	1.5 9413.27 %	1.74 8458.8 %	2.04 2636.27 %	2.05 4611.07 %	2.05 4611.07 %
			Tb Error(%)	8.57 99.45 %	0.05 100.6 %	0.05 26.92 %	- - %	- - %
0.700	Tb1 Mn6 Sn6	MSG 191.240 ($P6/mm'm'$)	Mn Error(%)	2.39 0.1 %	2.38 8.21 %	3.57 8.19 %	- - %	- - %
			Tb Error(%)	5.82 97.2 %	0.16 101.62 %	0.09 99.81 %	0.01 111.44 %	0.67 111.44 %
			Mn Error(%)	2.01 3.13 %	2.39 13.16 %	3.6 13.05 %	3.58 13.06 %	3.59 13.06 %
0.703	Ho1 Mn6 Sn6	MSG 12.62 ($C2'/m'$)	Ho Error(%)	8.43 110.79 %	3.76 108.13 %	3.89 - %	- - %	3.22 124.82 %
			Mn Error(%)	2.39 0.32 %	2.41 16.62 %	3.58 - %	- - %	3.59 16.48 %
			Ho Error(%)	5.27 204.48 %	0.18 43.41 %	3.89 - %	- - %	4.23 54.22 %
0.704	Ho1 Mn6 Sn6	MSG 12.62 ($C2'/m'$)	Mn Error(%)	2.18 4.55 %	2.41 23.83 %	3.58 - %	- - %	3.57 19.96 %
			Ho Error(%)	4.68 95.71 %	0.2 16.18 %	3.92 13.63 %	4.04 10.38 %	4.19 10.38 %
			Mn Error(%)	2.18 1.81 %	2.42 10.65 %	3.57 10.67 %	3.58 10.62 %	3.57 10.62 %
0.715	W1 Ho1 Cr1 O6	MSG 33.144 ($Pna2_1$)	Ho Error(%)	8.68 247.8 %	3.68 - %	- 168.24 %	3.88 165.67 %	3.94 165.67 %
			Ho Error(%)	8.68 248.04 %	3.68 - %	- 168.26 %	3.87 165.67 %	3.94 165.67 %
			Ho Error(%)	8.68 124.0 %	3.68 - %	- 84.13 %	3.87 82.84 %	3.94 82.84 %
			Cr Error(%)	2.32 91.77 %	0.29 - %	- 220.17 %	2.8 220.6 %	2.8 220.6 %
			Cr Error(%)	2.32 30.66 %	0.28 - %	- 73.38 %	2.8 73.38 %	2.8 73.52 %
			Er Error(%)	8.7 35.6 %	2.51 35.26 %	2.56 33.95 %	2.79 33.28 %	2.91 33.28 %
0.729	Er1 Ni4 B1	MSG 191.240 ($P6/mm'm'$)	Tb Error(%)	5.7 102.44 %	0.13 104.26 %	0.37 118.84 %	1.22 - %	- - %
0.730	Tb1 Ni4 B1	MSG 12.62 ($C2'/m'$)	Ho Error(%)	6.7 35.21 %	3.64 47.69 %	3.56 42.33 %	3.9 40.48 %	3.97 40.48 %
0.731	Ho1 Ni4 B1	MSG 12.62 ($C2'/m'$)	Fe Error(%)	4.05 65.04 %	1.42 3.21 %	3.92 2.25 %	3.96 2.2 %	3.96 2.2 %
0.758	Ce1 Fe1 O3	MSG 62.441 ($Pnma$)	Fe Error(%)	4.05 21.46 %	1.45 1.07 %	3.92 0.77 %	3.96 0.75 %	3.96 0.75 %
			Ce Error(%)	0.11 393.64 %	0.32 12.73 %	0.1 268.18 %	0.18 90.91 %	0.01 90.91 %
			Ce Error(%)	0.11 393.64 %	0.35 0.09	0.09 0.19	0.19 0.01	0.01 0.01
0.759	Ce1 Fe1 O3	MSG 62.441 ($Pnma$)						

			Error(%)		140.0 %	5.45 %	90.0 %	30.91 %
			Fe	4.17	1.37	3.93	3.96	3.96
			Error(%)		67.36 %	5.9 %	5.16 %	5.04 %
			Fe	4.17	1.4	3.93	3.95	3.96
			Error(%)		22.25 %	1.97 %	1.73 %	1.69 %
0.771	Pr1 Mn1 Si2	MSG 63.464 ($Cm'cm'$)	Mn	2.06	2.01	3.48	3.45	3.44
			Error(%)		1.26 %	34.39 %	33.67 %	33.59 %
0.772	Pr1 Mn1 Si2	MSG 63.464 ($Cm'cm'$)	Mn	1.93	0.45	3.51	3.48	-
			Error(%)		61.61 %	41.04 %	40.1 %	- %
0.773	Nd1 Mn1 Si2	MSG 12.62 ($C2'/m'$)	Nd	1.8	3.14	3.03	3.27	2.96
			Error(%)		9.58 %	33.83 %	40.39 %	30.58 %
0.774	Nd1 Mn1 Si2	MSG 63.464 ($Cm'cm'$)	Mn	2.29	2.13	3.44	3.44	3.43
			Error(%)		98.8 %	49.66 %	49.29 %	49.32 %
0.775	Nd1 Mn1 Si2	MSG 63.464 ($Cm'cm'$)	Mn	2.06	0.02	3.44	3.44	3.43
			Error(%)		50.46 %	33.47 %	33.42 %	33.35 %
0.776	Ce1 Mn1 Si2	MSG 63.464 ($Cm'cm'$)	Ce	0.23	0.38	0.65	-	0.54
			Error(%)		31.52 %	91.96 %	- %	67.61 %
0.777	Ce1 Mn1 Si2	MSG 63.464 ($Cm'cm'$)	Mn	2.24	2.03	3.47	-	3.48
			Error(%)		4.75 %	27.37 %	- %	27.72 %
0.778	Ce1 Mn1 Si2	MSG 63.464 ($Cm'cm'$)	Mn	2.18	2.03	3.44	3.49	3.48
			Error(%)		3.51 %	28.92 %	30.0 %	29.77 %
0.781	Ce1 Mn1 Si2	MSG 63.464 ($Cm'cm'$)	Ce	0.1	0.35	0.57	0.15	0.08
			Error(%)		122.5 %	233.0 %	25.5 %	8.0 %
0.784	Nd1 Co1 O3	MSG 62.441 ($Pnma$)	Mn	2.7	1.99	3.43	3.39	3.45
			Error(%)		13.22 %	13.59 %	12.83 %	13.83 %
0.789	Ce1 Cu1 Si1	MSG 63.463 ($Cmc'm'$)	Nd	1.39	2.82	2.93	-	3.05
			Error(%)		102.81 %	110.72 %	- %	119.28 %
0.791	Sr2 Tb1 Ru1 O6	MSG 14.75 ($P2_1/c$)	Nd	1.39	2.85	2.93	-	3.04
			Error(%)		34.92 %	36.91 %	- %	39.52 %
0.792	Sr2 Ho1 Ru1 O6	MSG 14.75 ($P2_1/c$)	Tb	5.0	5.95	5.89	5.97	6.11
			Error(%)		40.17 %	41.81 %	23.91 %	26.42 %
0.794	Sr2 Ho1 Ru1 O6	MSG 14.75 ($P2_1/c$)	Tb	5.0	5.95	5.89	5.97	6.11
			Error(%)		40.13 %	41.81 %	23.91 %	26.42 %
0.840	Dy1 Fe1 O3	MSG 62.441 ($Pnma$)	Ru	3.0	0.02	2.03	2.06	2.07
			Error(%)		201.87 %	69.25 %	70.98 %	63.03 %
0.841	Dy1 Fe1 O3	MSG 62.441 ($Pnma$)	Ru	3.0	0.02	2.03	2.06	2.07
			Error(%)		202.1 %	69.25 %	70.98 %	63.03 %
			Ho	6.66	0.3	3.82	3.9	3.99
			Error(%)		432.26 %	1457.3 %	298.57 %	1254.71 %
			Ho	6.66	0.28	3.82	3.9	3.99
			Error(%)		432.49 %	1457.3 %	298.57 %	1254.71 %
			Ru	2.74	0.08	2.04	2.05	2.06
			Error(%)		461.12 %	207.26 %	879.73 %	688.64 %
			Ru	2.74	0.07	2.04	2.05	2.06
			Error(%)		452.28 %	207.26 %	879.73 %	688.67 %
			Ho	7.94	0.24	3.85	3.91	4.0
			Error(%)		192.54 %	89.66 %	82.25 %	175.19 %
			Ho	7.94	0.25	3.84	3.91	4.0
			Error(%)		193.45 %	90.03 %	82.25 %	175.2 %
			Ru	1.8	0.06	0.05	2.05	0.26
			Error(%)		215.14 %	207.23 %	66.1 %	210.71 %
			Ru	1.8	0.07	0.06	2.05	0.25
			Error(%)		219.3 %	209.36 %	66.1 %	210.35 %
			Fe	4.0	0.05	3.96	3.97	-
			Error(%)		100.82 %	1.02 %	0.7 %	- %
			Fe	4.0	0.02	3.96	3.97	-
			Error(%)		33.45 %	0.33 %	0.23 %	- %
			Fe	4.0	0.05	3.96	-	1.23
			Error(%)		100.6 %	1.15 %	- %	129.6 %

			Fe Error(%)	4.0 33.4 %	0.02 0.37 %	3.96 -	- - %	1.23 43.21 %
0.867	Ir1 Nd2 Ni1 O6	MSG 14.75 ($P2_1/c$)	Ir Error(%)	0.32 -	- %	0.25 19.53 %	0.28 7.66 %	0.26 89.06 %
			Ni Error(%)	1.71 -	- %	1.56 8.22 %	1.56 7.05 %	1.56 94.06 %
			Ni Error(%)	1.64 394.37 %	1.33 206.98 %	1.37 256.01 %	1.37 89.07 %	1.36
0.869	Ni1 Ir1 Pr2 O6	MSG 14.75 ($P2_1/c$)	Ni Error(%)	1.64 397.76 %	1.36 207.05 %	1.39 257.31 %	1.4 86.53 %	1.39
			Ir Error(%)	0.39 156.35 %	0.25 168.56 %	0.07 138.24 %	0.11 151.74 %	0.13
			Ir Error(%)	0.39 156.32 %	0.25 166.38 %	0.07 134.97 %	0.12 149.47 %	0.13
			Pr Error(%)	1.58 29.14 %	1.71 30.04 %	1.87 30.24 %	1.95 47.02 %	1.95
			Pr Error(%)	1.58 9.72 %	1.71 9.93 %	1.87 10.08 %	1.95 15.65 %	1.95
			Ni Error(%)	1.79 298.45 %	0.01 570.43 %	1.57 121.26 %	1.56 137.17 %	1.56
			Ni Error(%)	1.79 298.08 %	0.01 570.08 %	1.57 121.12 %	1.56 137.35 %	1.56
0.870	Ni1 Ir1 Pr2 O6	MSG 14.75 ($P2_1/c$)	Ir Error(%)	0.59 292.06 %	0.1 464.78 %	0.24 195.63 %	0.29 208.2 %	0.26
			Ir Error(%)	0.59 289.99 %	0.1 462.64 %	0.24 195.99 %	0.29 208.37 %	0.27
			Pr Error(%)	1.21 135.38 %	1.76 154.39 %	1.92 270.26 %	1.95 249.02 %	1.96
			Pr Error(%)	1.21 45.25 %	1.76 51.46 %	1.92 90.36 %	1.95 83.01 %	1.96
			Ni Error(%)	1.84 186.98 %	0.28 123.14 %	1.56 262.67 %	0.59 139.25 %	1.56
			Ni Error(%)	1.84 187.16 %	0.27 123.08 %	1.56 262.36 %	0.58 139.37 %	1.56
0.871	Ni1 Ir1 Pr2 O6	MSG 14.75 ($P2_1/c$)	Ir Error(%)	0.45 179.06 %	0.18 122.81 %	0.25 224.69 %	0.16 136.56 %	0.24
			Ir Error(%)	0.45 179.38 %	0.18 123.13 %	0.25 225.0 %	0.17 136.88 %	0.25
			Pr Error(%)	0.41 654.57 %	1.78 768.57 %	1.91 747.62 %	1.85 711.71 %	1.96
			Pr Error(%)	0.41 217.94 %	1.77 256.19 %	1.91 248.51 %	1.85 237.24 %	1.96
			Ni Error(%)	1.62 205.08 %	0.04 71.8 %	1.56 428.9 %	1.57 22.64 %	1.57
			Ni Error(%)	1.62 205.08 %	0.04 71.8 %	1.56 428.75 %	1.57 22.93 %	1.57
0.872	Ni1 Ir1 Pr2 O6	MSG 14.75 ($P2_1/c$)	Ir Error(%)	0.43 185.42 %	0.04 119.31 %	0.27 282.08 %	0.22 201.11 %	0.07
			Ir Error(%)	0.43 185.42 %	0.04 120.28 %	0.27 280.83 %	0.22 202.5 %	0.07
			Pr Error(%)	0.18 165.35 %	0.04 2216.04 %	1.91 2012.78 %	1.95 2208.96 %	1.96
			Pr Error(%)	0.18 57.64 %	0.04 738.47 %	1.91 671.3 %	1.95 736.32 %	1.96
			Ni Error(%)	1.54 166.86 %	0.29 137.79 %	1.56 330.28 %	1.57 204.6 %	0.06
			Ni Error(%)	1.54 165.74 %	0.3 137.86 %	1.56 330.28 %	1.57 205.41 %	0.07
0.873	Ni1 Ir1 Pr2 O6	MSG 14.75 ($P2_1/c$)	Ir Error(%)	0.41 164.23 %	0.09 140.08 %	0.24 257.1 %	0.16 162.8 %	0.31
			Ir Error(%)	0.41 164.37 %	0.09 140.22 %	0.24 256.09 %	0.16 164.99 %	0.32
			Pr Error(%)	0.15 57.64 %	0.08 738.47 %	1.91 671.3 %	1.95 736.32 %	1.96
			Ni Error(%)	1.54 166.86 %	0.29 137.79 %	1.56 330.28 %	1.57 204.6 %	0.06
			Ni Error(%)	1.54 165.74 %	0.3 137.86 %	1.56 330.28 %	1.57 205.41 %	0.07

			Error(%)		311.21 %	2852.09 %	2107.58 %	2760.66 %
			Pr	0.15	0.08	1.91	1.95	1.96
			Error(%)		103.48 %	951.17 %	702.27 %	920.22 %
0.874	Ni1 Ir1 Nd2 O6	MSG 14.75 (P_{21}/c)	Ni	1.55	1.41	1.59	1.58	1.58
			Error(%)		98.36 %	19.55 %	448.07 %	172.58 %
			Ni	1.55	1.41	1.58	1.58	1.58
			Error(%)		97.7 %	20.34 %	448.58 %	172.15 %
			Ir	0.48	0.17	0.4	0.24	0.27
			Error(%)		178.12 %	175.72 %	169.54 %	211.72 %
0.875	Ni1 Ir1 Nd2 O6	MSG 14.75 (P_{21}/c)	Ir	0.48	0.17	0.4	0.24	0.27
			Error(%)		178.35 %	176.55 %	169.63 %	211.83 %
			Nd	0.56	2.88	2.93	2.94	2.95
			Error(%)		103.71 %	105.45 %	105.89 %	105.04 %
			Ni	0.93	1.47	1.59	1.59	1.58
			Error(%)		380.01 %	267.9 %	641.27 %	201.95 %
0.897	Tb1 Mn2 Ge2	MSG 139.537 ($I4/mm'm'$)	Ni	0.93	1.47	1.59	1.58	1.58
			Error(%)		380.11 %	267.18 %	639.35 %	201.5 %
			Ir	0.44	0.35	0.34	0.33	0.25
			Error(%)		108.06 %	142.69 %	102.5 %	215.14 %
			Ir	0.44	0.35	0.34	0.33	0.25
			Error(%)		107.75 %	143.61 %	104.17 %	215.0 %
0.902	Dy1 Mn2 Ge2	MSG 139.537 ($I4/mm'm'$)	Nd	0.27	2.88	2.93	2.94	2.95
			Error(%)		240.0 %	244.17 %	243.98 %	246.57 %
			Tb	8.8	0.42	1.44	6.0	6.05
			Error(%)		95.18 %	116.39 %	31.84 %	31.31 %
			Mn	2.2	2.31	1.22	3.61	3.61
			Error(%)		2.55 %	22.2 %	32.11 %	31.95 %
0.910	Ni1 Si2 Tb1	MSG 63.459 ($Cm'cm$)	Dy	10.2	0.02	4.64	4.78	4.99
			Error(%)		100.11 %	54.5 %	53.13 %	51.11 %
			Mn	2.3	2.32	0.88	3.66	3.65
			Error(%)		0.46 %	30.98 %	29.65 %	29.3 %
			Tb	8.7	5.81	5.88	5.97	6.01
			Error(%)		33.25 %	32.47 %	31.44 %	30.87 %
0.919	Eu1 Mn1 Bi2	MSG 139.536 ($I4'/m'm'm'$)	Tb	8.7	5.81	5.88	5.97	6.01
			Error(%)		33.25 %	32.47 %	31.44 %	30.87 %
			Mn	2.1	0.12	4.18	4.17	4.16
			Error(%)		94.19 %	98.86 %	98.62 %	97.86 %
			Mn	2.1	0.12	4.18	4.17	4.15
			Error(%)		94.19 %	98.86 %	98.62 %	97.81 %
0.920	N1 P1 Mn1 Th1	MSG 129.416 ($P4'/n'm'm'$)	Mn	2.69	-	3.91	-	3.9
			Error(%)		- %	245.28 %	- %	245.09 %
			Mn	2.69	-	3.91	-	3.9
			Error(%)		- %	245.28 %	- %	245.09 %
			Mn	2.3	-	4.02	-	4.01
			Error(%)		- %	274.65 %	- %	274.52 %
0.922	N1 As1 Mn1 Th1	MSG 129.416 ($P4'/n'm'm'$)	Mn	2.3	-	4.02	-	4.01
			Error(%)		- %	274.65 %	- %	274.52 %
			Mn	2.3	-	4.02	-	4.01
			Error(%)		- %	274.65 %	- %	274.52 %
			Mn	3.41	3.53	4.01	-	4.01
			Error(%)		203.55 %	17.54 %	- %	17.45 %
0.923	N1 As1 Mn1 Th1	MSG 129.416 ($P4'/n'm'm'$)	Mn	3.41	3.53	4.01	-	4.01
			Error(%)		203.55 %	17.54 %	- %	17.45 %
			Mn	3.41	3.53	4.01	-	4.01
			Error(%)		203.55 %	17.54 %	- %	17.45 %
			Yb	0.57	0.0	0.49	0.56	0.64
			Error(%)		75.45 %	10.53 %	2.05 %	8.79 %
0.944	Yb2 Ir2 O7	MSG 166.101 ($R\bar{3}m'$)	Ir	0.44	0.0	0.05	0.05	0.44
			Error(%)		300.79 %	262.6 %	264.57 %	4.33 %
			Ir	0.44	0.0	0.05	0.09	0.43
			Error(%)		299.61 %	309.06 %	329.92 %	13.39 %
			Ir	0.44	0.0	0.06	0.09	0.43
			Error(%)		150.0 %	154.92 %	164.17 %	7.09 %
0.945	Yb2 Ir2 O7	MSG 227.131 ($Fd\bar{3}m'$)	Ir	0.4	0.0	0.0	0.42	0.43
			Error(%)		300.0 %	297.83 %	15.65 %	22.17 %
			Ir	0.4	0.0	0.0	0.42	0.43
			Error(%)		300.0 %	297.39 %	16.96 %	23.48 %

			Ir Error(%)	0.4 150.0 %	0.0 149.13 %	0.0 7.17 %	0.42 11.74 %	0.43
0.954	Nd2 Ir2 O7	MSG 227.131 ($Fd\bar{3}m'$)	Nd Error(%)	1.27 386.77 %	2.91 392.77 %	2.93 396.73 %	2.95 397.82 %	2.95
			Nd Error(%)	1.27 387.59 %	2.91 391.81 %	2.93 396.86 %	2.95 397.82 %	2.95
			Nd Error(%)	1.27 192.7 %	2.9 197.0 %	2.94 198.29 %	2.95 198.91 %	2.95
			Ir Error(%)	0.34 272.31 %	0.03 29.23 %	0.37 75.38 %	0.42 318.97 %	0.02
			Ir Error(%)	0.34 270.26 %	0.03 29.23 %	0.37 76.41 %	0.42 318.46 %	0.02
			Ir Error(%)	0.34 137.44 %	0.03 15.64 %	0.37 38.72 %	0.43 159.49 %	0.02
			Pr Error(%)	3.0 34.23 %	1.97 34.27 %	1.97 34.27 %	1.97 90.17 %	0.3
0.970	Pr1 Ru2 Si2	MSG 139.537 ($I4/mm'm'$)	Er Error(%)	5.2 17.64 %	2.45 16.75 %	2.59 15.97 %	2.71 14.76 %	2.9
0.978	Er1 In1 Ni1	MSG 189.225 ($P\bar{6}2'm'$)	V Error(%)	1.25 100.08 %	0.0 99.92 %	0.01 100.24 %	0.01 110.16 %	0.27
			V Error(%)	1.25 33.33 %	0.0 33.39 %	0.01 33.49 %	0.01 36.64 %	0.27
0.979	Tm1 V1 O3	MSG 62.446 ($Pn'm'a$)	V Error(%)	1.3 100.08 %	0.0 101.69 %	0.03 - %	- % - %	- %
			V Error(%)	1.3 33.36 %	0.0 33.97 %	0.03 - %	- % - %	- %
0.980	Tm1 V1 O3	MSG 62.446 ($Pn'm'a$)	Tm Error(%)	2.15 99.95 %	0.02 96.14 %	0.08 30.79 %	1.49 15.77 %	1.81
			Tm Error(%)	2.15 33.43 %	0.02 32.19 %	0.07 10.29 %	1.49 5.26 %	1.81
			V Error(%)	1.3 100.15 %	0.0 98.54 %	0.03 115.77 %	0.26 25.77 %	1.8
			V Error(%)	1.3 33.41 %	0.0 33.28 %	0.03 39.21 %	0.28 8.74 %	1.79
0.981	Tm1 V1 O3	MSG 62.441 ($Pnma$)	V Error(%)	1.0 202.18 %	0.01 205.57 %	0.05 200.82 %	0.01 - %	- %
			V Error(%)	1.0 67.23 %	0.01 69.89 %	0.06 66.8 %	0.01 - %	- %
0.982	Tm1 V1 O3	MSG 14.75 (P_{21}/c)	V Error(%)	0.99 99.6 %	0.01 104.14 %	0.05 - %	- % 200.71 %	1.8
			V Error(%)	0.99 33.13 %	0.01 33.74 %	0.02 - %	- % 67.14 %	1.83
1.272	Ce1 Ni1 As1 O1	MSG 4.10 (P_a2_1)	Ce Error(%)	0.37 102.39 %	0.17 181.52 %	0.04 414.03 %	0.91 139.33 %	0.44
			Ce Error(%)	0.37 101.03 %	0.18 180.15 %	0.04 414.03 %	0.91 138.88 %	0.44
			Ce Error(%)	0.37 76.14 %	0.11 108.24 %	0.04 354.27 %	0.93 57.39 %	0.22
1.292	Ho1 Ni2 B2 C1	MSG 64.480 (C_Amca)	Ho Error(%)	9.16 122.58 %	3.55 123.72 %	3.5 - %	- % - %	- %
			Ho Error(%)	9.16 122.58 %	3.55 123.72 %	3.5 - %	- % - %	- %
1.293	Nd1 Ni2 B2 C1	MSG 15.90 (C_c2/c)	Nd Error(%)	2.1 36.19 %	3.04 42.1 %	2.99 - %	- % - %	- %
			Nd Error(%)	2.1 36.0 %	3.03 42.1 %	2.99 - %	- % - %	- %
1.294	Ho1 Ni2 B2 C1	MSG 64.480 (C_Amca)	Ho Error(%)	8.62 117.74 %	3.55 112.06 %	3.79 - %	- % - %	- %
			Ho Error(%)	8.62 117.74 %	3.55 112.06 %	3.79 - %	- % - %	- %
1.295	Dy1 Ni2 B2 C1	MSG 64.480 (C_Amca)	Dy Error(%)	8.47 90.27 %	4.65 86.14 %	4.82 - %	- % - %	- %
			Dy Error(%)	8.47 90.27 %	4.65 86.14 %	4.82 - %	- % - %	- %

			Error(%)		90.27 %	86.14 %	- %	- %
1.296	Pr1 Ni2 B2 C1	MSG 64.480 ($C_A mca$)	Pr	0.81	1.81	1.94	1.93	1.96
			Error(%)		248.6 %	280.88 %	280.0 %	285.09 %
			Pr	0.81	1.81	1.94	1.93	1.96
			Error(%)		248.6 %	280.88 %	280.0 %	285.09 %
1.312	Ho1 Ni2 B2 C1	MSG 64.480 ($C_A mca$)	Ho	9.16	3.55	3.5	-	-
			Error(%)		61.23 %	61.84 %	- %	- %
			Ho	9.16	3.55	3.5	-	-
			Error(%)		61.23 %	61.84 %	- %	- %
1.350	Ba1 Nd2 Co1 O5	MSG 15.90 ($C_{c2/c}$)	Nd	2.55	2.96	2.92	2.94	2.94
			Error(%)		16.12 %	32.04 %	14.63 %	15.37 %
			Nd	2.55	2.96	2.92	2.94	2.94
			Error(%)		5.39 %	10.68 %	4.88 %	5.12 %
			Co	3.08	0.13	2.55	2.54	2.55
			Error(%)		177.7 %	184.52 %	105.3 %	113.43 %
1.363	Tb1 Cu2 Si2	MSG 2.7 ($P_S\bar{I}$)	Co	3.08	0.13	2.55	2.54	2.55
			Error(%)		177.43 %	184.52 %	105.3 %	113.43 %
			Tb	8.5	5.77	5.9	5.95	6.01
			Error(%)		334.53 %	54.5 %	54.62 %	46.15 %
1.364	Ho1 Cu2 Si2	MSG 2.7 ($P_S\bar{I}$)	Tb	8.5	5.77	5.89	5.96	6.01
			Error(%)		87.29 %	97.21 %	55.9 %	45.55 %
			Ho	8.81	3.57	3.69	3.51	3.92
			Error(%)		118.49 %	104.81 %	109.33 %	102.84 %
1.365	Cu2 Si2 Tb1	MSG 2.7 ($P_S\bar{I}$)	Ho	8.81	3.57	3.68	3.77	3.92
			Error(%)		119.37 %	88.85 %	84.28 %	105.98 %
			Tb	8.6	0.58	5.91	5.96	6.01
			Error(%)		202.38 %	62.63 %	61.46 %	60.25 %
1.366	Cu2 Ho1 Si2	MSG 12.63 ($C_{c2/m}$)	Tb	8.6	0.7	5.91	5.96	6.01
			Error(%)		185.1 %	62.6 %	61.45 %	60.26 %
			Ho	6.5	3.57	3.5	3.66	3.92
			Error(%)		45.14 %	46.17 %	43.68 %	39.72 %
1.369	Ho1 Fe2 Ge2	MSG 64.480 ($C_A mca$)	Ho	6.5	3.56	3.62	3.7	3.9
			Error(%)		45.17 %	44.34 %	43.06 %	39.92 %
			Ho	6.6	3.55	3.59	3.62	3.62
			Error(%)		46.27 %	45.59 %	45.2 %	45.09 %
1.487	Ce1 Ir1 Al4 Si2	MSG 124.360 (P_c4/mcc)	Ho	6.6	3.55	3.59	3.61	3.62
			Error(%)		46.27 %	45.58 %	45.26 %	45.09 %
			Ce	1.41	-	-	0.75	0.04
			Error(%)		- %	- %	46.67 %	96.95 %
1.488	Ce1 Mn2 Si2	MSG 126.386 (P_I4/nnc)	Ce	1.41	-	-	0.75	0.04
			Error(%)		- %	- %	46.67 %	96.95 %
			Mn	2.3	1.88	2.52	2.52	2.55
			Error(%)		9.15 %	4.8 %	4.67 %	5.41 %
1.489	Ce1 Mn2 Si2	MSG 126.386 (P_I4/nnc)	Mn	2.3	1.88	2.52	2.52	2.55
			Error(%)		9.15 %	4.8 %	4.67 %	5.41 %
			Mn	2.01	1.99	3.38	3.4	-
			Error(%)		0.5 %	34.03 %	34.5 %	- %
1.491	Pr1 Mn2 Si2	MSG 126.386 (P_I4/nnc)	Mn	2.01	1.99	3.38	3.4	-
			Error(%)		0.5 %	34.03 %	34.5 %	- %
			Mn	2.48	-	3.49	3.49	3.49
			Error(%)		- %	20.26 %	20.36 %	20.4 %
1.492	Pr1 Mn2 Si2	MSG 126.386 (P_I4/nnc)	Mn	2.48	-	3.49	3.49	3.49
			Error(%)		- %	20.26 %	20.38 %	20.4 %
			Mn	2.03	2.08	3.47	3.47	3.48
			Error(%)		1.33 %	35.47 %	35.47 %	35.64 %
1.493	Pr1 Mn2 Si2	MSG 126.386 (P_I4/nnc)	Mn	2.03	2.08	3.47	3.47	3.48
			Error(%)		1.33 %	35.47 %	35.47 %	35.64 %
			Mn	1.92	-	3.41	3.42	3.42
			Error(%)		- %	38.83 %	38.98 %	39.09 %
1.494	Nd1 Mn2 Si2	MSG 126.386 (P_I4/nnc)	Mn	2.57	0.02	3.32	3.27	3.28
			Error(%)		50.0 %	14.49 %	13.58 %	13.81 %

			Mn Error(%)	2.57 50.0 %	0.02 14.49 %	3.32 13.58 %	3.27 13.81 %	3.28
1.504	Gd1 Cu1 Sn1	MSG 33.154 (P_Cna2_1)	Gd Error(%)	6.0 49.97 %	0.0 49.97 %	0.0 49.97 %	0.0 49.97 %	0.0
			Gd Error(%)	6.0 50.03 %	0.0 50.03 %	0.0 50.03 %	0.0 50.03 %	0.0
			Tb Error(%)	8.8 98.08 %	0.17 32.64 %	5.93 31.98 %	5.99 31.61 %	6.02
1.511	Ni2 Tb1 Si2	MSG 64.480 (C_{Amca})	Tb Error(%)	8.8 98.08 %	0.17 32.64 %	5.93 31.98 %	5.99 31.61 %	6.02
			Er Error(%)	8.7 - %	- 69.38 %	2.66 67.47 %	2.83 66.41 %	2.92
			Er Error(%)	8.7 - %	- 69.38 %	2.66 67.47 %	2.83 66.41 %	2.92
1.516	Er1 Co2 Si2	MSG 58.404 (P_{Innm})	U Error(%)	0.92 - %	- 140.52 %	1.56 89.52 %	1.33 - %	-
			U Error(%)	0.92 - %	- 20.07 %	1.56 12.79 %	1.33 - %	-
			Yb Error(%)	1.0 119.1 %	0.19 46.6 %	0.53 - %	- 36.9 %	0.63
1.566	Ba2 Yb1 Ru1 O6	MSG 128.410 ($P_{I4/mnc}$)	Yb Error(%)	1.0 119.1 %	0.19 46.6 %	0.53 - %	- 36.9 %	0.63
			Ru Error(%)	2.57 100.0 %	0.0 25.49 %	1.92 - %	- 26.38 %	1.89
			Ru Error(%)	2.57 100.0 %	0.0 25.49 %	1.92 - %	- 26.38 %	1.89
			Tm Error(%)	1.91 95.97 %	0.08 23.51 %	1.46 11.31 %	1.69 8.59 %	1.75
			Tm Error(%)	1.91 95.97 %	0.08 23.51 %	1.46 11.31 %	1.69 8.59 %	1.75
1.567	Ba2 Tm1 Ru1 O6	MSG 128.410 ($P_{I4/mnc}$)	Ru Error(%)	2.13 104.32 %	0.09 6.06 %	2.0 6.43 %	1.99 5.68 %	2.01
			Ru Error(%)	2.13 104.32 %	0.09 6.06 %	2.0 6.43 %	1.99 5.68 %	2.01
			Gd Error(%)	7.2 100.0 %	0.0 100.0 %	0.0 100.0 %	0.0 100.0 %	0.0
			Gd Error(%)	7.2 100.0 %	0.0 100.0 %	0.0 100.0 %	0.0 100.0 %	0.0
			Pr Error(%)	0.84 116.31 %	0.14 128.81 %	1.92 132.5 %	1.95 134.64 %	1.97
1.584	Pr1 Fe1 As1 O1	MSG 54.350 (P_{Bcca})	Pr Error(%)	0.84 38.69 %	0.14 42.98 %	1.92 44.17 %	1.95 45.08 %	1.98
			Fe Error(%)	0.48 103.54 %	0.02 50.62 %	0.24 149.79 %	0.24 481.04 %	2.79
			Fe Error(%)	0.48 34.79 %	0.02 17.36 %	0.23 50.42 %	0.25 160.63 %	2.79
			Fe Error(%)	0.35 679.71 %	2.03 146.0 %	0.16 171.43 %	0.25 168.29 %	0.24
			Fe Error(%)	0.35 226.95 %	2.03 49.05 %	0.17 57.81 %	0.26 56.76 %	0.25
1.586	Pr1 Fe1 As1 O1	MSG 27.85 (P_{Acc2})	Pr Error(%)	1.0 40.25 %	1.82 47.1 %	1.95 44.7 %	1.94 47.75 %	1.96
			Pr Error(%)	1.0 43.25 %	1.88 47.7 %	1.97 44.75 %	1.94 47.65 %	1.95
			Fe Error(%)	0.5 26.0 %	0.37 97.0 %	0.02 459.6 %	2.8 135.6 %	0.18
			Fe Error(%)	0.5 8.2 %	0.38 31.87 %	0.02 153.2 %	2.8 44.53 %	0.17
			Tb Error(%)	7.8 26.52 %	5.73 25.81 %	5.79 23.57 %	5.96 23.02 %	6.0
1.596	Tb1 Cu1 Sb2	MSG 2.7 ($P_S\bar{1}$)	Tb Error(%)	7.8 26.58 %	5.73 26.48 %	5.73 24.35 %	5.96 23.02 %	6.0
			Pr	2.35	1.96	2.04	1.97	1.97

			Error(%)		16.6 %	13.06 %	16.26 %	16.21 %
			Pr	2.35	1.96	2.04	1.97	1.97
			Error(%)		5.53 %	4.35 %	5.42 %	5.4 %
			Mn	2.04	2.1	3.45	3.46	3.46
			Error(%)		3.14 %	69.31 %	69.36 %	69.66 %
			Mn	2.04	2.1	3.45	3.46	3.46
			Error(%)		1.05 %	23.1 %	23.12 %	23.22 %
1.635	Er1 Fe2 Si2	MSG 62.450 (P_{anma})	Er	7.4	2.55	2.69	2.84	2.92
			Error(%)		65.54 %	63.64 %	61.62 %	60.5 %
			Er	7.4	2.55	2.69	2.84	2.92
			Error(%)		21.85 %	21.21 %	20.54 %	20.17 %
1.636	Er1 Mn2 Si2	MSG 126.386 ($P_{I4/nnc}$)	Mn	2.17	0.02	2.57	2.58	2.59
			Error(%)		50.07 %	9.15 %	9.35 %	9.77 %
			Mn	2.17	0.02	2.57	2.58	2.59
			Error(%)		50.07 %	9.15 %	9.35 %	9.77 %
1.637	Er1 Mn2 Si2	MSG 126.386 ($P_{I4/nnc}$)	Mn	2.24	0.02	2.58	2.58	2.59
			Error(%)		50.04 %	7.48 %	7.57 %	7.88 %
			Mn	2.24	0.02	2.58	2.58	2.59
			Error(%)		50.04 %	7.48 %	7.57 %	7.88 %
1.638	Er1 Mn2 Ge2	MSG 126.386 ($P_{I4/nnc}$)	Mn	1.7	0.02	0.91	3.48	3.44
			Error(%)		50.0 %	76.71 %	52.35 %	51.21 %
			Mn	1.7	0.02	0.91	3.48	3.44
			Error(%)		50.0 %	76.79 %	52.35 %	51.21 %
1.639	Er1 Mn2 Ge2	MSG 126.386 ($P_{I4/nnc}$)	Mn	2.2	0.02	0.1	3.46	3.43
			Error(%)		49.95 %	51.86 %	28.57 %	27.95 %
			Mn	2.2	0.02	0.1	3.46	3.43
			Error(%)		49.95 %	51.84 %	28.57 %	27.95 %
1.640	Er1 Mn2 Ge2	MSG 126.386 ($P_{I4/nnc}$)	Mn	2.21	0.02	0.02	3.59	3.6
			Error(%)		50.0 %	49.46 %	31.11 %	31.45 %
			Mn	2.21	0.02	0.02	3.59	3.6
			Error(%)		50.0 %	49.46 %	31.11 %	31.45 %
1.664	Dy1 V1 O4	MSG 62.456 (P_{Inma})	Dy	9.0	4.8	4.87	4.91	4.99
			Error(%)		46.66 %	45.86 %	45.43 %	44.61 %
			Dy	9.0	4.8	4.87	4.91	4.98
			Error(%)		15.54 %	15.29 %	15.15 %	14.88 %
1.666	Tb1 Co1 Ga5	MSG 67.509 (C_{amma})	Tb	8.32	0.35	5.81	5.99	5.72
			Error(%)		104.17 %	30.18 %	28.02 %	31.2 %
			Tb	8.32	0.34	5.81	5.99	5.72
			Error(%)		104.13 %	30.18 %	28.02 %	31.2 %
1.668	Ho1 Co1 Ga5	MSG 67.509 (C_{amma})	Ho	8.6	3.55	3.68	3.76	3.94
			Error(%)		58.74 %	57.2 %	56.33 %	54.23 %
			Ho	8.6	3.55	3.68	3.76	3.94
			Error(%)		58.74 %	57.2 %	56.33 %	54.23 %
1.670	Np1 Fe1 Ga5	MSG 67.509 (C_{amma})	Np	0.86	0.0	3.43	0.11	3.77
			Error(%)		100.0 %	298.6 %	87.56 %	338.49 %
			Np	0.86	0.0	3.43	0.12	3.77
			Error(%)		100.0 %	298.6 %	86.98 %	338.49 %
1.683	Ga5 Ni1 U1	MSG 140.550 ($I_{c4/mcm}$)	Fe	0.24	0.0	0.27	0.03	0.14
			Error(%)		97.92 %	13.75 %	86.25 %	42.92 %
			Fe	0.24	0.0	0.27	0.03	0.14
			Error(%)		97.92 %	13.75 %	89.58 %	42.92 %
1.690	Tm1 Mn2 Ge2	MSG 126.386 ($P_{I4/nnc}$)	U	0.75	1.6	2.12	2.38	2.57
			Error(%)		113.87 %	182.67 %	217.87 %	243.2 %
			U	0.75	1.6	2.12	2.38	2.57
			Error(%)		113.87 %	182.67 %	217.87 %	243.2 %
1.694	Mn2 Tb1 Ge2	MSG 126.386 ($P_{I4/nnc}$)	Mn	2.19	2.27	3.48	3.48	3.47
			Error(%)		1.87 %	29.41 %	29.36 %	29.13 %
			Mn	2.19	2.27	3.48	3.48	3.47
			Error(%)		1.87 %	29.41 %	29.36 %	29.13 %
1.694	Mn2 Tb1 Ge2	MSG 126.386 ($P_{I4/nnc}$)	Mn	2.1	2.17	3.44	3.44	3.45
			Error(%)		1.71 %	31.98 %	31.83 %	32.07 %
			Mn	2.1	2.17	3.44	3.44	3.45
			Error(%)		1.71 %	31.98 %	31.83 %	32.07 %

1.721	U1 Cu5	MSG 161.72 (R_I3c)	U Error(%)	0.9	0.05 317.31 %	1.55 215.38 %	2.25 449.04 %	2.47 524.23 %
			U Error(%)	0.9	0.06 280.0 %	1.51 203.27 %	2.26 451.35 %	2.47 523.27 %
1.729	Gd2 Fe2 Si2 C1	MSG 12.63 (C_c2/m)	Gd Error(%)	6.2	0.0 50.0 %	0.0 49.99 %	0.0 49.99 %	0.0 49.99 %
			Gd Error(%)	6.2	0.0 50.0 %	0.0 50.01 %	0.0 50.01 %	0.0 50.01 %
1.738	Tb1 Al1 Ni1	MSG 46.247 ($I_a ma2$)	Tb Error(%)	7.9	5.83 26.18 %	5.95 24.67 %	6.03 23.72 %	- - %
			Tb Error(%)	7.9	5.87 8.57 %	5.95 8.24 %	6.02 7.92 %	- - %
			Tb Error(%)	1.2	5.83 386.17 %	0.82 31.75 %	0.02 101.5 %	- - %
			Tb Error(%)	1.2	5.83 385.75 %	0.82 31.75 %	0.02 101.75 %	- - %
			Er Error(%)	7.3	2.47 33.09 %	2.64 31.95 %	2.78 30.95 %	2.9 30.17 %
2.81	Er1 Mn2 Si2	MSG 59.409 ($Pm'm'n$)	Mn Error(%)	2.3	1.93 16.13 %	2.48 7.65 %	2.45 6.48 %	2.44 6.04 %
			Mn Error(%)	2.3	1.93 5.43 %	2.47 2.49 %	2.45 2.1 %	2.44 1.97 %
			Er Error(%)	8.9	2.51 35.92 %	0.28 51.55 %	2.78 34.39 %	2.9 33.69 %
2.82	Er1 Mn2 Si2	MSG 59.409 ($Pm'm'n$)	Mn Error(%)	2.3	1.93 17.57 %	2.49 7.43 %	2.46 6.91 %	2.44 6.22 %
			Mn Error(%)	2.3	1.92 5.97 %	2.49 2.48 %	2.46 2.26 %	2.44 2.04 %
			Er Error(%)	7.7	2.47 33.99 %	2.64 32.88 %	0.16 51.01 %	- - %
2.83	Er1 Mn2 Ge2	MSG 59.409 ($Pm'm'n$)	Mn Error(%)	2.3	2.22 4.26 %	2.85 23.91 %	3.37 46.35 %	- - %
			Mn Error(%)	2.3	2.21 1.51 %	2.84 7.88 %	3.37 15.45 %	- - %
			Er Error(%)	6.81	2.47 31.84 %	2.59 30.96 %	2.75 29.83 %	- - %
2.84	Er1 Mn2 Ge2	MSG 59.409 ($Pm'm'n$)	Mn Error(%)	2.34	2.35 0.47 %	3.62 54.83 %	3.61 54.15 %	- - %
			Mn Error(%)	2.34	2.34 0.04 %	3.62 18.26 %	3.6 17.99 %	- - %
			Tm Error(%)	6.63	0.06 99.74 %	- - %	1.32 82.31 %	- - %
2.94	Tm1 Mn2 Ge2	MSG 26.70 ($Pm'c'2_1$)	Tm Error(%)	6.63	0.06 33.25 %	- - %	1.33 27.44 %	- - %
			Mn Error(%)	2.28	2.28 17.51 %	- - %	3.49 97.04 %	- - %
			Mn Error(%)	2.28	2.28 5.79 %	- - %	3.5 32.39 %	- - %
			Mn Error(%)	2.28	2.28 1.89 %	- - %	3.49 23.65 %	- - %
			Mn Error(%)	2.3	0.02 49.65 %	3.43 29.07 %	3.45 24.96 %	3.45 25.0 %
3.20	Mn2 Tb1 Ge2	MSG 2.4 ($P\bar{I}$)	Mn Error(%)	2.3	0.01 16.72 %	3.42 35.43 %	3.45 8.33 %	3.46 8.37 %
			Tb Error(%)	9.38	0.23 147.02 %	5.92 57.94 %	5.98 55.45 %	6.0 56.08 %
			Tb Error(%)	9.38	0.12 151.33 %	5.9 197.15 %	5.98 55.5 %	6.0 56.59 %

TAB. S4: Magnetic momenta prediction of materials with both d and f electrons. In the first, second and third columns, we list the BCSID, chemical formula and MSG of each compound. In columns 4 and 5, we show the label of each magnetic atom in the structure and the experimentally measured magnetic momenta. In columns 6-9, we list the computed magnetizations per independent atom and the relative error (see Eq. C1 as function of the Hubbard U parameter).

Appendix D: Topological classification and gap

The topological phase diagram with gap information is illustrated herein. Similar to the previous table, in this table we list the BCS ID, chemical formula and MSG of the materials in the first three columns. Thereafter, we present the topological diagnosis of the system, as well as the electronic gaps in eV; first the indirect and second the smallest direct gaps. Notice that a negative sign in the indirect denotes a metallic system. We tabulate these results as a function of the Hubbard U parameter. In Table S5 we show the described information for compounds with only d electrons, in Table S6 we display the compounds with only f electrons and in Table S7 we show compounds with both d and f electrons. If the gap between the last valence and first conduction bands is small, we denote these systems as accidental Fermi degeneracies (AF). Since the topology is very sensitive to band inversions, we cannot confidently predict the topological phase of the system.

BCS ID	Formula	MSG	U=0	U=1	U=2	U=3	U=4
0.229	Ba2 Mn1 Si2 O7	MSG 113.267 ($P\bar{4}2_1m$)	AI 2.212 2.235	AI 2.566 2.599	AI 2.861 2.906	AI 3.12 3.179	AI 3.346 3.422
0.230	K2 Co1 P2 O7	MSG 58.395 ($Pn'nm$)	AI 1.112 1.14	AI 1.813 1.838	AI 2.507 2.531	AI 3.176 3.198	AI 3.797 3.817
0.234	Mn2 La1 Sb1 O6	MSG 13.69 ($P2'/c'$)	AI -0.028 0.004	AI 1.504 1.848	AI 1.068 1.088	AI 1.517 1.537	AI 2.068 2.578
0.236	Ca1 Fe4 Al8	MSG 139.535 ($I4'/mmm'$)	ES -0.306 0.002	ES -0.578 0.002	ES -0.724 0.006	-0.896 0.009	-0.882 0.007
0.239	Ca3 Li1 Ru1 O6	MSG 15.89 ($C2'/c'$)	AI 0.854 0.865	AI 1.169 1.179	AI 1.473 1.48	AI 1.767 1.772	AI 2.05 2.054
0.254	Cu1 O6 C4 H9 N3	MSG 33.144 ($Pna2_1$)	AI -0.052 0.001	AI -0.052 0.0	AI -0.05 0.001	-0.049 0.001	-0.048 0.0
0.258	Fe2 P3 O12 Li3	MSG 14.79 ($P2'_1/c'$)	AI 1.085 1.097	AI 1.486 1.493	AI 1.824 1.827	AI 2.122 2.124	AI 2.394 2.394
0.260	Cu1 Fe1 P1 O5	MSG 62.441 ($Pnma$)	AI 0.573 0.653	AI 0.894 0.961	AI 1.235 1.291	AI 1.587 1.635	AI 1.945 1.986
0.261	Ni1 Fe1 P1 O5	MSG 62.441 ($Pnma$)	AI 0.52 0.53	AI 0.971 0.977	AI 1.408 1.414	AI 1.812 1.829	AI 2.19 2.22
0.262	Co1 Fe1 P1 O5	MSG 62.447 ($Pnm'a'$)	AI 0.385 0.407	AI 0.893 0.894	AI 1.354 1.356	AI 1.804 1.814	AI 2.197 2.208
0.263	Fe2 P1 O5	MSG 62.441 ($Pnma$)	AI 0.117 0.128	AI 0.311 0.345	AI 0.523 0.565	AI 0.913 0.957	AI 1.399 1.425
0.264	Fe3 P2 O8	MSG 14.78 ($P2_1/c'$)	AI 0.363 0.376	AI 0.908 0.915	AI 1.53 1.536	AI 2.18 2.186	AI 2.846 2.852
0.266	Na2 Ba1 Mn1 V2 O8	MSG 164.89 ($P\bar{3}m'1$)	AI 1.338 1.354	AI 1.837 1.849	AI 2.304 2.317	AI 2.75 2.765	AI 3.179 3.196
0.273	Mn3 Zn1 N1	MSG 166.97 ($R\bar{3}m$)	AF -1.81 0.0	AF -2.174 0.0	ES -2.631 0.0	AF -3.117 0.0	AF -3.525 0.0
0.275	Al1 Mn3 N1	MSG 166.101 ($R\bar{3}m'$)	ES -1.096 0.003	ES -0.609 0.009	ES -0.574 0.013	AF -1.748 0.021	AF -1.093 0.012
0.276	Al1 Mn3 N1	MSG 65.486 ($Cmm'm'$)	ES -1.098 0.0	ES -1.142 0.004	ES -1.273 0.001	AF -0.759 0.006	AF -0.72 0.003
0.277	Mg1 Mn1 O3	MSG 148.19 ($R\bar{3}'$)	AI 1.982 2.011	AI 2.306 2.359	AI 2.51 2.576	AI 2.605 2.666	AI 2.624 2.675
0.279	Mn3 As1	MSG 63.463 ($Cmc'm'$)	NLC -0.469 0.003	AI -0.411 0.009	ES -0.466 0.006	ES -0.551 0.0	ES -0.624 0.0
0.280	Mn3 As1	MSG 63.464 ($Cm'cm'$)	ES -0.467 0.001	ES -0.411 0.0	AF -0.466 0.001	AF -0.55 0.0	AF -0.625 0.0
0.284	K1 Os1 O4	MSG 88.85 ($I4'_1/a'$)	AI 0.077 0.271	AI 0.223 0.413	AI 0.42 0.601	AI 0.629 0.805	AI 0.841 1.015

0.285	K1 Ru1 O4	MSG 88.85 ($I4'_1/a'$)	AI -0.091 0.132	AI 0.003 0.213	AI 0.157 0.361	AI 0.33 0.533	0.487 0.691
0.292	Te2 Ni1 O5	MSG 62.441 ($Pnma$)	AI 1.279 1.295	AI 1.723 1.749	AI 2.108 2.138	AI 2.408 2.408	AI 2.581 2.588
0.296	Cu2 Cl1 O3	MSG 14.75 ($P2_1/c$)	ES -0.272 0.007	NLC -0.268 0.006	AF -0.268 0.007	ES -0.262 0.0	ES -0.224 0.001
0.297	Na1 Cr1 Ge2 O6	MSG 15.89 ($C2'/c'$)	AI 1.527 1.606	AI 1.974 2.092	AI 2.391 2.553	AI 2.765 2.943	3.087 3.25
0.298	Na2 Ba1 Fe1 V2 O8	MSG 15.89 ($C2'/c'$)	AI -0.038 0.057	AI 0.612 0.673	AI 1.164 1.222	AI 1.696 1.749	AI 2.22 2.263
0.299	Fe2 O3	MSG 33.147 ($Pna'2'_1$)	0.391 0.4	0.765 0.782	1.15 1.176	1.526 1.555	1.793 1.816
0.300	Fe2 O3	MSG 33.147 ($Pna'2'_1$)	AI 0.356 0.375	AI 0.768 0.781	AI 1.167 1.173	AI 1.455 1.533	AI 1.714 1.792
0.301	Sr2 Co1 Te1 O6	MSG 14.75 ($P2_1/c$)	AI 0.425 0.534	AI 1.18 1.276	AI 1.55 1.73	AI 1.878 2.095	2.169 2.334
0.303	Ba1 F5 Cr1	MSG 19.27 ($P2'_12'_12_1$)	AI 2.345 2.347	AI 2.905 2.909	AI 3.448 3.453	AI 3.971 3.976	AI 4.464 4.471
0.307	Sc1 Cr1 O3	MSG 62.441 ($Pnma$)	AI 1.356 1.431	AI 1.871 1.904	AI 2.355 2.355	AI 2.781 2.781	3.175 3.175
0.308	In1 Cr1 O3	MSG 62.441 ($Pnma$)	AI 0.817 0.849	AI 1.179 1.27	AI 1.496 1.688	AI 1.767 2.089	1.996 2.452
0.310	Na1 Mn1 Fe1 F6	MSG 150.27 ($P32'1$)	AI 0.528 0.55	AI 0.71 0.749	AI 0.99 1.04	AI 1.36 1.416	AI 1.791 1.848
0.311	Co1 Ge1 O3	MSG 61.435 ($Pb'ca$)	AI 0.33 0.33	AI 0.985 1.027	AI 1.534 1.551	AI 1.913 1.927	AI 2.231 2.231
0.312	Mn1 Ge1 O3	MSG 15.87 ($C2'/c$)	AI 0.267 0.434	AI 0.524 0.706	AI 0.783 0.985	AI 1.031 1.255	1.262 1.507
0.313	Mn1 Ge1 O3	MSG 61.435 ($Pb'ca$)	AI 0.529 0.564	AI 0.804 0.84	AI 1.075 1.113	AI 1.331 1.372	AI 1.566 1.611
0.315	Zr1 Mn2 Ge4 O12	MSG 125.367 ($P4'/nbm'$)	AI 1.125 1.125	AI 1.456 1.456	AI 1.766 1.766	AI 2.053 2.053	AI 2.315 2.315
0.323	La1 Cr1 O3	MSG 62.441 ($Pnma$)	AI 1.42 1.44	AI 1.919 1.938	AI 2.404 2.422	AI 2.866 2.882	3.296 3.311
0.327	Mn1 Cs1 F4	MSG 59.410 ($Pmm'n'$)	ES -0.069 0.032	ES -0.083 0.021	ES -0.072 0.023	ES -0.05 0.004	AI 0.249 0.249
0.328	Mn1 F4 K1	MSG 14.79 ($P2'_1/c'$)	AI 1.072 1.188	AI 1.501 1.606	AI 1.906 2.003	AI 2.278 2.371	AI 2.614 2.702
0.329	Mn1 F4 Rb1	MSG 2.4 ($P\bar{I}$)	AI 0.497 0.699	AI 0.875 1.053	AI 1.25 1.41	AI 1.601 1.748	AI 1.925 2.06

			AI	AI	AI	AI	AI
0.331	Fe2 Mo3 O8	MSG 186.205 ($P6'_3m'c$)	-0.041 0.0	0.051 0.064	0.274 0.285	0.617 0.62	1.001 1.003
0.332	Co2 Mo3 O8	MSG 186.205 ($P6'_3m'c$)	-0.001 0.021	0.495 0.506	1.047 1.073	1.582 1.593	1.963 1.969
0.333	Mn2 Mo3 O8	MSG 186.207 ($P6_3m'c'$)	-0.038 0.002	1.085 1.085	1.401 1.401	1.724 1.724	2.036 2.051
0.334	Co1 F3	MSG 167.103 ($R\bar{3}c$)	-0.048 0.0	0.425 0.555	1.07 1.162	1.667 1.733	2.202 2.249
0.335	Fe1 F3	MSG 15.89 ($C2'/c'$)	1.614 1.615	2.214 2.214	2.773 2.773	3.29 3.29	3.765 3.765
0.338	Co2 Mo3 O8	MSG 186.205 ($P6'_3m'c$)	-0.026 0.005	0.603 0.629	1.227 1.242	1.747 1.758	2.197 2.287
0.348	Bi2 Cu1 O4	MSG 130.431 ($P4/n'c'c'$)	0.614 0.697	0.858 0.947	1.094 1.187	1.322 1.421	1.545 1.651
0.357	Ca1 Fe5 O7	MSG 11.50 ($P2_1/m$)	-0.562 0.0	-0.75 0.003	-0.746 0.004	-0.729 0.099	-0.63 0.199
0.361	Sr3 Li1 Ru1 O6	MSG 15.89 ($C2'/c'$)	0.914 0.925	1.218 1.226	1.51 1.516	1.791 1.795	2.057 2.065
0.368	Co1 C4 N1 O6 H9	MSG 62.448 ($Pn'ma'$)	0.623 0.623	1.435 1.435	2.216 2.216	2.934 2.934	3.551 3.551
0.369	N1 C4 O6 Co1 H9	MSG 14.79 ($P2'_1/c'$)	0.019 0.062	0.0 0.07	0.37 0.42	0.388 0.43	0.397 0.435
0.375	La2 Co1 Ir1 O6	MSG 14.75 ($P2_1/c$)	-0.167 0.009	-0.069 0.11	0.554 0.635	0.905 0.98	1.324 1.367
0.395	Ga1 Mn1 Pt1	MSG 63.462 ($Cm'c'm$)	-1.889 0.0	-2.18 0.002	-2.629 0.001	-3.099 0.0	-3.499 0.003
0.396	Ga1 Mn1 Pt1	MSG 63.462 ($Cm'c'm$)	-1.796 0.001	-2.257 0.003	-2.643 0.004	-3.11 0.007	-3.431 0.001
0.399	Fe1 O2 H1	MSG 62.445 ($Pnma'$)	0.337 0.337	0.756 0.756	1.172 1.172	1.573 1.573	1.958 1.958
0.414	Fe2 B2 Al1	MSG 65.486 ($Cmm'm'$)	-1.413 0.009	-1.472 0.009	-1.441 0.023	-1.354 0.028	-1.2 0.016
0.416	La1 Cr1 O3	MSG 167.103 ($R\bar{3}c$)	1.46 1.478	1.965 1.975	2.456 2.462	2.926 2.928	3.367 3.368
0.433	K1 Mn1 F3	MSG 140.541 ($I4/mcm$)	2.519 2.687	2.916 3.056	3.299 3.418	3.665 3.767	4.013 4.099
0.447	Ge1 Mn1 Co1	MSG 194.270 ($P6_3/mm'c'$)	-1.448 0.006	-1.686 0.001	-1.869 0.001	-2.322 0.008	-2.573 0.001
0.464	Ba1 Mn2 P2	MSG 139.536 ($I4'/m'm'm$)	0.151 0.321	0.359 0.488	- -	0.487 0.686	- -

0.470	Ba1 Mn2 Sb2	MSG 139.536 ($I4'/m'm'm$)	AI 0.149 0.352	AI 0.244 0.406	-	-	-
0.471	Ba2 Mn3 Sb2 O2	MSG 139.536 ($I4'/m'm'm$)	- - -	-0.635 0.0 -	- -0.833 0.0 0.0	ESFD -0.833 0.0 0.0	ESFD -0.867 0.0 0.0
0.473	La1 Mn2 Si2	MSG 44.231 ($Im'm2'$)	ES -0.327 0.011	ES -0.471 0.008	ES -0.439 0.019	ES -0.342 0.012	ES -0.304 0.02
0.482	Sr1 Mn2 As2	MSG 12.60 ($C2'/m$)	AI -0.071 0.646	AI 0.082 0.941	AI 0.235 1.21	AI 0.371 1.243	AI 0.488 1.271
0.495	La1 Mn2 Si2	MSG 44.231 ($Im'm2'$)	ES -0.309 0.003	ES -0.48 0.005	ES -0.441 0.001	ES -0.338 0.035	ES -0.295 0.0
0.496	La1 Mn2 Si2	MSG 44.231 ($Im'm2'$)	ES -0.306 0.005	ES -0.458 0.008	ES -0.477 0.002	ES -0.346 0.031	ES -0.269 0.007
0.497	La1 Mn2 Si2	MSG 44.231 ($Im'm2'$)	ES -0.307 0.004	ES -0.457 0.008	ES -0.481 0.001	ES -0.347 0.03	ES -0.268 0.016
0.512	Mn3 As2	MSG 12.58 ($C2/m$)	ES -0.605 0.005	ES -0.725 0.009	ES -0.757 0.008	ES -0.751 0.008	ES -0.773 0.009
0.513	Y1 Ru1 O3	MSG 62.448 ($Pn'ma'$)	AI -0.252 0.003	AI -0.001 0.06	AI 0.48 0.504	AI 0.993 0.995	AI 1.415 1.415
0.523	Ca1 Mn2 Sb2	MSG 2.6 ($P\bar{1}'$)	- -	AI 0.096 0.753	AI 0.202 0.989	AI 0.294 1.229	AI 0.367 1.363
0.524	Mn1 P1 Se3	MSG 2.6 ($P\bar{1}'$)	- -	AI 1.301 1.417	AI 1.521 1.622	AI 1.688 1.771	AI 1.815 1.88
0.526	Mn4 Ta2 O9	MSG 165.94 ($P\bar{3}'c'1$)	AI 1.168 1.168	AI 1.554 1.555	AI 1.883 1.902	AI 2.134 2.206	AI 2.36 2.472
0.528	Cr1 Sb1	MSG 194.268 ($P6'_3/m'm'c$)	OAI -0.605 0.024	OAI -0.85 0.04	OAI -0.994 0.257	OAI -1.078 0.324	OAI -1.18 0.313
0.529	Co4 Nb2 O9	MSG 15.88 ($C2/c'$)	- -	AI 0.42 0.483	AI 1.17 1.187	AI 1.36 1.407	AI 2.366 2.389
0.552	Pb2 Mn1 O4	MSG 114.278 ($P\bar{4}'2_1c'$)	AI 1.301 1.427	AI 1.435 1.569	AI 1.48 1.606	AI 1.468 1.597	AI 1.422 1.553
0.571	Co1 S1 O4	MSG 62.441 ($Pnma$)	AI 0.683 0.695	AI 1.442 1.446	AI 2.186 2.194	AI 2.844 2.855	AI 3.433 3.448
0.572	Na2 F7 Ni1 Cr1	MSG 74.558 ($Im'm'a$)	AI 1.349 1.36	AI 2.09 2.099	AI 2.82 2.821	AI 3.44 3.44	AI 3.998 3.998
0.573	Na2 F7 Ni1 Cr1	MSG 74.558 ($Im'm'a$)	AI 1.361 1.372	AI 2.084 2.093	AI 2.807 2.807	AI 3.425 3.425	AI 3.978 3.978
0.574	Mn1 Fe1 F5 O2 H4	MSG 5.15 ($C2'$)	- -	AI 0.566 0.566	AI 0.889 0.889	AI 1.306 1.306	AI 1.767 1.767
0.575	Zn1 Fe1 F5 O2 H4	MSG 44.229 ($Imm2$)	- -	AI 1.812 1.835	AI 2.191 2.191	AI 2.481 2.481	AI 2.747 2.747

0.576	Cr2 F5	MSG 15.85 ($C2/c$)	-	AI 0.94 -	AI 1.337 1.391	AI 1.824 1.871	AI 2.289 2.336
0.577	Ba1 Mn1 Fe1 F7	MSG 14.79 ($P2_1'/c'$)	-	AI 0.776 0.79	AI 1.084 1.097	AI 1.482 1.491	AI 1.936 1.943
0.578	Fe2 Na1 Ba1 F9	MSG 14.75 ($P2_1/c$)	AI 1.45 1.45	AI 1.943 1.943	AI 2.426 2.426	AI 2.882 2.882	AI 3.315 3.315
0.579	Na2 Ni1 Fe1 F7	MSG 74.559 ($Imm'a'$)	AI 0.214 0.214	AI 0.431 0.431	AI 0.776 0.776	AI 1.184 1.184	AI 1.649 1.649
0.580	Na2 Ni1 Fe1 F7	MSG 74.559 ($Imm'a'$)	-	AI 0.529 0.529	AI 0.908 0.908	AI 1.344 1.344	AI 1.812 1.812
0.581	Fe1 F3	MSG 15.89 ($C2'/c'$)	-	AI 2.209 2.209	AI 2.765 2.765	AI 3.28 3.28	AI 3.753 3.753
0.582	Fe3 F8 O2 H4	MSG 12.62 ($C2'/m'$)	-	AI 0.433 0.464	AI 0.677 0.708	AI 1.178 1.198	AI 1.793 1.81
0.583	Fe2 F5 O2 H4	MSG 74.559 ($Imm'a'$)	-	AI 0.012 0.061	AI 0.025 0.069	AI 0.232 0.267	AI 0.714 0.751
0.584	Fe2 F5 O2 H4	MSG 15.89 ($C2'/c'$)	AI 0.036 0.069	AI 0.073 0.106	AI 0.102 0.131	AI 0.331 0.355	AI 0.801 0.828
0.586	Y1 Cr1 O3	MSG 62.448 ($Pn'ma'$)	AI 1.502 1.517	AI 1.995 2.028	AI 2.463 2.522	AI 2.906 2.963	AI 3.313 3.367
0.598	Al1 Cr2	MSG 14.83 (P_{A2_1}/c)	OAI -0.971 0.002	OAI -0.683 0.009	OAI -0.509 0.006	OAI -0.876 0.009	OAI -1.231 0.005
0.599	Mn1 Ca1 Si1	MSG 129.416 ($P4'/n'm'm$)	SEBR 0.008 0.015	SEBR 0.011 0.011	SEBR -0.004 0.007	SEBR -0.018 0.002	- -
0.600	Mn1 Ca1 Si1	MSG 129.416 ($P4'/n'm'm$)	SEBR 0.011 0.015	SEBR 0.009 0.011	SEBR -0.006 0.006	AF -0.021 0.001	AI -0.031 0.004
0.601	Mn1 Ca1 Ge1	MSG 11.53 ($P2_1/m'$)	AI 0.02 0.026	- -	- -	AI 0.018 0.028	- -
0.603	Ca1 Mn2 Ge2	MSG 139.536 ($I4'/m'm'm$)	NLC -0.453 0.019	NLC -0.388 0.008	AF -0.463 0.003	OAI -0.536 0.015	- -
0.604	Ca1 Mn2 Ge2	MSG 139.536 ($I4'/m'm'm$)	-	-0.406 0.008	-0.478 0.003	OAI -0.55 0.016	- -
0.605	Ba1 Mn2 Ge2	MSG 139.536 ($I4'/m'm'm$)	-	-0.208 0.012	-0.229 0.002	OAI -0.249 0.016	- -
0.606	Ba1 Mn2 Ge2	MSG 139.536 ($I4'/m'm'm$)	NLC -0.289 0.022	NLC -0.21 0.008	OAI -0.233 0.001	OAI -0.257 0.019	- -
0.607	Ru1 O2	MSG 136.499 ($P4'_2/mnm'$)	-	AI -1.259 0.017	AI -1.359 0.073	AI -1.353 0.123	AI -0.984 0.307
0.612	Cu2 S1 O5	MSG 12.58 ($C2/m$)	AI -0.002 0.034	AI 0.375 0.375	AI 0.716 0.716	AI 1.063 1.063	AI 1.415 1.415

0.613	Fe1 Cr2 S4	MSG 141.557 ($I4_1/am'd'$)	-	ES -0.079 0.016	ES -0.079 0.021	ES -0.073 0.014	AI 0.79 1.136
0.617	Mn1 K1 Sb1	MSG 129.416 ($P4'/n'm'm$)	AI 0.66 0.751	AI 0.839 0.908	AI 0.993 1.002	AI 1.04 1.052	AI 1.058 1.072
0.618	Mn1 K1 Bi1	MSG 129.416 ($P4'/n'm'm$)	AI 0.426 0.428	AI 0.42 0.424	AI 0.381 0.387	AI 0.337 0.344	AI 0.279 0.288
0.619	Mn1 La1 As1 O1	MSG 129.416 ($P4'/n'm'm$)	AI 0.472 0.614	AI 0.707 0.926	AI 0.892 1.052	AI 1.046 1.103	- -
0.624	Mn1 La1 As1 O1	MSG 129.416 ($P4'/n'm'm$)	AI 0.467 0.603	AI 0.704 0.916	AI 0.891 1.049	AI 1.047 1.1	AI 1.107 1.133
0.626	Na1 Mn1 P1	MSG 129.416 ($P4'/n'm'm$)	-	AI 0.598 1.008	AI 0.821 1.275	AI 1.013 1.456	AI 1.171 1.565
0.627	Na1 Mn1 P1	MSG 129.416 ($P4'/n'm'm$)	-	AI 0.601 1.011	AI 0.823 1.274	AI 1.014 1.45	- -
0.628	Mn1 Na1 P1	MSG 129.416 ($P4'/n'm'm$)	AI 0.365 0.681	AI 0.619 1.029	AI 0.842 1.282	AI 1.034 1.446	- -
0.629	Mn1 Na1 As1	MSG 129.416 ($P4'/n'm'm$)	AI 0.454 0.69	AI 0.652 0.888	AI 0.821 0.99	AI 0.962 1.043	AI 1.067 1.067
0.630	Mn1 Na1 As1	MSG 129.416 ($P4'/n'm'm$)	-	AI 0.668 0.862	AI 0.841 0.952	AI 0.986 0.999	- -
0.633	Fe1 K1 S2	MSG 15.87 ($C2'/c$)	-	AI 0.97 1.152	AI 1.224 1.393	AI 1.416 1.545	AI 1.487 1.654
0.634	Mn1 Na1 Bi1	MSG 129.416 ($P4'/n'm'm$)	-	AI 0.228 0.233	- -	AI 0.13 0.13	- -
0.636	Fe1 Rb1 S2	MSG 15.87 ($C2'/c$)	AI 0.59 0.782	AI 0.846 1.003	AI 1.084 1.225	AI 1.265 1.447	AI 1.389 1.644
0.637	Fe1 K1 Se2	MSG 15.88 ($C2/c'$)	AI -0.021 0.415	AI 0.297 0.722	AI 0.632 0.983	AI 0.943 1.097	AI 1.13 1.21
0.638	Fe1 Rb1 Se2	MSG 15.88 ($C2/c'$)	AI 0.475 0.676	AI 0.717 0.904	AI 0.93 1.121	AI 1.034 1.307	AI 1.11 1.391
0.639	Au1 Mn2	MSG 71.535 ($Im'mm$)	-	ESFD -2.323 0.0	ESFD -2.167 0.0	ESFD -2.492 0.0	ESFD -2.802 0.0
0.640	Au1 Mn2	MSG 71.535 ($Im'mm$)	ESFD -1.716 0.0	ESFD -2.314 0.0	ESFD -2.178 0.0	ESFD -2.496 0.0	ESFD -2.807 0.0
0.641	Ga1 Mn3	MSG 12.62 ($C2'/m'$)	NLC -1.199 0.003	SEBR -0.844 0.003	NLC -0.868 0.011	NLC -0.934 0.013	NLC -0.999 0.003
0.642	La1 Mn1 O3	MSG 62.448 ($Pn'ma'$)	AI 0.283 0.715	AI 0.56 0.95	AI 0.809 1.175	AI 1.032 1.382	AI 1.22 1.557
0.662	Mn3 Sn2	MSG 62.448 ($Pn'ma'$)	ES -0.472 0.004	ES -0.484 0.004	ES -0.496 0.005	ES -0.859 0.003	ES -0.811 0.001

0.663	Mn3 Sn2	MSG 62.448 ($Pn'ma'$)	ES -0.146 0.007	ES -0.22 0.009	ES -0.387 0.01	ES -0.529 0.011	ES -0.716 0.008
0.664	Mn3 Sn2	MSG 14.79 ($P2'_1/c'$)	NLC -0.122 0.002	NLC -0.24 0.001	NLC -0.337 0.005	NLC -0.471 0.018	OAI -0.67 0.011
0.682	Ca2 Fe1 Os1 O6	MSG 14.79 ($P2'_1/c'$)	- -	AI 0.631 0.652	AI 0.901 0.924	AI 1.188 1.222	AI 1.489 1.534
0.692	Ru3 Ba4 O10	MSG 64.471 ($Cm'ca$)	AI 0.094 0.176	AI 0.258 0.32	AI 0.431 0.455	AI 0.716 0.731	AI 1.005 1.018
0.693	Ru3 Ba4 O10	MSG 64.472 ($Cmc'a$)	AI 0.135 0.196	AI 0.304 0.357	AI 0.449 0.475	AI 0.705 0.72	AI 1.002 1.002
0.694	Bi2 Cu1 O4	MSG 130.431 ($P4/n'c'c'$)	AI 0.215 0.362	AI 0.384 0.534	AI 0.537 0.689	AI 0.683 0.837	AI 0.831 0.978
0.695	Bi2 Cu1 O4	MSG 56.367 ($Pc'cn$)	- AI 0.613 0.698	- AI 0.856 0.946	- AI 1.09 1.185	- AI 1.316 1.417	- AI 1.537 1.645
0.699	Mn6 Sn6 Li1	MSG 65.486 ($Cmm'm'$)	ES -1.096 0.001	ES -0.737 0.001	ES -1.116 0.0	ES -1.164 0.001	ES -1.562 0.003
0.708	Nb4 Cr1 S8	MSG 194.268 ($P6'_3/m'm'c$)	SEBR -0.47 0.037	AI -0.561 0.01	AI -0.605 0.019	AI -0.643 0.021	AI -0.678 0.011
0.709	Nb4 Mn1 S8	MSG 63.463 ($Cmc'm'$)	- AF -0.388 0.0	- AF -0.33 0.0	- AF -0.28 0.0	- AF -0.252 0.0	- AF -0.252 0.0
0.711	Ta4 Mn1 S8	MSG 63.463 ($Cmc'm'$)	- AF -0.217 0.0	- AF -0.211 0.0	- ES -0.223 0.0	- ES -0.208 0.0	- ES -0.2 0.0
0.712	Nb3 V1 S6	MSG 20.33 ($C2'2'2_1$)	- AI -0.075 0.027	- AI -0.09 0.022	- AI -0.08 0.072	- AI -0.068 0.118	- AI -0.054 0.162
0.714	Ni1 Li2 S2 O8	MSG 14.75 ($P2_1/c$)	- AI 1.646 1.679	- AI 2.196 2.23	- AI 2.701 2.737	- AI 3.159 3.196	- AI 3.585 3.623
0.722	Mn4 Nb2 O9	MSG 9.37 (Cc)	- AI 0.476 0.525	- AI 0.655 0.71	- AI 0.828 0.878	- AI 1.002 1.047	- AI 1.176 1.218
0.724	Ba1 Co1 Si1 O4	MSG 173.129 ($P6_3$)	- AI 1.003 1.025	- AI - -	- AI - -	- AI - -	- AI 3.36 3.377
0.726	Mn2 Cs1 F6	MSG 62.447 ($Pnm'a'$)	- AI 0.379 0.43	- AI - -	- AI - -	- AI 1.225 1.278	- AI 1.489 1.522
0.732	Sr1 Ru1 O3	MSG 62.446 ($Pn'm'a$)	- AI -0.311 0.007	- ES -0.537 0.008	- ES -0.559 0.012	- ES -0.512 0.022	- ES -0.293 0.014
0.733	Ru1 Ag1 O3	MSG 167.106 ($R\bar{3}'c'$)	- AI 0.035 0.047	- AI 0.283 0.336	- AI 0.494 0.613	- AI 0.668 0.865	- AI 0.822 1.005
0.735	La1 Ba1 Mn2 O5	MSG 129.417 ($P4/nm'm'$)	- AI 0.615 0.812	- AI 0.738 1.032	- AI 0.89 1.257	- AI 1.045 1.456	- AI 1.19 1.605
0.737	La1 Ba1 Mn2 O6	MSG 123.345 ($P4/mm'm'$)	- ES -2.245 0.006	- ES -2.147 0.007	- ES -2.064 0.016	- ES -2.008 0.023	- ES -1.941 0.003

0.738	La1 Ba1 Mn2 O6	MSG 123.345 ($P4/mm'm'$)	ES -2.232 0.02	ES -2.136 0.005	ES -2.053 0.025	ES -2.002 0.028	ES -1.945 0.011
0.739	Y1 Ba1 Mn2 O5	MSG 129.417 ($P4/nm'm'$)	AI 0.829 0.928	AI 0.972 1.196	AI 1.107 1.41	AI 1.25 1.605	AI 1.385 1.761
0.747	Ba3 Co1 Ir2 O9	MSG 15.85 ($C2/c$)	NLC -0.005 0.003	OAI -0.0 0.016	ES -0.016 0.001	ES -0.0 0.012	AI 0.299 0.299
0.748	Ba3 Ni1 Ru2 O9	MSG 194.268 ($P6'_3/m'm'c$)	AI 0.57 0.57	AI 0.823 0.823	AI 1.072 1.072	AI 1.32 1.32	AI 1.572 1.572
0.755	Mn2 Se1 F2 O3	MSG 62.448 ($Pn'ma'$)	AI 2.278 2.282	- -	- -	- -	AI 3.873 3.941
0.756	Gal V4 S8	MSG 160.67 ($R3m'$)	AI -0.187 0.058	AI -0.065 0.04	AI -0.076 0.46	ES -0.225 0.011	AI 0.127 0.285
0.760	Fe1 S1 O5 H1	MSG 15.89 ($C2'/c'$)	AI 0.425 0.596	AI 0.928 1.081	AI 1.396 1.519	AI 1.831 1.904	AI 2.239 2.239
0.761	Sr1 Fe2 Se2 O1	MSG 59.411 ($Pm'm'n'$)	AI 0.432 0.466	AI 0.938 1.013	AI 1.424 1.543	AI 1.864 1.962	AI 2.243 2.302
0.762	Sr1 Fe2 S2 O1	MSG 59.411 ($Pm'm'n'$)	AI 0.364 0.394	AI 0.87 0.932	AI 1.377 1.515	AI 1.856 1.99	AI 2.285 2.366
0.768	Sr1 Mn1 Sb2	MSG 33.148 ($Pn'a'2_1$)	AI 0.01 0.19	AI 0.025 0.192	AI 0.038 0.195	AI 0.047 0.198	AI 0.052 0.201
0.778	La1 Mn1 Si2	MSG 63.464 ($Cm'cm'$)	ES -0.577 0.023	ES -0.399 0.006	ES -0.653 0.002	ES -0.513 0.0	ES -0.689 0.009
0.779	La1 Mn1 Si2	MSG 63.464 ($Cm'cm'$)	ES -0.577 0.023	ES -0.398 0.004	ES -0.401 0.002	ES -0.513 0.0	ES -0.504 0.018
0.780	La1 Mn1 Si2	MSG 63.464 ($Cm'cm'$)	ES -0.577 0.023	ES -0.415 0.003	ES -0.564 0.002	ES -0.513 0.0	ES -0.503 0.018
0.787	Y1 V1 O3	MSG 62.446 ($Pn'm'a$)	AI -0.055 0.073	AI 0.548 0.624	AI 1.121 1.189	AI 1.712 1.775	AI 2.3 2.365
0.788	Y1 V1 O3	MSG 2.4 ($P\bar{1}$)	AI -0.152 0.022	AI 0.46 0.506	AI 1.078 1.089	AI 1.677 1.677	AI 2.053 2.178
0.795	Sr2 Y1 Ru1 O6	MSG 14.75 ($P2_1/c$)	AI 0.329 0.536	AI 0.682 0.881	AI 1.021 1.211	AI 1.356 1.533	AI 1.69 1.848
0.796	Ca2 Ni1 Os1 O6	MSG 14.79 ($P2'_1/c'$)	AI -0.076 0.025	AI 0.0 0.045	AI 0.209 0.209	AI 0.443 0.443	AI 0.631 0.645
0.798	Mn1 Pd2	MSG 62.445 ($Pnma'$)	AI -0.471 0.012	AI -0.541 0.025	AI -0.621 0.038	AI -0.692 0.04	AI -0.763 0.036
0.799	Sr2 Co2 O5	MSG 30.122 (P_{Iinc2})	AI -0.175 0.004	AI -0.164 0.003	AI 0.277 0.327	AI 0.543 0.629	AI 0.783 0.894
0.800	Mn1 Te1	MSG 63.457 ($Cmcm$)	AI 0.053 0.481	AI 0.402 0.835	AI 0.587 1.148	AI 0.661 1.427	AI 0.711 1.675

				ES	AF	AF	
				-0.068	-0.072	-0.113	-0.131
				0.0	0.0	0.001	0.002
0.801	Tl3 Fe2 S4	MSG 62.445 ($Pnma'$)	-	AI	AI	AI	AI
0.802	Cu1 Fe1 S2	MSG 122.333 ($I\bar{4}2d$)	-0.002 0.299	0.233 0.5	0.489 0.687	0.762 0.862	0.902 1.011
0.803	Mn1 Nb1 P1	MSG 31.125 ($Pm'n2'_1$)	-0.495 0.005	AI 0.0	AI 0.001	AI 0.002	ES 0.002
0.804	Mo1 P3 Si1 O11	MSG 15.88 ($C2/c'$)	AI 0.264 0.27	AI 0.372 0.389	AI 0.541 0.588	AI 0.665 0.717	AI 0.692 0.714
0.809	W1 Fe2 O6	MSG 14.78 ($P2_1/c'$)	AI -0.037 0.019	AI 0.936 1.004	AI 1.317	AI 1.664	AI 1.968
0.810	Fe2 W1 O6	MSG 60.423 ($Pbc'n'$)	AI 0.27 0.29	AI 0.531 0.56	AI 0.826 0.861	AI 1.114	AI 1.345
0.811	Fe2 W1 O6	MSG 60.423 ($Pbc'n'$)	AI 0.281 0.287	AI 0.534 0.556	AI 0.832 0.858	AI 1.12	AI 1.351
0.812	Fe2 W1 O6	MSG 30.113 ($Pn'c2'$)	AI 0.278 0.284	AI 0.526 0.542	AI 0.828 0.848	AI 1.121	AI 1.366
0.813	Fe2 W1 O6	MSG 60.423 ($Pbc'n'$)	- -	AI 0.521 0.528	AI 0.777 0.784	AI 1.008	AI 1.199
0.814	Fe2 W1 O6	MSG 60.419 ($Pb'cn$)	AI 0.291 0.298	AI 0.588 0.603	AI 0.884 0.893	AI 1.151	AI 1.376
0.815	Mn1 Nb2 O6	MSG 60.419 ($Pb'cn$)	AI 2.16 2.208	AI 2.526 2.575	AI 2.838 2.887	AI 3.112	AI 3.351
0.816	Mn1 Ta2 O6	MSG 60.419 ($Pb'cn$)	AI 1.858 1.894	AI 2.145 2.195	AI 2.413 2.47	AI 2.661	AI 2.888
0.818	Mn1 Ta2 O6	MSG 60.419 ($Pb'cn$)	AI 1.856 1.872	AI 2.146 2.169	AI 2.415 2.446	AI 2.665	AI 2.888
0.819	Mn1 Nb2 O6	MSG 60.419 ($Pb'cn$)	AI 2.146 2.189	AI 2.52 2.565	AI 2.836 2.881	AI 3.112	AI 3.352
0.823	Mn1 Sr2 Ga1 O5	MSG 46.243 ($Im'a2'$)	AI 0.427 0.613	AI 0.726 0.928	AI 0.98 1.167	AI 1.18	AI 1.318
0.825	Ca2 Mn1 Ga1 O5	MSG 62.447 ($Pnm'a'$)	AI 0.117 0.287	AI 0.172 0.376	AI 0.238 0.474	AI 0.317 0.56	AI 0.387 0.628
0.834	Cr1 Sb1 Se3	MSG 62.447 ($Pnm'a'$)	AI 0.5 0.697	AI 0.545 0.806	AI 0.551 0.823	AI 0.541 0.827	AI 0.52 0.825
0.855	Mn2 Sb1	MSG 129.417 ($P4/nm'm'$)	ES -1.039 0.004	ES -1.097 0.01	ES -1.161 0.007	ES -1.122 0.004	ES -1.269 0.007
0.859	Y1 Co3	MSG 166.101 ($R\bar{3}m'$)	ES -0.16 0.001	SEBR -0.366 0.0	ES -0.28 0.002	ES -0.368 0.001	ES -0.511 0.0
0.860	Sn2 Co3 S2	MSG 166.101 ($R\bar{3}m'$)	SEBR -0.057 0.056	SEBR -0.161 0.005	SEBR -0.115 0.039	SEBR -0.174 0.02	SEBR -1.191 0.0

			SEBR	SEBR	SEBR	ES	ES
0.861	Sn2 Co3 S2	MSG 166.101 ($R\bar{3}m'$)	-0.061 0.056	-0.158 0.01	-0.113 0.04	-0.171 0.022	-0.857 0.004
0.881	Mn1 Cu1 As1	MSG 59.407 ($Pm'mn$)	AI -0.824 0.01	AI -0.75 0.013	AI -0.604 0.026	AI -0.767 0.036	AI -0.88 0.177
0.891	Cu1 Cr2 O4	MSG 15.89 ($C2'/c'$)	NLC -0.339 0.029	AI -0.199 0.024	AI 0.111 0.375	AI 0.495 0.742	AI 0.951 1.125
0.892	Ni1 Cr2 O4	MSG 70.530 ($Fd'd'd$)	-0.08 0.001	-0.018 0.015	0.141 0.22	AI 1.134 1.237	AI 1.64 1.673
0.893	Ni1 Cr2 O4	MSG 70.530 ($Fd'd'd$)	ES -0.281 0.004	-0.198 0.0 0.041	AI 0.027 0.909	AI 0.989	AI 1.639 1.671
0.896	Ni1 Cr1 O4	MSG 63.457 ($Cmcm$)	AI 0.74 1.002	AI 1.089 1.298	AI 1.405 1.559	AI 1.677 1.755	AI 1.87 1.932
0.898	Mn3 Ir1 Si1	MSG 198.9 ($P2_{13}$)	AI -0.073 0.01	AI -0.135 0.035	AI -0.227 0.046	AI -0.312 0.031	AI -0.412 0.019
0.899	Mn3 Ir1 Ge1	MSG 198.9 ($P2_{13}$)	AI -0.142 0.006	AI -0.229 0.013	AI -0.311 0.001	AF -0.351	ES -0.387 0.007
0.900	Mn3 Co1 Ge1	MSG 198.9 ($P2_{13}$)	AI -0.057 0.019	AI -0.077 0.018	AI -0.215 0.013	AI -0.304	ES -0.313 0.004
0.916	Cd2 Os2 O7	MSG 227.131 ($Fd\bar{3}m'$)	NLC -0.146 0.028	AI 0.108 0.352	AI 0.447 0.652	AI 0.75 0.876	AI 1.026 1.107
0.917	Sr2 Os1 Sc1 O6	MSG 14.75 ($P2_1/c$)	AI -0.281 0.132	AI 0.155 0.483	AI 0.535 0.851	AI 0.905 1.216	AI 1.283 1.586
0.918	Ag2 Ru1 O4	MSG 62.444 ($Pnm'a$)	AI 0.212 0.243	AI 0.403 0.427	AI 0.581 0.599	AI 0.744 0.759	AI 0.908 0.921
0.924	Rb1 Ru1 O4	MSG 62.449 ($Pn'm'a'$)	AI -0.085 0.009	AI -0.066 0.017	AI 0.044 0.126	AI 0.286 0.366	AI 0.473 0.551
0.933	Ru1 Na2 O4	MSG 14.78 ($P2_1/c'$)	AI 0.563 0.596	AI 0.784 0.784	AI 1.0 1.0	AI 1.219 1.219	AI 1.434 1.434
0.934	Sr2 O6 Ni1 Te1	MSG 14.75 ($P2_1/c$)	AI 0.726 0.774	AI 1.203 1.288	AI 1.66 1.799	AI 2.085 2.103	AI 2.249 2.249
0.936	Sr2 O6 Mn1 Te1	MSG 14.75 ($P2_1/c$)	AI 0.722 0.722	AI 1.011 1.011	AI 1.289 1.289	AI 1.552 1.552	AI 1.797 1.797
0.937	Sr2 O6 Co1 Te1	MSG 14.75 ($P2_1/c$)	AI 0.424 0.535	AI 1.178 1.285	AI 1.676 1.789	AI 2.0 2.219	AI 2.287 2.463
0.947	Cr1 Y1 O3	MSG 62.448 ($Pn'ma'$)	AI 1.504 1.518	AI 1.993 2.029	AI 2.464 2.523	AI 2.907 2.966	AI 3.316 3.372
0.948	Ca1 Ni3 P4 O14	MSG 14.75 ($P2_1/c$)	AI 1.314 1.321	AI 1.878 1.883	AI 2.42 2.425	AI 2.929 2.934	AI 3.406 3.412
0.959	Cr2 Te1 O6	MSG 58.395 ($Pn'nm$)	AI 0.939	AI 1.342	AI 1.709	AI 2.032	AI 2.309
			0.939	1.342	1.709	2.032	2.309

0.960	Fe2 Te1 O6	MSG 136.503 ($P4_2/m'n'm'$)	AI 0.22 0.371	AI 0.724 0.862	AI 1.161 1.261	AI 1.528 1.594	AI 1.698 1.78
0.961	Li1 Cr1 Ge2 O6	MSG 14.77 ($P2'_1/c$)	AI 2.042 2.043	AI 2.505 2.511	AI 2.901 2.901	AI 3.23 3.23	AI 3.486 3.486
0.962	Li1 Cr1 Ge2 O6	MSG 14.77 ($P2'_1/c$)	AI 2.042 2.043	AI 2.505 2.511	AI 2.901 2.901	AI 3.23 3.23	AI 3.486 3.486
0.963	Li1 Cr1 Ge2 O6	MSG 14.77 ($P2'_1/c$)	AI 2.042 2.043	AI 2.505 2.511	AI 2.901 2.901	AI 3.23 3.23	AI 3.486 3.486
0.964	Li1 Cr1 Ge2 O6	MSG 14.77 ($P2'_1/c$)	AI 2.042 2.043	AI 2.505 2.511	AI 2.901 2.901	AI 3.23 3.23	AI 3.486 3.486
0.965	Lu1 Fe2 O4	MSG 1.3 (P_S1)	AI 0.227 0.292	AI 0.304 0.355	AI 0.362 0.393	AI 0.49 0.501	AI 0.866 0.87
0.966	W1 V2 O6	MSG 58.395 ($Pn'nm$)	- -	AI 0.021 0.023	AI 0.623 0.623	AI 1.041 1.091	AI 1.402 1.471
0.968	Fe2 Ca1 O4	MSG 62.448 ($Pn'ma'$)	AI -0.057 0.027	AI 0.31 0.359	AI 0.665 0.69	AI 1.012 1.031	AI 1.35 1.372
0.969	Fe2 Ca1 O4	MSG 62.445 ($Pnma'$)	AI -0.268 0.002	AI 0.019 0.065	AI 0.422 0.434	AI 0.843 0.848	AI 1.251 1.259
0.984	V1 Lu1 O3	MSG 62.446 ($Pn'm'a$)	AI -0.174 0.005	AI 0.456 0.476	AI 1.044 1.048	AI 1.669 1.673	AI 2.263 2.292
1.277	Li1 Fe1 Cr4 O8	MSG 119.319 ($I\bar{4}m'2'$)	AI 0.301 0.412	AI 0.607 0.769	AI 0.989 1.145	AI 1.4 1.546	AI 1.822 1.928
1.278	Cu1 C2 N2 S2	MSG 2.7 ($P_S\bar{1}$)	AI 0.529 0.559	AI 0.698 0.698	AI 0.831 0.831	AI 0.966 0.966	AI 1.107 1.107
1.281	Y1 Ba1 Fe1 Cu1 O5	MSG 42.223 (F_Smm2)	AI -0.333 0.037	AI -0.213 0.049	AI -0.735 0.002	AI -0.87 0.026	AI 0.797 0.97
1.286	Fe1 C3 O8 H4	MSG 2.7 ($P_S\bar{1}$)	AI 0.286 0.3	AI 0.005 0.005	AI 0.005 0.008	AI 0.031 0.031	AI 0.632 0.663
1.287	V2 O3	MSG 14.84 (P_C2_1/c)	NLC -0.205 0.001	AI -0.191 0.006	AI 0.364 0.432	AI 0.98 1.078	AI 1.559 1.66
1.304	Mg1 Mn1 O3	MSG 2.7 ($P_S\bar{1}$)	AI 1.668 1.777	AI 2.055 2.18	AI 2.317 2.419	AI 2.454 2.532	AI 2.488 2.56
1.305	Mn5 Si3	MSG 60.431 (P_Cbcn)	NLC -0.472 0.0	OAI -0.44 0.0	ES -0.446 0.001	OAI -0.501 0.004	OAI -0.512 0.001
1.308	Mn1 Bi2 Te4	MSG 167.108 ($R_I\bar{3}c$)	SEBR 0.032 0.032	SEBR 0.077 0.077	SEBR 0.085 0.085	SEBR 0.09 0.09	SEBR 0.096 0.096
1.311	Ba1 Mo1 P2 O8	MSG 2.7 ($P_S\bar{1}$)	AI 0.081 0.093	AI 0.444 0.465	AI 0.918 0.933	AI 1.373 1.385	AI 1.819 1.829
1.314	Na1 Fe1 Si2 O6	MSG 14.84 (P_C2_1/c)	AI 0.948 0.996	AI 1.418 1.463	AI 1.854 1.865	AI 2.225 2.225	AI 2.561 2.561

1.319	Sr2 Ru1 O4	MSG 63.466 ($C_c mcm$)	OAI -0.493 0.012	ES -0.364 0.01	ES -0.196 0.002	AI -0.075 0.0	AI -0.178 0.024
1.321	Ba2 Fe1 W1 O6	MSG 2.7 ($P_S\bar{1}$)	AI -0.437 0.025	AI -0.457 0.029	AI -0.445 0.027	AI 0.911 1.022	AI 1.314 1.376
1.323	Co1 Ge1 O3	MSG 14.84 (P_C2_1/c)	NLC 0.082 0.083	AI 0.945 0.949	AI 1.367 1.373	AI 1.78 1.791	AI 2.119 2.129
1.345	Na1 Mn1 F4	MSG 14.80 (P_a2_1/c)	AI 1.436 1.521	AI 1.857 1.943	AI 2.249 2.339	AI 2.608 2.703	AI 2.929 3.029
1.347	Cu1 Fe1 O2	MSG 15.91 (C_a2/c)	OAI 0.188 0.259	OAI 0.423 0.516	OAI 0.635 0.742	0.855 0.982	1.104 1.244
1.351	Ba2 Co2 Cl1 F7	MSG 11.55 (P_a2_1/m)	0.286 0.287	1.138 1.139	1.94 1.941	2.741 2.741	3.514 3.515
1.370	Li2 Cu1 O2	MSG 58.404 (P_{Innm})	AI 0.527 1.066	AI 0.793 1.322	AI 1.054 1.571	1.319 1.821	1.59 2.076
1.383	Fe1 Ca2 O3 Br1	MSG 113.273 ($P_C\bar{4}2_1m$)	AI 1.04 1.107	AI 1.431 1.487	AI 1.813 1.849	AI 2.183 2.21	SEBR 2.539 2.562
1.495	Y1 Mn2 Si2	MSG 126.386 (P_I4/nnc)	ESFD -1.087 0.0	ESFD -1.155 0.0	ESFD -1.098 0.0	ESFD -1.436 0.0	ESFD -1.816 0.0
1.496	Y1 Mn2 Ge2	MSG 126.386 (P_I4/nnc)	ESFD -0.971 0.0	ESFD -0.897 0.0	ESFD -1.531 0.0	ESFD -1.743 0.0	ESFD -1.775 0.0
1.498	Cu1 Si1 O4 H2	MSG 148.20 ($R_I\bar{3}$)	-	AI 1.286	AI 1.64	AI 1.991	AI 2.349
1.499	Cs1 Fe1 Mo2 O8	MSG 143.3 (P_c3)	-	-	-	2.385 2.387	AI 2.709 2.715
1.500	Co1 Cu2 S2 Sr2 O2	MSG 2.7 ($P_S\bar{1}$)	-	AI -0.955 0.02	AI -0.963 0.001	AI -0.943 0.003	AI -0.901 0.005
1.508	Al1 B2 Mn2	MSG 63.466 ($C_c mcm$)	SEBR -0.094 0.096	OAI -0.128 0.07	-	-	SEBR -1.312 0.004
1.519	Co1 S1 O4	MSG 60.431 (P_Cbcn)	AI 0.59 0.591	AI 1.344 1.371	AI 2.133 2.142	AI 2.872 2.903	AI 3.414 3.414
1.520	Ni1 S1 O4	MSG 60.431 (P_Cbcn)	-	AI 1.404 1.594	AI 1.866 2.132	AI 2.289 2.366	AI 2.475 2.475
1.521	Fe1 S1 O4	MSG 60.431 (P_Cbcn)	-	AI 0.867 0.893	AI 1.68 1.707	AI 2.498 2.526	AI 3.313 3.346
1.522	Cr1 V1 O4	MSG 2.4 ($P\bar{1}$)	AI 1.503 1.667	AI 1.939 2.094	AI 2.356 2.495	AI 2.71 2.839	AI 2.977 3.108
1.523	V1 P1 O4	MSG 62.452 ($P_c nma$)	-	AI 0.683 0.683	AI 1.335 1.335	AI 1.98 1.98	AI 2.604 2.604
1.524	In1 Mn1 O3	MSG 159.64 (P_c31c)	0.637 0.794	AI 0.911 1.078	AI 1.162 1.342	AI 1.377 1.569	AI 1.552 1.747

1.528	Fe4 Bi2 O9	MSG 12.64 (C_a2/m)	AI 0.707 0.707	AI 1.092 1.092	AI 1.468 1.468	AI 1.829 1.829	AI 2.169 2.169
1.538	Mn1 Ba2 Te1 O6	MSG 14.83 ($P_{A21/c}$)	AI 0.853 0.854	AI 1.151 1.151	AI 1.432 1.433	AI 1.694 1.695	AI 1.935 1.936
1.542	Mn1 Rb1 P1	MSG 138.528 ($P_{c42/ncm}$)	AI 0.764 0.852	- -	- -	AI 1.399 1.399	- -
1.544	Mn1 Rb1 As1	MSG 138.528 ($P_{c42/ncm}$)	AI 0.809 0.852	AI 0.954 0.954	AI 1.0 1.0	- -	- -
1.545	Mn1 Rb1 Bi1	MSG 138.528 ($P_{c42/ncm}$)	AI 0.361 0.361	AI 0.334 0.334	AI 0.285 0.285	AI 0.237 0.237	AI 0.177 0.177
1.546	Mn1 Cs1 Bi1	MSG 138.528 ($P_{c42/ncm}$)	AI 0.376 0.376	AI 0.4 0.4	AI 0.387 0.387	AI 0.367 0.367	AI 0.327 0.327
1.547	Mn1 Cs1 P1	MSG 138.528 ($P_{c42/ncm}$)	AI 0.593 0.593	AI 0.811 0.812	AI 0.954 0.954	AI 1.05 1.05	AI 1.114 1.114
1.548	Mn1 Cs1 P1	MSG 138.528 ($P_{c42/ncm}$)	- -	AI 0.792 0.792	- -	AI 1.01 1.01	- -
1.550	Mn1 Li1 As1	MSG 138.528 ($P_{c42/ncm}$)	AI 0.405 0.768	AI 0.581 1.087	- -	AI 0.828 1.361	AI 0.91 1.39
1.553	Mn1 K1 As1	MSG 138.528 ($P_{c42/ncm}$)	AI 0.761 0.861	AI 0.989 0.989	- -	AI 1.09 1.09	AI 1.105 1.105
1.554	Mn1 K1 As1	MSG 138.528 ($P_{c42/ncm}$)	- -	AI 0.959 0.959	AI 1.019 1.019	- -	AI 1.065 1.065
1.555	Mn3 B4	MSG 58.404 (P_{Innm})	- -	AF -0.663 0.0	ES -0.86 0.004	ES -1.146 0.006	ES -0.662 0.013
1.556	Fe1 Sn2	MSG 60.432 (P_{Ibcn})	OAI -0.421 0.018	OAI -0.573 0.023	OAI -0.754 0.047	ES -0.878 0.0	ES -0.915 0.012
1.557	Fe1 Ge2	MSG 60.432 (P_{Ibcn})	OAI -0.164 0.018	OAI -0.401 0.025	OAI -0.723 0.038	OAI -0.991 0.048	ES -1.213 0.012
1.558	Mn1 Sn2	MSG 68.520 (C_{Acca})	NLC -1.236 0.012	NLC -1.422 0.048	NLC -1.442 0.011	OAI -1.517 0.03	OAI -1.866 0.007
1.559	Mn1 Sn2	MSG 66.498 (C_{ccm})	ES -1.095 0.007	- -	ES -1.302 0.015	ES -1.452 0.007	OAI -1.595 0.017
1.560	Ge1 Ni2 O4	MSG 12.63 (C_c2/m)	SEBR -0.2 0.005	-0.165 0.002	AI 0.478 0.69	AI 0.995 1.218	AI 1.49 1.49
1.561	Ge1 Ni2 O4	MSG 8.35 (C_cm)	AI 1.259 1.259	AI 1.746 1.768	AI 1.988 1.989	AI 2.149 2.149	AI 2.283 2.283
1.562	Ge1 Ni2 O4	MSG 5.16 (C_c2)	AI 1.223 1.223	AI 1.729 1.738	AI 1.973 1.986	AI 2.136 2.146	AI 2.273 2.28
1.563	Ge1 Ni2 O4	MSG 8.35 (C_cm)	AI 1.208 1.208	AI 1.593 1.596	AI 1.769 1.769	AI 1.913 1.913	AI 2.032 2.032

1.569	Sr1 Ru2 O6	MSG 162.78 ($P_c\bar{3}1m$)	AI 0.349 0.425	AI 0.694 0.789	AI 1.039 1.122	AI 1.381 1.43	AI 1.72 1.72
1.580	Ni1 Ti1 O3	MSG 2.7 ($P_S\bar{1}$)	AI 1.032 1.101	AI 1.563 1.633	AI 2.042 2.16	AI 2.495 2.644	AI 2.934 3.085
1.593	Ba1 Co1 S1 O1	MSG 57.386 (P_abcm)	AI 0.43 0.448	- -	- -	- -	AI 2.218 2.285
1.594	Ba1 Co1 S1 O1	MSG 57.386 (P_abcm)	AI 0.415 0.434	- -	- -	- -	AI 2.198 2.265
1.617	Mo2 Fe1 Li1 O8	MSG 2.7 ($P_S\bar{1}$)	AI 0.911 0.952	- -	- -	- -	AI 2.504 2.544
1.619	Mn1 S1	MSG 12.63 (C_c2/m)	AI 0.847 1.217	AI 1.269 1.712	AI 1.648 2.153	AI 1.985 2.524	AI 2.249 2.79
1.625	Sr2 Fe3 S2 O3	MSG 62.451 (P_bnma)	AI -0.097 0.005	- -	- -	- -	AI 2.5 2.529
1.629	Fe1 Ge1	MSG 192.252 (P_c6/mcc)	ES -0.63 0.003	ES -0.683 0.003	ES -0.977 0.003	ES -1.245 0.002	AF -1.64 0.001
1.630	Lu1 Mn6 Sn6	MSG 63.466 (C_cmcm)	AF -0.815 0.0	AF -0.656 0.001	ES -0.89 0.004	OAI -0.925 0.008	SEBR -0.991 0.01
1.641	Ba2 Fe1 Si2 O7	MSG 36.177 (C_cmc2_1)	AI 0.49 0.49	AI 1.182 1.182	AI 1.903 1.903	AI 2.42 2.42	AI 2.755 2.755
1.649	Sr3 Zn1 O6 Ir1	MSG 13.74 (P_C2/c)	AI -0.039 0.002	AI 0.404 0.474	AI 0.76 0.798	AI 1.14 1.158	AI 1.547 1.552
1.653	Fe1 W1 O4	MSG 13.70 (P_a2/c)	OAI 0.027 0.034	AI 0.491 0.498	AI 0.947 0.963	AI 1.364 1.372	AI 1.639 1.667
1.661	La2 Ni1 Ir1 O6	MSG 2.7 ($P_S\bar{1}$)	AI -0.009 0.1	AI 0.346 0.467	AI 0.703 0.802	AI 1.072 1.145	AI 1.463 1.517
1.662	La2 Ni1 Ir1 O6	MSG 2.7 ($P_S\bar{1}$)	AI 0.023 0.081	AI 0.406 0.465	AI 0.774 0.82	AI 1.164 1.193	AI 1.59 1.597
1.678	Cr1 N1	MSG 62.450 (P_anma)	SEBR -0.403 0.002	AI -0.107 0.215	AI 0.287 0.594	AI 0.51 0.88	AI 0.717 1.063
1.689	Lu1 Mn2 Ge2	MSG 126.386 (P_I4/nnc)	ESFD -1.055 0.0	ESFD -1.003 0.0	ESFD -1.368 2.0	ESFD -2.026 3.0	ESFD -2.12 4.0
1.691	Mn2 Y1 Ge2	MSG 126.386 (P_I4/nnc)	ESFD -1.065 0.0	ESFD -0.978 0.0	ESFD -1.519 2.0	ESFD -1.759 3.0	ESFD -1.801 4.0
1.692	Mn2 Y1 Ge2	MSG 126.386 (P_I4/nnc)	ESFD -1.009 0.0	ESFD -0.932 1.0	ESFD -1.536 2.0	ESFD -1.773 3.0	ESFD -1.813 4.0
1.702	Ba1 Y1 Co2 O5	MSG 65.489 (C_ammm)	SEBR -0.067 0.003	AF -0.15 0.006	AF -0.301 0.006	AF -0.396 0.006	SEBR -0.491 0.006
1.703	Ba1 Y1 Co2 O5	MSG 53.330 (P_amna)	AI -0.078 0.009	AI 0.368 0.371	AI 0.634 0.71	AI 0.835 1.02	AI 1.014 1.204

1.706	Ba2 Mn1 Te1 O6	MSG 64.480 (C_{Amca})	AI 0.473 0.473	AI 0.757 0.757	AI 1.028 1.029	AI 1.283 1.283	AI 1.518 1.519
1.708	Cr1 P1 S4	MSG 5.16 (C_c2)	AI 0.798 0.798	AI 1.02 1.02	AI 1.191 1.191	AI 1.324 1.324	AI 1.391 1.425
1.709	Cs1 Cr1 F4	MSG 46.247 ($I_a ma2$)	AI 1.669 1.669	AI 2.235 2.236	AI 2.789 2.792	AI 3.321 3.327	AI 3.823 3.831
1.715	Sr2 Co1 W1 O6	MSG 2.7 ($P_S\bar{1}$)	AI -0.191 0.003	AI -0.037 0.066	AI 1.34 1.38	AI 1.83 1.83	AI 2.237 2.237
1.716	Sr2 Mn1 Mo1 O6	MSG 14.80 (P_a2_1/c)	AI 0.351 0.377	AI 0.631 0.65	AI 0.931 0.943	AI 1.235 1.246	- -
1.717	Sr2 Mn1 W1 O6	MSG 14.80 (P_a2_1/c)	AI 0.854 0.862	AI 1.184 1.194	AI 1.479 1.485	AI 1.749 1.756	- -
1.718	Ca2 Mn1 W1 O6	MSG 2.7 ($P_S\bar{1}$)	AI 0.973 0.978	AI 1.276 1.28	AI 1.554 1.557	AI 1.809 1.813	- -
1.719	Ca2 Mn1 W1 O6	MSG 2.7 ($P_S\bar{1}$)	AI 0.969 0.969	AI 1.285 1.294	AI 1.564 1.583	AI 1.82 1.84	AI 2.054 2.074
1.724	Ba2 Ni1 Te1 O6	MSG 14.83 (P_A2_1/c)	AI 1.096 1.107	AI 1.572 1.588	AI 1.984 2.054	AI 2.345 2.487	AI 2.675 2.765
1.726	Ru1 Cl3	MSG 5.16 (C_c2)	AI -0.033 0.002	AI 0.311 0.314	AI 0.921 0.921	AI 1.483 1.486	AI 1.954 1.959
1.730	Cu2 Mn1 Si1 S4	MSG 7.27 (P_ac)	AI 1.104 1.105	AI 1.4 1.401	AI 1.667 1.667	AI 1.881 1.881	AI 2.034 2.034
1.731	Cu2 Fe1 Si1 S4	MSG 9.41 (C_ac)	AI 0.281 0.289	AI 0.79 0.796	AI 1.115 1.137	AI 1.365 1.438	AI 1.592 1.687
1.732	Mn1 Sn1 Cu2 S4	MSG 5.16 (C_c2)	AI 0.354 0.36	AI 0.486 0.486	AI 0.587 0.587	AI 0.675 0.675	AI 0.758 0.758
1.733	Ge1 Mn1 Cu2 S4	MSG 7.27 (P_ac)	AI 0.331 0.348	AI 0.485 0.488	AI 0.594 0.594	AI 0.68 0.68	AI 0.755 0.755
1.734	Fe1 Ge1 Cu2 S4	MSG 1.3 (P_S1)	AI 0.191 0.285	AI 0.616 0.682	AI 0.956 1.045	AI 1.114 1.383	AI 1.239 1.413
1.736	Co1 S2 O8 N4 H10	MSG 2.7 ($P_S\bar{1}$)	AI -0.206 0.005	AI -0.227 0.004	AI -0.223 0.012	AI 0.032 0.062	AI -0.195 0.006
1.741	Ni1 K1 As1 O4	MSG 2.7 ($P_S\bar{1}$)	AI 1.445 1.455	AI 1.975 2.021	AI 2.465 2.511	AI 2.925 2.971	AI 3.139 3.216
1.742	Ni1 K1 As1 O4	MSG 2.7 ($P_S\bar{1}$)	AI 1.552 1.613	AI 2.152 2.235	AI 2.704 2.803	AI 3.153 3.157	AI 3.315 3.326
1.745	Co3 La2	MSG 61.439 (P_Cbca)	ES -0.304 0.002	ES -0.258 0.005	ES -0.363 0.001	ES -0.472 0.005	OAI -0.381 0.0
1.746	Mn2 Y1	MSG 4.12 (P_C2_1)	AI -0.19 0.001	AI -0.241 0.005	AI -0.432 0.002	AI -0.653 0.004	AI -0.84 0.007

1.752	Cs1 Co2 Mo2 O9 H1	MSG 11.55 (P_{a21}/m)	AI -0.102 0.006	AI -0.02 0.095	NLC -0.305 0.003	AI 0.149 0.418	AI 0.181 0.399
2.31	Mn3 Zn1 N1	MSG 60.432 (P_Ibcn)	AF -0.211 0.0	ES -0.143 0.01	ES -0.19 0.006	ES -0.166 0.003	ES -0.436 0.001
2.35	Cr1 Se1	MSG 157.55 ($P31m'$)	- -	AI -0.507 0.02	AI -0.585 0.008	AI -0.787 0.015	AI -0.675 0.017
2.61	Fe3 F8 O2 H4	MSG 12.62 ($C2'/m'$)	- -	AI 0.248 0.259	AI 0.36 0.375	AI 0.538 0.543	AI 0.89 0.895
2.66	Fe1 Sn2	MSG 68.513 ($Cc'ca$)	AI -0.437 0.031	AI -0.574 0.023	AI -0.761 0.031	- -	-0.805 0.004
2.68	Ge2 Fe1	MSG 56.367 ($Pc'cn$)	AI -0.171 0.016	AI -0.381 0.018	AI -0.694 0.047	-0.981 0.032	-1.204 0.014
2.93	Co1 Cr1 O4	MSG 60.417 ($Pbcn$)	AI 0.038 0.077	AI 0.682 0.682	AI 1.228 1.249	AI 1.634 1.663	AI 1.909 1.921
3.24	Ca1 Fe3 Ti4 O12	MSG 148.17 ($R\bar{3}$)	AI 0.224 0.27	AI 0.612 0.612	AI 1.01 1.01	AI 1.468 1.468	AI 1.958 1.958

TAB. S5: Topological diagnosis and gap calculations for materials with only d electrons. In the first, second and third columns, we list the BCSID, chemical formula and MSG of each compound. In columns 4-8, we provide the topological classification, indirect and direct gaps as a function of the Hubbard U parameter.

BCS ID	Formula	MSG	U=0	U=2	U=4	U=6
0.237	Er2 Sn2 O7	MSG 141.555 ($I4'_1/AMD'$)	AI 0.925 0.933	AI 1.883 1.892	AI 2.629 2.637	AI 2.608 2.614
0.238	Er2 Sn2 O7	MSG 141.555 ($I4'_1/AMD'$)	AI 0.903 0.913	AI 2.083 2.092	AI 2.85 2.862	AI 2.823 2.832
0.320	U2 Pd2 In1	MSG 127.394 ($P4'/m'bm'$)	ESFD -0.303 0.0	ESFD -1.1 0.0	ESFD -0.961 0.0	ESFD -1.23 0.0
0.321	U2 Sn1 Pd2	MSG 127.394 ($P4'/m'bm'$)	NLC -0.259 0.02	NLC -1.073 0.036	NLC -0.761 0.033	NLC -0.875 0.081
0.324	Cd1 Yb2 S4	MSG 141.551 ($I4_1/AMD$)	AF -0.484 0.0	-	-	AI 0.017 0.117
0.326	Nd2 Sn2 O7	MSG 227.131 ($Fd\bar{3}m'$)	AI 0.642 0.653	AI 2.439 2.47	AI 3.078 3.078	AI 3.072 3.072
0.330	Er1 Ge3	MSG 11.53 ($P2_1/m'$)	AI -0.257 0.028	AI -1.812 0.05	AI -2.146 0.004	AI -2.234 0.005
0.339	Nd2 Hf2 O7	MSG 227.131 ($Fd\bar{3}m'$)	AI 0.607 0.645	AI 2.418 2.453	AI 3.272 3.352	AI 3.511 3.513
0.340	Nd2 Zr2 O7	MSG 227.131 ($Fd\bar{3}m'$)	AI 0.607 0.643	AI 2.427 2.463	AI 3.504 3.504	AI 3.452 3.457
0.343	Tb1 Ge2	MSG 65.483 ($Cm'mm$)	AI -0.085 0.003	AI -0.864 0.001	AI -0.943 0.016	AI -1.151 0.018
0.350	Tb1 Al1 O3	MSG 62.449 ($Pn'm'a'$)	ES 0.078 0.1	AI 0.785 0.794	AI 2.724 2.733	AI 4.371 4.385
0.410	Gd1 Al1 O3	MSG 62.449 ($Pn'm'a'$)	AI 5.0 5.075	AI 5.0 5.075	AI 5.0 5.075	AI 5.0 5.075
0.525	Ce1 Na1 O2	MSG 141.556 ($I4'_1/a'm'd$)	AI 0.019 0.058	AI 0.84 0.84	AI 1.924 1.939	AI 2.704 2.713
0.527	Er2 Si2 O7	MSG 12.60 ($C2'/m$)	AI 0.901 0.906	AI 2.294 2.295	AI 2.409 2.41	AI 3.267 3.27
0.593	U1 Se1 P1	MSG 129.417 ($P4/nm'm'$)	ES -0.086 0.003	SEBR -0.209 0.019	ES -1.362 0.026	ES -1.034 0.004
0.594	U1 S1 As1	MSG 129.417 ($P4/nm'm'$)	SEBR -0.137 0.017	SEBR -0.482 0.004	ES -0.449 0.046	ES -0.538 0.015
0.595	U1 Te1 P1	MSG 139.537 ($I4/mm'm'$)	- -	ES -0.727 0.01	ES -1.168 0.028	ES -1.124 0.058
0.596	U1 Te1 As1	MSG 139.537 ($I4/mm'm'$)	- -	ES -0.713 0.01	ES -0.874 0.011	ES -1.127 0.002
0.616	Ho1 B2	MSG 12.62 ($C2'/m'$)	NLC -1.041 0.012	SEBR -1.194 0.053	SEBR -1.529 0.053	SEBR -2.227 0.02
0.625	U2 In1 Pd2	MSG 127.394 ($P4'/m'bm'$)	- -	ESFD -1.112 0.0	ESFD -0.952 0.0	ESFD -1.218 0.0

0.650	Er2 Si2 O7	MSG 12.60 ($C2'/m$)	AI 0.909 0.914	AI 2.319 2.328	AI 2.414 2.435	AI 3.247 3.258
0.681	Sb3 Ce4	MSG 122.336 ($I\bar{4}'2d'$)	ESFD -0.029 0.0	ESFD -0.395 0.004	-0.417 0.0	- -
0.684	Pt1 Tb1	MSG 62.446 ($Pn'm'a$)	ES -0.041 0.002	NLC -0.659 0.015	NLC -0.912 0.002	NLC -0.924 0.006
0.685	Er1 Pt1	MSG 62.447 ($Pnm'a'$)	AI -0.551 0.001	AI -0.625 0.017	AI -0.718 0.008	NLC -1.059 0.012
0.686	Ho1 Pt1	MSG 62.447 ($Pnm'a'$)	AI -0.248 0.01	AI -0.204 0.009	AI -0.326 0.014	ES -0.612 0.001
0.687	Dy1 Pt1	MSG 62.446 ($Pn'm'a$)	ES -0.109 0.0	AI -0.052 0.001	-0.368 0.002	NLC -0.689 0.013
0.688	Tm1 Pt1	MSG 62.447 ($Pnm'a'$)	AF -0.038 0.0	AI -0.53 0.019	AI -0.426 0.006	AI -0.577 0.01
0.689	Pt1 Pr1	MSG 63.462 ($Cm'c'm$)	ES -0.337 0.005	ES -0.614 0.002	OAI -2.156 0.033	ES -0.46 0.001
0.690	Nd1 Pt1	MSG 15.89 ($C2'/c'$)	NLC -0.642 0.008	OAI -1.241 0.007	NLC -1.237 0.033	NLC -1.834 0.029
0.743	Ho3 Al5 O12	MSG 230.148 ($Ia\bar{3}d'$)	AF 0.859 0.861	AI - -	AI 3.19 3.19	- -
0.782	Nd1 Sc1 O3	MSG 62.444 ($Pnm'a$)	AI 0.65 0.683	AI 2.322 2.368	AI 3.562 3.562	AI 3.64 3.64
0.783	Nd1 In1 O3	MSG 62.444 ($Pnm'a$)	AI 0.646 0.646	AI 2.427 2.434	AI 3.032 3.032	AI 3.057 3.057
0.821	Sr1 Gd2 O4	MSG 62.445 ($Pnma'$)	AI 3.59 3.59	AI 3.59 3.59	AI 3.59 3.59	AI 3.59 3.59
0.832	Ce1 Au1 Ge1	MSG 36.175 ($Cmc'2'_1$)	ES -0.036 0.001	AI -0.236 0.003	AI -0.34 0.016	-0.434 0.013
0.842	Dy1 Al1 O3	MSG 62.449 ($Pn'm'a'$)	ES -0.002 0.0	AI 2.101 2.13	AI 2.513 2.52	AI 3.439 3.44
0.854	Gd2 Pt2 O7	MSG 141.555 ($I4'_1/amd'$)	AI 1.189 1.446	AI 1.189 1.446	AI 1.189 1.446	AI 1.189 1.446
0.863	Eu1 Cd2 As2	MSG 12.62 ($C2'/m'$)	OAI -0.176 0.01	SEBR -0.156 0.018	SEBR -0.018 0.005	NLC 0.008 0.008
0.941	Er2 O3	MSG 206.37 ($Ia\bar{3}$)	AI -0.0 0.0	AI 2.196 2.213	AI 2.534 2.537	3.797 3.798
0.950	Er1 La1 O3	MSG 62.441 ($Pnma$)	AI 0.757 0.761	AI 2.304 2.32	AI 2.996 3.026	AI 3.65 3.683
0.952	Yb1 Pd1 Si1	MSG 59.409 ($Pm'm'n$)	OAI -1.073 0.0	SEBR -1.184 0.0	SEBR -1.394 0.001	SEBR -1.644 0.003

0.972	Ho1 Pd1 In1	MSG 189.225 ($P\bar{6}2'm'$)	ES -0.555 0.001	-1.179 0.001	ES -1.262 0.002	-1.202 0.0
0.973	Ho1 Pd1 In1	MSG 189.225 ($P\bar{6}2'm'$)	ES -0.658 0.003	-0.818 0.001	-1.232 0.0	-1.189 0.001
0.974	Er1 Pd1 In1	MSG 189.225 ($P\bar{6}2'm'$)	-0.289 0.001	-0.977 0.0	-1.364 0.001	-1.289 0.0
0.975	Er1 Pd1 In1	MSG 189.225 ($P\bar{6}2'm'$)	-0.279 0.0	-0.95 0.0	-1.319 0.001	-1.248 0.002
0.976	Nd1 Pd1 In1	MSG 38.191 ($Am'm'2$)	ES -0.415 0.008	AI -1.012 0.001	ES -1.116 0.003	ES -1.27 0.0
0.977	Nd1 Pd1 In1	MSG 8.34 (Cm')	AI -0.465 0.01	AI -0.866 0.008	AI -1.087 0.009	AI -1.509 0.014
0.985	Eu1 Pd3 Si2	MSG 74.559 ($Imm'a'$)	ES -0.623 0.001	ES -0.828 0.0	ES -1.001 0.002	ES -1.045 0.001
1.288	Ce1 Pd2 Si2	MSG 66.500 (C_{Accm})	SEBR -0.679 0.004	SEBR -0.697 0.007	AF -2.04 0.0	ES -2.173 0.001
1.290	Ce1 Rh2 Si2	MSG 64.480 (C_{Amca})	SEBR -0.287 0.019	OAI -0.594 0.008	ES -1.432 0.003	ES -1.466 0.003
1.291	Au2 Ce1 Si2	MSG 128.410 (P_I4/mnc)	ES -0.255 0.01	ES -1.601 0.001	ES -2.796 0.001	ES -3.252 0.0
1.334	Pr2 Pd2 In1	MSG 62.451 (P_bnma)	ES -0.032 0.0	AI -0.395 0.005	ES -0.406 0.001	ES -0.408 0.0
1.339	Eu1 As3	MSG 12.63 (C_c2/m)	OAI -0.188 0.002	OAI -0.33 0.009	OAI -0.478 0.003	SEBR -0.504 0.007
1.361	Dy1 Ge1	MSG 15.90 (C_c2/c)	OAI -0.061 0.004	SEBR -0.07 0.018	SEBR -0.176 0.018	OAI -0.319 0.02
1.367	Pu2 O3	MSG 15.90 (C_c2/c)	SEBR -0.098 0.006	AI 1.301 1.427	AI 2.314 2.354	AI 3.024 3.15
1.486	Ce1 Rh1 Al4 Si2	MSG 124.360 (P_c4/mcc)	- -	ES -0.373 0.003	ES -0.342 0.006	ES -0.41 0.005
1.497	Eu1 Bi2 Mg2	MSG 12.63 (C_c2/m)	SEBR -0.216 0.044	SEBR -0.108 0.029	SEBR -0.018 0.027	SEBR -0.0 0.027
1.505	Gd1 Ag1 Sn1	MSG 33.154 (P_Cna2_1)	AI -0.732 0.016	AI -0.732 0.016	AI -0.732 0.016	AI -0.732 0.016
1.507	Al2 Pd5 Nd1	MSG 62.450 ($P_a nma$)	SEBR -0.136 0.001	SEBR -0.562 0.0	OAI -1.205 0.001	OAI -1.421 0.001
1.530	Ce1 C2	MSG 128.410 (P_I4/mnc)	ES -0.493 0.005	ES -0.4 0.026	ES -2.584 0.001	ES -3.888 0.0
1.531	Pr1 C2	MSG 128.410 (P_I4/mnc)	ES -0.183 0.003	ES -1.632 0.005	ES -3.267 0.003	ES -3.67 0.003

1.532	Nd1 C2	MSG 128.410 (P_{I4}/mnc)	ES -0.443 0.054	ES -2.029 0.013	ES -2.963 0.001	ES -3.492 0.001
1.536	U1 Pd2 Si2	MSG 128.410 (P_{I4}/mnc)	- - -	ES -0.624 0.043	OAI -0.843 0.033	OAI -1.137 0.048
1.574	Nd1 Bi1 Pt1	MSG 118.314 ($P_I\bar{4}n2$)	AI -0.216 0.053	AI -0.059 0.122	AI 0.083 0.083	AI 0.048 0.048
1.576	O2 S1 Yb2	MSG 12.63 (C_{c2}/m)	SEBR -0.381 0.002	SEBR -0.128 0.01	AI -0.024 0.034	AI 0.271 0.302
1.578	K1 Er1 Se2	MSG 12.63 (C_{c2}/m)	-0.367 0.009	AI 0.329 0.393	AI 0.491 0.565	AI 1.12 1.225
1.623	Bi2 Eu1 Mg2	MSG 12.63 (C_{c2}/m)	SEBR -0.2 0.045	SEBR -0.09 0.027	SEBR -0.017 0.015	SEBR 0.012 0.013
1.627	Ce1 K1 S2	MSG 15.90 (C_{c2}/c)	AI -0.135 0.012	SEBR -1.048 0.028	AI -1.005 0.01	AI -1.044 0.013
1.643	Cl1 Dy1 O1	MSG 62.450 (P_anma)	AI -0.106 0.007	AI 0.824 0.858	AI 2.182 2.224	AI 3.183 3.235
1.648	Nd2 O3	MSG 12.63 (C_{c2}/m)	- -	AI 1.591 1.591	AI 2.873 2.873	AI 3.535 3.561
1.658	Dy1 Ga3	MSG 15.90 (C_{c2}/c)	AI -0.084 0.004	AI -0.103 0.003	OAI -0.534 0.01	OAI -0.582 0.006
1.667	U1 Pd1 Ga5	MSG 67.509 (C_amma)	NLC -0.237 0.009	OAI -1.111 0.033	OAI -1.532 0.021	OAI -1.592 0.021
1.672	Eu1 Zn2 As2	MSG 12.63 (C_{c2}/m)	SEBR -0.098 0.025	SEBR -0.09 0.003	AI 0.026 0.036	AI 0.12 0.127
1.714	Ce1 Bi2 Au1	MSG 130.432 (P_{c4}/ncc)	ES -0.379 0.003	SEBR -0.539 0.022	SEBR -0.675 0.024	SEBR -0.768 0.015
1.740	Ce1 Au1 Sb2	MSG 39.201 (A_bb2)	ES -0.192 0.0	AI -0.131 0.002	AI -0.859 0.001	AI -0.903 0.0
1.744	Pr1 Pd1 Sn1	MSG 14.80 (P_a2_1/c)	NLC -0.116 0.002	NLC -0.528 0.008	NLC -0.597 0.012	NLC -0.6 0.004
1.747	Er1 In1 Au1	MSG 174.136 ($P_c\bar{6}$)	AF -0.163 0.0	AF -0.214 0.001	AF -0.226 0.001	AF -0.339 0.0
1.749	Ho1 Sb1 Te1	MSG 11.55 (P_a2_1/m)	NLC -0.161 0.03	OAI -0.301 0.0	OAI -0.365 0.011	OAI -0.401 0.011
1.753	Ho1 Bi1	MSG 15.90 (C_{c2}/c)	-0.285 0.006	AF -0.389 0.0	AF -1.11 0.011	AF -0.87 0.07
1.755	K1 Er1 Se2	MSG 12.63 (C_{c2}/m)	AI 0.117 0.26	AI 0.313 0.367	AI 0.288 0.406	AI 0.773 0.835
2.100	Ho1 P1	MSG 15.89 ($C2'/c'$)	AF -0.39 0.001	NLC -0.863 0.034	NLC -0.917 0.006	NLC -0.864 0.003

2.103	Eu3 Pb1 O1	MSG 47.252 ($Pm'm'm$)	ES -0.037 0.001	ES -0.063 0.001	OAI -0.112 0.0	OAI -0.115 0.001
2.71	H01 Rh1	MSG 11.57 (P_C2_1/m)	NLC -0.078 0.037	-0.245 0.014	-0.191 0.007	-0.371 0.007
3.21	Ga3 Tm1	MSG 229.143 ($Im\bar{3}m'$)	-0.066 0.0	-0.19 0.002	-1.033 0.0	-1.131 0.001
3.23	Eu3 Pb1 O1	MSG 123.345 ($P4/mm'm'$)	ES -0.024 0.0	ES -0.064 0.002	SEBR -0.022 0.01	SEBR -0.01 0.014

TAB. S6: Topological diagnosis and gap calculations for materials with only f electrons. In the first, second and third columns, we list the BCSID, chemical formula and MSG of each compound. In columns 4-8, we provide the topological classification, indirect and direct gaps as a function of the Hubbard U parameter.

BCS ID	Formula	MSG	U=0	U=2	U=4	U=6
0.231	Tm1 Mn3 O6	MSG 59.410 ($Pmm'n'$)	ES -0.057 0.0	ES -0.455 0.004	ES -0.603 0.004	- -
0.232	Tm1 Mn3 O6	MSG 59.409 ($Pm'm'n$)	AF -0.04 0.0	ES -0.364 0.006	ES -0.514 0.006	ES -0.843 0.002
0.235	Mn2 Pr1 Sb1 O6	MSG 86.67 ($P4_2/n$)	AI -0.015 0.005	AI 0.0 0.002	AI 0.829 0.848	AI 1.454 1.758
0.289	Nd1 Mn1 O3	MSG 62.448 ($Pn'ma'$)	AF -0.135 0.004	-0.012 0.425	0.021 0.107	0.461 0.767
0.290	Ce1 Cu2	MSG 74.560 ($Im'm'a'$)	AI -0.341 0.021	-0.42 0.014	-0.465 0.019	AF -0.532 0.004
0.318	Tm2 Co1 Mn1 O6	MSG 14.79 ($P2'_1/c'$)	NLC -0.032 0.0	AI -0.015 0.114	-0.176 0.024	AI -0.002 0.118
0.319	Tm2 Co1 Mn1 O6	MSG 14.79 ($P2'_1/c'$)	AF -0.029 0.002	-0.008 0.1	-0.221 0.049	-0.019 0.095
0.367	Eu1 Cr2 As2	MSG 119.319 ($I\bar{4}m'2'$)	AF -0.98 0.001	ES -1.329 0.002	ES -1.678 0.005	AF -2.091 0.005
0.372	Dy1 Cr1 O4	MSG 15.87 ($C2'/c$)	AI -0.035 0.027	AI 0.482 0.557	-0.223 0.013	AI -0.216 0.015
0.374	Tb1 Ni4 Si1	MSG 65.486 ($Cmm'm'$)	ES -0.351 0.001	ES -0.726 0.002	ES -1.595 0.0	ES -1.573 0.001
0.406	Gd1 Ni1 Si3	MSG 65.484 ($Cmmm'$)	AI -1.885 0.001	AI -1.981 0.003	AI -1.981 0.003	AI -1.981 0.003
0.519	Ho1 Cr2 Si2	MSG 139.536 ($I4'/m'm'm$)	AF -0.154 0.0	- -	ESFD -0.445 0.0	- -
0.561	Ni1 Nd1 Ge2	MSG 63.462 ($Cm'c'm$)	- -	ES -2.037 0.001	OAI -2.09 0.001	ES -2.182 0.002
0.566	Ge2 Ni1 Tb1	MSG 63.459 ($Cm'cm$)	ES -0.104 0.02	ES -0.901 0.022	ES -2.3 0.006	ES -2.458 0.011
0.587	Tm1 Cr1 O3	MSG 62.448 ($Pn'ma'$)	OAI -0.008 0.001	- -	0.617 0.617	- -
0.590	Er1 Cr1 O3	MSG 11.50 ($P2_1/m$)	- -	- -	AI 1.46 1.487	AI 2.365 2.41
0.620	Mn1 Nd1 As1 O1	MSG 129.416 ($P4'/n'm'm$)	SEBR -0.09 0.008	- -	SEBR -0.135 0.022	AI -0.077 0.005
0.621	Mn1 Nd1 As1 O1	MSG 59.407 ($Pm'mn$)	AI -0.157 0.006	AI 0.558 0.585	-0.765 0.139	AI 0.716 0.957
0.622	Mn1 Nd1 As1 O1	MSG 59.407 ($Pm'mn$)	AI -0.101 0.004	AI -0.144 0.003	0.708 0.9	- -
0.623	Mn1 Nd1 As1 O1	MSG 129.416 ($P4'/n'm'm$)	SEBR -0.089 0.008	- -	SEBR -0.155 0.021	AI -0.063 0.01

0.656	Nd1 Mn2 Ge2	MSG 44.231 ($Im'm2'$)	ES -0.244 0.001	ES -0.382 0.006	-0.402 0.004	ES -0.416 0.012
0.657	Pr1 Mn2 Ge2	MSG 44.231 ($Im'm2'$)	ES -0.224 0.001	ES -0.414 0.007	ES -0.432 0.001	ES -0.392 0.006
0.666	Ce1 Mn1 Sb1 O1	MSG 59.407 ($Pm'mn$)	AI -0.086 0.009	AI 0.348 0.348	AI 0.411 0.726	AI 0.406 0.726
0.668	Pr1 Mn1 Sb1 O1	MSG 59.407 ($Pm'mn$)	AF -0.164 0.0	AI -1.121 0.062	AI 0.375 0.675	AI 0.366 0.696
0.671	Sr2 Tm1 Ru1 O6	MSG 14.75 ($P2_1/c$)	AF -0.041 0.001	AI 0.992 1.147	AI 1.006 1.186	AI 0.997 1.205
0.700	Tb1 Mn6 Sn6	MSG 191.240 ($P6/mm'm'$)	ES -0.375 0.001	-0.854 0.001	-0.933 0.0	- -
0.701	Tb1 Mn6 Sn6	MSG 191.240 ($P6/mm'm'$)	ES -0.387 0.0	AF -0.741 0.0	ES -0.863 0.001	ES -0.888 0.0
0.703	Ho1 Mn6 Sn6	MSG 12.62 ($C2'/m'$)	SEBR -0.778 0.001	SEBR -0.872 0.001	-	SEBR -0.892 0.006
0.704	Ho1 Mn6 Sn6	MSG 12.62 ($C2'/m'$)	NLC -0.434 0.002	SEBR -0.848 0.003	-	NLC -0.853 0.003
0.705	Ho1 Mn6 Sn6	MSG 65.486 ($Cmm'm'$)	ES -0.145 0.007	ES -0.785 0.004	AF -0.763 0.0	ES -0.775 0.0
0.715	W1 Ho1 Cr1 O6	MSG 33.144 ($Pna2_1$)	AI -0.02 0.013	-	AI 1.534 1.55	AI 1.81 1.926
0.729	Er1 Ni4 B1	MSG 191.240 ($P6/mm'm'$)	ES -0.261 0.0	AF -0.568 0.0	ES -0.671 0.0	ES -0.798 0.0
0.730	Tb1 Ni4 B1	MSG 12.62 ($C2'/m'$)	SEBR -0.457 0.001	SEBR -0.671 0.002	SEBR -0.665 0.003	- -
0.731	Ho1 Ni4 B1	MSG 12.62 ($C2'/m'$)	SEBR -0.535 0.001	AF -0.525 0.001	NLC -0.6 0.001	NLC -0.641 0.001
0.758	Ce1 Fe1 O3	MSG 62.441 ($Pnma$)	AI 0.047 0.076	AI 0.37 0.413	AI 1.3 1.325	AI 1.568 1.568
0.759	Ce1 Fe1 O3	MSG 62.441 ($Pnma$)	AI 0.046 0.076	AI 0.358 0.432	AI 1.086 1.129	AI 1.57 1.57
0.771	Pr1 Mn1 Si2	MSG 63.464 ($Cm'cm'$)	ES -0.126 0.001	ES -0.514 0.006	ES -0.748 0.024	ES -0.747 0.012
0.772	Pr1 Mn1 Si2	MSG 63.464 ($Cm'cm'$)	ES -0.111 0.001	ES -0.538 0.023	ES -0.682 0.017	- -
0.773	Nd1 Mn1 Si2	MSG 12.62 ($C2'/m'$)	NLC -0.09 0.009	NLC -0.759 0.009	SEBR -0.465 0.012	SEBR -1.03 0.014
0.774	Nd1 Mn1 Si2	MSG 63.464 ($Cm'cm'$)	SEBR -0.615 0.003	ES -0.724 0.006	ES -0.712 0.03	ES -0.661 0.004

0.775	Nd1 Mn1 Si2	MSG 63.464 ($Cm'cm'$)	ES -0.069 0.002	ES -0.62 0.013	ES -0.699 0.016	ES -0.661 0.004
0.776	Ce1 Mn1 Si2	MSG 63.464 ($Cm'cm'$)	ES -0.373 0.002	ES -0.335 0.009	-	ES -0.746 0.006
0.777	Ce1 Mn1 Si2	MSG 63.464 ($Cm'cm'$)	ES -0.373 0.002	ES -0.376 0.003	ES -0.72 0.003	ES -0.727 0.004
0.781	Ce1 Mn1 Si2	MSG 63.464 ($Cm'cm'$)	ES -0.375 0.002	ES -0.415 0.004	ES -0.274 0.016	ES -0.788 0.006
0.784	Nd1 Co1 O3	MSG 62.441 ($Pnma$)	NLC -0.035 0.002	AI 0.654 0.654	-	ES -0.09 0.0
0.789	Ce1 Cu1 Si1	MSG 63.463 ($Cmc'm'$)	ES -0.198 0.003	ES -0.504 0.0	ES -1.25 0.001	ES -1.31 0.0
0.791	Sr2 Tb1 Ru1 O6	MSG 14.75 ($P2_1/c$)	NLC -0.199 0.024	AI 0.209 0.219	AI 1.049 1.177	AI 1.056 1.212
0.792	Sr2 Ho1 Ru1 O6	MSG 14.75 ($P2_1/c$)	ES -0.257 0.015	AI 1.036 1.175	AI 1.042 1.218	AI 1.047 1.243
0.794	Sr2 Ho1 Ru1 O6	MSG 14.75 ($P2_1/c$)	ES -0.17 0.004	NLC -0.035 0.024	AI 1.023 1.106	AI -0.281 0.046
0.840	Dy1 Fe1 O3	MSG 62.441 ($Pnma$)	OAI -0.005 0.002	AI 0.785 0.835	AI 1.529 1.53	-
0.841	Dy1 Fe1 O3	MSG 62.441 ($Pnma$)	OAI -0.004 0.004	AI 0.79 0.829	-	AI 1.042 1.271
0.867	Ir1 Nd2 Ni1 O6	MSG 14.75 ($P2_1/c$)	- -	AI 0.317 0.419	AI 0.488 0.654	AI 0.515 0.7
0.869	Ni1 Ir1 Pr2 O6	MSG 14.75 ($P2_1/c$)	ES -0.018 0.015	ES 0.01 0.034	ES -0.036 0.026	ES -0.042 0.016
0.870	Ni1 Ir1 Pr2 O6	MSG 14.75 ($P2_1/c$)	ES -0.072 0.002	AI 0.33 0.374	AI 0.445 0.56	AI 0.465 0.597
0.871	Ni1 Ir1 Pr2 O6	MSG 14.75 ($P2_1/c$)	ES -0.023 0.002	AI 0.285 0.352	NLC -0.05 0.008	AI 0.472 0.609
0.872	Ni1 Ir1 Pr2 O6	MSG 14.75 ($P2_1/c$)	AI -0.057 0.001	AI 0.269 0.356	AI 0.604 0.619	AI 0.54 0.619
0.873	Ni1 Ir1 Pr2 O6	MSG 14.75 ($P2_1/c$)	ES -0.015 0.005	AI 0.267 0.367	AI 0.531 0.686	AI 0.468 0.498
0.874	Ni1 Ir1 Nd2 O6	MSG 14.75 ($P2_1/c$)	ES -0.113 0.007	AI 0.494 0.646	AI 0.574 0.697	AI 0.57 0.701
0.875	Ni1 Ir1 Nd2 O6	MSG 14.75 ($P2_1/c$)	AI 0.029 0.039	AI 0.52 0.691	AI 0.577 0.659	AI 0.568 0.696
0.897	Tb1 Mn2 Ge2	MSG 139.537 ($I4/mm'm'$)	ES -0.311 0.005	ES -0.627 0.0	ES -1.038 0.001	ES -1.137 0.005

0.902	Dy1 Mn2 Ge2	MSG 139.537 ($I4/mm'm'$)	ES -0.47 0.003	ES -0.472 0.0	ES -0.968 0.003	ES -0.948 0.008
0.910	Ni1 Si2 Tb1	MSG 63.459 ($Cm'cm$)	ES -0.175 0.001	ES -0.989 0.016	AF -2.474 0.0	ES -2.627 0.002
0.919	Eu1 Mn1 Bi2	MSG 139.536 ($I4'/m'm'm$)	AF -0.182 0.003	NLC -0.301 0.013	NLC -0.283 0.012	AF -0.404 0.001
0.920	N1 P1 Mn1 Th1	MSG 129.416 ($P4'/n'm'm$)	- -	AI 0.677 0.817	-	AI 0.636 0.854
0.922	N1 As1 Mn1 Th1	MSG 129.416 ($P4'/n'm'm$)	- -	AI 0.622 0.822	-	AI 0.578 0.799
0.923	N1 As1 Mn1 Th1	MSG 129.416 ($P4'/n'm'm$)	AI 0.279 0.316	AI 0.616 0.82	-	AI 0.574 0.796
0.944	Yb2 Ir2 O7	MSG 166.101 ($R\bar{3}m'$)	SEBR -0.072 0.012	ES -0.138 0.0	ES -0.125 0.001	AI 0.226 0.242
0.945	Yb2 Ir2 O7	MSG 227.131 ($Fd\bar{3}m'$)	NLC -0.077 0.013	NLC -0.079 0.015	AI 0.041 0.043	AI 0.235 0.24
0.954	Nd2 Ir2 O7	MSG 227.131 ($Fd\bar{3}m'$)	AF -0.07 0.0	AI -0.014 0.003	AI 0.306 0.467	NLC -0.113 0.001
0.970	Pr1 Ru2 Si2	MSG 139.537 ($I4/mm'm'$)	ES -0.645 0.015	ES -1.401 0.001	ES -1.983 0.007	ES -1.214 0.023
0.978	Er1 In1 Ni1	MSG 189.225 ($P\bar{6}2'm'$)	-0.331 0.0	-1.027 0.001	-1.183 0.001	-1.098 0.001
0.979	Tm1 V1 O3	MSG 62.446 ($Pn'm'a$)	NLC -0.025 0.004	AI -0.074 0.006	AI -0.028 0.06	0.576 0.577
0.980	Tm1 V1 O3	MSG 62.446 ($Pn'm'a$)	NLC -0.025 0.002	-0.075 0.002	-	-
0.981	Tm1 V1 O3	MSG 62.441 ($Pnma$)	NLC -0.025 0.002	NLC -0.278 0.0	AI 0.219 0.231	AI 0.482 0.541
0.982	Tm1 V1 O3	MSG 14.75 ($P2_1/c$)	NLC -0.026 0.002	ES -0.111 0.009	AI -0.051 0.031	-
0.983	Tm1 V1 O3	MSG 14.75 ($P2_1/c$)	NLC -0.026 0.003	AI -0.125 0.012	-	AI 0.741 0.786
1.272	Ce1 Ni1 As1 O1	MSG 4.10 (P_a2_1)	AI -0.458 0.003	AI -0.525 0.004	AI -1.179 0.002	AI -1.241 0.007
1.292	Ho1 Ni2 B2 C1	MSG 64.480 (C_{Amca})	AI -0.603 0.0	AI -1.176 0.001	AI -1.27 0.004	AI -1.739 0.001
1.293	Nd1 Ni2 B2 C1	MSG 15.90 (C_c2/c)	OAI -0.193 0.03	SEBR -0.963 0.025	SEBR -1.161 0.015	SEBR -1.257 0.013
1.294	Ho1 Ni2 B2 C1	MSG 64.480 (C_{Amca})	SEBR -0.233 0.01	AI -1.168 0.003	AI -1.282 0.0	AI -1.664 0.001

1.295	Dy1 Ni2 B2 C1	MSG 64.480 (C_{Amca})	ES -0.333 0.002	AI -1.128 0.0	AI -0.316 0.006	AI -1.802 0.0
1.296	Pr1 Ni2 B2 C1	MSG 64.480 (C_{Amca})	SEBR -0.39 0.002	ES -1.553 0.001	AF -1.695 0.0	AF -1.865 0.0
1.312	Ho1 Ni2 B2 C1	MSG 64.480 (C_{Amca})	AI -0.603 0.0	AI -1.177 0.0	AI -1.363 0.009	AI -1.745 0.001
1.350	Ba1 Nd2 Co1 O5	MSG 15.90 (C_c2/c)	AI -0.05 0.0	AI 1.482 1.482	AI 1.568 1.568	AI 1.585 1.585
1.363	Tb1 Cu2 Si2	MSG 2.7 ($P_S\bar{1}$)	OAI -0.123 0.015	AF -1.46 0.019	-1.718 0.019	OAI -2.019 0.007
1.364	Ho1 Cu2 Si2	MSG 2.7 ($P_S\bar{1}$)	OAI -0.862 0.016	OAI -1.414 0.007	OAI -1.415 0.016	-2.034 0.007
1.365	Cu2 Si2 Tb1	MSG 2.7 ($P_S\bar{1}$)	OAI -0.515 0.018	NLC -1.407 0.003	NLC -1.686 0.024	NLC -1.988 0.013
1.366	Cu2 Ho1 Si2	MSG 12.63 (C_c2/m)	ES -0.92 0.007	-1.415 0.004	-1.67 0.0	-1.927 0.007
1.369	Ho1 Fe2 Ge2	MSG 64.480 (C_{Amca})	SEBR -0.131 0.003	AF -0.419 0.0	ES -0.372 0.0	ES -0.441 0.003
1.487	Ce1 Ir1 Al4 Si2	MSG 124.360 (P_c4/mcc)	- -	- -	-0.231 0.005	-0.255 0.012
1.488	Ce1 Mn2 Si2	MSG 126.386 (P_I4/nnc)	ES -0.054 0.025	ES -0.151 0.028	ES -0.143 0.049	ES -0.105 0.002
1.489	Ce1 Mn2 Si2	MSG 126.386 (P_I4/nnc)	ES 0.021 0.024	ES -0.278 0.008	ES -0.292 0.029	- -
1.491	Pr1 Mn2 Si2	MSG 126.386 (P_I4/nnc)	- -	ESFD -0.828 0.0	ESFD -1.206 0.0	ESFD -1.264 0.0
1.492	Pr1 Mn2 Si2	MSG 126.386 (P_I4/nnc)	ESFD -0.052 0.0	ESFD -0.842 0.0	ESFD -1.184 0.0	ESFD -1.246 0.0
1.493	Pr1 Mn2 Si2	MSG 126.386 (P_I4/nnc)	- -	ESFD -0.788 0.0	ESFD -1.105 0.0	ESFD -1.162 0.0
1.494	Nd1 Mn2 Si2	MSG 126.386 (P_I4/nnc)	OAI -0.233 0.001	ES -0.145 0.006	ES -0.451 0.022	AF -0.552 0.0
1.504	Gd1 Cu1 Sn1	MSG 33.154 (P_{Cna2_1})	AI -0.774 0.014	-0.8 0.015	-0.8 0.015	-0.8 0.015
1.511	Ni2 Tb1 Si2	MSG 64.480 (C_{Amca})	SEBR -0.283 0.004	OAI -1.054 0.008	OAI -1.687 0.006	OAI -1.707 0.009
1.516	Er1 Co2 Si2	MSG 58.404 (P_{Innm})	- -	ES -0.906 0.006	ES -1.127 0.004	AF -1.223 0.0
1.549	U2 In1 Ni2	MSG 128.408 (P_c4/mnc)	- -	ES -0.24 0.013	ES -0.372 0.011	- -

1.566	Ba2 Yb1 Ru1 O6	MSG 128.410 (P_{I4}/mnc)	ES -0.207 0.008	ES -0.218 0.001	-	ES -0.203 0.002
1.567	Ba2 Tm1 Ru1 O6	MSG 128.410 (P_{I4}/mnc)	SEBR -0.027 0.03	AI 0.817 0.828	ES -0.021 0.002	AI 0.842 0.993
1.568	Cu2 Gd1 Si2	MSG 12.63 (C_{c2}/m)	AF -2.25 0.0	AF -2.297 0.0	AF -2.297 0.0	AF -2.297 0.0
1.584	Pr1 Fe1 As1 O1	MSG 54.350 (P_{Bcca})	OAI -0.027 0.012	OAI 0.002 0.002	OAI 0.006 0.01	ES -0.097 0.015
1.585	Pr1 Fe1 As1 O1	MSG 54.350 (P_{Bcca})	NLC -0.018 0.006	NLC -0.014 0.005	OAI 0.005 0.019	OAI 0.007 0.007
1.586	Pr1 Fe1 As1 O1	MSG 27.85 (P_{Acc2})	AI -0.04 0.003	AI -0.072 0.004	AI 0.182 0.382	AI -0.102 0.061
1.596	Tb1 Cu1 Sb2	MSG 2.7 ($P_{S\bar{1}}$)	OAI -0.046 0.012	OAI -0.509 0.004	-0.87 0.022	OAI -0.847 0.043
1.628	Pr1 Mn1 Si2	MSG 52.318 (P_{Bnna})	ES -0.145 0.001	ES -0.222 0.009	ES -0.5 0.0	ES -0.405 0.004
1.635	Er1 Fe2 Si2	MSG 62.450 (P_{anma})	ES -0.403 0.004	SEBR -0.506 0.001	SEBR -0.491 0.001	SEBR -0.568 0.0
1.636	Er1 Mn2 Si2	MSG 126.386 ($P_{I4}/nncc$)	SEBR -0.211 0.002	ES -0.548 0.012	ES -0.585 0.022	OAI -0.67 0.008
1.637	Er1 Mn2 Si2	MSG 126.386 ($P_{I4}/nncc$)	AI -0.243 0.001	OAI -0.565 0.014	OAI -0.59 0.011	ES -0.715 0.011
1.638	Er1 Mn2 Ge2	MSG 126.386 ($P_{I4}/nncc$)	AI -0.211 0.001	ES -0.385 0.004	SEBR -0.843 0.004	ES -0.794 0.0
1.639	Er1 Mn2 Ge2	MSG 126.386 ($P_{I4}/nncc$)	AI -0.21 0.001	SEBR -0.608 0.001	ES -0.843 0.006	ES -0.844 0.002
1.640	Er1 Mn2 Ge2	MSG 126.386 ($P_{I4}/nncc$)	AI -0.207 0.0	ES -0.328 0.002	SEBR -0.844 0.01	ES -0.974 0.017
1.664	Dy1 V1 O4	MSG 62.456 (P_{Inma})	AI -0.009 0.003	AI 2.094 2.105	AI 2.326 2.357	AI 2.915 2.918
1.666	Tb1 Co1 Ga5	MSG 67.509 (C_{amma})	OAI -0.384 0.007	OAI -0.949 0.008	NLC -1.368 0.008	OAI -0.938 0.009
1.668	Ho1 Co1 Ga5	MSG 67.509 (C_{amma})	NLC -1.005 0.015	NLC -1.356 0.012	NLC -1.218 0.011	NLC -1.331 0.014
1.670	Np1 Fe1 Ga5	MSG 67.509 (C_{amma})	AI -0.03 0.003	AI -0.592 0.015	AI -0.85 0.027	NLC -1.089 0.02
1.683	Ga5 Ni1 U1	MSG 140.550 (I_{c4}/mcm)	ES -0.198 0.004	SEBR -0.72 0.038	SEBR -0.9 0.038	OAI -1.103 0.045
1.690	Tm1 Mn2 Ge2	MSG 126.386 ($P_{I4}/nncc$)	AF -0.179 0.0	ESFD -0.59 0.0	ESFD -0.588 0.0	ESFD -1.115 0.0

1.694	Mn2 Tb1 Ge2	MSG 126.386 (P_I4/nnc)	ESFD -0.02 0.0	ESFD -1.094 0.0	ESFD -1.139 4.0	ESFD -1.132 0.0
1.721	U1 Cu5	MSG 161.72 (R_I3c)	AF -0.073 0.0	AI -0.344 0.029	AI -0.245 0.043	AI -0.221 0.041
1.729	Gd2 Fe2 Si2 C1	MSG 12.63 (C_c2/m)	SEBR -0.315 0.004	AF -0.269 0.005	AF -0.269 0.005	AF -0.269 0.005
1.738	Tb1 Al1 Ni1	MSG 46.247 ($I_a ma2$)	ES -0.012 0.0	AI -0.101 0.008	-0.12 0.003	- -
2.81	Er1 Mn2 Si2	MSG 59.409 ($Pm'm'n$)	OAI -0.355 0.002	ES -0.681 0.0	ES -0.841 0.0	AF -1.053 0.0
2.82	Er1 Mn2 Si2	MSG 59.409 ($Pm'm'n$)	OAI -0.712 0.003	AF -0.64 0.0	ES -0.762 0.0	ES -0.949 0.0
2.83	Er1 Mn2 Ge2	MSG 59.409 ($Pm'm'n$)	ES -0.356 0.001	ES -0.511 0.0	ES -0.964 0.0	- -
2.84	Er1 Mn2 Ge2	MSG 59.409 ($Pm'm'n$)	AF -0.663 0.0	ES -1.428 0.0	AF -1.372 0.0	- -
2.94	Tm1 Mn2 Ge2	MSG 26.70 ($Pm'c'2_1$)	AI -0.112 0.002	- -	AI -1.124 0.007	- -
3.20	Mn2 Tb1 Ge2	MSG 2.4 ($P\bar{1}$)	NLC -0.311 0.003	NLC -0.364 0.009	NLC -0.489 0.001	NLC -0.483 0.003

TAB. S7: Topological diagnosis and gap calculations for materials with both d and f electrons. In the first, second and third columns, we list the BCSID, chemical formula and MSG of each compound. In columns 4-8, we provide the topological classification, indirect and direct gaps as a function of the Hubbard U parameter.

Appendix E: Physical interpretation of systems with non-trivial symmetry indicators

In this section we provide the physical interpretation of the topological phase predicted by symmetry indicators according to the definitions in Ref. [2]. For each compound, for each Hubbard U value, we compute the symmetry indicators. Then, by subducing to their minimal SSG (see Ref. [2]) we provide the physical interpretation corresponding to their layer construction [2, 8]. As discussed in the main text (see Sec. II), the symmetry diagnosable topological phases are AXI, 3DQAH, SISM and MTCI. If two topological phases cannot be distinguished by symmetry indicators, we write both possibilities. For example, a set of symmetry indicators $(\eta_{4I}, z_{2I,1}, z_{2I,2}, z_{2I,3}) = (2, 0, 0, 0)$ indicates AXI. However, if the MSG does not forbid zero net Chern number, since the $z_{2I,i}$ indicators can only diagnose the Chern number mod(2), we cannot rule out that the system is in the 3DQAH phase.

BCS ID	Formula	U(eV)	MSG	minimal SSG	Indices	Interpretation
1.752	Cs1 Co2 Mo2 O9 H1	2	MSG 11.55 ($P_a 2_1/m$)	MSG 2.4 ($P\bar{1}$)	$\eta_{4I} = 2$ $z_{2I,1} = 0$ $z_{2I,2} = 0$ $z_{2I,3} = 0$	AXI
1.749	Ho1 Sb1 Te1	0	MSG 11.55 ($P_a 2_1/m$)	MSG 2.4 ($P\bar{1}$)	$\eta_{4I} = 2$ $z_{2I,1} = 0$ $z_{2I,2} = 0$ $z_{2I,3} = 0$	AXI
2.71	Ho1 Rh1	0	MSG 11.57 ($P_C 2_1/m$)	MSG 2.4 ($P\bar{1}$)	$\eta_{4I} = 2$ $z_{2I,1} = 0$ $z_{2I,2} = 0$ $z_{2I,3} = 0$	AXI
1.383	Fe1 Ca2 O3 Br1	4	MSG 113.273 ($P_C \bar{4}2_1m$)	MSG 81.33 ($P\bar{4}$)	$\delta_{2S} = 0$ $z_2 = 1$ $z_{4S} = 0$	AXI
0.863	Eu1 Cd2 As2	2	MSG 12.62 ($C2'/m'$)	MSG 2.4 ($P\bar{1}$)	$\eta_{4I} = 2$ $z_{2I,1} = 0$ $z_{2I,2} = 0$ $z_{2I,3} = 0$	AXI/3DQAH
0.863	Eu1 Cd2 As2	4	MSG 12.62 ($C2'/m'$)	MSG 2.4 ($P\bar{1}$)	$\eta_{4I} = 2$ $z_{2I,1} = 0$ $z_{2I,2} = 0$ $z_{2I,3} = 0$	AXI/3DQAH
0.863	Eu1 Cd2 As2	6	MSG 12.62 ($C2'/m'$)	MSG 2.4 ($P\bar{1}$)	$\eta_{4I} = 3$ $z_{2I,1} = 0$ $z_{2I,2} = 0$ $z_{2I,3} = 0$	SISM
0.616	Ho1 B2	0	MSG 12.62 ($C2'/m'$)	MSG 2.4 ($P\bar{1}$)	$\eta_{4I} = 1$ $z_{2I,1} = 1$ $z_{2I,2} = 1$ $z_{2I,3} = 0$	SISM
0.616	Ho1 B2	2	MSG 12.62 ($C2'/m'$)	MSG 2.4 ($P\bar{1}$)	$\eta_{4I} = 2$ $z_{2I,1} = 0$ $z_{2I,2} = 0$ $z_{2I,3} = 0$	AXI/3DQAH
0.616	Ho1 B2	4	MSG 12.62 ($C2'/m'$)	MSG 2.4 ($P\bar{1}$)	$\eta_{4I} = 2$ $z_{2I,1} = 0$ $z_{2I,2} = 0$ $z_{2I,3} = 0$	AXI/3DQAH
0.616	Ho1 B2	6	MSG 12.62 ($C2'/m'$)	MSG 2.4 ($P\bar{1}$)	$\eta_{4I} = 2$ $z_{2I,1} = 0$ $z_{2I,2} = 0$ $z_{2I,3} = 0$	AXI/3DQAH
0.703	Ho1 Mn6 Sn6	0	MSG 12.62 ($C2'/m'$)	MSG 2.4 ($P\bar{1}$)	$\eta_{4I} = 0$ $z_{2I,1} = 0$ $z_{2I,2} = 0$ $z_{2I,3} = 1$	3DQAH
0.703	Ho1 Mn6 Sn6	2	MSG 12.62 ($C2'/m'$)	MSG 2.4 ($P\bar{1}$)	$\eta_{4I} = 2$ $z_{2I,1} = 0$ $z_{2I,2} = 0$	AXI/3DQAH

					$z_{2I,3} = 0$	
0.703	Ho1 Mn6 Sn6	6	MSG 12.62 ($C2'/m'$)	MSG 2.4 ($P\bar{1}$)	$\eta_{4I} = 0$ $z_{2I,1} = 0$ $z_{2I,2} = 0$ $z_{2I,3} = 1$	3DQAH
0.704	Ho1 Mn6 Sn6	0	MSG 12.62 ($C2'/m'$)	MSG 2.4 ($P\bar{1}$)	$\eta_{4I} = 3$ $z_{2I,1} = 0$ $z_{2I,2} = 0$ $z_{2I,3} = 1$	SISM
0.704	Ho1 Mn6 Sn6	2	MSG 12.62 ($C2'/m'$)	MSG 2.4 ($P\bar{1}$)	$\eta_{4I} = 2$ $z_{2I,1} = 0$ $z_{2I,2} = 0$ $z_{2I,3} = 0$	AXI/3DQAH
0.704	Ho1 Mn6 Sn6	6	MSG 12.62 ($C2'/m'$)	MSG 2.4 ($P\bar{1}$)	$\eta_{4I} = 3$ $z_{2I,1} = 0$ $z_{2I,2} = 0$ $z_{2I,3} = 0$	SISM
0.731	Ho1 Ni4 B1	0	MSG 12.62 ($C2'/m'$)	MSG 2.4 ($P\bar{1}$)	$\eta_{4I} = 2$ $z_{2I,1} = 0$ $z_{2I,2} = 0$ $z_{2I,3} = 0$	AXI/3DQAH
0.731	Ho1 Ni4 B1	4	MSG 12.62 ($C2'/m'$)	MSG 2.4 ($P\bar{1}$)	$\eta_{4I} = 1$ $z_{2I,1} = 0$ $z_{2I,2} = 0$ $z_{2I,3} = 0$	SISM
0.731	Ho1 Ni4 B1	6	MSG 12.62 ($C2'/m'$)	MSG 2.4 ($P\bar{1}$)	$\eta_{4I} = 1$ $z_{2I,1} = 0$ $z_{2I,2} = 0$ $z_{2I,3} = 0$	SISM
0.641	Ga1 Mn3	0	MSG 12.62 ($C2'/m'$)	MSG 2.4 ($P\bar{1}$)	$\eta_{4I} = 1$ $z_{2I,1} = 1$ $z_{2I,2} = 1$ $z_{2I,3} = 0$	SISM
0.641	Ga1 Mn3	1	MSG 12.62 ($C2'/m'$)	MSG 2.4 ($P\bar{1}$)	$\eta_{4I} = 2$ $z_{2I,1} = 1$ $z_{2I,2} = 1$ $z_{2I,3} = 0$	3DQAH
0.641	Ga1 Mn3	2	MSG 12.62 ($C2'/m'$)	MSG 2.4 ($P\bar{1}$)	$\eta_{4I} = 1$ $z_{2I,1} = 0$ $z_{2I,2} = 0$ $z_{2I,3} = 0$	SISM
0.641	Ga1 Mn3	3	MSG 12.62 ($C2'/m'$)	MSG 2.4 ($P\bar{1}$)	$\eta_{4I} = 1$ $z_{2I,1} = 0$ $z_{2I,2} = 0$ $z_{2I,3} = 0$	SISM
0.641	Ga1 Mn3	4	MSG 12.62 ($C2'/m'$)	MSG 2.4 ($P\bar{1}$)	$\eta_{4I} = 1$ $z_{2I,1} = 0$ $z_{2I,2} = 0$ $z_{2I,3} = 0$	SISM
0.773	Nd1 Mn1 Si2	0	MSG 12.62 ($C2'/m'$)	MSG 2.4 ($P\bar{1}$)	$\eta_{4I} = 3$ $z_{2I,1} = 0$ $z_{2I,2} = 0$ $z_{2I,3} = 0$	SISM
0.773	Nd1 Mn1 Si2	2	MSG 12.62 ($C2'/m'$)	MSG 2.4 ($P\bar{1}$)	$\eta_{4I} = 3$ $z_{2I,1} = 1$ $z_{2I,2} = 1$ $z_{2I,3} = 0$	SISM
0.773	Nd1 Mn1 Si2	4	MSG 12.62 ($C2'/m'$)	MSG 2.4 ($P\bar{1}$)	$\eta_{4I} = 2$ $z_{2I,1} = 0$ $z_{2I,2} = 0$ $z_{2I,3} = 0$	AXI/3DQAH
0.773	Nd1 Mn1 Si2	6	MSG 12.62 ($C2'/m'$)	MSG 2.4 ($P\bar{1}$)	$\eta_{4I} = 0$ $z_{2I,1} = 1$	3DQAH

					$z_{2I,2} = 1$ $z_{2I,3} = 0$	
0.730	Tb1 Ni4 B1	0	MSG 12.62 ($C2'/m'$)	MSG 2.4 ($P\bar{1}$)	$\eta_{4I} = 0$ $z_{2I,1} = 0$ $z_{2I,2} = 0$ $z_{2I,3} = 1$	3DQAH
0.730	Tb1 Ni4 B1	2	MSG 12.62 ($C2'/m'$)	MSG 2.4 ($P\bar{1}$)	$\eta_{4I} = 2$ $z_{2I,1} = 0$ $z_{2I,2} = 0$ $z_{2I,3} = 0$	AXI/3DQAH
0.730	Tb1 Ni4 B1	4	MSG 12.62 ($C2'/m'$)	MSG 2.4 ($P\bar{1}$)	$\eta_{4I} = 2$ $z_{2I,1} = 0$ $z_{2I,2} = 0$ $z_{2I,3} = 0$	AXI/3DQAH
1.339	Eu1 As3	6	MSG 12.63 (C_c2/m)	MSG 2.4 ($P\bar{1}$)	$\eta_{4I} = 2$ $z_{2I,1} = 0$ $z_{2I,2} = 0$ $z_{2I,3} = 0$	AXI
1.497	Eu1 Bi2 Mg2	0	MSG 12.63 (C_c2/m)	MSG 2.4 ($P\bar{1}$)	$\eta_{4I} = 2$ $z_{2I,1} = 0$ $z_{2I,2} = 0$ $z_{2I,3} = 0$	AXI
1.497	Eu1 Bi2 Mg2	2	MSG 12.63 (C_c2/m)	MSG 2.4 ($P\bar{1}$)	$\eta_{4I} = 2$ $z_{2I,1} = 0$ $z_{2I,2} = 0$ $z_{2I,3} = 0$	AXI
1.497	Eu1 Bi2 Mg2	4	MSG 12.63 (C_c2/m)	MSG 2.4 ($P\bar{1}$)	$\eta_{4I} = 2$ $z_{2I,1} = 0$ $z_{2I,2} = 0$ $z_{2I,3} = 0$	AXI
1.497	Eu1 Bi2 Mg2	6	MSG 12.63 (C_c2/m)	MSG 2.4 ($P\bar{1}$)	$\eta_{4I} = 2$ $z_{2I,1} = 0$ $z_{2I,2} = 0$ $z_{2I,3} = 0$	AXI
1.623	Bi2 Eu1 Mg2	0	MSG 12.63 (C_c2/m)	MSG 2.4 ($P\bar{1}$)	$\eta_{4I} = 2$ $z_{2I,1} = 0$ $z_{2I,2} = 0$ $z_{2I,3} = 0$	AXI
1.623	Bi2 Eu1 Mg2	2	MSG 12.63 (C_c2/m)	MSG 2.4 ($P\bar{1}$)	$\eta_{4I} = 2$ $z_{2I,1} = 0$ $z_{2I,2} = 0$ $z_{2I,3} = 0$	AXI
1.623	Bi2 Eu1 Mg2	4	MSG 12.63 (C_c2/m)	MSG 2.4 ($P\bar{1}$)	$\eta_{4I} = 2$ $z_{2I,1} = 0$ $z_{2I,2} = 0$ $z_{2I,3} = 0$	AXI
1.623	Bi2 Eu1 Mg2	6	MSG 12.63 (C_c2/m)	MSG 2.4 ($P\bar{1}$)	$\eta_{4I} = 2$ $z_{2I,1} = 0$ $z_{2I,2} = 0$ $z_{2I,3} = 0$	AXI
1.672	Eu1 Zn2 As2	0	MSG 12.63 (C_c2/m)	MSG 2.4 ($P\bar{1}$)	$\eta_{4I} = 2$ $z_{2I,1} = 0$ $z_{2I,2} = 0$ $z_{2I,3} = 0$	AXI
1.672	Eu1 Zn2 As2	2	MSG 12.63 (C_c2/m)	MSG 2.4 ($P\bar{1}$)	$\eta_{4I} = 2$ $z_{2I,1} = 0$ $z_{2I,2} = 0$ $z_{2I,3} = 0$	AXI
1.729	Gd2 Fe2 Si2 C1	0	MSG 12.63 (C_c2/m)	MSG 2.4 ($P\bar{1}$)	$\eta_{4I} = 2$ $z_{2I,1} = 0$ $z_{2I,2} = 0$ $z_{2I,3} = 0$	AXI
1.560	Ge1 Ni2 O4	0	MSG 12.63 (C_c2/m)	MSG 2.4 ($P\bar{1}$)	$\eta_{4I} = 2$	AXI

					$z_{2I,1} = 0$ $z_{2I,2} = 0$ $z_{2I,3} = 0$	
1.576	O2 S1 Yb2	0	MSG 12.63 (C_c2/m)	MSG 2.4 ($P\bar{1}$)	$\eta_{4I} = 2$ $z_{2I,1} = 0$ $z_{2I,2} = 0$ $z_{2I,3} = 0$	AXI
1.576	O2 S1 Yb2	2	MSG 12.63 (C_c2/m)	MSG 2.4 ($P\bar{1}$)	$\eta_{4I} = 2$ $z_{2I,1} = 0$ $z_{2I,2} = 0$ $z_{2I,3} = 0$	AXI
3.23	Eu3 Pb1 O1	4	MSG 123.345 ($P4/mm'm'$)	MSG 83.43 ($P4/m$)	$\delta_{4m} = 2$ $z_{4m,\pi}^- = 0$ $z_{4m,\pi}^+ = 0$	MTCI
3.23	Eu3 Pb1 O1	6	MSG 123.345 ($P4/mm'm'$)	MSG 83.43 ($P4/m$)	$\delta_{4m} = 2$ $z_{4m,\pi}^- = 0$ $z_{4m,\pi}^+ = 0$	MTCI
1.638	Er1 Mn2 Ge2	4	MSG 126.386 (P_I4/nnc)	MSG 2.4 ($P\bar{1}$)	$\eta_{4I} = 2$ $z_{2I,1} = 0$ $z_{2I,2} = 0$ $z_{2I,3} = 0$	AXI
1.639	Er1 Mn2 Ge2	2	MSG 126.386 (P_I4/nnc)	MSG 2.4 ($P\bar{1}$)	$\eta_{4I} = 2$ $z_{2I,1} = 0$ $z_{2I,2} = 0$ $z_{2I,3} = 0$	AXI
1.640	Er1 Mn2 Ge2	4	MSG 126.386 (P_I4/nnc)	MSG 2.4 ($P\bar{1}$)	$\eta_{4I} = 2$ $z_{2I,1} = 0$ $z_{2I,2} = 0$ $z_{2I,3} = 0$	AXI
1.636	Er1 Mn2 Si2	0	MSG 126.386 (P_I4/nnc)	MSG 2.4 ($P\bar{1}$)	$\eta_{4I} = 2$ $z_{2I,1} = 0$ $z_{2I,2} = 0$ $z_{2I,3} = 0$	AXI
0.321	U2 Sn1 Pd2	0	MSG 127.394 ($P4'/m'bm'$)	MSG 81.33 ($P\bar{4}$)	$\delta_{2S} = 0$ $z_2 = 1$ $z_{4S} = 0$	AXI
0.321	U2 Sn1 Pd2	2	MSG 127.394 ($P4'/m'bm'$)	MSG 81.33 ($P\bar{4}$)	$\delta_{2S} = 0$ $z_2 = 1$ $z_{4S} = 0$	AXI
0.321	U2 Sn1 Pd2	4	MSG 127.394 ($P4'/m'bm'$)	MSG 81.33 ($P\bar{4}$)	$\delta_{2S} = 0$ $z_2 = 1$ $z_{4S} = 0$	AXI
0.321	U2 Sn1 Pd2	6	MSG 127.394 ($P4'/m'bm'$)	MSG 81.33 ($P\bar{4}$)	$\delta_{2S} = 0$ $z_2 = 1$ $z_{4S} = 0$	AXI
1.567	Ba2 Tm1 Ru1 O6	0	MSG 128.410 (P_I4/mnc)	MSG 83.43 ($P4/m$)	$\delta_{4m} = 2$ $z_{4m,\pi}^- = 0$ $z_{4m,\pi}^+ = 0$	MTCI
0.599	Mn1 Ca1 Si1	0	MSG 129.416 ($P4'/n'm'm$)	MSG 81.33 ($P\bar{4}$)	$\delta_{2S} = 0$ $z_2 = 1$ $z_{4S} = 0$	AXI
0.599	Mn1 Ca1 Si1	1	MSG 129.416 ($P4'/n'm'm$)	MSG 81.33 ($P\bar{4}$)	$\delta_{2S} = 0$ $z_2 = 1$ $z_{4S} = 0$	AXI
0.599	Mn1 Ca1 Si1	2	MSG 129.416 ($P4'/n'm'm$)	MSG 81.33 ($P\bar{4}$)	$\delta_{2S} = 0$ $z_2 = 1$ $z_{4S} = 0$	AXI
0.599	Mn1 Ca1 Si1	3	MSG 129.416 ($P4'/n'm'm$)	MSG 81.33 ($P\bar{4}$)	$\delta_{2S} = 0$ $z_2 = 1$ $z_{4S} = 0$	AXI
0.600	Mn1 Ca1 Si1	0	MSG 129.416 ($P4'/n'm'm$)	MSG 81.33 ($P\bar{4}$)	$\delta_{2S} = 0$ $z_2 = 1$	AXI

					$z_{4S} = 0$	
0.600	Mn1 Ca1 Si1	1	MSG 129.416 ($P4'/n'm'm$)	MSG 81.33 ($P\bar{4}$)	$\delta_{2S} = 0$ $z_2 = 1$ $z_{4S} = 0$	AXI
0.600	Mn1 Ca1 Si1	2	MSG 129.416 ($P4'/n'm'm$)	MSG 81.33 ($P\bar{4}$)	$\delta_{2S} = 0$ $z_2 = 1$ $z_{4S} = 0$	AXI
0.620	Mn1 Nd1 As1 O1	0	MSG 129.416 ($P4'/n'm'm$)	MSG 81.33 ($P\bar{4}$)	$\delta_{2S} = 0$ $z_2 = 1$ $z_{4S} = 0$	AXI
0.620	Mn1 Nd1 As1 O1	4	MSG 129.416 ($P4'/n'm'm$)	MSG 81.33 ($P\bar{4}$)	$\delta_{2S} = 0$ $z_2 = 1$ $z_{4S} = 0$	AXI
0.623	Mn1 Nd1 As1 O1	0	MSG 129.416 ($P4'/n'm'm$)	MSG 81.33 ($P\bar{4}$)	$\delta_{2S} = 0$ $z_2 = 1$ $z_{4S} = 0$	AXI
0.623	Mn1 Nd1 As1 O1	4	MSG 129.416 ($P4'/n'm'm$)	MSG 81.33 ($P\bar{4}$)	$\delta_{2S} = 0$ $z_2 = 1$ $z_{4S} = 0$	AXI
0.594	U1 S1 As1	0	MSG 129.417 ($P4/nm'm'$)	MSG 81.33 ($P\bar{4}$)	$\delta_{2S} = 0$ $z_2 = 0$ $z_{4S} = 3$	3DQAH
0.594	U1 S1 As1	2	MSG 129.417 ($P4/nm'm'$)	MSG 81.33 ($P\bar{4}$)	$\delta_{2S} = 0$ $z_2 = 1$ $z_{4S} = 1$	3DQAH
0.593	U1 Se1 P1	2	MSG 129.417 ($P4/nm'm'$)	MSG 81.33 ($P\bar{4}$)	$\delta_{2S} = 0$ $z_2 = 1$ $z_{4S} = 3$	3DQAH
1.714	Ce1 Bi2 Au1	2	MSG 130.432 (P_c4/ncc)	MSG 2.4 ($P\bar{1}$)	$\eta_{4I} = 2$ $z_{2I,1} = 0$ $z_{2I,2} = 0$ $z_{2I,3} = 0$	AXI
1.714	Ce1 Bi2 Au1	4	MSG 130.432 (P_c4/ncc)	MSG 2.4 ($P\bar{1}$)	$\eta_{4I} = 2$ $z_{2I,1} = 0$ $z_{2I,2} = 0$ $z_{2I,3} = 0$	AXI
1.714	Ce1 Bi2 Au1	6	MSG 130.432 (P_c4/ncc)	MSG 2.4 ($P\bar{1}$)	$\eta_{4I} = 2$ $z_{2I,1} = 0$ $z_{2I,2} = 0$ $z_{2I,3} = 0$	AXI
0.605	Ba1 Mn2 Ge2	1	MSG 139.536 ($I4'/m'm'm$)	MSG 81.33 ($P\bar{4}$)	$\delta_{2S} = 0$ $z_2 = 1$ $z_{4S} = 0$	AXI
0.605	Ba1 Mn2 Ge2	2	MSG 139.536 ($I4'/m'm'm$)	MSG 81.33 ($P\bar{4}$)	$\delta_{2S} = 0$ $z_2 = 1$ $z_{4S} = 0$	AXI
0.606	Ba1 Mn2 Ge2	0	MSG 139.536 ($I4'/m'm'm$)	MSG 81.33 ($P\bar{4}$)	$\delta_{2S} = 0$ $z_2 = 1$ $z_{4S} = 0$	AXI
0.606	Ba1 Mn2 Ge2	1	MSG 139.536 ($I4'/m'm'm$)	MSG 81.33 ($P\bar{4}$)	$\delta_{2S} = 0$ $z_2 = 1$ $z_{4S} = 0$	AXI
0.603	Ca1 Mn2 Ge2	0	MSG 139.536 ($I4'/m'm'm$)	MSG 81.33 ($P\bar{4}$)	$\delta_{2S} = 0$ $z_2 = 1$ $z_{4S} = 0$	AXI
0.603	Ca1 Mn2 Ge2	1	MSG 139.536 ($I4'/m'm'm$)	MSG 81.33 ($P\bar{4}$)	$\delta_{2S} = 0$ $z_2 = 1$ $z_{4S} = 0$	AXI
0.919	Eu1 Mn1 Bi2	2	MSG 139.536 ($I4'/m'm'm$)	MSG 81.33 ($P\bar{4}$)	$\delta_{2S} = 0$ $z_2 = 1$ $z_{4S} = 0$	AXI
0.919	Eu1 Mn1 Bi2	4	MSG 139.536 ($I4'/m'm'm$)	MSG 81.33 ($P\bar{4}$)	$\delta_{2S} = 0$ $z_2 = 1$	AXI

					$z_{4S} = 0$	
0.296	Cu2 Cl1 O3	1	MSG 14.75 ($P2_1/c$)	MSG 2.4 ($P\bar{1}$)	$\eta_{4I} = 2$ $z_{2I,1} = 0$ $z_{2I,2} = 0$ $z_{2I,3} = 0$	AXI/3DQAH
0.871	Ni1 Ir1 Pr2 O6	4	MSG 14.75 ($P2_1/c$)	MSG 2.4 ($P\bar{1}$)	$\eta_{4I} = 2$ $z_{2I,1} = 0$ $z_{2I,2} = 0$ $z_{2I,3} = 0$	AXI/3DQAH
0.794	Sr2 Ho1 Ru1 O6	2	MSG 14.75 ($P2_1/c$)	MSG 2.4 ($P\bar{1}$)	$\eta_{4I} = 2$ $z_{2I,1} = 0$ $z_{2I,2} = 0$ $z_{2I,3} = 0$	AXI/3DQAH
0.791	Sr2 Tb1 Ru1 O6	0	MSG 14.75 ($P2_1/c$)	MSG 2.4 ($P\bar{1}$)	$\eta_{4I} = 2$ $z_{2I,1} = 0$ $z_{2I,2} = 0$ $z_{2I,3} = 0$	AXI/3DQAH
0.982	Tm1 V1 O3	0	MSG 14.75 ($P2_1/c$)	MSG 2.4 ($P\bar{1}$)	$\eta_{4I} = 2$ $z_{2I,1} = 0$ $z_{2I,2} = 0$ $z_{2I,3} = 0$	AXI/3DQAH
0.983	Tm1 V1 O3	0	MSG 14.75 ($P2_1/c$)	MSG 2.4 ($P\bar{1}$)	$\eta_{4I} = 2$ $z_{2I,1} = 0$ $z_{2I,2} = 0$ $z_{2I,3} = 0$	AXI/3DQAH
0.664	Mn3 Sn2	0	MSG 14.79 ($P2'_1/c'$)	MSG 2.4 ($P\bar{1}$)	$\eta_{4I} = 1$ $z_{2I,1} = 0$ $z_{2I,2} = 0$ $z_{2I,3} = 0$	SISM
0.664	Mn3 Sn2	1	MSG 14.79 ($P2'_1/c'$)	MSG 2.4 ($P\bar{1}$)	$\eta_{4I} = 2$ $z_{2I,1} = 0$ $z_{2I,2} = 0$ $z_{2I,3} = 0$	AXI/3DQAH
0.664	Mn3 Sn2	2	MSG 14.79 ($P2'_1/c'$)	MSG 2.4 ($P\bar{1}$)	$\eta_{4I} = 2$ $z_{2I,1} = 0$ $z_{2I,2} = 0$ $z_{2I,3} = 0$	AXI/3DQAH
0.664	Mn3 Sn2	3	MSG 14.79 ($P2'_1/c'$)	MSG 2.4 ($P\bar{1}$)	$\eta_{4I} = 2$ $z_{2I,1} = 0$ $z_{2I,2} = 0$ $z_{2I,3} = 0$	AXI/3DQAH
0.318	Tm2 Co1 Mn1 O6	0	MSG 14.79 ($P2'_1/c'$)	MSG 2.4 ($P\bar{1}$)	$\eta_{4I} = 2$ $z_{2I,1} = 1$ $z_{2I,2} = 0$ $z_{2I,3} = 0$	3DQAH
1.744	Pr1 Pd1 Sn1	0	MSG 14.80 (P_a2_1/c)	MSG 2.4 ($P\bar{1}$)	$\eta_{4I} = 2$ $z_{2I,1} = 0$ $z_{2I,2} = 0$ $z_{2I,3} = 0$	AXI
1.744	Pr1 Pd1 Sn1	2	MSG 14.80 (P_a2_1/c)	MSG 2.4 ($P\bar{1}$)	$\eta_{4I} = 2$ $z_{2I,1} = 0$ $z_{2I,2} = 0$ $z_{2I,3} = 0$	AXI
1.744	Pr1 Pd1 Sn1	4	MSG 14.80 (P_a2_1/c)	MSG 2.4 ($P\bar{1}$)	$\eta_{4I} = 2$ $z_{2I,1} = 0$ $z_{2I,2} = 0$ $z_{2I,3} = 0$	AXI
1.744	Pr1 Pd1 Sn1	6	MSG 14.80 (P_a2_1/c)	MSG 2.4 ($P\bar{1}$)	$\eta_{4I} = 2$ $z_{2I,1} = 0$ $z_{2I,2} = 0$ $z_{2I,3} = 0$	AXI
1.323	Co1 Ge1 O3	0	MSG 14.84 (P_C2_1/c)	MSG 2.4 ($P\bar{1}$)	$\eta_{4I} = 2$ $z_{2I,1} = 0$	AXI

					$z_{2I,2} = 0$ $z_{2I,3} = 0$	
1.287	V2 O3	0	MSG 14.84 (P_C2_1/c)	MSG 2.4 ($P\bar{1}$)	$\eta_{4I} = 2$ $z_{2I,1} = 0$ $z_{2I,2} = 0$ $z_{2I,3} = 0$	AXI
1.683	Ga5 Ni1 U1	2	MSG 140.550 (I_c4/mcm)	MSG 47.249 ($Pmmm$)	$z_{2w,1} = 0$ $z_{2w,2} = 0$ $z_{2w,3} = 0$ $z_4 = 3$	AXI
1.683	Ga5 Ni1 U1	4	MSG 140.550 (I_c4/mcm)	MSG 47.249 ($Pmmm$)	$z_{2w,1} = 0$ $z_{2w,2} = 0$ $z_{2w,3} = 0$ $z_4 = 3$	AXI
0.747	Ba3 Co1 Ir2 O9	0	MSG 15.85 ($C2/c$)	MSG 2.4 ($P\bar{1}$)	$\eta_{4I} = 2$ $z_{2I,1} = 1$ $z_{2I,2} = 1$ $z_{2I,3} = 0$	3DQAH
0.891	Cu1 Cr2 O4	0	MSG 15.89 ($C2'/c'$)	MSG 2.4 ($P\bar{1}$)	$\eta_{4I} = 1$ $z_{2I,1} = 0$ $z_{2I,2} = 0$ $z_{2I,3} = 0$	SISM
2.100	Ho1 P1	2	MSG 15.89 ($C2'/c'$)	MSG 2.4 ($P\bar{1}$)	$\eta_{4I} = 0$ $z_{2I,1} = 1$ $z_{2I,2} = 1$ $z_{2I,3} = 0$	3DQAH
2.100	Ho1 P1	4	MSG 15.89 ($C2'/c'$)	MSG 2.4 ($P\bar{1}$)	$\eta_{4I} = 0$ $z_{2I,1} = 1$ $z_{2I,2} = 1$ $z_{2I,3} = 0$	3DQAH
2.100	Ho1 P1	6	MSG 15.89 ($C2'/c'$)	MSG 2.4 ($P\bar{1}$)	$\eta_{4I} = 1$ $z_{2I,1} = 0$ $z_{2I,2} = 0$ $z_{2I,3} = 0$	SISM
0.690	Nd1 Pt1	0	MSG 15.89 ($C2'/c'$)	MSG 2.4 ($P\bar{1}$)	$\eta_{4I} = 1$ $z_{2I,1} = 1$ $z_{2I,2} = 1$ $z_{2I,3} = 0$	SISM
0.690	Nd1 Pt1	4	MSG 15.89 ($C2'/c'$)	MSG 2.4 ($P\bar{1}$)	$\eta_{4I} = 2$ $z_{2I,1} = 1$ $z_{2I,2} = 1$ $z_{2I,3} = 0$	3DQAH
0.690	Nd1 Pt1	6	MSG 15.89 ($C2'/c'$)	MSG 2.4 ($P\bar{1}$)	$\eta_{4I} = 1$ $z_{2I,1} = 0$ $z_{2I,2} = 0$ $z_{2I,3} = 0$	SISM
1.361	Dy1 Ge1	2	MSG 15.90 (C_c2/c)	MSG 2.4 ($P\bar{1}$)	$\eta_{4I} = 2$ $z_{2I,1} = 0$ $z_{2I,2} = 0$ $z_{2I,3} = 0$	AXI
1.361	Dy1 Ge1	4	MSG 15.90 (C_c2/c)	MSG 2.4 ($P\bar{1}$)	$\eta_{4I} = 2$ $z_{2I,1} = 0$ $z_{2I,2} = 0$ $z_{2I,3} = 0$	AXI
1.627	Ce1 K1 S2	2	MSG 15.90 (C_c2/c)	MSG 2.4 ($P\bar{1}$)	$\eta_{4I} = 2$ $z_{2I,1} = 0$ $z_{2I,2} = 0$ $z_{2I,3} = 0$	AXI
1.293	Nd1 Ni2 B2 C1	4	MSG 15.90 (C_c2/c)	MSG 2.4 ($P\bar{1}$)	$\eta_{4I} = 2$ $z_{2I,1} = 0$ $z_{2I,2} = 0$ $z_{2I,3} = 0$	AXI
1.293	Nd1 Ni2 B2 C1	6	MSG 15.90 (C_c2/c)	MSG 2.4 ($P\bar{1}$)	$\eta_{4I} = 2$	AXI

					$z_{2I,1} = 0$ $z_{2I,2} = 0$ $z_{2I,3} = 0$	
1.367	Pu2 O3	0	MSG 15.90 (C_c2/c)	MSG 2.4 ($P\bar{1}$)	$\eta_{4I} = 2$ $z_{2I,1} = 0$ $z_{2I,2} = 0$ $z_{2I,3} = 0$	AXI
0.860	Sn2 Co3 S2	0	MSG 166.101 ($R\bar{3}m'$)	MSG 2.4 ($P\bar{1}$)	$\eta_{4I} = 3$ $z_{2I,1} = 0$ $z_{2I,2} = 0$ $z_{2I,3} = 0$	SISM
0.860	Sn2 Co3 S2	1	MSG 166.101 ($R\bar{3}m'$)	MSG 2.4 ($P\bar{1}$)	$\eta_{4I} = 0$ $z_{2I,1} = 1$ $z_{2I,2} = 1$ $z_{2I,3} = 1$	3DQAH
0.860	Sn2 Co3 S2	2	MSG 166.101 ($R\bar{3}m'$)	MSG 2.4 ($P\bar{1}$)	$\eta_{4I} = 0$ $z_{2I,1} = 1$ $z_{2I,2} = 1$ $z_{2I,3} = 1$	3DQAH
0.860	Sn2 Co3 S2	4	MSG 166.101 ($R\bar{3}m'$)	MSG 2.4 ($P\bar{1}$)	$\eta_{4I} = 2$ $z_{2I,1} = 1$ $z_{2I,2} = 1$ $z_{2I,3} = 1$	3DQAH
0.861	Sn2 Co3 S2	0	MSG 166.101 ($R\bar{3}m'$)	MSG 2.4 ($P\bar{1}$)	$\eta_{4I} = 3$ $z_{2I,1} = 0$ $z_{2I,2} = 0$ $z_{2I,3} = 0$	SISM
0.861	Sn2 Co3 S2	1	MSG 166.101 ($R\bar{3}m'$)	MSG 2.4 ($P\bar{1}$)	$\eta_{4I} = 0$ $z_{2I,1} = 1$ $z_{2I,2} = 1$ $z_{2I,3} = 1$	3DQAH
0.861	Sn2 Co3 S2	2	MSG 166.101 ($R\bar{3}m'$)	MSG 2.4 ($P\bar{1}$)	$\eta_{4I} = 0$ $z_{2I,1} = 1$ $z_{2I,2} = 1$ $z_{2I,3} = 1$	3DQAH
0.859	Y1 Co3	1	MSG 166.101 ($R\bar{3}m'$)	MSG 2.4 ($P\bar{1}$)	$\eta_{4I} = 2$ $z_{2I,1} = 0$ $z_{2I,2} = 0$ $z_{2I,3} = 0$	AXI/3DQAH
0.944	Yb2 Ir2 O7	0	MSG 166.101 ($R\bar{3}m'$)	MSG 2.4 ($P\bar{1}$)	$\eta_{4I} = 2$ $z_{2I,1} = 0$ $z_{2I,2} = 0$ $z_{2I,3} = 0$	AXI/3DQAH
1.308	Mn1 Bi2 Te4	0	MSG 167.108 ($R_I\bar{3}c$)	MSG 2.4 ($P\bar{1}$)	$\eta_{4I} = 2$ $z_{2I,1} = 0$ $z_{2I,2} = 0$ $z_{2I,3} = 0$	AXI
1.308	Mn1 Bi2 Te4	1	MSG 167.108 ($R_I\bar{3}c$)	MSG 2.4 ($P\bar{1}$)	$\eta_{4I} = 2$ $z_{2I,1} = 0$ $z_{2I,2} = 0$ $z_{2I,3} = 0$	AXI
1.308	Mn1 Bi2 Te4	2	MSG 167.108 ($R_I\bar{3}c$)	MSG 2.4 ($P\bar{1}$)	$\eta_{4I} = 2$ $z_{2I,1} = 0$ $z_{2I,2} = 0$ $z_{2I,3} = 0$	AXI
1.308	Mn1 Bi2 Te4	3	MSG 167.108 ($R_I\bar{3}c$)	MSG 2.4 ($P\bar{1}$)	$\eta_{4I} = 2$ $z_{2I,1} = 0$ $z_{2I,2} = 0$ $z_{2I,3} = 0$	AXI
1.308	Mn1 Bi2 Te4	4	MSG 167.108 ($R_I\bar{3}c$)	MSG 2.4 ($P\bar{1}$)	$\eta_{4I} = 2$ $z_{2I,1} = 0$ $z_{2I,2} = 0$ $z_{2I,3} = 0$	AXI

0.708	Nb ₄ Cr ₁ S ₈	0	MSG 194.268 ($P6'_3/m'm'c$)	MSG 2.4 ($P\bar{1}$)	$\eta_{4I} = 2$ $z_{2I,1} = 0$ $z_{2I,2} = 0$ $z_{2I,3} = 0$	AXI
3.20	Mn ₂ Tb ₁ Ge ₂	0	MSG 2.4 ($P\bar{1}$)	MSG 2.4 ($P\bar{1}$)	$\eta_{4I} = 2$ $z_{2I,1} = 0$ $z_{2I,2} = 0$ $z_{2I,3} = 0$	AXI/3DQAH
3.20	Mn ₂ Tb ₁ Ge ₂	2	MSG 2.4 ($P\bar{1}$)	MSG 2.4 ($P\bar{1}$)	$\eta_{4I} = 2$ $z_{2I,1} = 0$ $z_{2I,2} = 0$ $z_{2I,3} = 0$	AXI/3DQAH
3.20	Mn ₂ Tb ₁ Ge ₂	4	MSG 2.4 ($P\bar{1}$)	MSG 2.4 ($P\bar{1}$)	$\eta_{4I} = 1$ $z_{2I,1} = 0$ $z_{2I,2} = 0$ $z_{2I,3} = 0$	SISM
3.20	Mn ₂ Tb ₁ Ge ₂	6	MSG 2.4 ($P\bar{1}$)	MSG 2.4 ($P\bar{1}$)	$\eta_{4I} = 1$ $z_{2I,1} = 0$ $z_{2I,2} = 0$ $z_{2I,3} = 0$	SISM
1.363	Tb ₁ Cu ₂ Si ₂	3	MSG 2.7 ($P_S\bar{1}$)	MSG 2.4 ($P\bar{1}$)	$\eta_{4I} = 2$ $z_{2I,1} = 0$ $z_{2I,2} = 0$ $z_{2I,3} = 0$	AXI
1.365	Cu ₂ Si ₂ Tb ₁	2	MSG 2.7 ($P_S\bar{1}$)	MSG 2.4 ($P\bar{1}$)	$\eta_{4I} = 2$ $z_{2I,1} = 0$ $z_{2I,2} = 0$ $z_{2I,3} = 0$	AXI
1.365	Cu ₂ Si ₂ Tb ₁	3	MSG 2.7 ($P_S\bar{1}$)	MSG 2.4 ($P\bar{1}$)	$\eta_{4I} = 2$ $z_{2I,1} = 0$ $z_{2I,2} = 0$ $z_{2I,3} = 0$	AXI
1.365	Cu ₂ Si ₂ Tb ₁	4	MSG 2.7 ($P_S\bar{1}$)	MSG 2.4 ($P\bar{1}$)	$\eta_{4I} = 2$ $z_{2I,1} = 0$ $z_{2I,2} = 0$ $z_{2I,3} = 0$	AXI
1.365	Cu ₂ Si ₂ Tb ₁	6	MSG 2.7 ($P_S\bar{1}$)	MSG 2.4 ($P\bar{1}$)	$\eta_{4I} = 2$ $z_{2I,1} = 0$ $z_{2I,2} = 0$ $z_{2I,3} = 0$	AXI
0.916	Cd ₂ Os ₂ O ₇	0	MSG 227.131 ($Fd\bar{3}m'$)	MSG 2.4 ($P\bar{1}$)	$\eta_{4I} = 2$ $z_{2I,1} = 0$ $z_{2I,2} = 0$ $z_{2I,3} = 0$	AXI
0.954	Nd ₂ Ir ₂ O ₇	6	MSG 227.131 ($Fd\bar{3}m'$)	MSG 2.4 ($P\bar{1}$)	$\eta_{4I} = 2$ $z_{2I,1} = 0$ $z_{2I,2} = 0$ $z_{2I,3} = 0$	AXI
0.945	Yb ₂ Ir ₂ O ₇	0	MSG 227.131 ($Fd\bar{3}m'$)	MSG 2.4 ($P\bar{1}$)	$\eta_{4I} = 2$ $z_{2I,1} = 0$ $z_{2I,2} = 0$ $z_{2I,3} = 0$	AXI
0.945	Yb ₂ Ir ₂ O ₇	2	MSG 227.131 ($Fd\bar{3}m'$)	MSG 2.4 ($P\bar{1}$)	$\eta_{4I} = 2$ $z_{2I,1} = 0$ $z_{2I,2} = 0$ $z_{2I,3} = 0$	AXI
1.585	Pr ₁ Fe ₁ As ₁ O ₁	0	MSG 54.350 (P_{Bcca})	MSG 2.4 ($P\bar{1}$)	$\eta_{4I} = 2$ $z_{2I,1} = 0$ $z_{2I,2} = 0$ $z_{2I,3} = 0$	AXI
1.585	Pr ₁ Fe ₁ As ₁ O ₁	2	MSG 54.350 (P_{Bcca})	MSG 2.4 ($P\bar{1}$)	$\eta_{4I} = 2$ $z_{2I,1} = 0$	AXI

					$z_{2I,2} = 0$ $z_{2I,3} = 0$	
0.952	Yb1 Pd1 Si1	2	MSG 59.409 ($Pm'm'n$)	MSG 2.4 ($P\bar{1}$)	$\eta_{4I} = 2$ $z_{2I,1} = 0$ $z_{2I,2} = 0$ $z_{2I,3} = 0$	AXI/3DQAH
0.952	Yb1 Pd1 Si1	4	MSG 59.409 ($Pm'm'n$)	MSG 2.4 ($P\bar{1}$)	$\eta_{4I} = 2$ $z_{2I,1} = 0$ $z_{2I,2} = 0$ $z_{2I,3} = 0$	AXI/3DQAH
0.952	Yb1 Pd1 Si1	6	MSG 59.409 ($Pm'm'n$)	MSG 2.4 ($P\bar{1}$)	$\eta_{4I} = 2$ $z_{2I,1} = 0$ $z_{2I,2} = 0$ $z_{2I,3} = 0$	AXI/3DQAH
1.305	Mn5 Si3	0	MSG 60.431 (P_Cbcn)	MSG 2.4 ($P\bar{1}$)	$\eta_{4I} = 2$ $z_{2I,1} = 0$ $z_{2I,2} = 0$ $z_{2I,3} = 0$	AXI
0.784	Nd1 Co1 O3	0	MSG 62.441 ($Pnma$)	MSG 2.4 ($P\bar{1}$)	$\eta_{4I} = 2$ $z_{2I,1} = 0$ $z_{2I,2} = 0$ $z_{2I,3} = 0$	AXI
0.981	Tm1 V1 O3	0	MSG 62.441 ($Pnma$)	MSG 2.4 ($P\bar{1}$)	$\eta_{4I} = 2$ $z_{2I,1} = 0$ $z_{2I,2} = 0$ $z_{2I,3} = 0$	AXI
0.981	Tm1 V1 O3	2	MSG 62.441 ($Pnma$)	MSG 2.4 ($P\bar{1}$)	$\eta_{4I} = 2$ $z_{2I,1} = 0$ $z_{2I,2} = 0$ $z_{2I,3} = 0$	AXI
0.687	Dy1 Pt1	6	MSG 62.446 ($Pn'm'a$)	MSG 2.4 ($P\bar{1}$)	$\eta_{4I} = 2$ $z_{2I,1} = 0$ $z_{2I,2} = 0$ $z_{2I,3} = 0$	AXI/3DQAH
0.684	Pt1 Tb1	2	MSG 62.446 ($Pn'm'a$)	MSG 2.4 ($P\bar{1}$)	$\eta_{4I} = 2$ $z_{2I,1} = 0$ $z_{2I,2} = 0$ $z_{2I,3} = 0$	AXI/3DQAH
0.684	Pt1 Tb1	4	MSG 62.446 ($Pn'm'a$)	MSG 2.4 ($P\bar{1}$)	$\eta_{4I} = 2$ $z_{2I,1} = 0$ $z_{2I,2} = 0$ $z_{2I,3} = 0$	AXI/3DQAH
0.684	Pt1 Tb1	6	MSG 62.446 ($Pn'm'a$)	MSG 2.4 ($P\bar{1}$)	$\eta_{4I} = 2$ $z_{2I,1} = 0$ $z_{2I,2} = 0$ $z_{2I,3} = 0$	AXI/3DQAH
0.979	Tm1 V1 O3	0	MSG 62.446 ($Pn'm'a$)	MSG 2.4 ($P\bar{1}$)	$\eta_{4I} = 2$ $z_{2I,1} = 0$ $z_{2I,2} = 0$ $z_{2I,3} = 0$	AXI/3DQAH
0.980	Tm1 V1 O3	0	MSG 62.446 ($Pn'm'a$)	MSG 2.4 ($P\bar{1}$)	$\eta_{4I} = 2$ $z_{2I,1} = 0$ $z_{2I,2} = 0$ $z_{2I,3} = 0$	AXI/3DQAH
0.685	Er1 Pt1	6	MSG 62.447 ($Pnm'a'$)	MSG 2.4 ($P\bar{1}$)	$\eta_{4I} = 2$ $z_{2I,1} = 0$ $z_{2I,2} = 0$ $z_{2I,3} = 0$	AXI/3DQAH
1.678	Cr1 N1	0	MSG 62.450 (P_anma)	MSG 2.4 ($P\bar{1}$)	$\eta_{4I} = 2$ $z_{2I,1} = 0$ $z_{2I,2} = 0$ $z_{2I,3} = 0$	AXI
1.635	Er1 Fe2 Si2	2	MSG 62.450 (P_anma)	MSG 2.4 ($P\bar{1}$)	$\eta_{4I} = 2$	AXI

					$z_{2I,1} = 0$ $z_{2I,2} = 0$ $z_{2I,3} = 0$	
1.635	Er1 Fe2 Si2	4	MSG 62.450 (P_{anma})	MSG 2.4 ($P\bar{1}$)	$\eta_{4I} = 2$ $z_{2I,1} = 0$ $z_{2I,2} = 0$ $z_{2I,3} = 0$	AXI
1.635	Er1 Fe2 Si2	6	MSG 62.450 (P_{anma})	MSG 2.4 ($P\bar{1}$)	$\eta_{4I} = 2$ $z_{2I,1} = 0$ $z_{2I,2} = 0$ $z_{2I,3} = 0$	AXI
1.507	Al2 Pd5 Nd1	0	MSG 62.450 (P_{anma})	MSG 2.4 ($P\bar{1}$)	$\eta_{4I} = 2$ $z_{2I,1} = 0$ $z_{2I,2} = 0$ $z_{2I,3} = 0$	AXI
1.507	Al2 Pd5 Nd1	2	MSG 62.450 (P_{anma})	MSG 2.4 ($P\bar{1}$)	$\eta_{4I} = 2$ $z_{2I,1} = 0$ $z_{2I,2} = 0$ $z_{2I,3} = 0$	AXI
0.279	Mn3 As1	0	MSG 63.463 ($Cmc'm'$)	MSG 2.4 ($P\bar{1}$)	$\eta_{4I} = 2$ $z_{2I,1} = 0$ $z_{2I,2} = 0$ $z_{2I,3} = 0$	AXI/3DQAH
0.774	Nd1 Mn1 Si2	0	MSG 63.464 ($Cm'cm'$)	MSG 2.4 ($P\bar{1}$)	$\eta_{4I} = 0$ $z_{2I,1} = 1$ $z_{2I,2} = 1$ $z_{2I,3} = 0$	3DQAH
1.630	Lu1 Mn6 Sn6	4	MSG 63.466 ($C_c mcm$)	MSG 2.4 ($P\bar{1}$)	$\eta_{4I} = 2$ $z_{2I,1} = 0$ $z_{2I,2} = 0$ $z_{2I,3} = 0$	AXI
1.508	Al1 B2 Mn2	0	MSG 63.466 ($C_c mcm$)	MSG 2.4 ($P\bar{1}$)	$\eta_{4I} = 2$ $z_{2I,1} = 0$ $z_{2I,2} = 0$ $z_{2I,3} = 0$	AXI
1.508	Al1 B2 Mn2	4	MSG 63.466 ($C_c mcm$)	MSG 2.4 ($P\bar{1}$)	$\eta_{4I} = 2$ $z_{2I,1} = 0$ $z_{2I,2} = 0$ $z_{2I,3} = 0$	AXI
1.290	Ce1 Rh2 Si2	0	MSG 64.480 ($C_A mca$)	MSG 2.4 ($P\bar{1}$)	$\eta_{4I} = 2$ $z_{2I,1} = 0$ $z_{2I,2} = 0$ $z_{2I,3} = 0$	AXI
1.369	Ho1 Fe2 Ge2	0	MSG 64.480 ($C_A mca$)	MSG 2.4 ($P\bar{1}$)	$\eta_{4I} = 2$ $z_{2I,1} = 0$ $z_{2I,2} = 0$ $z_{2I,3} = 0$	AXI
1.294	Ho1 Ni2 B2 C1	0	MSG 64.480 ($C_A mca$)	MSG 2.4 ($P\bar{1}$)	$\eta_{4I} = 2$ $z_{2I,1} = 0$ $z_{2I,2} = 0$ $z_{2I,3} = 0$	AXI
1.296	Pr1 Ni2 B2 C1	0	MSG 64.480 ($C_A mca$)	MSG 2.4 ($P\bar{1}$)	$\eta_{4I} = 2$ $z_{2I,1} = 0$ $z_{2I,2} = 0$ $z_{2I,3} = 0$	AXI
1.511	Ni2 Tb1 Si2	0	MSG 64.480 ($C_A mca$)	MSG 2.4 ($P\bar{1}$)	$\eta_{4I} = 2$ $z_{2I,1} = 0$ $z_{2I,2} = 0$ $z_{2I,3} = 0$	AXI
1.702	Ba1 Y1 Co2 O5	0	MSG 65.489 ($C_a mmm$)	MSG 47.249 ($Pmmm$)	$z_{2w,1} = 0$ $z_{2w,2} = 0$ $z_{2w,3} = 1$ $z_4 = 2$	MTCI

1.702	Ba1 Y1 Co2 O5	4	MSG 65.489 ($C_{a}mmm$)	MSG 47.249 ($Pmmm$)	$z_{2w,1} = 0$ $z_{2w,2} = 0$ $z_{2w,3} = 1$ $z_4 = 2$	MTCI
1.288	Ce1 Pd2 Si2	0	MSG 66.500 (C_{Accm})	MSG 2.4 ($P\bar{1}$)	$\eta_{4I} = 2$ $z_{2I,1} = 0$ $z_{2I,2} = 0$ $z_{2I,3} = 0$	AXI
1.288	Ce1 Pd2 Si2	2	MSG 66.500 (C_{Accm})	MSG 2.4 ($P\bar{1}$)	$\eta_{4I} = 2$ $z_{2I,1} = 0$ $z_{2I,2} = 0$ $z_{2I,3} = 0$	AXI
1.668	Ho1 Co1 Ga5	0	MSG 67.509 (C_{amma})	MSG 2.4 ($P\bar{1}$)	$\eta_{4I} = 2$ $z_{2I,1} = 0$ $z_{2I,2} = 0$ $z_{2I,3} = 0$	AXI
1.668	Ho1 Co1 Ga5	2	MSG 67.509 (C_{amma})	MSG 2.4 ($P\bar{1}$)	$\eta_{4I} = 2$ $z_{2I,1} = 0$ $z_{2I,2} = 0$ $z_{2I,3} = 0$	AXI
1.668	Ho1 Co1 Ga5	4	MSG 67.509 (C_{amma})	MSG 2.4 ($P\bar{1}$)	$\eta_{4I} = 2$ $z_{2I,1} = 0$ $z_{2I,2} = 0$ $z_{2I,3} = 0$	AXI
1.668	Ho1 Co1 Ga5	6	MSG 67.509 (C_{amma})	MSG 2.4 ($P\bar{1}$)	$\eta_{4I} = 2$ $z_{2I,1} = 0$ $z_{2I,2} = 0$ $z_{2I,3} = 0$	AXI
1.670	Np1 Fe1 Ga5	6	MSG 67.509 (C_{amma})	MSG 2.4 ($P\bar{1}$)	$\eta_{4I} = 2$ $z_{2I,1} = 0$ $z_{2I,2} = 0$ $z_{2I,3} = 0$	AXI
1.666	Tb1 Co1 Ga5	4	MSG 67.509 (C_{amma})	MSG 2.4 ($P\bar{1}$)	$\eta_{4I} = 2$ $z_{2I,1} = 0$ $z_{2I,2} = 0$ $z_{2I,3} = 0$	AXI
1.667	U1 Pd1 Ga5	0	MSG 67.509 (C_{amma})	MSG 2.4 ($P\bar{1}$)	$\eta_{4I} = 2$ $z_{2I,1} = 0$ $z_{2I,2} = 0$ $z_{2I,3} = 0$	AXI
1.558	Mn1 Sn2	0	MSG 68.520 (C_{Acca})	MSG 2.4 ($P\bar{1}$)	$\eta_{4I} = 2$ $z_{2I,1} = 0$ $z_{2I,2} = 0$ $z_{2I,3} = 0$	AXI
1.558	Mn1 Sn2	1	MSG 68.520 (C_{Acca})	MSG 2.4 ($P\bar{1}$)	$\eta_{4I} = 2$ $z_{2I,1} = 0$ $z_{2I,2} = 0$ $z_{2I,3} = 0$	AXI
1.558	Mn1 Sn2	2	MSG 68.520 (C_{Acca})	MSG 2.4 ($P\bar{1}$)	$\eta_{4I} = 2$ $z_{2I,1} = 0$ $z_{2I,2} = 0$ $z_{2I,3} = 0$	AXI

TAB. S8: Physical interpretation of symmetry indicators for the systems with non-trivial symmetry indicators. In the first three columns we give the BCSID, chemical formula and Hubbard U value of the diagnosed compounds. In the 4th and 5th columns we give the MSG of the material and its minimal SSG. On the alst two columns, we give the symmetry indicators in the minimal SSG and the physical interpretation according to Ref. [2].

Appendix F: Full tables with structure, bands and topological classification

The complete tables with information on the crystal and magnetic structure, magnetic space group, topological classification, and electronic structure are presented herein.

BCS ID	Formula	ICSD	MSG	T.C.	Picture
0.229	Ba2 Mn1 Si2 O7		MSG 113.267 ($P\bar{4}2_1m$)	z_2	
Topology	 U=0 eV AI	 U= 1 eV AI	 U= 2 eV AI	 U= 3 eV AI	 U=4 eV AI

TAB. S9. Topology phase diagram of Ba2 Mn1 Si2 O7

BCS ID	Formula	ICSD	MSG	T.C.	Picture
0.230	K2 Co1 P2 O7		MSG 58.395 ($Pn'nm$)	None	
Topology	 U=0 eV AI	 U= 1 eV AI	 U= 2 eV AI	 U= 3 eV AI	 U=4 eV AI

TAB. S10. Topology phase diagram of K2 Co1 P2 O7

BCS ID	Formula	ICSD	MSG	T.C.	Picture
0.234	Mn2 La1 Sb1 O6		MSG 13.69 ($P2'/c'$)	$\eta_{4I} z_{2I,1} z_{2I,2}$	
Topology	 U=0 eV AI	 U= 1 eV AI	 U= 2 eV AI	 U= 3 eV AI	 U=4 eV AI

TAB. S11. Topology phase diagram of Mn2 La1 Sb1 O6

BCS ID	Formula	ICSD	MSG	T.C.	Picture
0.236	Ca1 Fe4 Al8		MSG 139.535 ($I4'/mmm'$)	None	
Topology	 U=0 eV ES	 U= 1 eV ES	 U= 2 eV ES	 U= 3 eV	 U=4 eV

TAB. S12. Topology phase diagram of Ca1 Fe4 Al8

BCS ID	Formula	ICSD	MSG	T.C.	Picture
0.239	Ca3 Li1 Ru1 O6		MSG 15.89 ($C2'/c'$)	$\eta_{4I} z_{2I,1} z_{2I,2}$	
Topology	 U=0 eV AI	 U= 1 eV AI	 U= 2 eV AI	 U= 3 eV AI	 U=4 eV AI

TAB. S13. Topology phase diagram of Ca3 Li1 Ru1 O6

BCS ID	Formula	ICSD	MSG	T.C.	Picture
0.254	Cu1 O6 C4 H9 N3		MSG 33.144 ($Pna2_1$)	None	
Topology	 U=0 eV AI	 U= 1 eV AI	 U= 2 eV AI	 U= 3 eV	 U=4 eV

TAB. S14. Topology phase diagram of Cu1 O6 C4 H9 N3

BCS ID	Formula	ICSD	MSG	T.C.	Picture
0.258	Fe2 P3 O12 Li3		MSG 14.79 ($P2'_1/c'$)	$\eta_{4I} z_{2I,1}$	
Topology	 U=0 eV AI	 U= 1 eV AI	 U= 2 eV AI	 U= 3 eV AI	 U=4 eV AI

TAB. S15. Topology phase diagram of Fe2 P3 O12 Li3

BCS ID	Formula	ICSD	MSG	T.C.	Picture
0.260	Cu1 Fe1 P1 O5		MSG 62.441 ($Pnma$)	η_{4I}	
Topology	 U=0 eV AI	 U= 1 eV AI	 U= 2 eV AI	 U= 3 eV AI	 U=4 eV AI

TAB. S16. Topology phase diagram of Cu1 Fe1 P1 O5

BCS ID	Formula	ICSD	MSG	T.C.	Picture
0.261	Ni1 Fe1 P1 O5		MSG 62.441 ($Pnma$)	η_{4I}	
Topology					

TAB. S17. Topology phase diagram of Ni1 Fe1 P1 O5

BCS ID	Formula	ICSD	MSG	T.C.	Picture
0.262	Co1 Fe1 P1 O5		MSG 62.447 ($Pnm'a'$)	η_{4I}	
Topology					

TAB. S18. Topology phase diagram of Co1 Fe1 P1 O5

BCS ID	Formula	ICSD	MSG	T.C.	Picture
0.263	Fe2 P1 O5		MSG 62.441 ($Pnma$)	η_{4I}	
Topology					

TAB. S19. Topology phase diagram of Fe2 P1 O5

BCS ID	Formula	ICSD	MSG	T.C.	Picture
0.264	Fe3 P2 O8		MSG 14.78 ($P2_1/c'$)	None	
Topology					

TAB. S20. Topology phase diagram of Fe3 P2 O8

BCS ID	Formula	ICSD	MSG	T.C.	Picture
0.266	Na2 Ba1 Mn1 V2 O8		MSG 164.89 ($P\bar{3}m'1$)	$\eta_{4I}z_{2I,3}z_{3R}$	
Topology	 U=0 eV AI	 U= 1 eV AI	 U= 2 eV AI	 U= 3 eV	 U=4 eV

TAB. S21. Topology phase diagram of Na2 Ba1 Mn1 V2 O8

BCS ID	Formula	ICSD	MSG	T.C.	Picture
0.273	Mn3 Zn1 N1		MSG 166.97 ($R\bar{3}m$)	None	
Topology	 U=0 eV AF	 U= 1 eV AF	 U= 2 eV ES	 U= 3 eV AF	 U=4 eV AF

TAB. S22. Topology phase diagram of Mn3 Zn1 N1

BCS ID	Formula	ICSD	MSG	T.C.	Picture
0.275	Al1 Mn3 N1		MSG 166.101 ($R\bar{3}m'$)	None	
Topology	 U=0 eV ES	 U= 1 eV ES	 U= 2 eV ES	 U= 3 eV	 U=4 eV

TAB. S23. Topology phase diagram of Al1 Mn3 N1

BCS ID	Formula	ICSD	MSG	T.C.	Picture
0.276	Al1 Mn3 N1		MSG 65.486 ($Cmm'm'$)	None	
Topology	 U=0 eV ES	 U= 1 eV ES	 U= 2 eV ES	 U= 3 eV	 U=4 eV

TAB. S24. Topology phase diagram of Al1 Mn3 N1

BCS ID	Formula	ICSD	MSG	T.C.	Picture
0.277	Mg1 Mn1 O3		MSG 148.19 ($R\bar{3}'$)	None	
Topology	 U=0 eV AI	 U= 1 eV AI	 U= 2 eV AI	 U= 3 eV	 U=4 eV

TAB. S25. Topology phase diagram of Mg1 Mn1 O3

BCS ID	Formula	ICSD	MSG	T.C.	Picture
0.279	Mn3 As1		MSG 63.463 ($Cmc'm'$)	$\eta_{4I}z_{2I,1}z_{2I,2}\delta_{2m}z_{2m,\pi}^-z_{2m,\pi}^+$	
Topology	 U=0 eV NLC (2, 0, 0, 1, 0, 0)	 U= 1 eV AI	 U= 2 eV ES	 U= 3 eV ES	 U=4 eV ES

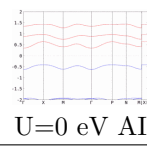
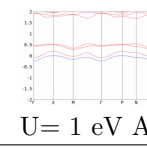
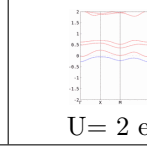
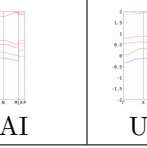
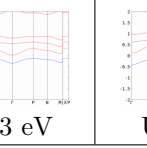
TAB. S26. Topology phase diagram of Mn3 As1

BCS ID	Formula	ICSD	MSG	T.C.	Picture
0.280	Mn3 As1		MSG 63.464 ($Cm'cm'$)	None	
Topology	 U=0 eV ES	 U= 1 eV ES	 U= 2 eV AF	 U= 3 eV	 U=4 eV

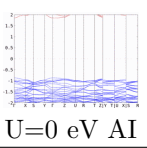
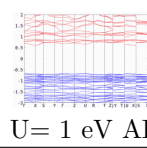
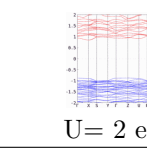
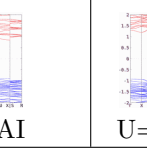
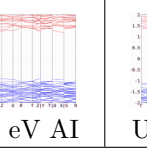
TAB. S27. Topology phase diagram of Mn3 As1

BCS ID	Formula	ICSD	MSG	T.C.	Picture
0.284	K1 Os1 O4		MSG 88.85 ($I4'_1/a'$)	z_2	
Topology	 U=0 eV AI	 U= 1 eV AI	 U= 2 eV	 U= 3 eV	 U=4 eV

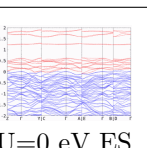
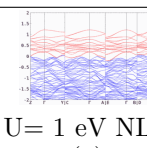
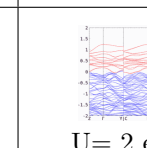
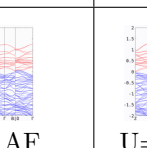
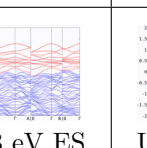
TAB. S28. Topology phase diagram of K1 Os1 O4

BCS ID	Formula	ICSD	MSG	T.C.	Picture
0.285	K1 Ru1 O4		MSG 88.85 ($I4'_1/a'$)	z_2	
Topology	 U=0 eV AI	 U= 1 eV AI	 U= 2 eV AI	 U= 3 eV	 U=4 eV

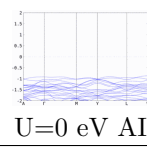
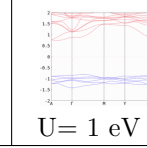
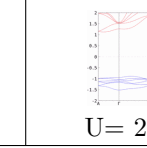
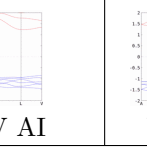
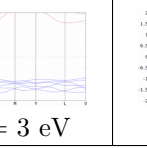
TAB. S29. Topology phase diagram of K1 Ru1 O4

BCS ID	Formula	ICSD	MSG	T.C.	Picture
0.292	Te2 Ni1 O5		MSG 62.441 ($Pnma$)	η_{4I}	
Topology	 U=0 eV AI	 U= 1 eV AI	 U= 2 eV AI	 U= 3 eV AI	 U=4 eV AI

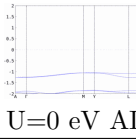
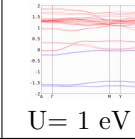
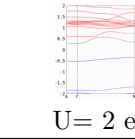
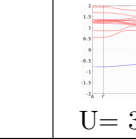
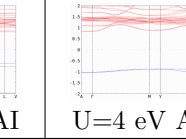
TAB. S30. Topology phase diagram of Te2 Ni1 O5

BCS ID	Formula	ICSD	MSG	T.C.	Picture
0.296	Cu2 Cl1 O3		MSG 14.75 ($P2_1/c$)	η_{4I}	
Topology	 U=0 eV ES	 U= 1 eV NLC (2)	 U= 2 eV AF	 U= 3 eV ES	 U=4 eV ES

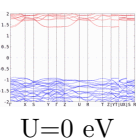
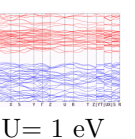
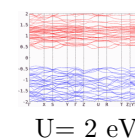
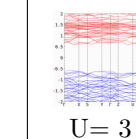
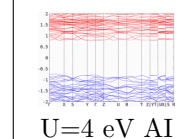
TAB. S31. Topology phase diagram of Cu2 Cl1 O3

BCS ID	Formula	ICSD	MSG	T.C.	Picture
0.297	Na1 Cr1 Ge2 O6		MSG 15.89 ($C2'/c'$)	$\eta_{4I} z_{2I,1} z_{2I,2}$	
Topology	 U=0 eV AI	 U= 1 eV AI	 U= 2 eV AI	 U= 3 eV	 U=4 eV

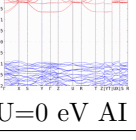
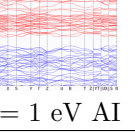
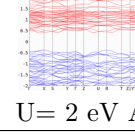
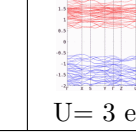
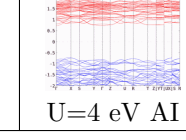
TAB. S32. Topology phase diagram of Na1 Cr1 Ge2 O6

BCS ID	Formula	ICSD	MSG	T.C.	Picture
0.298	Na2 Ba1 Fe1 V2 O8		MSG 15.89 ($C2'/c'$)	$\eta_{4I} z_{2I,1} z_{2I,2}$	
Topology	 U=0 eV AI	 U= 1 eV AI	 U= 2 eV AI	 U= 3 eV AI	 U=4 eV AI

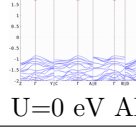
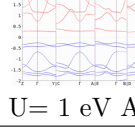
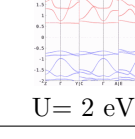
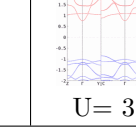
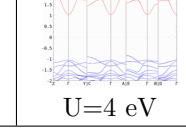
TAB. S33. Topology phase diagram of Na2 Ba1 Fe1 V2 O8

BCS ID	Formula	ICSD	MSG	T.C.	Picture
0.299	Fe2 O3		MSG 33.147 ($Pna'2'_1$)	<i>None</i>	
Topology	 U=0 eV	 U= 1 eV	 U= 2 eV	 U= 3 eV	 U=4 eV AI

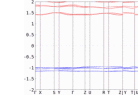
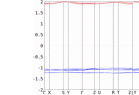
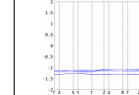
TAB. S34. Topology phase diagram of Fe2 O3

BCS ID	Formula	ICSD	MSG	T.C.	Picture
0.300	Fe2 O3		MSG 33.147 ($Pna'2'_1$)	<i>None</i>	
Topology	 U=0 eV AI	 U= 1 eV AI	 U= 2 eV AI	 U= 3 eV AI	 U=4 eV AI

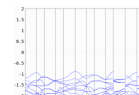
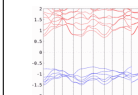
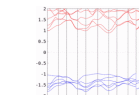
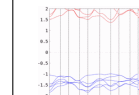
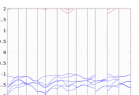
TAB. S35. Topology phase diagram of Fe2 O3

BCS ID	Formula	ICSD	MSG	T.C.	Picture
0.301	Sr2 Co1 Te1 O6		MSG 14.75 ($P2_1/c$)	η_{4I}	
Topology	 U=0 eV AI	 U= 1 eV AI	 U= 2 eV AI	 U= 3 eV	 U=4 eV

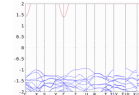
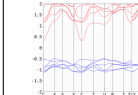
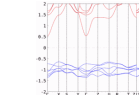
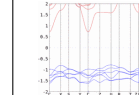
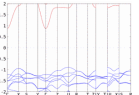
TAB. S36. Topology phase diagram of Sr2 Co1 Te1 O6

BCS ID	Formula	ICSD	MSG	T.C.	Picture
0.303	Ba1 F5 Cr1		MSG 19.27 ($P2'_12'_12_1$)	None	
Topology	 U=0 eV AI	 U= 1 eV AI	 U= 2 eV AI	 U= 3 eV AI	 U=4 eV AI

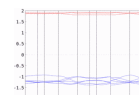
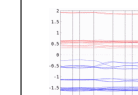
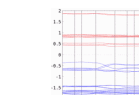
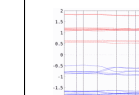
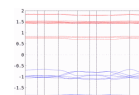
TAB. S37. Topology phase diagram of Ba1 F5 Cr1

BCS ID	Formula	ICSD	MSG	T.C.	Picture
0.307	Sc1 Cr1 O3		MSG 62.441 ($Pnma$)	η_{4I}	
Topology	 U=0 eV AI	 U= 1 eV AI	 U= 2 eV AI	 U=3 eV	 U=4 eV

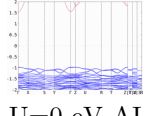
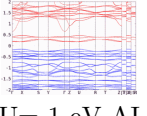
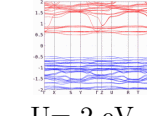
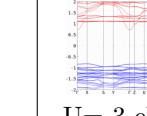
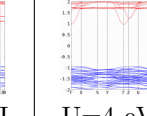
TAB. S38. Topology phase diagram of Sc1 Cr1 O3

BCS ID	Formula	ICSD	MSG	T.C.	Picture
0.308	In1 Cr1 O3		MSG 62.441 ($Pnma$)	η_{4I}	
Topology	 U=0 eV AI	 U= 1 eV AI	 U= 2 eV AI	 U=3 eV	 U=4 eV

TAB. S39. Topology phase diagram of In1 Cr1 O3

BCS ID	Formula	ICSD	MSG	T.C.	Picture
0.310	Na1 Mn1 Fe1 F6		MSG 150.27 ($P32'1$)	z_{3R}	
Topology	 U=0 eV AI	 U= 1 eV AI	 U= 2 eV	 U=3 eV AI	 U=4 eV AI

TAB. S40. Topology phase diagram of Na1 Mn1 Fe1 F6

BCS ID	Formula	ICSD	MSG	T.C.	Picture
0.311	Co1 Ge1 O3		MSG 61.435 ($Pb'ca$)	None	
Topology	 U=0 eV AI	 U= 1 eV AI	 U= 2 eV AI	 U= 3 eV AI	 U=4 eV AI

TAB. S41. Topology phase diagram of Co1 Ge1 O3

BCS ID	Formula	ICSD	MSG	T.C.	Picture
			MSG 15.87 ($C2'/c$)		
0.312	Mn1 Ge1 O3			None	

TAB. S42. Topology phase diagram of Mn1 Ge1 O3

BCS ID	Formula	ICSD	MSG	T.C.	Picture
			MSG 61.435 ($Pb'ca$)	None	
0.313	Mn1 Ge1 O3				

TAB. S43. Topology phase diagram of Mn1 Ge1 O3

BCS ID	Formula	ICSD	MSG	T.C.	Picture
			MSG 125.367 ($P4'/nbm'$)		
0.315	Zr1 Mn2 Ge4 O12			η_{4I}	

TAB. S44. Topology phase diagram of Zr1 Mn2 Ge4 O12

BCS ID	Formula	ICSD	MSG	T.C.	Picture
			MSG 62.441 ($Pnma$)		
0.323	La1 Cr1 O3			η_{4I}	

TAB. S45. Topology phase diagram of La1 Cr1 O3

BCS ID	Formula	ICSD	MSG	T.C.	Picture
	0.327 Mn1 Cs1 F4		MSG 59.410 ($Pmm'm'n'$)	None	
Topology	 U=0 eV ES	 U= 1 eV ES	 U = 2 eV ES	 U = 3 eV ES	 U=4 eV AI

TAB. S46. Topology phase diagram of Mn1 Cs1 F4

BCS ID	Formula	ICSD	MSG	T.C.	Picture
	0.328 Mn1 F4 K1		MSG 14.79 ($P2'_1/c'$)	$\eta_{4I}z_{2I,1}$	
Topology	 U=0 eV AI	 U= 1 eV AI	 U = 2 eV AI	 U = 3 eV AI	 U=4 eV AI

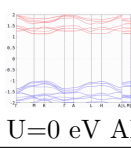
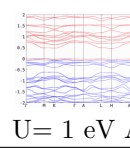
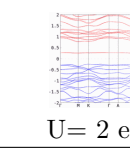
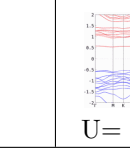
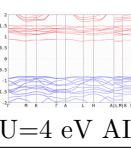
TAB. S47. Topology phase diagram of Mn1 F4 K1

BCS ID	Formula	ICSD	MSG	T.C.	Picture
	0.329 Mn1 F4 Rb1		MSG 2.4 ($P\bar{1}$)	$\eta_{4I}z_{2I,1}z_{2I,2}z_{2I,3}$	
Topology	 U=0 eV AI	 U= 1 eV AI	 U = 2 eV AI	 U = 3 eV AI	 U=4 eV AI

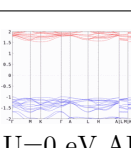
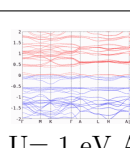
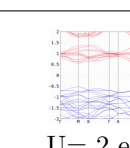
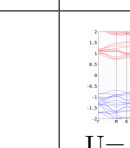
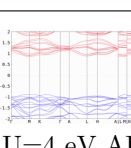
TAB. S48. Topology phase diagram of Mn1 F4 Rb1

BCS ID	Formula	ICSD	MSG	T.C.	Picture
	0.331 Fe2 Mo3 O8		MSG 186.205 ($P6'_3m'c$)	None	
Topology	 U=0 eV AI	 U= 1 eV AI	 U = 2 eV AI	 U = 3 eV AI	 U=4 eV AI

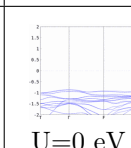
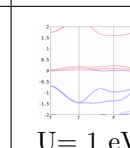
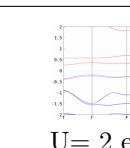
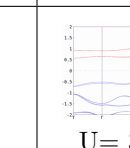
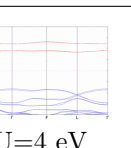
TAB. S49. Topology phase diagram of Fe2 Mo3 O8

BCS ID	Formula	ICSD	MSG	T.C.	Picture
	Co2 Mo3 O8		MSG 186.205 ($P6'_3m'c$)	None	
Topology	 U=0 eV AI	 U= 1 eV AI	 U= 2 eV AI	 U= 3 eV AI	 U=4 eV AI

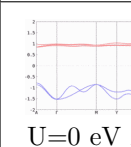
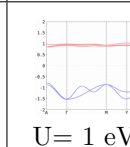
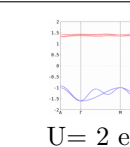
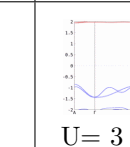
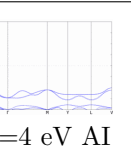
TAB. S50. Topology phase diagram of Co2 Mo3 O8

BCS ID	Formula	ICSD	MSG	T.C.	Picture
	Mn2 Mo3 O8		MSG 186.207 ($P6_3m'c'$)	z_{3R}	
Topology	 U=0 eV AI	 U= 1 eV AI	 U= 2 eV AI	 U= 3 eV AI	 U=4 eV AI

TAB. S51. Topology phase diagram of Mn2 Mo3 O8

BCS ID	Formula	ICSD	MSG	T.C.	Picture
	Co1 F3		MSG 167.103 ($R\bar{3}c$)	η_{4I}	
Topology	 U=0 eV AI	 U= 1 eV AI	 U= 2 eV AI	 U= 3 eV	 U=4 eV

TAB. S52. Topology phase diagram of Co1 F3

BCS ID	Formula	ICSD	MSG	T.C.	Picture
	Fe1 F3		MSG 15.89 ($C2'/c'$)	$\eta_{4I}z_{2I,1}z_{2I,2}$	
Topology	 U=0 eV AI	 U= 1 eV AI	 U= 2 eV AI	 U= 3 eV AI	 U=4 eV AI

TAB. S53. Topology phase diagram of Fe1 F3

BCS ID	Formula	ICSD	MSG	T.C.	Picture
			MSG 186.205 ($P6'_3m'c$)		
0.338	Co2 Mo3 O8			None	

TAB. S54. Topology phase diagram of Co2 Mo3 O8

BCS ID	Formula	ICSD	MSG	T.C.	Picture
			MSG 130.431 ($P4/n'c'c'$)		
0.348	Bi2 Cu1 O4			None	

TAB. S55. Topology phase diagram of Bi2 Cu1 O4

BCS ID	Formula	ICSD	MSG	T.C.	Picture
			MSG 11.50 ($P2_1/m$)		
0.357	Ca1 Fe5 O7			None	

TAB. S56. Topology phase diagram of Ca1 Fe5 O7

BCS ID	Formula	ICSD	MSG	T.C.	Picture
			MSG 15.89 ($C2'/c'$)		
0.361	Sr3 Li1 Ru1 O6			$\eta_{4I}z_{2I,1}z_{2I,2}$	

TAB. S57. Topology phase diagram of Sr3 Li1 Ru1 O6

BCS ID	Formula	ICSD	MSG	T.C.	Picture
0.368	Co1 C4 N1 O6 H9		MSG 62.448 ($Pn'ma'$)	η_{4I}	
Topology	 U=0 eV AI	 U= 1 eV AI	 U= 2 eV AI	 U= 3 eV AI	 U=4 eV AI

TAB. S58. Topology phase diagram of Co1 C4 N1 O6 H9

BCS ID	Formula	ICSD	MSG	T.C.	Picture
0.369	N1 C4 O6 Co1 H9		MSG 14.79 ($P2'_1/c'$)	$\eta_{4I}z_{2I,1}$	
Topology	 U=0 eV	 U= 1 eV	 U= 2 eV AI	 U= 3 eV AI	 U=4 eV AI

TAB. S59. Topology phase diagram of N1 C4 O6 Co1 H9

BCS ID	Formula	ICSD	MSG	T.C.	Picture
0.375	La2 Co1 Ir1 O6		MSG 14.75 ($P2_1/c$)	η_{4I}	
Topology	 U=0 eV AI	 U= 1 eV AI	 U= 2 eV AI	 U= 3 eV	 U=4 eV

TAB. S60. Topology phase diagram of La2 Co1 Ir1 O6

BCS ID	Formula	ICSD	MSG	T.C.	Picture
0.395	Ga1 Mn1 Pt1		MSG 63.462 ($Cm'c'm$)	None	
Topology	 U=0 eV ES	 U= 1 eV ES	 U= 2 eV ES	 U= 3 eV ES	 U=4 eV ES

TAB. S61. Topology phase diagram of Ga1 Mn1 Pt1

BCS ID	Formula	ICSD	MSG	T.C.	Picture
0.396	Ga1 Mn1 Pt1		MSG 63.462 ($Cm'c'm$)	None	
Topology					

TAB. S62. Topology phase diagram of Ga1 Mn1 Pt1

BCS ID	Formula	ICSD	MSG	T.C.	Picture
0.399	Fe1 O2 H1		MSG 62.445 ($Pnma'$)	None	
Topology					

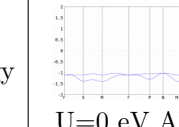
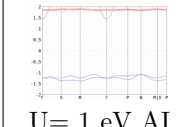
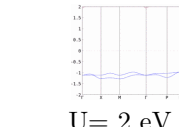
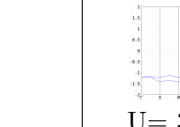
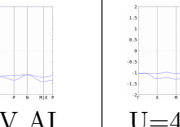
TAB. S63. Topology phase diagram of Fe1 O2 H1

BCS ID	Formula	ICSD	MSG	T.C.	Picture
0.414	Fe2 B2 Al1		MSG 65.486 ($Cmm'm'$)	None	
Topology					

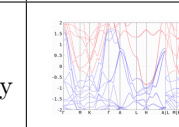
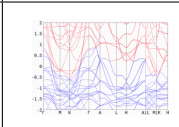
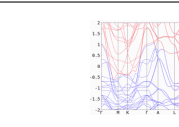
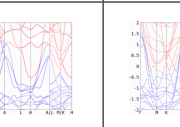
TAB. S64. Topology phase diagram of Fe2 B2 Al1

BCS ID	Formula	ICSD	MSG	T.C.	Picture
0.416	La1 Cr1 O3		MSG 167.103 ($R\bar{3}c$)	η_{4I}	
Topology					

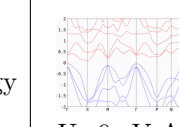
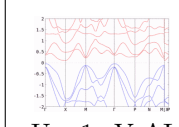
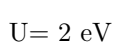
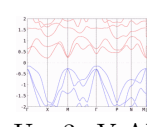
TAB. S65. Topology phase diagram of La1 Cr1 O3

BCS ID	Formula	ICSD	MSG	T.C.	Picture
0.433	K1 Mn1 F3		MSG 140.541 ($I4/mcm$)	$\eta_{4I}\delta_{2m}z_2\delta_{4m}z_{4m,0}^+$	
Topology	 $U=0 \text{ eV AI}$  $U=1 \text{ eV AI}$  $U=2 \text{ eV AI}$  $U=3 \text{ eV AI}$  $U=4 \text{ eV AI}$				

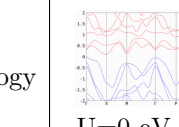
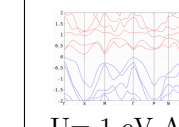
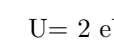
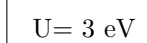
TAB. S66. Topology phase diagram of K1 Mn1 F3

BCS ID	Formula	ICSD	MSG	T.C.	Picture
0.447	Ge1 Mn1 Co1		MSG 194.270 ($P6_3/mm'c'$)	None	
Topology	 $U=0 \text{ eV ES}$  $U=1 \text{ eV ES}$  $U=2 \text{ eV ES}$  $U=3 \text{ eV ES}$  $U=4 \text{ eV ES}$				

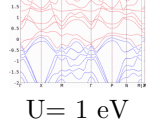
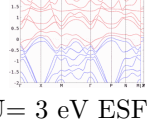
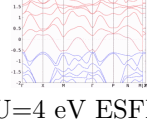
TAB. S67. Topology phase diagram of Ge1 Mn1 Co1

BCS ID	Formula	ICSD	MSG	T.C.	Picture	
0.464	Ba1 Mn2 P2		MSG 139.536 ($I4'/m'm'm$)	z_2		
Topology	 $U=0 \text{ eV AI}$  $U=1 \text{ eV AI}$		 $U=2 \text{ eV}$		 $U=3 \text{ eV AI}$	 $U=4 \text{ eV}$

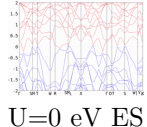
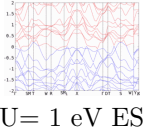
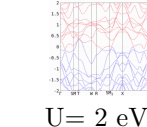
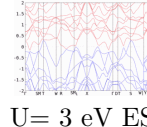
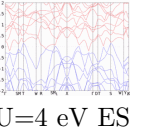
TAB. S68. Topology phase diagram of Ba1 Mn2 P2

BCS ID	Formula	ICSD	MSG	T.C.	Picture
0.470	Ba1 Mn2 Sb2		MSG 139.536 ($I4'/m'm'm$)	z_2	
Topology	 $U=0 \text{ eV AI}$  $U=1 \text{ eV AI}$		 $U=2 \text{ eV}$	 $U=3 \text{ eV}$	 $U=4 \text{ eV}$

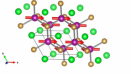
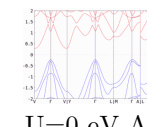
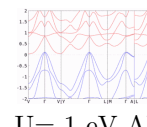
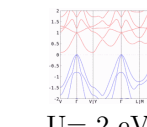
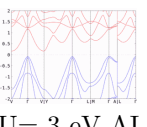
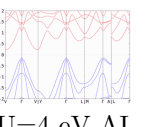
TAB. S69. Topology phase diagram of Ba1 Mn2 Sb2

BCS ID	Formula	ICSD	MSG	T.C.	Picture
0.471	Ba2 Mn3 Sb2 O2		MSG 139.536 ($I4'/m'm'm$)	None	
Topology	U=0 eV	 U= 1 eV	U= 2 eV	U= 3 eV ESFD	 

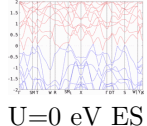
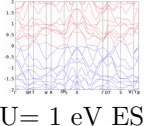
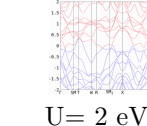
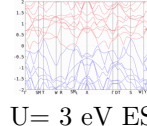
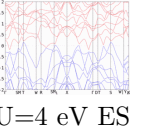
TAB. S70. Topology phase diagram of Ba2 Mn3 Sb2 O2

BCS ID	Formula	ICSD	MSG	T.C.	Picture
0.473	La1 Mn2 Si2		MSG 44.231 ($Im'm2'$)	None	
Topology	 U=0 eV ES	 U= 1 eV ES	 U= 2 eV ES	 U= 3 eV ES	 U=4 eV ES

TAB. S71. Topology phase diagram of La1 Mn2 Si2

BCS ID	Formula	ICSD	MSG	T.C.	Picture
0.482	Sr1 Mn2 As2		MSG 12.60 ($C2'/m$)	None	
Topology	 U=0 eV AI	 U= 1 eV AI	 U= 2 eV AI	 U= 3 eV AI	 U=4 eV AI

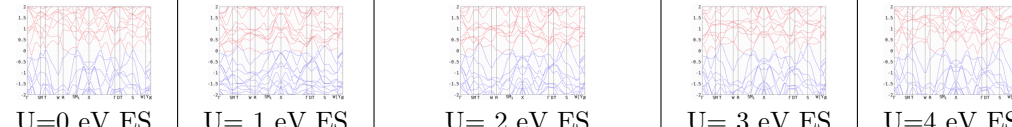
TAB. S72. Topology phase diagram of Sr1 Mn2 As2

BCS ID	Formula	ICSD	MSG	T.C.	Picture
0.495	La1 Mn2 Si2		MSG 44.231 ($Im'm2'$)	None	
Topology	 U=0 eV ES	 U= 1 eV ES	 U= 2 eV ES	 U= 3 eV ES	 U=4 eV ES

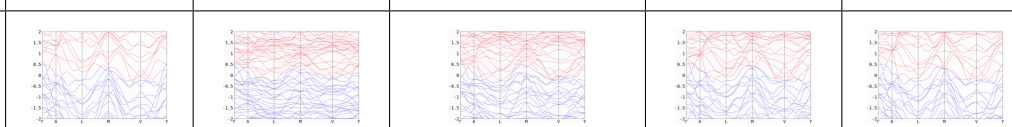
TAB. S73. Topology phase diagram of La1 Mn2 Si2

BCS ID	Formula	ICSD	MSG	T.C.	Picture
0.496	La1 Mn2 Si2		MSG 44.231 ($Im'm2'$)	None	
Topology	 U=0 eV ES	 U= 1 eV ES	 U= 2 eV ES	 U= 3 eV ES	 U=4 eV ES

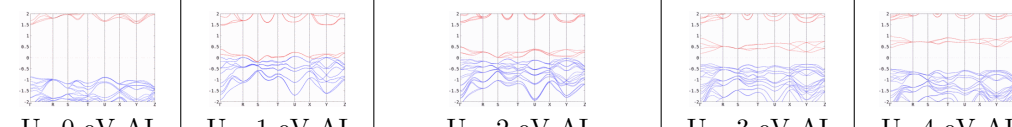
TAB. S74. Topology phase diagram of La1 Mn2 Si2

BCS ID	Formula	ICSD	MSG	T.C.	Picture
0.497	La1 Mn2 Si2		MSG 44.231 ($Im'm2'$)	None	
Topology	 U=0 eV ES U= 1 eV ES U= 2 eV ES U= 3 eV ES U=4 eV ES				

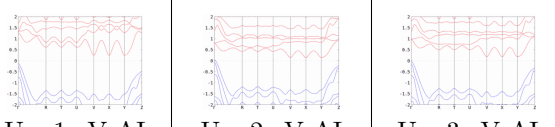
TAB. S75. Topology phase diagram of La1 Mn2 Si2

BCS ID	Formula	ICSD	MSG	T.C.	Picture
0.512	Mn3 As2		MSG 12.58 ($C2/m$)	None	
Topology	 U=0 eV ES U= 1 eV ES U= 2 eV ES U= 3 eV ES U=4 eV ES				

TAB. S76. Topology phase diagram of Mn3 As2

BCS ID	Formula	ICSD	MSG	T.C.	Picture
0.513	Y1 Ru1 O3		MSG 62.448 ($Pn'ma'$)	η_{4I}	
Topology	 U=0 eV AI U= 1 eV AI U= 2 eV AI U= 3 eV AI U=4 eV AI				

TAB. S77. Topology phase diagram of Y1 Ru1 O3

BCS ID	Formula	ICSD	MSG	T.C.	Picture
0.523	Ca1 Mn2 Sb2		MSG 2.6 ($P\bar{1}'$)	None	
Topology	 U=0 eV U= 1 eV AI U= 2 eV AI U= 3 eV AI U=4 eV AI				

TAB. S78. Topology phase diagram of Ca1 Mn2 Sb2

BCS ID	Formula	ICSD	MSG	T.C.	Picture	
0.524	Mn1 P1 Se3		MSG 2.6 ($P\bar{1}'$)	None		
Topology	U=0 eV					

TAB. S79. Topology phase diagram of Mn1 P1 Se3

BCS ID	Formula	ICSD	MSG	T.C.	Picture	
0.526	Mn4 Ta2 O9		MSG 165.94 ($P\bar{3}'c'1$)	None		
Topology	U=0 eV AI					

TAB. S80. Topology phase diagram of Mn4 Ta2 O9

BCS ID	Formula	ICSD	MSG	T.C.	Picture	
0.528	Cr1 Sb1		MSG 194.268 ($P6'_3/m'm'c$)	η_{4I}		
Topology	U=0 eV OAI					

TAB. S81. Topology phase diagram of Cr1 Sb1

BCS ID	Formula	ICSD	MSG	T.C.	Picture	
0.529	Co4 Nb2 O9		MSG 15.88 ($C2/c'$)	None		
Topology	U=0 eV					

TAB. S82. Topology phase diagram of Co4 Nb2 O9

BCS ID	Formula	ICSD	MSG	T.C.	Picture
0.552	Pb2 Mn1 O4		MSG 114.278 ($P\bar{4}'2_1c'$)	None	
Topology	 U=0 eV AI	 U= 1 eV AI	 U = 2 eV AI	 U = 3 eV AI	 U=4 eV AI

TAB. S83. Topology phase diagram of Pb2 Mn1 O4

BCS ID	Formula	ICSD	MSG	T.C.	Picture
0.571	Co1 S1 O4		MSG 62.441 ($Pnma$)	η_{4I}	
Topology	 U=0 eV AI	 U= 1 eV AI	 U = 2 eV AI	 U = 3 eV AI	 U=4 eV AI

TAB. S84. Topology phase diagram of Co1 S1 O4

BCS ID	Formula	ICSD	MSG	T.C.	Picture
0.572	Na2 F7 Ni1 Cr1		MSG 74.558 ($Im'm'a$)	$\eta_{4I}z_{2I,1}z_{2I,2}z_{2I,3}$	
Topology	 U=0 eV AI	 U= 1 eV AI	 U = 2 eV AI	 U = 3 eV AI	 U=4 eV AI

TAB. S85. Topology phase diagram of Na2 F7 Ni1 Cr1

BCS ID	Formula	ICSD	MSG	T.C.	Picture
0.573	Na2 F7 Ni1 Cr1		MSG 74.558 ($Im'm'a$)	$\eta_{4I}z_{2I,1}z_{2I,2}z_{2I,3}$	
Topology	 U=0 eV AI	 U= 1 eV AI	 U = 2 eV AI	 U = 3 eV AI	 U=4 eV AI

TAB. S86. Topology phase diagram of Na2 F7 Ni1 Cr1

BCS ID	Formula	ICSD	MSG	T.C.	Picture	
0.574	Mn1 Fe1 F5 O2 H4		MSG 5.15 ($C2'$)	None		
Topology	U=0 eV					

TAB. S87. Topology phase diagram of Mn1 Fe1 F5 O2 H4

BCS ID	Formula	ICSD	MSG	T.C.	Picture	
0.575	Zn1 Fe1 F5 O2 H4		MSG 44.229 ($Imm2$)	None		
Topology	U=0 eV					

TAB. S88. Topology phase diagram of Zn1 Fe1 F5 O2 H4

BCS ID	Formula	ICSD	MSG	T.C.	Picture	
0.576	Cr2 F5		MSG 15.85 ($C2/c$)	$\eta_{4I} z_{2I,1} z_{2I,2}$		
Topology	U=0 eV					

TAB. S89. Topology phase diagram of Cr2 F5

BCS ID	Formula	ICSD	MSG	T.C.	Picture	
0.577	Ba1 Mn1 Fe1 F7		MSG 14.79 ($P2'_1/c'$)	$\eta_{4I} z_{2I,1}$		
Topology	U=0 eV					

TAB. S90. Topology phase diagram of Ba1 Mn1 Fe1 F7

BCS ID	Formula	ICSD	MSG	T.C.	Picture
0.578	Fe2 Na1 Ba1 F9		MSG 14.75 ($P2_1/c$)	η_{4I}	
Topology	 $U=0 \text{ eV AI}$	 $U=1 \text{ eV AI}$	 $U=2 \text{ eV AI}$	 $U=3 \text{ eV AI}$	 $U=4 \text{ eV AI}$

TAB. S91. Topology phase diagram of Fe2 Na1 Ba1 F9

BCS ID	Formula	ICSD	MSG	T.C.	Picture
0.579	Na2 Ni1 Fe1 F7		MSG 74.559 ($Imm'a'$)	$\eta_{4I}z_{2I,1}z_{2I,2}z_{2I,3}\delta_{2m}z_{2m,\pi}^-z_{2m,\pi}^+$	
Topology	 $U=0 \text{ eV AI}$	 $U=1 \text{ eV AI}$	 $U=2 \text{ eV}$	 $U=3 \text{ eV AI}$	 $U=4 \text{ eV}$

TAB. S92. Topology phase diagram of Na2 Ni1 Fe1 F7

BCS ID	Formula	ICSD	MSG	T.C.	Picture
0.580	Na2 Ni1 Fe1 F7		MSG 74.559 ($Imm'a'$)	$\eta_{4I}z_{2I,1}z_{2I,2}z_{2I,3}\delta_{2m}z_{2m,\pi}^-z_{2m,\pi}^+$	
Topology	$U=0 \text{ eV}$	 $U=1 \text{ eV AI}$	 $U=2 \text{ eV}$	 $U=3 \text{ eV AI}$	 $U=4 \text{ eV}$

TAB. S93. Topology phase diagram of Na2 Ni1 Fe1 F7

BCS ID	Formula	ICSD	MSG	T.C.	Picture
0.581	Fe1 F3		MSG 15.89 ($C2'/c'$)	$\eta_{4I}z_{2I,1}z_{2I,2}$	
Topology	$U=0 \text{ eV}$	 $U=1 \text{ eV AI}$	 $U=2 \text{ eV}$	 $U=3 \text{ eV}$	 $U=4 \text{ eV}$

TAB. S94. Topology phase diagram of Fe1 F3

BCS ID	Formula	ICSD	MSG	T.C.	Picture	
0.582	Fe3 F8 O2 H4		MSG 12.62 ($C2'/m'$)	$\eta_{4I} z_{2I,1} z_{2I,2} z_{2I,3}$		
Topology	U=0 eV					

TAB. S95. Topology phase diagram of Fe3 F8 O2 H4

BCS ID	Formula	ICSD	MSG	T.C.	Picture	
0.583	Fe2 F5 O2 H4		MSG 74.559 ($Imm'a'$)	$\eta_{4I} z_{2I,1} z_{2I,2} z_{2I,3} \delta_{2m} z_{2m,\pi}^- z_{2m,\pi}^+$		
Topology	U=0 eV					

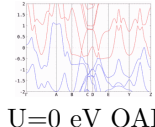
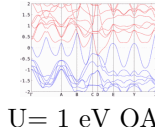
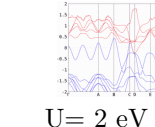
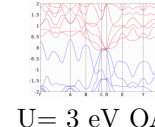
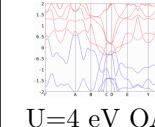
TAB. S96. Topology phase diagram of Fe2 F5 O2 H4

BCS ID	Formula	ICSD	MSG	T.C.	Picture	
0.584	Fe2 F5 O2 H4		MSG 15.89 ($C2'/c'$)	$\eta_{4I} z_{2I,1} z_{2I,2}$		
Topology	U=0 eV AI					

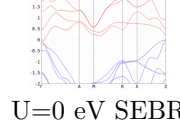
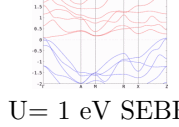
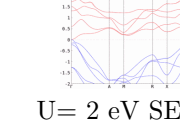
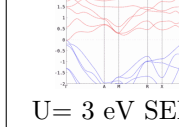
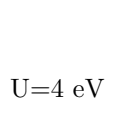
TAB. S97. Topology phase diagram of Fe2 F5 O2 H4

BCS ID	Formula	ICSD	MSG	T.C.	Picture	
0.586	Y1 Cr1 O3		MSG 62.448 ($Pn'ma'$)	η_{4I}		
Topology	U=0 eV AI					

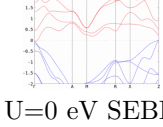
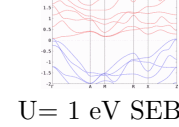
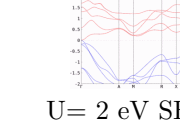
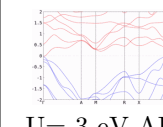
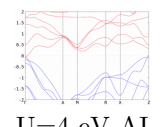
TAB. S98. Topology phase diagram of Y1 Cr1 O3

BCS ID	Formula	ICSD	MSG	T.C.	Picture
0.598	Al1 Cr2		MSG 14.83 (P_A2_1/c)	η_{4I}	
Topology	 $U=0 \text{ eV OAI}$	 $U= 1 \text{ eV OAI}$	 $U= 2 \text{ eV OAI}$	 $U= 3 \text{ eV OAI}$	 $U=4 \text{ eV OAI}$

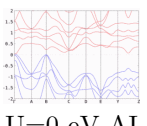
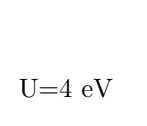
TAB. S99. Topology phase diagram of Al1 Cr2

BCS ID	Formula	ICSD	MSG	T.C.	Picture
0.599	Mn1 Ca1 Si1		MSG 129.416 ($P4'/n'm'm$)	z_2	
Topology	 $U=0 \text{ eV SEBR (1)}$	 $U= 1 \text{ eV SEBR (1)}$	 $U= 2 \text{ eV SEBR (1)}$	 $U= 3 \text{ eV SEBR (1)}$	 $U=4 \text{ eV}$

TAB. S100. Topology phase diagram of Mn1 Ca1 Si1

BCS ID	Formula	ICSD	MSG	T.C.	Picture
0.600	Mn1 Ca1 Si1		MSG 129.416 ($P4'/n'm'm$)	z_2	
Topology	 $U=0 \text{ eV SEBR (1)}$	 $U= 1 \text{ eV SEBR (1)}$	 $U= 2 \text{ eV SEBR (1)}$	 $U= 3 \text{ eV AF}$	 $U=4 \text{ eV AI}$

TAB. S101. Topology phase diagram of Mn1 Ca1 Si1

BCS ID	Formula	ICSD	MSG	T.C.	Picture
0.601	Mn1 Ca1 Ge1		MSG 11.53 ($P2_1/m'$)	<i>None</i>	
Topology	 $U=0 \text{ eV AI}$	$U= 1 \text{ eV}$	$U= 2 \text{ eV}$	$U= 3 \text{ eV AI}$	 $U=4 \text{ eV}$

TAB. S102. Topology phase diagram of Mn1 Ca1 Ge1

BCS ID	Formula	ICSD	MSG	T.C.	Picture
0.603	Ca1 Mn2 Ge2		MSG 139.536 ($I4'/m'm'm$)	z_2	
Topology	U=0 eV NLC (1)	 U = 1 eV NLC (1)	 U = 2 eV AF	 U = 3 eV OAI	U=4 eV

TAB. S103. Topology phase diagram of Ca1 Mn2 Ge2

BCS ID	Formula	ICSD	MSG	T.C.	Picture
0.604	Ca1 Mn2 Ge2		MSG 139.536 ($I4'/m'm'm$)	z_2	
Topology	U=0 eV	 U = 1 eV	 U = 2 eV	 U = 3 eV OAI	U=4 eV

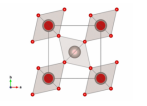
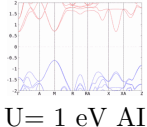
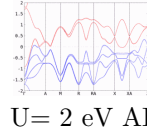
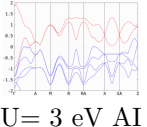
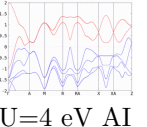
TAB. S104. Topology phase diagram of Ca1 Mn2 Ge2

BCS ID	Formula	ICSD	MSG	T.C.	Picture
0.605	Ba1 Mn2 Ge2		MSG 139.536 ($I4'/m'm'm$)	z_2	
Topology	U=0 eV	 U = 1 eV NLC (1)	 U = 2 eV NLC (1)	 U = 3 eV OAI	U=4 eV

TAB. S105. Topology phase diagram of Ba1 Mn2 Ge2

BCS ID	Formula	ICSD	MSG	T.C.	Picture
0.606	Ba1 Mn2 Ge2		MSG 139.536 ($I4'/m'm'm$)	z_2	
Topology	U=0 eV NLC (1)	 U = 1 eV NLC (1)	 U = 2 eV OAI	 U = 3 eV OAI	U=4 eV

TAB. S106. Topology phase diagram of Ba1 Mn2 Ge2

BCS ID	Formula	ICSD	MSG	T.C.	Picture
0.607	Ru1 O2		MSG 136.499 ($P4_2'/mnm'$)	$\eta_{4I}\delta_{2m}$	
Topology	U=0 eV	 U= 1 eV AI	 U= 2 eV AI	 U= 3 eV AI	 U=4 eV AI

TAB. S107. Topology phase diagram of Ru1 O2

BCS ID	Formula	ICSD	MSG	T.C.	Picture
0.612	Cu2 S1 O5		MSG 12.58 ($C2/m$)	$\eta_{4I} z_{2I,1} z_{2I,2} \delta_{2m} z_{2m,\pi}^- z_{2m,\pi}^+$	
Topology	U=0 eV AI U= 1 eV AI U= 2 eV AI U= 3 eV AI U=4 eV AI	 	 	 	

TAB. S108. Topology phase diagram of Cu2 S1 O5

BCS ID	Formula	ICSD	MSG	T.C.	Picture
0.613	Fe1 Cr2 S4		MSG 141.557 ($I4_1/am'd'$)	None	
Topology	U=0 eV U= 1 eV ES U= 2 eV ES U= 3 eV ES U=4 eV AI	 	 	 	

TAB. S109. Topology phase diagram of Fe1 Cr2 S4

BCS ID	Formula	ICSD	MSG	T.C.	Picture
0.617	Mn1 K1 Sb1		MSG 129.416 ($P4'/n'm'm$)	z_2	
Topology	U=0 eV AI U= 1 eV AI U= 2 eV AI U= 3 eV AI U=4 eV AI	 	 	 	

TAB. S110. Topology phase diagram of Mn1 K1 Sb1

BCS ID	Formula	ICSD	MSG	T.C.	Picture
0.618	Mn1 K1 Bi1		MSG 129.416 ($P4'/n'm'm$)	z_2	
Topology	U=0 eV AI U= 1 eV AI U= 2 eV AI U= 3 eV AI U=4 eV AI	 	 	 	

TAB. S111. Topology phase diagram of Mn1 K1 Bi1

BCS ID	Formula	ICSD	MSG	T.C.	Picture
0.619	Mn1 La1 As1 O1		MSG 129.416 ($P4'/n'm'm$)	z_2	
Topology	 U=0 eV AI	 U= 1 eV AI	 U= 2 eV AI	 U= 3 eV AI	 U=4 eV

TAB. S112. Topology phase diagram of Mn1 La1 As1 O1

BCS ID	Formula	ICSD	MSG	T.C.	Picture
0.624	Mn1 La1 As1 O1		MSG 129.416 ($P4'/n'm'm$)	z_2	
Topology	 U=0 eV AI	 U= 1 eV AI	 U= 2 eV AI	 U= 3 eV AI	 U=4 eV AI

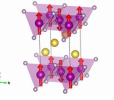
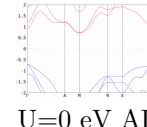
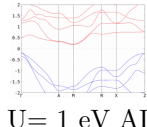
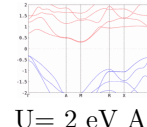
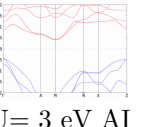
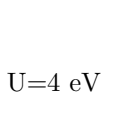
TAB. S113. Topology phase diagram of Mn1 La1 As1 O1

BCS ID	Formula	ICSD	MSG	T.C.	Picture
0.626	Na1 Mn1 P1		MSG 129.416 ($P4'/n'm'm$)	z_2	
Topology	 U=0 eV	 U= 1 eV AI	 U= 2 eV AI	 U= 3 eV AI	 U=4 eV AI

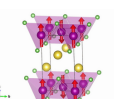
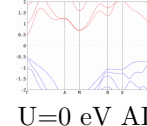
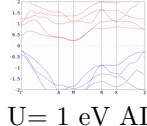
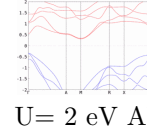
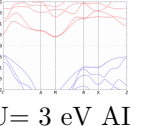
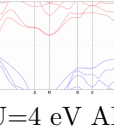
TAB. S114. Topology phase diagram of Na1 Mn1 P1

BCS ID	Formula	ICSD	MSG	T.C.	Picture
0.627	Na1 Mn1 P1		MSG 129.416 ($P4'/n'm'm$)	z_2	
Topology	 U=0 eV	 U= 1 eV AI	 U= 2 eV AI	 U= 3 eV AI	 U=4 eV

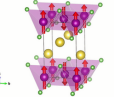
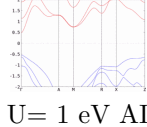
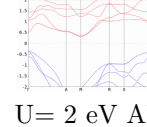
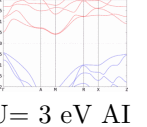
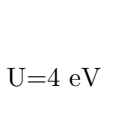
TAB. S115. Topology phase diagram of Na1 Mn1 P1

BCS ID	Formula	ICSD	MSG	T.C.	Picture
0.628	Mn1 Na1 P1		MSG 129.416 ($P4'/n'm'm$)	z_2	
Topology	 U=0 eV AI	 U= 1 eV AI	 U = 2 eV AI	 U= 3 eV AI	 U=4 eV

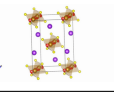
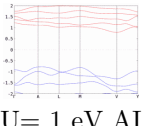
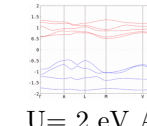
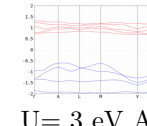
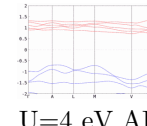
TAB. S116. Topology phase diagram of Mn1 Na1 P1

BCS ID	Formula	ICSD	MSG	T.C.	Picture
0.629	Mn1 Na1 As1		MSG 129.416 ($P4'/n'm'm$)	z_2	
Topology	 U=0 eV AI	 U= 1 eV AI	 U = 2 eV AI	 U= 3 eV AI	 U=4 eV AI

TAB. S117. Topology phase diagram of Mn1 Na1 As1

BCS ID	Formula	ICSD	MSG	T.C.	Picture
0.630	Mn1 Na1 As1		MSG 129.416 ($P4'/n'm'm$)	z_2	
Topology	U=0 eV	 U= 1 eV AI	 U = 2 eV AI	 U= 3 eV AI	 U=4 eV

TAB. S118. Topology phase diagram of Mn1 Na1 As1

BCS ID	Formula	ICSD	MSG	T.C.	Picture
0.633	Fe1 K1 S2		MSG 15.87 ($C2'/c$)	None	
Topology	U=0 eV	 U= 1 eV AI	 U = 2 eV AI	 U= 3 eV AI	 U=4 eV AI

TAB. S119. Topology phase diagram of Fe1 K1 S2

BCS ID	Formula	ICSD	MSG	T.C.	Picture
0.634	Mn1 Na1 Bi1		MSG 129.416 ($P4'/n'm'm$)	z_2	
Topology	U=0 eV		U= 2 eV		U=4 eV

TAB. S120. Topology phase diagram of Mn1 Na1 Bi1

BCS ID	Formula	ICSD	MSG	T.C.	Picture
0.636	Fe1 Rb1 S2		MSG 15.87 ($C2'/c$)	None	
Topology	U=0 eV AI		U= 1 eV AI		U=2 eV AI

TAB. S121. Topology phase diagram of Fe1 Rb1 S2

BCS ID	Formula	ICSD	MSG	T.C.	Picture
0.637	Fe1 K1 Se2		MSG 15.88 ($C2/c'$)	None	
Topology	U=0 eV AI		U= 1 eV AI		U=2 eV AI

TAB. S122. Topology phase diagram of Fe1 K1 Se2

BCS ID	Formula	ICSD	MSG	T.C.	Picture
0.638	Fe1 Rb1 Se2		MSG 15.88 ($C2/c'$)	None	
Topology	U=0 eV AI		U= 1 eV AI		U=2 eV AI

TAB. S123. Topology phase diagram of Fe1 Rb1 Se2

BCS ID	Formula	ICSD	MSG	T.C.	Picture	
0.639	Au1 Mn2		MSG 71.535 ($Im'mm$)	None		
Topology	U=0 eV					
		U= 1 eV ESFD	U= 2 eV ESFD	U= 3 eV ESFD	U=4 eV ESFD	

TAB. S124. Topology phase diagram of Au1 Mn2

BCS ID	Formula	ICSD	MSG	T.C.	Picture	
0.640	Au1 Mn2		MSG 71.535 ($Im'mm$)	None		
Topology	U=0 eV					
		U= 0 eV ESFD	U= 1 eV ESFD	U= 2 eV ESFD	U=3 eV ESFD	U=4 eV ESFD

TAB. S125. Topology phase diagram of Au1 Mn2

BCS ID	Formula	ICSD	MSG	T.C.	Picture	
0.641	Ga1 Mn3		MSG 12.62 ($C2'/m'$)	$\eta_{4I} z_{2I,1} z_{2I,2} z_{2I,3}$		
Topology	U=0 eV NLC (1, 1, 1, 0)					
		(1, 1, 1, 0)	(2, 1, 1, 0)	(1, 0, 0, 0)	(1, 0, 0, 0)	(1, 0, 0, 0)

TAB. S126. Topology phase diagram of Ga1 Mn3

BCS ID	Formula	ICSD	MSG	T.C.	Picture	
0.642	La1 Mn1 O3		MSG 62.448 ($Pn'ma'$)	η_{4I}		
Topology	U=0 eV AI					
		U= 0 eV AI	U= 1 eV AI	U= 2 eV AI	U=3 eV AI	U=4 eV AI

TAB. S127. Topology phase diagram of La1 Mn1 O3

BCS ID	Formula	ICSD	MSG	T.C.	Picture
0.662	Mn ₃ Sn ₂		MSG 62.448 ($Pn'ma'$)	None	
Topology	 U=0 eV ES	 U=1 eV ES	 U=2 eV ES	 U=3 eV ES	 U=4 eV

TAB. S128. Topology phase diagram of Mn₃ Sn₂

BCS ID	Formula	ICSD	MSG	T.C.	Picture
0.663	Mn ₃ Sn ₂		MSG 62.448 ($Pn'ma'$)	None	
Topology	 U=0 eV ES	 U=1 eV ES	 U=2 eV ES	 U=3 eV ES	 U=4 eV

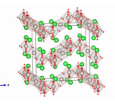
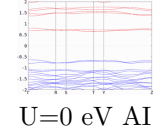
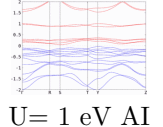
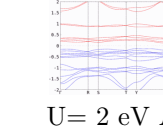
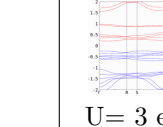
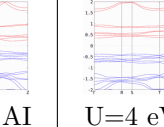
TAB. S129. Topology phase diagram of Mn₃ Sn₂

BCS ID	Formula	ICSD	MSG	T.C.	Picture
0.664	Mn ₃ Sn ₂		MSG 14.79 ($P2'_1/c'$)	$\eta_{4I}z_{2I,1}$	
Topology	 U=0 eV NLC (1, 0)	 U=1 eV NLC (2, 0)	 U=2 eV NLC (2, 0)	 U=3 eV NLC (2, 0)	 U=4 eV OAI

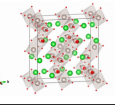
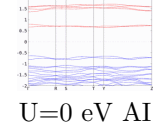
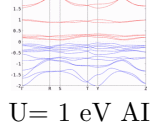
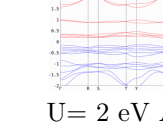
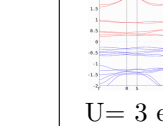
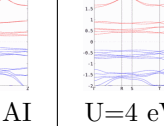
TAB. S130. Topology phase diagram of Mn₃ Sn₂

BCS ID	Formula	ICSD	MSG	T.C.	Picture
0.682	Ca ₂ Fe ₁ Os ₁ O ₆		MSG 14.79 ($P2'_1/c'$)	$\eta_{4I}z_{2I,1}$	
Topology	 U=0 eV	 U=1 eV AI	 U=2 eV AI	 U=3 eV AI	 U=4 eV AI

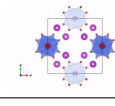
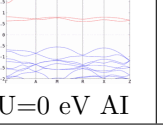
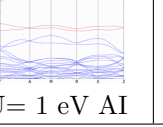
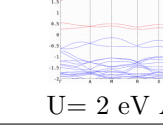
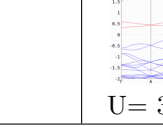
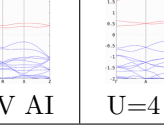
TAB. S131. Topology phase diagram of Ca₂ Fe₁ Os₁ O₆

BCS ID	Formula	ICSD	MSG	T.C.	Picture
0.692	Ru3 Ba4 O10		MSG 64.471 ($Cm'ca$)	None	
Topology	 U=0 eV AI	 U= 1 eV AI	 U= 2 eV AI	 U= 3 eV AI	 U=4 eV AI

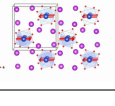
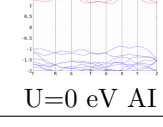
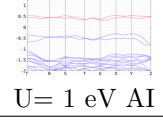
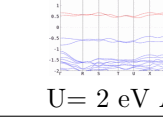
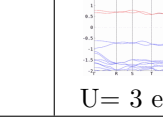
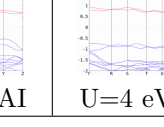
TAB. S132. Topology phase diagram of Ru3 Ba4 O10

BCS ID	Formula	ICSD	MSG	T.C.	Picture
0.693	Ru3 Ba4 O10		MSG 64.472 ($Cmc'a$)	None	
Topology	 U=0 eV AI	 U= 1 eV AI	 U= 2 eV AI	 U= 3 eV AI	 U=4 eV AI

TAB. S133. Topology phase diagram of Ru3 Ba4 O10

BCS ID	Formula	ICSD	MSG	T.C.	Picture
0.694	Bi2 Cu1 O4		MSG 130.431 ($P4/n'c'c'$)	None	
Topology	 U=0 eV AI	 U= 1 eV AI	 U= 2 eV AI	 U= 3 eV AI	 U=4 eV AI

TAB. S134. Topology phase diagram of Bi2 Cu1 O4

BCS ID	Formula	ICSD	MSG	T.C.	Picture
0.695	Bi2 Cu1 O4		MSG 56.367 ($Pc'cn$)	None	
Topology	 U=0 eV AI	 U= 1 eV AI	 U= 2 eV AI	 U= 3 eV AI	 U=4 eV AI

TAB. S135. Topology phase diagram of Bi2 Cu1 O4

BCS ID	Formula	ICSD	MSG	T.C.	Picture
			MSG 65.486 ($Cmm'm'$)		
0.699	Mn6 Sn6 Li1			None	

TAB. S136. Topology phase diagram of Mn6 Sn6 Li1

BCS ID	Formula	ICSD	MSG	T.C.	Picture
			MSG 194.268 ($P6'_3/m'm'c$)		
0.708	Nb4 Cr1 S8			η_{4I}	

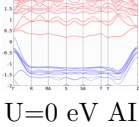
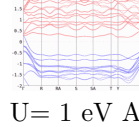
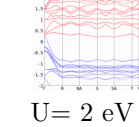
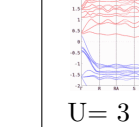
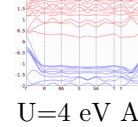
TAB. S137. Topology phase diagram of Nb4 Cr1 S8

BCS ID	Formula	ICSD	MSG	T.C.	Picture
			MSG 63.463 ($Cmc'm'$)	$\eta_{4I}z_{2I,1}z_{2I,2}\delta_{2m}z_{2m,\pi}^-z_{2m,\pi}^+$	
0.709	Nb4 Mn1 S8				

TAB. S138. Topology phase diagram of Nb4 Mn1 S8

BCS ID	Formula	ICSD	MSG	T.C.	Picture
			MSG 63.463 ($Cmc'm'$)	None	
0.711	Ta4 Mn1 S8				

TAB. S139. Topology phase diagram of Ta4 Mn1 S8

BCS ID	Formula	ICSD	MSG	T.C.	Picture
0.712	Nb3 V1 S6		MSG 20.33 ($C2'2'2_1$)	None	
Topology	 U=0 eV AI	 U= 1 eV AI	 U= 2 eV AI	 U= 3 eV AI	 U=4 eV AI

TAB. S140. Topology phase diagram of Nb3 V1 S6

BCS ID	Formula	ICSD	MSG	T.C.	Picture
0.714	Ni1 Li2 S2 O8		MSG 14.75 ($P2_1/c$)	η_{4I}	
Topology	 U=0 eV AI	 U= 1 eV AI	 U= 2 eV AI	 U= 3 eV AI	 U=4 eV AI

TAB. S141. Topology phase diagram of Ni1 Li2 S2 O8

BCS ID	Formula	ICSD	MSG	T.C.	Picture
0.722	Mn4 Nb2 O9		MSG 9.37 (Cc)	None	
Topology	 U=0 eV AI	 U= 1 eV AI	 U= 2 eV AI	 U= 3 eV AI	 U=4 eV AI

TAB. S142. Topology phase diagram of Mn4 Nb2 O9

BCS ID	Formula	ICSD	MSG	T.C.	Picture
0.724	Ba1 Co1 Si1 O4		MSG 173.129 ($P6_3$)	z_{3R}	
Topology	 U=0 eV AI	 U= 1 eV	 U= 2 eV	 U= 3 eV	 U=4 eV AI

TAB. S143. Topology phase diagram of Ba1 Co1 Si1 O4

BCS ID	Formula	ICSD	MSG	T.C.	Picture
0.726	Mn2 Cs1 F6		MSG 62.447 ($Pnm'a'$)	η_{4I}	
Topology	 U=0 eV AI	 U= 1 eV	 U= 2 eV	 U= 3 eV AI	 U=4 eV AI

TAB. S144. Topology phase diagram of Mn2 Cs1 F6

BCS ID	Formula	ICSD	MSG	T.C.	Picture
0.732	Sr1 Ru1 O3		MSG 62.446 ($Pn'm'a$)	None	
Topology	 U=0 eV AI	 U= 1 eV ES	 U= 2 eV ES	 U= 3 eV ES	 U=4 eV ES

TAB. S145. Topology phase diagram of Sr1 Ru1 O3

BCS ID	Formula	ICSD	MSG	T.C.	Picture
0.733	Ru1 Ag1 O3		MSG 167.106 ($R\bar{3}'c'$)	None	
Topology	 U=0 eV AI	 U= 1 eV AI	 U= 2 eV AI	 U= 3 eV AI	 U=4 eV AI

TAB. S146. Topology phase diagram of Ru1 Ag1 O3

BCS ID	Formula	ICSD	MSG	T.C.	Picture
0.735	La1 Ba1 Mn2 O5		MSG 129.417 ($P4/nm'm'$)	$\eta_{4I}z_{2I,3}z_{2R}z_{4R}z_2z_{4S}$	
Topology	 U=0 eV AI	 U= 1 eV AI	 U= 2 eV AI	 U= 3 eV AI	 U=4 eV AI

TAB. S147. Topology phase diagram of La1 Ba1 Mn2 O5

BCS ID	Formula	ICSD	MSG	T.C.	Picture
0.737	La1 Ba1 Mn2 O6		MSG 123.345 ($P4/mm'm'$)	None	
Topology	 U=0 eV ES	 U= 1 eV ES	 U= 2 eV ES	 U= 3 eV ES	 U=4 eV ES

TAB. S148. Topology phase diagram of La1 Ba1 Mn2 O6

BCS ID	Formula	ICSD	MSG	T.C.	Picture
0.738	La1 Ba1 Mn2 O6		MSG 123.345 ($P4/mm'm'$)	None	
Topology	 U=0 eV ES	 U= 1 eV ES	 U= 2 eV ES	 U= 3 eV ES	 U=4 eV ES

TAB. S149. Topology phase diagram of La1 Ba1 Mn2 O6

BCS ID	Formula	ICSD	MSG	T.C.	Picture
0.739	Y1 Ba1 Mn2 O5		MSG 129.417 ($P4/nm'm'$)	$\eta_{4I}z_{2I,3}z_{2R}z_{4R}z_2z_{4S}$	
Topology	 U=0 eV AI	 U= 1 eV AI	 U= 2 eV AI	 U= 3 eV AI	 U=4 eV AI

TAB. S150. Topology phase diagram of Y1 Ba1 Mn2 O5

BCS ID	Formula	ICSD	MSG	T.C.	Picture
0.747	Ba3 Co1 Ir2 O9		MSG 15.85 ($C2/c$)	$\eta_{4I}z_{2I,1}z_{2I,2}$	
Topology	 U=0 eV NLC (2, 1, 1)	 U= 1 eV OAI	 U= 2 eV ES	 U= 3 eV ES	 U=4 eV AI

TAB. S151. Topology phase diagram of Ba3 Co1 Ir2 O9

BCS ID	Formula	ICSD	MSG	T.C.	Picture
0.748	Ba3 Ni1 Ru2 O9		MSG 194.268 ($P6'_3/m'm'c$)	η_{4I}	
Topology	 U=0 eV AI	 U= 1 eV AI	 U= 2 eV AI	 U= 3 eV AI	 U=4 eV AI

TAB. S152. Topology phase diagram of Ba3 Ni1 Ru2 O9

BCS ID	Formula	ICSD	MSG	T.C.	Picture
0.755	Mn2 Se1 F2 O3		MSG 62.448 ($Pn'ma'$)	η_{4I}	
Topology	 U=0 eV AI	U= 1 eV	U= 2 eV	U= 3 eV	 U=4 eV AI

TAB. S153. Topology phase diagram of Mn2 Se1 F2 O3

BCS ID	Formula	ICSD	MSG	T.C.	Picture
0.756	Ga1 V4 S8		MSG 160.67 ($R3m'$)	None	
Topology	 U=0 eV AI U= 1 eV AI U= 2 eV AI U= 3 eV ES U=4 eV AI	U= 1 eV AI	U= 2 eV AI	U= 3 eV ES	U=4 eV AI

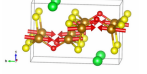
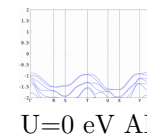
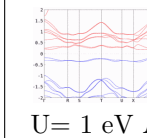
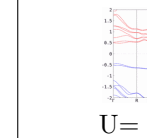
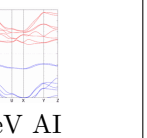
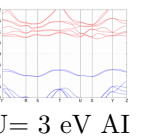
TAB. S154. Topology phase diagram of Ga1 V4 S8

BCS ID	Formula	ICSD	MSG	T.C.	Picture
0.760	Fe1 S1 O5 H1		MSG 15.89 ($C2'/c'$)	$\eta_{4I} z_{2I,1} z_{2I,2}$	
Topology	 U=0 eV AI U= 1 eV AI U= 2 eV AI U= 3 eV AI U=4 eV AI	U= 1 eV AI	U= 2 eV AI	U= 3 eV AI	U=4 eV AI

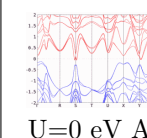
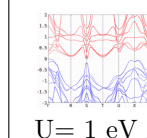
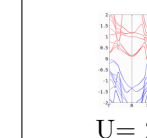
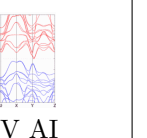
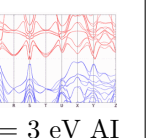
TAB. S155. Topology phase diagram of Fe1 S1 O5 H1

BCS ID	Formula	ICSD	MSG	T.C.	Picture
0.761	Sr1 Fe2 Se2 O1		MSG 59.411 ($Pm'm'n'$)	None	
Topology	 U=0 eV AI U= 1 eV AI U= 2 eV AI U= 3 eV AI U=4 eV AI	U= 1 eV AI	U= 2 eV AI	U= 3 eV AI	U=4 eV AI

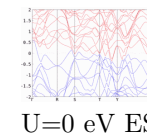
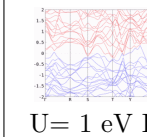
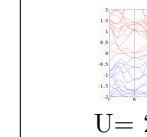
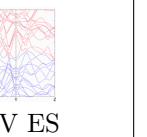
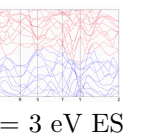
TAB. S156. Topology phase diagram of Sr1 Fe2 Se2 O1

BCS ID	Formula	ICSD	MSG	T.C.	Picture
	0.762 Sr1 Fe2 S2 O1		MSG 59.411 ($Pm'm'n'$)	None	
Topology	 U=0 eV AI	 U= 1 eV AI	 U= 2 eV AI	 U= 3 eV AI	 U=4 eV AI

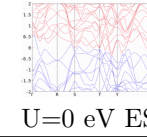
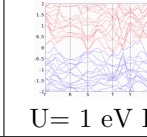
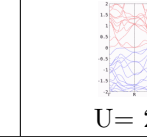
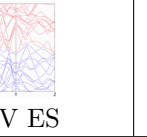
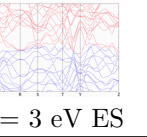
TAB. S157. Topology phase diagram of Sr1 Fe2 S2 O1

BCS ID	Formula	ICSD	MSG	T.C.	Picture
	0.768 Sr1 Mn1 Sb2		MSG 33.148 ($Pn'a'2_1$)	None	
Topology	 U=0 eV AI	 U= 1 eV AI	 U= 2 eV AI	 U= 3 eV AI	 U=4 eV AI

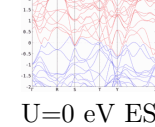
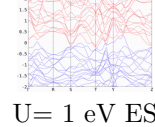
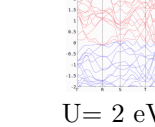
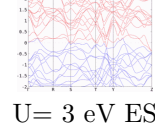
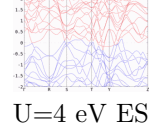
TAB. S158. Topology phase diagram of Sr1 Mn1 Sb2

BCS ID	Formula	ICSD	MSG	T.C.	Picture
	0.778 La1 Mn1 Si2		MSG 63.464 ($Cm'cm'$)	None	
Topology	 U=0 eV ES	 U= 1 eV ES	 U= 2 eV ES	 U= 3 eV ES	 U=4 eV ES

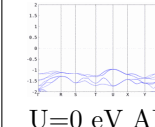
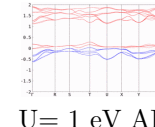
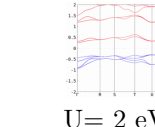
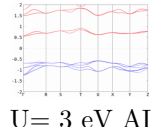
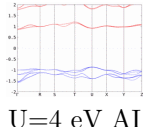
TAB. S159. Topology phase diagram of La1 Mn1 Si2

BCS ID	Formula	ICSD	MSG	T.C.	Picture
	0.779 La1 Mn1 Si2		MSG 63.464 ($Cm'cm'$)	None	
Topology	 U=0 eV ES	 U= 1 eV ES	 U= 2 eV ES	 U= 3 eV ES	 U=4 eV ES

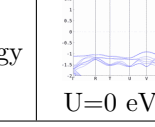
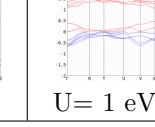
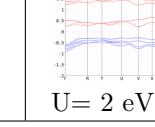
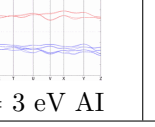
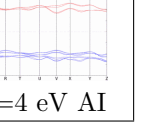
TAB. S160. Topology phase diagram of La1 Mn1 Si2

BCS ID	Formula	ICSD	MSG	T.C.	Picture
0.780	La1 Mn1 Si2		MSG 63.464 ($Cm'cm'$)	None	
Topology	 U=0 eV ES	 U= 1 eV ES	 U= 2 eV ES	 U= 3 eV ES	 U=4 eV ES

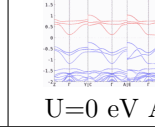
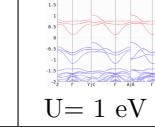
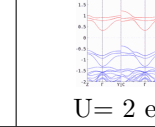
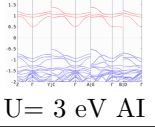
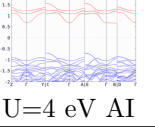
TAB. S161. Topology phase diagram of La1 Mn1 Si2

BCS ID	Formula	ICSD	MSG	T.C.	Picture
0.787	Y1 V1 O3		MSG 62.446 ($Pn'm'a$)	η_{4I}	
Topology	 U=0 eV AI	 U= 1 eV AI	 U= 2 eV AI	 U= 3 eV AI	 U=4 eV AI

TAB. S162. Topology phase diagram of Y1 V1 O3

BCS ID	Formula	ICSD	MSG	T.C.	Picture
0.788	Y1 V1 O3		MSG 2.4 ($P\bar{1}$)	$\eta_{4I}z_{2I,1}z_{2I,2}z_{2I,3}$	
Topology	 U=0 eV AI	 U= 1 eV AI	 U= 2 eV AI	 U= 3 eV AI	 U=4 eV AI

TAB. S163. Topology phase diagram of Y1 V1 O3

BCS ID	Formula	ICSD	MSG	T.C.	Picture
0.795	Sr2 Y1 Ru1 O6		MSG 14.75 ($P2_1/c$)	η_{4I}	
Topology	 U=0 eV AI	 U= 1 eV AI	 U= 2 eV AI	 U= 3 eV AI	 U=4 eV AI

TAB. S164. Topology phase diagram of Sr2 Y1 Ru1 O6

BCS ID	Formula	ICSD	MSG	T.C.	Picture
0.796	Ca2 Ni1 Os1 O6		MSG 14.79 ($P2_1'/c'$)	$\eta_{4I}z_{2I,1}$	
Topology	 U=0 eV AI	 U= 1 eV	 U= 2 eV AI	 U= 3 eV AI	 U=4 eV AI

TAB. S165. Topology phase diagram of Ca2 Ni1 Os1 O6

BCS ID	Formula	ICSD	MSG	T.C.	Picture
0.798	Mn1 Pd2		MSG 62.445 ($Pnma'$)	None	
Topology	 U=0 eV AI	 U= 1 eV AI	 U= 2 eV AI	 U= 3 eV AI	 U=4 eV AI

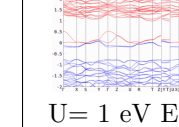
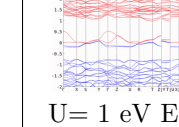
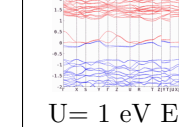
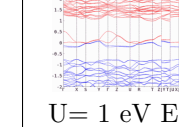
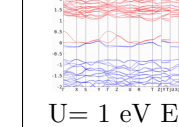
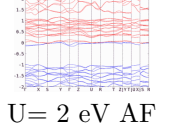
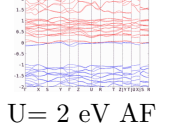
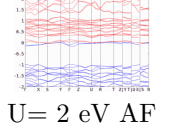
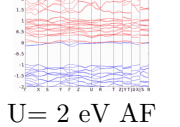
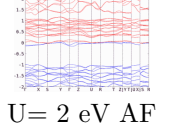
TAB. S166. Topology phase diagram of Mn1 Pd2

BCS ID	Formula	ICSD	MSG	T.C.	Picture
0.799	Sr2 Co2 O5		MSG 30.122 (P_{Inc2})	None	
Topology	 U=0 eV AI	 U= 1 eV	 U= 2 eV AI	 U= 3 eV AI	 U=4 eV AI

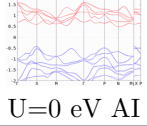
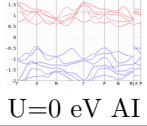
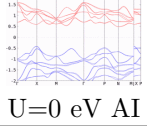
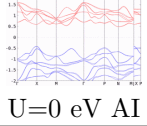
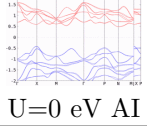
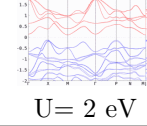
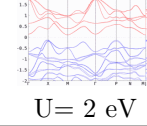
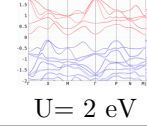
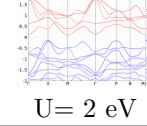
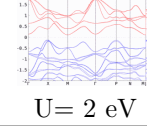
TAB. S167. Topology phase diagram of Sr2 Co2 O5

BCS ID	Formula	ICSD	MSG	T.C.	Picture
0.800	Mn1 Te1		MSG 63.457 ($Cmcm$)	$\eta_{4I}\delta_{2m}$	
Topology	 U=0 eV AI	 U= 1 eV AI	 U= 2 eV AI	 U= 3 eV AI	 U=4 eV AI

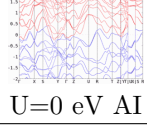
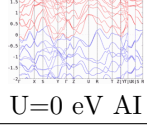
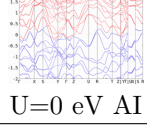
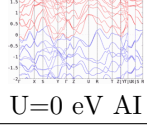
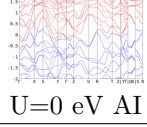
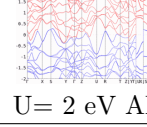
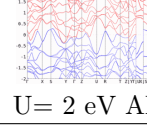
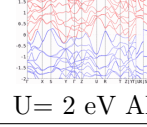
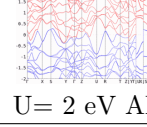
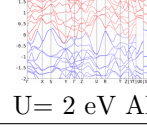
TAB. S168. Topology phase diagram of Mn1 Te1

BCS ID	Formula	ICSD	MSG	T.C.	Picture
0.801	Tl3 Fe2 S4		MSG 62.445 ($Pnma'$)	None	
Topology	U=0 eV U= 1 eV ES U= 2 eV AF U= 3 eV AF U=4 eV	    	    		

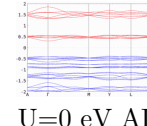
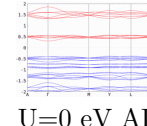
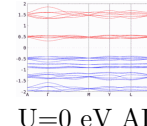
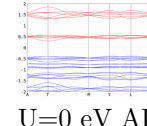
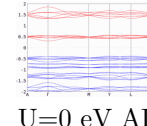
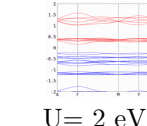
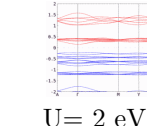
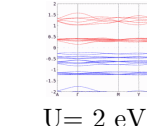
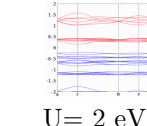
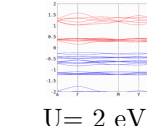
TAB. S169. Topology phase diagram of Tl3 Fe2 S4

BCS ID	Formula	ICSD	MSG	T.C.	Picture
0.802	Cu1 Fe1 S2		MSG 122.333 ($I\bar{4}2d$)	z_2	
Topology	U=0 eV AI U= 1 eV AI U= 2 eV U= 3 eV AI U=4 eV AI	    	    		

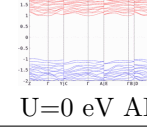
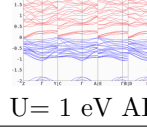
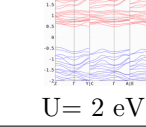
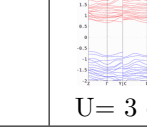
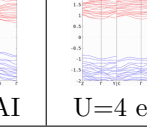
TAB. S170. Topology phase diagram of Cu1 Fe1 S2

BCS ID	Formula	ICSD	MSG	T.C.	Picture
0.803	Mn1 Nb1 P1		MSG 31.125 ($Pm'n2'_1$)	None	
Topology	U=0 eV AI U= 1 eV AI U= 2 eV AI U= 3 eV ES U=4 eV AI	    	    		

TAB. S171. Topology phase diagram of Mn1 Nb1 P1

BCS ID	Formula	ICSD	MSG	T.C.	Picture
0.804	Mo1 P3 Si1 O11		MSG 15.88 ($C2/c'$)	None	
Topology	U=0 eV AI U= 1 eV U= 2 eV AI U= 3 eV AI U=4 eV AI	    	    		

TAB. S172. Topology phase diagram of Mo1 P3 Si1 O11

BCS ID	Formula	ICSD	MSG	T.C.	Picture
0.809	W1 Fe2 O6		MSG 14.78 ($P2_1/c'$)	None	
Topology	 U=0 eV AI	 U= 1 eV AI	 U= 2 eV AI	 U= 3 eV AI	 U=4 eV AI

TAB. S173. Topology phase diagram of W1 Fe2 O6

BCS ID	Formula	ICSD	MSG	T.C.	Picture
0.810	Fe2 W1 O6		MSG 60.423 ($Pbc'n'$)	η_{4I}	
Topology	 U=0 eV AI	 U= 1 eV AI	 U= 2 eV AI	 U= 3 eV AI	 U=4 eV AI

TAB. S174. Topology phase diagram of Fe2 W1 O6

BCS ID	Formula	ICSD	MSG	T.C.	Picture
0.811	Fe2 W1 O6		MSG 60.423 ($Pbc'n'$)	η_{4I}	
Topology	 U=0 eV AI	 U= 1 eV AI	 U= 2 eV AI	 U= 3 eV AI	 U=4 eV AI

TAB. S175. Topology phase diagram of Fe2 W1 O6

BCS ID	Formula	ICSD	MSG	T.C.	Picture
0.812	Fe2 W1 O6		MSG 30.113 ($Pn'c2'$)	None	
Topology	 U=0 eV AI	 U= 1 eV AI	 U= 2 eV AI	 U= 3 eV AI	 U=4 eV AI

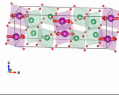
TAB. S176. Topology phase diagram of Fe2 W1 O6

BCS ID	Formula	ICSD	MSG	T.C.	Picture
0.813	Fe2 W1 O6		MSG 60.423 ($Pbc'n'$)	η_{4I}	
Topology	U=0 eV	 U= 1 eV AI	 U= 2 eV AI	 U= 3 eV AI	 U=4 eV AI

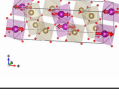
TAB. S177. Topology phase diagram of Fe2 W1 O6

BCS ID	Formula	ICSD	MSG	T.C.	Picture
0.814	Fe2 W1 O6		MSG 60.419 ($Pb'cn$)	None	
Topology	 U=0 eV AI	 U= 1 eV AI	 U= 2 eV AI	 U= 3 eV AI	 U=4 eV AI

TAB. S178. Topology phase diagram of Fe2 W1 O6

BCS ID	Formula	ICSD	MSG	T.C.	Picture
0.815	Mn1 Nb2 O6		MSG 60.419 ($Pb'cn$)	None	
Topology	 U=0 eV AI	 U= 1 eV AI	 U= 2 eV AI	 U= 3 eV AI	 U=4 eV AI

TAB. S179. Topology phase diagram of Mn1 Nb2 O6

BCS ID	Formula	ICSD	MSG	T.C.	Picture
0.816	Mn1 Ta2 O6		MSG 60.419 ($Pb'cn$)	None	
Topology	 U=0 eV AI	 U= 1 eV AI	 U= 2 eV AI	 U= 3 eV AI	 U=4 eV AI

TAB. S180. Topology phase diagram of Mn1 Ta2 O6

BCS ID	Formula	ICSD	MSG	T.C.	Picture
0.818	Mn1 Ta2 O6		MSG 60.419 ($Pb'cn$)	None	
Topology	 U=0 eV AI	 U= 1 eV AI	 U= 2 eV AI	 U= 3 eV AI	 U=4 eV AI

TAB. S181. Topology phase diagram of Mn1 Ta2 O6

BCS ID	Formula	ICSD	MSG	T.C.	Picture
0.819	Mn1 Nb2 O6		MSG 60.419 ($Pb'cn$)	None	
Topology	 U=0 eV AI	 U=1 eV AI	 U=2 eV AI	 U=3 eV AI	 U=4 eV AI

TAB. S182. Topology phase diagram of Mn1 Nb2 O6

BCS ID	Formula	ICSD	MSG	T.C.	Picture
0.823	Mn1 Sr2 Ga1 O5		MSG 46.243 ($Im'a2'$)	None	
Topology	 U=0 eV AI	 U=1 eV AI	 U=2 eV AI	 U=3 eV AI	 U=4 eV AI

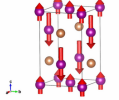
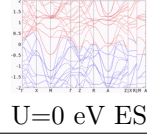
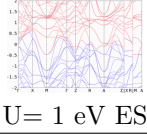
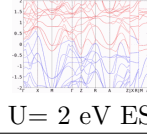
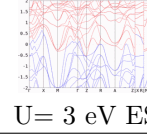
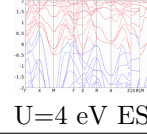
TAB. S183. Topology phase diagram of Mn1 Sr2 Ga1 O5

BCS ID	Formula	ICSD	MSG	T.C.	Picture
0.825	Ca2 Mn1 Ga1 O5		MSG 62.447 ($Pnm'a'$)	η_{4I}	
Topology	 U=0 eV AI	 U=1 eV AI	 U=2 eV AI	 U=3 eV AI	 U=4 eV AI

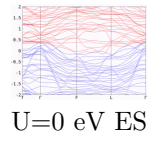
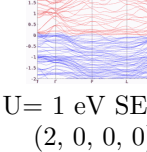
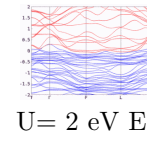
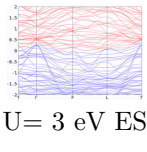
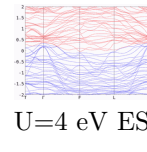
TAB. S184. Topology phase diagram of Ca2 Mn1 Ga1 O5

BCS ID	Formula	ICSD	MSG	T.C.	Picture
0.834	Cr1 Sb1 Se3		MSG 62.447 ($Pnm'a'$)	η_{4I}	
Topology	 U=0 eV AI	 U=1 eV AI	 U=2 eV AI	 U=3 eV AI	 U=4 eV AI

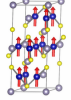
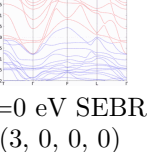
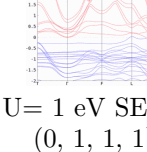
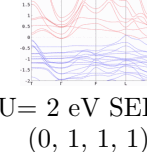
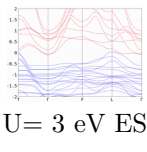
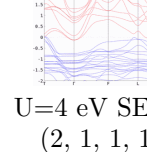
TAB. S185. Topology phase diagram of Cr1 Sb1 Se3

BCS ID	Formula	ICSD	MSG	T.C.	Picture
0.855	Mn2 Sb1		MSG 129.417 ($P4/nm'm'$)	None	
Topology	 U=0 eV ES	 U= 1 eV ES	 U= 2 eV ES	 U= 3 eV ES	 U=4 eV ES

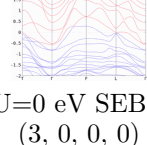
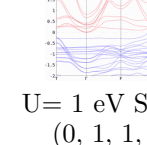
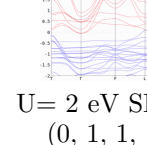
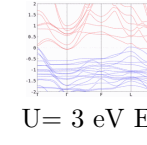
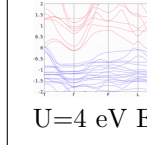
TAB. S186. Topology phase diagram of Mn2 Sb1

BCS ID	Formula	ICSD	MSG	T.C.	Picture
0.859	Y1 Co3		MSG 166.101 ($R\bar{3}m'$)	$\eta_{4I}z_{2I,1}z_{2I,2}z_{2I,3}$	
Topology	 U=0 eV SEBR (2, 0, 0, 0)	 U= 1 eV SEBR (2, 0, 0, 0)	 U= 2 eV SEBR (2, 0, 0, 0)	 U= 3 eV ES	 U=4 eV ES

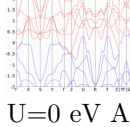
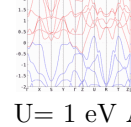
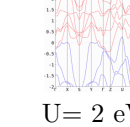
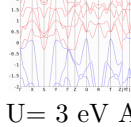
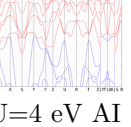
TAB. S187. Topology phase diagram of Y1 Co3

BCS ID	Formula	ICSD	MSG	T.C.	Picture
0.860	Sn2 Co3 S2		MSG 166.101 ($R\bar{3}m'$)	$\eta_{4I}z_{2I,1}z_{2I,2}z_{2I,3}$	
Topology	 U=0 eV SEBR (3, 0, 0, 0)	 U= 1 eV SEBR (0, 1, 1, 1)	 U= 2 eV SEBR (0, 1, 1, 1)	 U= 3 eV ES	 U=4 eV ES (2, 1, 1, 1)

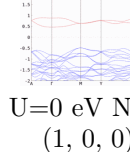
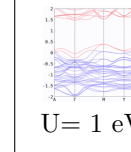
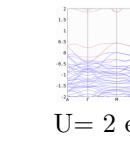
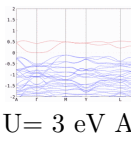
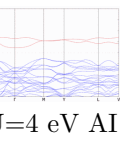
TAB. S188. Topology phase diagram of Sn2 Co3 S2

BCS ID	Formula	ICSD	MSG	T.C.	Picture
0.861	Sn2 Co3 S2		MSG 166.101 ($R\bar{3}m'$)	$\eta_{4I}z_{2I,1}z_{2I,2}z_{2I,3}$	
Topology	 U=0 eV SEBR (3, 0, 0, 0)	 U= 1 eV SEBR (0, 1, 1, 1)	 U= 2 eV SEBR (0, 1, 1, 1)	 U= 3 eV ES	 U=4 eV ES

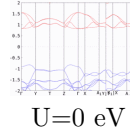
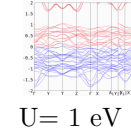
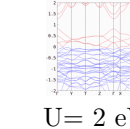
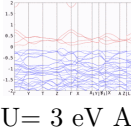
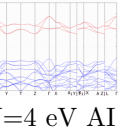
TAB. S189. Topology phase diagram of Sn2 Co3 S2

BCS ID	Formula	ICSD	MSG	T.C.	Picture
0.881	Mn1 Cu1 As1		MSG 59.407 ($Pm'mn$)	None	
Topology	 U=0 eV AI	 U= 1 eV AI	 U= 2 eV AI	 U= 3 eV AI	 U=4 eV AI

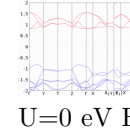
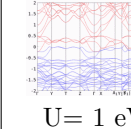
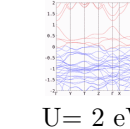
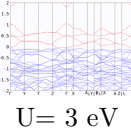
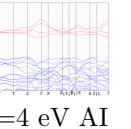
TAB. S190. Topology phase diagram of Mn1 Cu1 As1

BCS ID	Formula	ICSD	MSG	T.C.	Picture
0.891	Cu1 Cr2 O4		MSG 15.89 ($C2'/c'$)	$\eta_{4I}z_{2I,1}z_{2I,2}$	
Topology	 U=0 eV NLC (1, 0, 0)	 U= 1 eV AI	 U= 2 eV AI	 U= 3 eV AI	 U=4 eV AI

TAB. S191. Topology phase diagram of Cu1 Cr2 O4

BCS ID	Formula	ICSD	MSG	T.C.	Picture
0.892	Ni1 Cr2 O4		MSG 70.530 ($Fd'd'd$)	None	
Topology	 U=0 eV	 U= 1 eV ES	 U= 2 eV AI	 U= 3 eV AI	 U=4 eV AI

TAB. S192. Topology phase diagram of Ni1 Cr2 O4

BCS ID	Formula	ICSD	MSG	T.C.	Picture
0.893	Ni1 Cr2 O4		MSG 70.530 ($Fd'd'd$)	None	
Topology	 U=0 eV ES	 U= 1 eV	 U= 2 eV AI	 U= 3 eV	 U=4 eV AI

TAB. S193. Topology phase diagram of Ni1 Cr2 O4

BCS ID	Formula	ICSD	MSG	T.C.	Picture
0.896	Ni1 Cr1 O4		MSG 63.457 ($Cmcm$)	$\eta_{4I}\delta_{2m}$	
Topology	 U=0 eV AI	 U= 1 eV AI	 U= 2 eV AI	 U= 3 eV AI	 U=4 eV AI

TAB. S194. Topology phase diagram of Ni1 Cr1 O4

BCS ID	Formula	ICSD	MSG	T.C.	Picture
0.898	Mn3 Ir1 Si1		MSG 198.9 ($P2_13$)	None	
Topology	 U=0 eV AI	 U= 1 eV AI	 U= 2 eV AI	 U= 3 eV AI	 U=4 eV AI

TAB. S195. Topology phase diagram of Mn3 Ir1 Si1

BCS ID	Formula	ICSD	MSG	T.C.	Picture
0.899	Mn3 Ir1 Ge1		MSG 198.9 ($P2_13$)	None	
Topology	 U=0 eV AI	 U= 1 eV AI	 U= 2 eV AI	 U= 3 eV AF	 U=4 eV ES

TAB. S196. Topology phase diagram of Mn3 Ir1 Ge1

BCS ID	Formula	ICSD	MSG	T.C.	Picture
0.900	Mn3 Co1 Ge1		MSG 198.9 ($P2_13$)	None	
Topology	 U=0 eV AI	 U= 1 eV AI	 U= 2 eV AI	 U= 3 eV AI	 U=4 eV ES

TAB. S197. Topology phase diagram of Mn3 Co1 Ge1

BCS ID	Formula	ICSD	MSG	T.C.	Picture
0.916	Cd2 Os2 O7		MSG 227.131 ($Fd\bar{3}m'$)	η_{4I}	
Topology	 U=0 eV NLC (2)	 U= 1 eV AI	 U= 2 eV AI	 U= 3 eV AI	 U=4 eV AI

TAB. S198. Topology phase diagram of Cd2 Os2 O7

BCS ID	Formula	ICSD	MSG	T.C.	Picture
0.917	Sr2 Os1 Sc1 O6		MSG 14.75 ($P2_1/c$)	η_{4I}	
Topology	 U=0 eV AI	 U= 1 eV AI	 U= 2 eV AI	 U= 3 eV AI	 U=4 eV AI

TAB. S199. Topology phase diagram of Sr2 Os1 Sc1 O6

BCS ID	Formula	ICSD	MSG	T.C.	Picture
0.918	Ag2 Ru1 O4		MSG 62.444 ($Pnm'a$)	None	
Topology	 U=0 eV AI	 U= 1 eV AI	 U= 2 eV AI	 U= 3 eV AI	 U=4 eV AI

TAB. S200. Topology phase diagram of Ag2 Ru1 O4

BCS ID	Formula	ICSD	MSG	T.C.	Picture
0.924	Rb1 Ru1 O4		MSG 62.449 ($Pn'm'a'$)	None	
Topology	 U=0 eV AI	 U= 1 eV AI	 U= 2 eV AI	 U= 3 eV AI	 U=4 eV AI

TAB. S201. Topology phase diagram of Rb1 Ru1 O4

BCS ID	Formula	ICSD	MSG	T.C.	Picture
0.933	Ru1 Na2 O4		MSG 14.78 ($P2_1/c'$)	None	
Topology	 U=0 eV AI	 U= 1 eV AI	 U = 2 eV AI	 U= 3 eV AI	 U=4 eV AI

TAB. S202. Topology phase diagram of Ru1 Na2 O4

BCS ID	Formula	ICSD	MSG	T.C.	Picture
0.934	Sr2 O6 Ni1 Te1		MSG 14.75 ($P2_1/c$)	η_{4I}	
Topology	 U=0 eV AI	 U= 1 eV AI	 U = 2 eV AI	 U= 3 eV AI	 U=4 eV AI

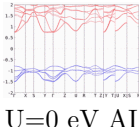
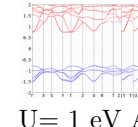
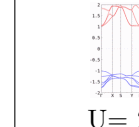
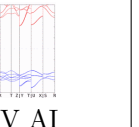
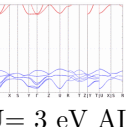
TAB. S203. Topology phase diagram of Sr2 O6 Ni1 Te1

BCS ID	Formula	ICSD	MSG	T.C.	Picture
0.936	Sr2 O6 Mn1 Te1		MSG 14.75 ($P2_1/c$)	η_{4I}	
Topology	 U=0 eV AI	 U= 1 eV AI	 U = 2 eV AI	 U= 3 eV AI	 U=4 eV AI

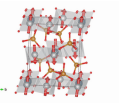
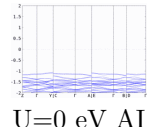
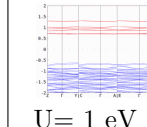
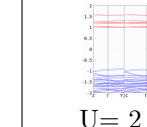
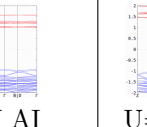
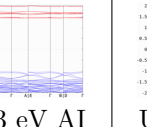
TAB. S204. Topology phase diagram of Sr2 O6 Mn1 Te1

BCS ID	Formula	ICSD	MSG	T.C.	Picture
0.937	Sr2 O6 Co1 Te1		MSG 14.75 ($P2_1/c$)	η_{4I}	
Topology	 U=0 eV AI	 U= 1 eV AI	 U = 2 eV AI	 U= 3 eV AI	 U=4 eV AI

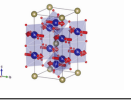
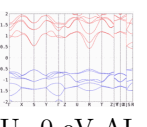
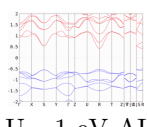
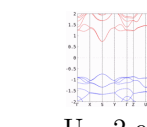
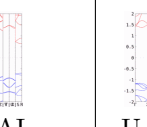
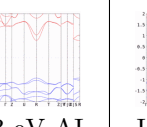
TAB. S205. Topology phase diagram of Sr2 O6 Co1 Te1

BCS ID	Formula	ICSD	MSG	T.C.	Picture
0.947	Cr1 Y1 O3		MSG 62.448 ($Pn'ma'$)	η_{4I}	
Topology	 U=0 eV AI	 U= 1 eV AI	 U= 2 eV AI	 U= 3 eV AI	 U=4 eV AI

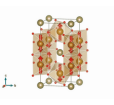
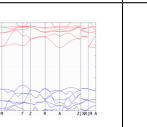
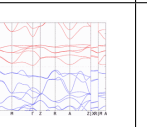
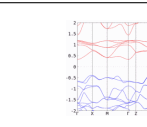
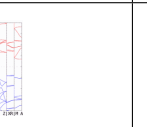
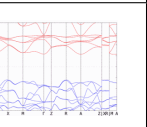
TAB. S206. Topology phase diagram of Cr1 Y1 O3

BCS ID	Formula	ICSD	MSG	T.C.	Picture
0.948	Ca1 Ni3 P4 O14		MSG 14.75 ($P2_1/c$)	η_{4I}	
Topology	 $U=0 \text{ eV AI}$  $U=1 \text{ eV AI}$  $U=2 \text{ eV AI}$  $U=3 \text{ eV AI}$  $U=4 \text{ eV AI}$				

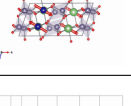
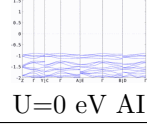
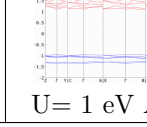
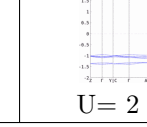
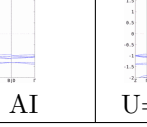
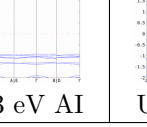
TAB. S207. Topology phase diagram of Ca1 Ni3 P4 O14

BCS ID	Formula	ICSD	MSG	T.C.	Picture
0.959	Cr2 Te1 O6		MSG 58.395 ($Pn'nm$)	<i>None</i>	
Topology	 $U=0 \text{ eV AI}$  $U=1 \text{ eV AI}$  $U=2 \text{ eV AI}$  $U=3 \text{ eV AI}$  $U=4 \text{ eV AI}$				

TAB. S208. Topology phase diagram of Cr2 Te1 O6

BCS ID	Formula	ICSD	MSG	T.C.	Picture
0.960	Fe2 Te1 O6		MSG 136.503 ($P4_2/m'n'm'$)	<i>None</i>	
Topology	 $U=0 \text{ eV AI}$  $U=1 \text{ eV AI}$  $U=2 \text{ eV AI}$  $U=3 \text{ eV AI}$  $U=4 \text{ eV AI}$				

TAB. S209. Topology phase diagram of Fe2 Te1 O6

BCS ID	Formula	ICSD	MSG	T.C.	Picture
0.961	Li1 Cr1 Ge2 O6		MSG 14.77 ($P2'_1/c$)	<i>None</i>	
Topology	 $U=0 \text{ eV AI}$  $U=1 \text{ eV AI}$  $U=2 \text{ eV AI}$  $U=3 \text{ eV AI}$  $U=4 \text{ eV AI}$				

TAB. S210. Topology phase diagram of Li1 Cr1 Ge2 O6

BCS ID	Formula	ICSD	MSG	T.C.	Picture
0.962	Li1 Cr1 Ge2 O6		MSG 14.77 ($P2'_1/c$)	None	
Topology	 U=0 eV AI	 U=1 eV AI	 U=2 eV AI	 U=3 eV AI	 U=4 eV AI

TAB. S211. Topology phase diagram of Li1 Cr1 Ge2 O6

BCS ID	Formula	ICSD	MSG	T.C.	Picture
0.963	Li1 Cr1 Ge2 O6		MSG 14.77 ($P2'_1/c$)	None	
Topology	 U=0 eV AI	 U=1 eV AI	 U=2 eV AI	 U=3 eV AI	 U=4 eV AI

TAB. S212. Topology phase diagram of Li1 Cr1 Ge2 O6

BCS ID	Formula	ICSD	MSG	T.C.	Picture
0.964	Li1 Cr1 Ge2 O6		MSG 14.77 ($P2'_1/c$)	None	
Topology	 U=0 eV AI	 U=1 eV AI	 U=2 eV AI	 U=3 eV AI	 U=4 eV AI

TAB. S213. Topology phase diagram of Li1 Cr1 Ge2 O6

BCS ID	Formula	ICSD	MSG	T.C.	Picture
0.965	Lu1 Fe2 O4		MSG 1.3 (P_S1)	None	
Topology	 U=0 eV AI	 U=1 eV AI	 U=2 eV AI	 U=3 eV AI	 U=4 eV AI

TAB. S214. Topology phase diagram of Lu1 Fe2 O4

BCS ID	Formula	ICSD	MSG	T.C.	Picture	
0.966	W1 V2 O6		MSG 58.395 ($Pn'nm$)	None		
Topology	U=0 eV					

TAB. S215. Topology phase diagram of W1 V2 O6

BCS ID	Formula	ICSD	MSG	T.C.	Picture	
0.968	Fe2 Ca1 O4		MSG 62.448 ($Pn'ma'$)	η_{4I}		
Topology	U=0 eV AI					

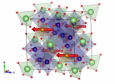
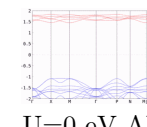
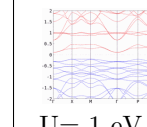
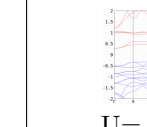
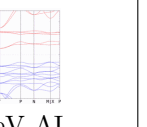
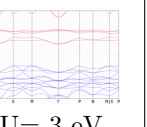
TAB. S216. Topology phase diagram of Fe2 Ca1 O4

BCS ID	Formula	ICSD	MSG	T.C.	Picture	
0.969	Fe2 Ca1 O4		MSG 62.445 ($Pnma'$)	None		
Topology	U=0 eV AI					

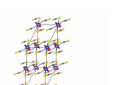
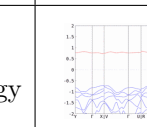
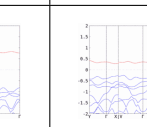
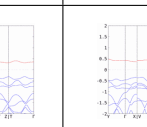
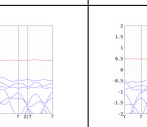
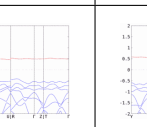
TAB. S217. Topology phase diagram of Fe2 Ca1 O4

BCS ID	Formula	ICSD	MSG	T.C.	Picture	
0.984	V1 Lu1 O3		MSG 62.446 ($Pn'm'a$)	η_{4I}		
Topology	U=0 eV AI					

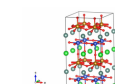
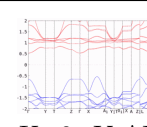
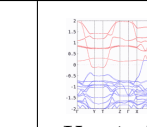
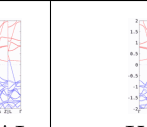
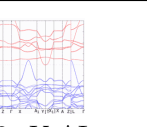
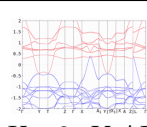
TAB. S218. Topology phase diagram of V1 Lu1 O3

BCS ID	Formula	ICSD	MSG	T.C.	Picture
1.277	Li1 Fe1 Cr4 O8		MSG 119.319 ($I\bar{4}m'2'$)	$\delta_{2S}z_2z_{4S}$	
Topology	 $U=0 \text{ eV AI}$  $U=1 \text{ eV AI}$  $U=2 \text{ eV AI}$  $U=3 \text{ eV}$  $U=4 \text{ eV}$				

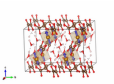
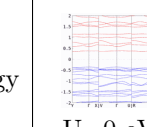
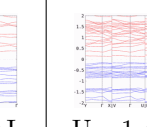
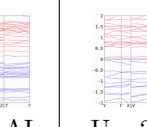
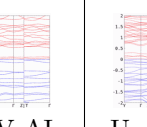
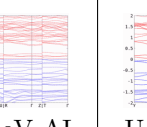
TAB. S219. Topology phase diagram of Li1 Fe1 Cr4 O8

BCS ID	Formula	ICSD	MSG	T.C.	Picture
1.278	Cu1 C2 N2 S2		MSG 2.7 ($P_S\bar{1}$)	η_{4I}	
Topology	 $U=0 \text{ eV AI}$  $U=1 \text{ eV AI}$  $U=2 \text{ eV AI}$  $U=3 \text{ eV}$  $U=4 \text{ eV}$				

TAB. S220. Topology phase diagram of Cu1 C2 N2 S2

BCS ID	Formula	ICSD	MSG	T.C.	Picture
1.281	Y1 Ba1 Fe1 Cu1 O5		MSG 42.223 (F_{Smm2})	<i>None</i>	
Topology	 $U=0 \text{ eV AI}$  $U=1 \text{ eV AI}$  $U=2 \text{ eV AI}$  $U=3 \text{ eV AI}$  $U=4 \text{ eV AI}$				

TAB. S221. Topology phase diagram of Y1 Ba1 Fe1 Cu1 O5

BCS ID	Formula	ICSD	MSG	T.C.	Picture
1.286	Fe1 C3 O8 H4		MSG 2.7 ($P_S\bar{1}$)	η_{4I}	
Topology	 $U=0 \text{ eV AI}$  $U=1 \text{ eV AI}$  $U=2 \text{ eV AI}$  $U=3 \text{ eV AI}$  $U=4 \text{ eV AI}$				

TAB. S222. Topology phase diagram of Fe1 C3 O8 H4

BCS ID	Formula	ICSD	MSG	T.C.	Picture
1.287	V2 O3		MSG 14.84 (P_C2_1/c)	η_{4I}	
Topology	 U=0 eV NLC (2)	 U= 1 eV AI	 U= 2 eV AI	 U= 3 eV	 U=4 eV

TAB. S223. Topology phase diagram of V2 O3

BCS ID	Formula	ICSD	MSG	T.C.	Picture
1.304	Mg1 Mn1 O3		MSG 2.7 ($P_S\bar{1}$)	η_{4I}	
Topology	 U=0 eV AI	 U= 1 eV AI	 U= 2 eV AI	 U= 3 eV	 U=4 eV

TAB. S224. Topology phase diagram of Mg1 Mn1 O3

BCS ID	Formula	ICSD	MSG	T.C.	Picture
1.305	Mn5 Si3		MSG 60.431 (P_Cbcn)	η_{4I}	
Topology	 U=0 eV NLC (2)	 U= 1 eV OAI	 U= 2 eV ES	 U= 3 eV OAI	 U=4 eV OAI

TAB. S225. Topology phase diagram of Mn5 Si3

BCS ID	Formula	ICSD	MSG	T.C.	Picture
1.308	Mn1 Bi2 Te4		MSG 167.108 ($R_I\bar{3}c$)	η_{4I}	
Topology	 U=0 eV SEBR (2)	 U= 1 eV SEBR (2)	 U= 2 eV SEBR (2)	 U= 3 eV SEBR (2)	 U=4 eV SEBR (2)

TAB. S226. Topology phase diagram of Mn1 Bi2 Te4

BCS ID	Formula	ICSD	MSG	T.C.	Picture
1.311	Ba1 Mo1 P2 O8		MSG 2.7 ($P_S\bar{1}$)	η_{4I}	
Topology	 U=0 eV AI	 U= 1 eV AI	 U= 2 eV AI	 U= 3 eV AI	 U=4 eV AI

TAB. S227. Topology phase diagram of Ba1 Mo1 P2 O8

BCS ID	Formula	ICSD	MSG	T.C.	Picture
1.314	Na1 Fe1 Si2 O6		MSG 14.84 (P_C2_1/c)	η_{4I}	
Topology	 U=0 eV AI	 U= 1 eV AI	 U= 2 eV AI	 U= 3 eV AI	 U=4 eV AI

TAB. S228. Topology phase diagram of Na1 Fe1 Si2 O6

BCS ID	Formula	ICSD	MSG	T.C.	Picture
1.319	Sr2 Ru1 O4		MSG 63.466 ($C_c mcm$)	None	
Topology	 U=0 eV OAI	 U= 1 eV ES	 U= 2 eV ES	 U= 3 eV AI	 U=4 eV AI

TAB. S229. Topology phase diagram of Sr2 Ru1 O4

BCS ID	Formula	ICSD	MSG	T.C.	Picture
1.321	Ba2 Fe1 W1 O6		MSG 2.7 ($P_S\bar{1}$)	η_{4I}	
Topology	 U=0 eV AI	 U= 1 eV AI	 U= 2 eV AI	 U= 3 eV AI	 U=4 eV AI

TAB. S230. Topology phase diagram of Ba2 Fe1 W1 O6

BCS ID	Formula	ICSD	MSG	T.C.	Picture	
1.323	Co1 Ge1 O3		MSG 14.84 (P_C2_1/c)	η_{4I}		
Topology	U=0 eV NLC (2)					

TAB. S231. Topology phase diagram of Co1 Ge1 O3

BCS ID	Formula	ICSD	MSG	T.C.	Picture	
1.345	Na1 Mn1 F4		MSG 14.80 (P_a2_1/c)	η_{4I}		
Topology	U=0 eV AI					

TAB. S232. Topology phase diagram of Na1 Mn1 F4

BCS ID	Formula	ICSD	MSG	T.C.	Picture	
1.347	Cu1 Fe1 O2		MSG 15.91 (C_a2/c)	η_{4I}		
Topology	U=0 eV OAI					

TAB. S233. Topology phase diagram of Cu1 Fe1 O2

BCS ID	Formula	ICSD	MSG	T.C.	Picture	
1.351	Ba2 Co2 Cl1 F7		MSG 11.55 (P_a2_1/m)	η_{4I}		
Topology	U=0 eV					

TAB. S234. Topology phase diagram of Ba2 Co2 Cl1 F7

BCS ID	Formula	ICSD	MSG	T.C.	Picture
1.370	Li2 Cu1 O2		MSG 58.404 (P_{Innm})	$\eta_{4I}\delta_{2m}$	
Topology	 U=0 eV AI	 U= 1 eV AI	 U= 2 eV AI	 U= 3 eV	 U=4 eV

TAB. S235. Topology phase diagram of Li2 Cu1 O2

BCS ID	Formula	ICSD	MSG	T.C.	Picture
1.383	Fe1 Ca2 O3 Br1		MSG 113.273 ($P_C\bar{4}2_1m$)	z_2	
Topology	 U=0 eV AI	 U= 1 eV AI	 U= 2 eV AI	 U= 3 eV	 U=4 eV SEBR (1)

TAB. S236. Topology phase diagram of Fe1 Ca2 O3 Br1

BCS ID	Formula	ICSD	MSG	T.C.	Picture
1.495	Y1 Mn2 Si2		MSG 126.386 (P_I4/nnc)	None	
Topology	 U=0 eV ESFD	 U= 1 eV ESFD	 U= 2 eV ESFD	 U= 3 eV ESFD	 U=4 eV ESFD

TAB. S237. Topology phase diagram of Y1 Mn2 Si2

BCS ID	Formula	ICSD	MSG	T.C.	Picture
1.496	Y1 Mn2 Ge2		MSG 126.386 (P_I4/nnc)	None	
Topology	 U=0 eV ESFD	 U= 1 eV ESFD	 U= 2 eV ESFD	 U= 3 eV ESFD	 U=4 eV ESFD

TAB. S238. Topology phase diagram of Y1 Mn2 Ge2

BCS ID	Formula	ICSD	MSG	T.C.	Picture
1.498	Cu1 Si1 O4 H2		MSG 148.20 ($R_I\bar{3}$)	η_{4I}	
Topology	U=0 eV				
	U= 1 eV AI		U= 2 eV AI	U= 3 eV AI	U=4 eV AI

TAB. S239. Topology phase diagram of Cu1 Si1 O4 H2

BCS ID	Formula	ICSD	MSG	T.C.	Picture	
1.499	Cs1 Fe1 Mo2 O8		MSG 143.3 (P_c3)	None		
Topology	U=0 eV	U= 1 eV	U= 2 eV	U= 3 eV		U=4 eV AI

TAB. S240. Topology phase diagram of Cs1 Fe1 Mo2 O8

BCS ID	Formula	ICSD	MSG	T.C.	Picture	
1.500	Co1 Cu2 S2 Sr2 O2		MSG 2.7 ($P_S\bar{1}$)	η_{4I}		
Topology	U=0 eV	U= 1 eV AI U= 2 eV AI U= 3 eV AI U= 4 eV AI	U= 1 eV AI U= 2 eV AI U= 3 eV AI U= 4 eV AI	U= 2 eV U= 3 eV		U=4 eV AI

TAB. S241. Topology phase diagram of Co1 Cu2 S2 Sr2 O2

BCS ID	Formula	ICSD	MSG	T.C.	Picture
1.508	Al1 B2 Mn2		MSG 63.466 ($C_c mcm$)	$\eta_{4I}\delta_{2m}$	
Topology	U=0 eV SEBR (2, 1) U= 1 eV OAI	U= 1 eV OAI	U= 2 eV	U= 3 eV	U= 4 eV SEBR (2, 1)

TAB. S242. Topology phase diagram of Al1 B2 Mn2

BCS ID	Formula	ICSD	MSG	T.C.	Picture
1.519	Co1 S1 O4		MSG 60.431 ($P_C bcn$)	η_{4I}	
Topology	U=0 eV AI U= 1 eV AI U= 2 eV AI U= 3 eV AI U= 4 eV AI	U= 1 eV AI U= 2 eV AI U= 3 eV AI U= 4 eV AI	U= 2 eV U= 3 eV	U= 4 eV AI	

TAB. S243. Topology phase diagram of Co1 S1 O4

BCS ID	Formula	ICSD	MSG	T.C.	Picture	
1.520	Ni1 S1 O4		MSG 60.431 (P_Cbcn)	η_{4I}		
Topology	U=0 eV					

TAB. S244. Topology phase diagram of Ni1 S1 O4

BCS ID	Formula	ICSD	MSG	T.C.	Picture	
1.521	Fe1 S1 O4		MSG 60.431 (P_Cbcn)	η_{4I}		
Topology	U=0 eV					

TAB. S245. Topology phase diagram of Fe1 S1 O4

BCS ID	Formula	ICSD	MSG	T.C.	Picture	
1.522	Cr1 V1 O4		MSG 2.4 ($P\bar{1}$)	$\eta_{4I}z_{2I,1}z_{2I,2}z_{2I,3}$		
Topology	U=0 eV AI					

TAB. S246. Topology phase diagram of Cr1 V1 O4

BCS ID	Formula	ICSD	MSG	T.C.	Picture	
1.523	V1 P1 O4		MSG 62.452 (P_cnma)	η_{4I}		
Topology	U=0 eV					

TAB. S247. Topology phase diagram of V1 P1 O4

BCS ID	Formula	ICSD	MSG	T.C.	Picture
1.524	In1 Mn1 O3		MSG 159.64 (P_c31c)	None	
Topology	 U=0 eV	 U= 1 eV AI	 U= 2 eV AI	 U= 3 eV AI	 U=4 eV

TAB. S248. Topology phase diagram of In1 Mn1 O3

BCS ID	Formula	ICSD	MSG	T.C.	Picture
1.528	Fe4 Bi2 O9		MSG 12.64 (C_a2/m)	$\eta_{4I}\delta_{2m}$	
Topology	 U=0 eV AI	 U= 1 eV AI	 U= 2 eV AI	 U= 3 eV AI	 U=4 eV AI

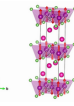
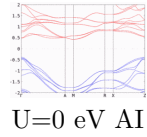
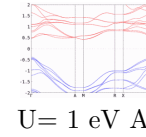
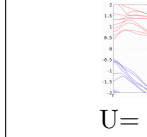
TAB. S249. Topology phase diagram of Fe4 Bi2 O9

BCS ID	Formula	ICSD	MSG	T.C.	Picture
1.538	Mn1 Ba2 Te1 O6		MSG 14.83 (P_A2_1/c)	η_{4I}	
Topology	 U=0 eV AI	 U= 1 eV AI	 U= 2 eV AI	 U= 3 eV AI	 U=4 eV AI

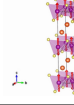
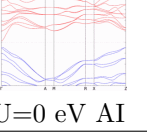
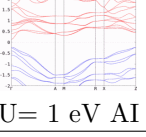
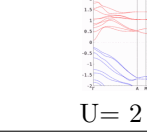
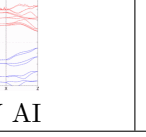
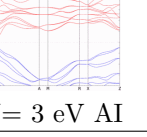
TAB. S250. Topology phase diagram of Mn1 Ba2 Te1 O6

BCS ID	Formula	ICSD	MSG	T.C.	Picture
1.542	Mn1 Rb1 P1		MSG 138.528 (P_c4_2/nmc)	$\eta_{4I}z_2$	
Topology	 U=0 eV AI	 U= 1 eV	 U= 2 eV	 U= 3 eV AI	 U=4 eV

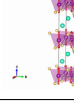
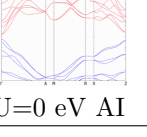
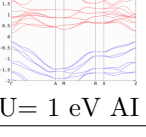
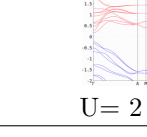
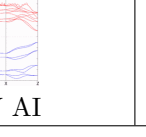
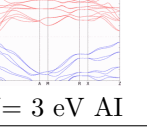
TAB. S251. Topology phase diagram of Mn1 Rb1 P1

BCS ID	Formula	ICSD	MSG	T.C.	Picture
1.544	Mn1 Rb1 As1		MSG 138.528 (P_c4_2/ncm)	$\eta_{4I}z_2$	
Topology	 U=0 eV AI	 U= 1 eV AI	 U= 2 eV AI	U= 3 eV	U=4 eV

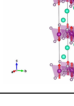
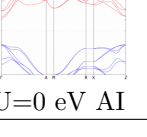
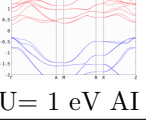
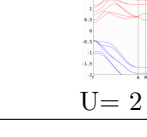
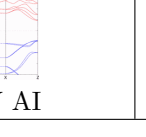
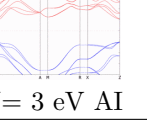
TAB. S252. Topology phase diagram of Mn1 Rb1 As1

BCS ID	Formula	ICSD	MSG	T.C.	Picture
1.545	Mn1 Rb1 Bi1		MSG 138.528 (P_c4_2/ncm)	$\eta_{4I}z_2$	
Topology	 U=0 eV AI	 U= 1 eV AI	 U= 2 eV AI	 U= 3 eV AI	 U=4 eV AI

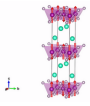
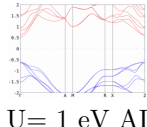
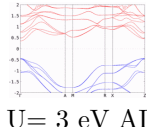
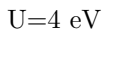
TAB. S253. Topology phase diagram of Mn1 Rb1 Bi1

BCS ID	Formula	ICSD	MSG	T.C.	Picture
1.546	Mn1 Cs1 Bi1		MSG 138.528 (P_c4_2/ncm)	$\eta_{4I}z_2$	
Topology	 U=0 eV AI	 U= 1 eV AI	 U= 2 eV AI	 U= 3 eV AI	 U=4 eV AI

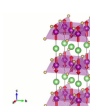
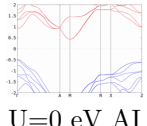
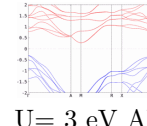
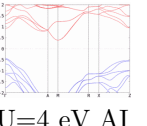
TAB. S254. Topology phase diagram of Mn1 Cs1 Bi1

BCS ID	Formula	ICSD	MSG	T.C.	Picture
1.547	Mn1 Cs1 P1		MSG 138.528 (P_c4_2/ncm)	$\eta_{4I}z_2$	
Topology	 U=0 eV AI	 U= 1 eV AI	 U= 2 eV AI	 U= 3 eV AI	 U=4 eV AI

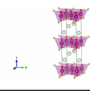
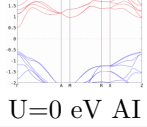
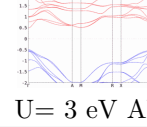
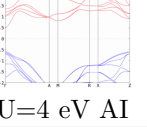
TAB. S255. Topology phase diagram of Mn1 Cs1 P1

BCS ID	Formula	ICSD	MSG	T.C.	Picture
1.548	Mn1 Cs1 P1		MSG 138.528 (P_c4_2/ncm)	$\eta_{4I}z_2$	
Topology	U=0 eV		U= 2 eV		U=4 eV 

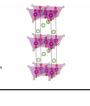
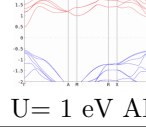
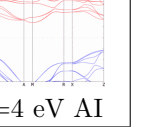
TAB. S256. Topology phase diagram of Mn1 Cs1 P1

BCS ID	Formula	ICSD	MSG	T.C.	Picture
1.550	Mn1 Li1 As1		MSG 138.528 (P_c4_2/ncm)	$\eta_{4I}z_2$	
Topology	U=0 eV AI		U= 2 eV		U=3 eV AI  U=4 eV AI

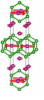
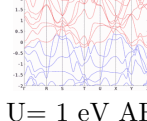
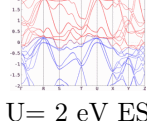
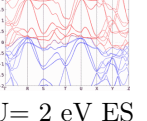
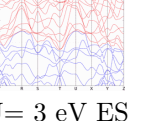
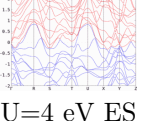
TAB. S257. Topology phase diagram of Mn1 Li1 As1

BCS ID	Formula	ICSD	MSG	T.C.	Picture
1.553	Mn1 K1 As1		MSG 138.528 (P_c4_2/ncm)	$\eta_{4I}z_2$	
Topology	U=0 eV AI		U= 2 eV		U=3 eV AI  U=4 eV AI

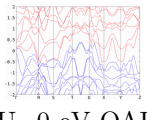
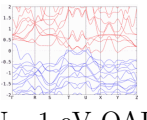
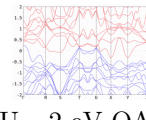
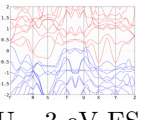
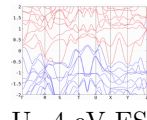
TAB. S258. Topology phase diagram of Mn1 K1 As1

BCS ID	Formula	ICSD	MSG	T.C.	Picture
1.554	Mn1 K1 As1		MSG 138.528 (P_c4_2/ncm)	$\eta_{4I}z_2$	
Topology	U=0 eV		U= 2 eV AI	U= 3 eV	U=4 eV AI 

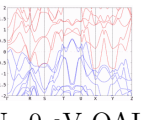
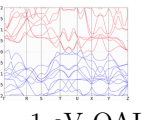
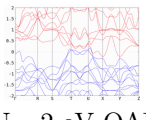
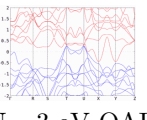
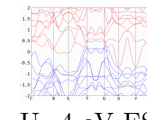
TAB. S259. Topology phase diagram of Mn1 K1 As1

BCS ID	Formula	ICSD	MSG	T.C.	Picture					
1.555	Mn3 B4		MSG 58.404 (P_{Innm})	None						
Topology	U=0 eV			U= 1 eV AF		U= 2 eV ES		U= 3 eV ES		U= 4 eV ES

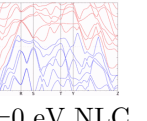
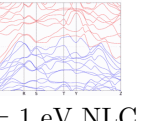
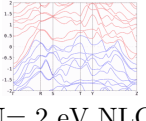
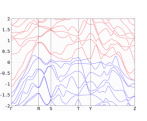
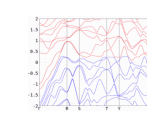
TAB. S260. Topology phase diagram of Mn3 B4

BCS ID	Formula	ICSD	MSG	T.C.	Picture					
1.556	Fe1 Sn2		MSG 60.432 (P_{Ibcn})	None						
Topology	U=0 eV OAI			U= 1 eV OAI		U= 2 eV OAI		U= 3 eV ES		U= 4 eV ES

TAB. S261. Topology phase diagram of Fe1 Sn2

BCS ID	Formula	ICSD	MSG	T.C.	Picture					
1.557	Fe1 Ge2		MSG 60.432 (P_{Ibcn})	None						
Topology	U=0 eV OAI			U= 1 eV OAI		U= 2 eV OAI		U= 3 eV ES		U= 4 eV ES

TAB. S262. Topology phase diagram of Fe1 Ge2

BCS ID	Formula	ICSD	MSG	T.C.	Picture					
1.558	Mn1 Sn2		MSG 68.520 (C_{Acca})	$\eta_{4I}\eta'_{2I}$						
Topology	U=0 eV NLC (2, 1)			U= 1 eV NLC (2, 1)		U= 2 eV NLC (2, 1)		U= 3 eV OAI		U= 4 eV OAI

TAB. S263. Topology phase diagram of Mn1 Sn2

BCS ID	Formula	ICSD	MSG	T.C.	Picture
1.559	Mn1 Sn2		MSG 66.498 ($C_c ccm$)	None	
Topology	 U=0 eV ES	U= 1 eV	 U= 2 eV ES	 U= 3 eV ES	 U=4 eV OAI

TAB. S264. Topology phase diagram of Mn1 Sn2

BCS ID	Formula	ICSD	MSG	T.C.	Picture
1.560	Ge1 Ni2 O4		MSG 12.63 ($C_c 2/m$)	$\eta_{4I}\delta_{2m}$	
Topology	 U=0 eV SEBR (2, 1)	 U= 1 eV	 U= 2 eV AI	 U= 3 eV AI	 U=4 eV AI

TAB. S265. Topology phase diagram of Ge1 Ni2 O4

BCS ID	Formula	ICSD	MSG	T.C.	Picture
1.561	Ge1 Ni2 O4		MSG 8.35 ($C_c m$)	None	
Topology	 U=0 eV AI	 U= 1 eV AI	 U= 2 eV AI	 U= 3 eV AI	 U=4 eV AI

TAB. S266. Topology phase diagram of Ge1 Ni2 O4

BCS ID	Formula	ICSD	MSG	T.C.	Picture
1.562	Ge1 Ni2 O4		MSG 5.16 ($C_c 2$)	None	
Topology	 U=0 eV AI	 U= 1 eV AI	 U= 2 eV AI	 U= 3 eV AI	 U=4 eV

TAB. S267. Topology phase diagram of Ge1 Ni2 O4

BCS ID	Formula	ICSD	MSG	T.C.	Picture
1.563	Ge1 Ni2 O4		MSG 8.35 (C_{cm})	None	
Topology	 U=0 eV AI	 U= 1 eV AI	 U= 2 eV AI	 U= 3 eV AI	 U=4 eV AI

TAB. S268. Topology phase diagram of Ge1 Ni2 O4

BCS ID	Formula	ICSD	MSG	T.C.	Picture
1.569	Sr1 Ru2 O6		MSG 162.78 ($P_c\bar{3}1m$)	η_{4I}	
Topology	 U=0 eV AI	 U= 1 eV AI	 U= 2 eV AI	 U= 3 eV AI	 U=4 eV AI

TAB. S269. Topology phase diagram of Sr1 Ru2 O6

BCS ID	Formula	ICSD	MSG	T.C.	Picture
1.580	Ni1 Ti1 O3		MSG 2.7 ($P_S\bar{1}$)	η_{4I}	
Topology	 U=0 eV AI	 U= 1 eV AI	 U= 2 eV AI	 U= 3 eV AI	 U=4 eV AI

TAB. S270. Topology phase diagram of Ni1 Ti1 O3

BCS ID	Formula	ICSD	MSG	T.C.	Picture
1.593	Ba1 Co1 S1 O1		MSG 57.386 (P_abcm)	$\eta_{4I}\eta'_{2I}$	
Topology	 U=0 eV AI	 U= 1 eV	 U= 2 eV	 U= 3 eV	 U=4 eV AI

TAB. S271. Topology phase diagram of Ba1 Co1 S1 O1

BCS ID	Formula	ICSD	MSG	T.C.	Picture
1.594	Ba1 Co1 S1 O1		MSG 57.386 ($P_a b c m$)	$\eta_{4I}\eta'_{2I}$	
Topology	 U=0 eV AI	U= 1 eV	U= 2 eV	U= 3 eV	 U=4 eV AI

TAB. S272. Topology phase diagram of Ba1 Co1 S1 O1

BCS ID	Formula	ICSD	MSG	T.C.	Picture
1.617	Mo2 Fe1 Li1 O8		MSG 2.7 ($P_S\bar{1}$)	η_{4I}	
Topology	 U=0 eV AI	U= 1 eV	U= 2 eV	U= 3 eV	 U=4 eV AI

TAB. S273. Topology phase diagram of Mo2 Fe1 Li1 O8

BCS ID	Formula	ICSD	MSG	T.C.	Picture
1.619	Mn1 S1		MSG 12.63 (C_c2/m)	$\eta_{4I}\delta_{2m}$	
Topology	 U=0 eV AI	 U= 1 eV AI	 U= 2 eV AI	 U= 3 eV AI	 U=4 eV AI

TAB. S274. Topology phase diagram of Mn1 S1

BCS ID	Formula	ICSD	MSG	T.C.	Picture
1.625	Sr2 Fe3 S2 O3		MSG 62.451 (P_bnma)	η_{4I}	
Topology	 U=0 eV AI	U= 1 eV	U= 2 eV	U= 3 eV	 U=4 eV AI

TAB. S275. Topology phase diagram of Sr2 Fe3 S2 O3

BCS ID	Formula	ICSD	MSG	T.C.	Picture
1.629	Fe1 Ge1		MSG 192.252 (P_c6/mcc)	None	
Topology	 U=0 eV ES	 U= 1 eV ES	 U= 2 eV ES	 U= 3 eV ES	 U=4 eV AF

TAB. S276. Topology phase diagram of Fe1 Ge1

BCS ID	Formula	ICSD	MSG	T.C.	Picture
1.630	Lu1 Mn6 Sn6		MSG 63.466 ($C_c mcm$)	$\eta_{4I}\delta_{2m}$	
Topology	 U=0 eV AF	 U= 1 eV AF	 U= 2 eV ES	 U= 3 eV OAI	 U=4 eV SEBR (2, 1)

TAB. S277. Topology phase diagram of Lu1 Mn6 Sn6

BCS ID	Formula	ICSD	MSG	T.C.	Picture
1.641	Ba2 Fe1 Si2 O7		MSG 36.177 ($C_c mc2_1$)	None	
Topology	 U=0 eV AI	 U= 1 eV AI	 U= 2 eV AI	 U= 3 eV AI	 U=4 eV AI

TAB. S278. Topology phase diagram of Ba2 Fe1 Si2 O7

BCS ID	Formula	ICSD	MSG	T.C.	Picture
1.649	Sr3 Zn1 O6 Ir1		MSG 13.74 (P_C2/c)	η_{4I}	
Topology	 U=0 eV AI	 U= 1 eV AI	 U= 2 eV AI	 U= 3 eV AI	 U=4 eV AI

TAB. S279. Topology phase diagram of Sr3 Zn1 O6 Ir1

BCS ID	Formula	ICSD	MSG	T.C.	Picture
1.653	Fe1 W1 O4		MSG 13.70 (P_a2/c)	η_{4I}	
Topology	 U=0 eV OAI	 U= 1 eV AI	 U= 2 eV AI	 U= 3 eV AI	 U=4 eV AI

TAB. S280. Topology phase diagram of Fe1 W1 O4

BCS ID	Formula	ICSD	MSG	T.C.	Picture
1.661	La2 Ni1 Ir1 O6		MSG 2.7 ($P_S\bar{1}$)	η_{4I}	
Topology	 U=0 eV AI	 U= 1 eV AI	 U= 2 eV AI	 U= 3 eV AI	 U=4 eV AI

TAB. S281. Topology phase diagram of La2 Ni1 Ir1 O6

BCS ID	Formula	ICSD	MSG	T.C.	Picture
1.662	La2 Ni1 Ir1 O6		MSG 2.7 ($P_S\bar{1}$)	η_{4I}	
Topology	 U=0 eV AI	 U= 1 eV AI	 U= 2 eV AI	 U= 3 eV AI	 U=4 eV AI

TAB. S282. Topology phase diagram of La2 Ni1 Ir1 O6

BCS ID	Formula	ICSD	MSG	T.C.	Picture
1.678	Cr1 N1		MSG 62.450 ($P_a nma$)	η_{4I}	
Topology	 U=0 eV SEBR (2)	 U= 1 eV AI	 U= 2 eV AI	 U= 3 eV AI	 U=4 eV AI

TAB. S283. Topology phase diagram of Cr1 N1

BCS ID	Formula	ICSD	MSG	T.C.	Picture
1.689	Lu1 Mn2 Ge2		MSG 126.386 (P_I4/nnc)	None	
Topology	 U=0 eV ESFD	 U= 1 eV ESFD	 U= 2 eV ESFD	 U= 3 eV ESFD	 U=4 eV ESFD

TAB. S284. Topology phase diagram of Lu1 Mn2 Ge2

BCS ID	Formula	ICSD	MSG	T.C.	Picture
1.691	Mn2 Y1 Ge2		MSG 126.386 (P_I4/nnc)	None	
Topology	 U=0 eV ESFD	 U= 1 eV ESFD	 U= 2 eV ESFD	 U= 3 eV ESFD	 U=4 eV ESFD

TAB. S285. Topology phase diagram of Mn2 Y1 Ge2

BCS ID	Formula	ICSD	MSG	T.C.	Picture
1.692	Mn2 Y1 Ge2		MSG 126.386 (P_I4/nnc)	None	
Topology	 U=0 eV ESFD	 U= 1 eV ESFD	 U= 2 eV ESFD	 U= 3 eV ESFD	 U=4 eV ESFD

TAB. S286. Topology phase diagram of Mn2 Y1 Ge2

BCS ID	Formula	ICSD	MSG	T.C.	Picture
1.702	Ba1 Y1 Co2 O5		MSG 65.489 (C_ammm)	$\eta_{4I}\delta_{2m}z_{2m,\pi}^-z_{2m,\pi}^+z_2w, 3z_4\eta'_{2I}$	
Topology	 U=0 eV SEBR (0, 0, 1, 1, 1, 2, 0)	 U= 1 eV AF	 U= 2 eV AF	 U= 3 eV AF	 U=4 eV SEBR (0, 0, 1, 1, 1, 2, 0)

TAB. S287. Topology phase diagram of Ba1 Y1 Co2 O5

BCS ID	Formula	ICSD	MSG	T.C.	Picture
1.703	Ba1 Y1 Co2 O5		MSG 53.330 ($P_a mna$)	$\eta_{4I}\delta_{2m}$	
Topology	 U=0 eV AI	 U= 1 eV AI	 U= 2 eV AI	 U= 3 eV AI	 U=4 eV AI

TAB. S288. Topology phase diagram of Ba1 Y1 Co2 O5

BCS ID	Formula	ICSD	MSG	T.C.	Picture
1.706	Ba2 Mn1 Te1 O6		MSG 64.480 ($C_A mca$)	$\eta_{4I} \delta_{2m}$	
Topology	 				

TAB. S289. Topology phase diagram of Ba2 Mn1 Te1 O6

BCS ID	Formula	ICSD	MSG	T.C.	Picture
1.708	Cr1 P1 S4		MSG 5.16 ($C_c 2$)	<i>None</i>	
Topology	 				

TAB. S290. Topology phase diagram of Cr1 P1 S4

BCS ID	Formula	ICSD	MSG	T.C.	Picture
1.709	Cs1 Cr1 F4		MSG 46.247 ($I_a ma2$)	<i>None</i>	
Topology	 				

TAB. S291. Topology phase diagram of Cs1 Cr1 F4

BCS ID	Formula	ICSD	MSG	T.C.	Picture
1.715	Sr2 Co1 W1 O6		MSG 2.7 ($P_S \bar{1}$)	η_{4I}	
Topology	 				

TAB. S292. Topology phase diagram of Sr2 Co1 W1 O6

BCS ID	Formula	ICSD	MSG	T.C.	Picture
1.716	Sr2 Mn1 Mo1 O6		MSG 14.80 (P_a2_1/c)	η_{4I}	
Topology	 U=0 eV AI	 U=1 eV AI	 U=2 eV AI	 U=3 eV AI	U=4 eV

TAB. S293. Topology phase diagram of Sr2 Mn1 Mo1 O6

BCS ID	Formula	ICSD	MSG	T.C.	Picture
1.717	Sr2 Mn1 W1 O6		MSG 14.80 (P_a2_1/c)	η_{4I}	
Topology	 U=0 eV AI	 U=1 eV AI	 U=2 eV AI	 U=3 eV AI	U=4 eV

TAB. S294. Topology phase diagram of Sr2 Mn1 W1 O6

BCS ID	Formula	ICSD	MSG	T.C.	Picture
1.718	Ca2 Mn1 W1 O6		MSG 2.7 ($P_S\bar{1}$)	η_{4I}	
Topology	 U=0 eV AI	 U=1 eV AI	 U=2 eV AI	 U=3 eV AI	U=4 eV

TAB. S295. Topology phase diagram of Ca2 Mn1 W1 O6

BCS ID	Formula	ICSD	MSG	T.C.	Picture
1.719	Ca2 Mn1 W1 O6		MSG 2.7 ($P_S\bar{1}$)	η_{4I}	
Topology	 U=0 eV AI	 U=1 eV AI	 U=2 eV AI	 U=3 eV AI	 U=4 eV AI

TAB. S296. Topology phase diagram of Ca2 Mn1 W1 O6

BCS ID	Formula	ICSD	MSG	T.C.	Picture
1.724	Ba2 Ni1 Te1 O6		MSG 14.83 (P_{A21}/c)	η_{4I}	
Topology	 U=0 eV AI	 U= 1 eV AI	 U= 2 eV AI	 U= 3 eV AI	 U=4 eV AI

TAB. S297. Topology phase diagram of Ba2 Ni1 Te1 O6

BCS ID	Formula	ICSD	MSG	T.C.	Picture
1.726	Ru1 Cl3		MSG 5.16 (C_c2)	None	
Topology	 U=0 eV AI	 U= 1 eV AI	 U= 2 eV AI	 U= 3 eV AI	 U=4 eV AI

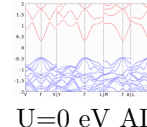
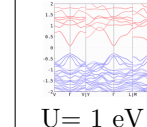
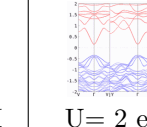
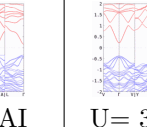
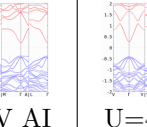
TAB. S298. Topology phase diagram of Ru1 Cl3

BCS ID	Formula	ICSD	MSG	T.C.	Picture
1.730	Cu2 Mn1 Si1 S4		MSG 7.27 ($P_a c$)	None	
Topology	 U=0 eV AI	 U= 1 eV AI	 U= 2 eV AI	 U= 3 eV AI	 U=4 eV AI

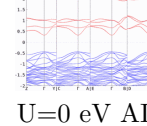
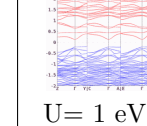
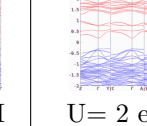
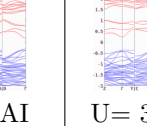
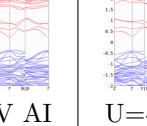
TAB. S299. Topology phase diagram of Cu2 Mn1 Si1 S4

BCS ID	Formula	ICSD	MSG	T.C.	Picture
1.731	Cu2 Fe1 Si1 S4		MSG 9.41 ($C_a c$)	None	
Topology	 U=0 eV AI	 U= 1 eV AI	 U= 2 eV AI	 U= 3 eV AI	 U=4 eV AI

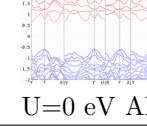
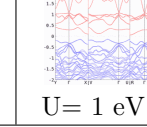
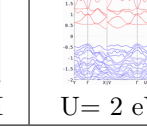
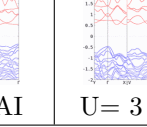
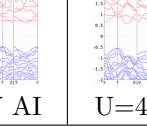
TAB. S300. Topology phase diagram of Cu2 Fe1 Si1 S4

BCS ID	Formula	ICSD	MSG	T.C.	Picture
1.732	Mn1 Sn1 Cu2 S4		MSG 5.16 (C_c2)	None	
Topology	 U=0 eV AI	 U= 1 eV AI	 U= 2 eV AI	 U= 3 eV AI	 U=4 eV AI

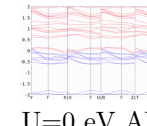
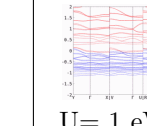
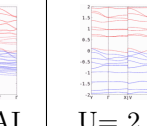
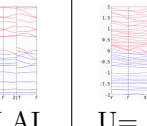
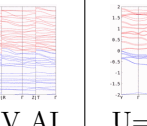
TAB. S301. Topology phase diagram of Mn1 Sn1 Cu2 S4

BCS ID	Formula	ICSD	MSG	T.C.	Picture
1.733	Ge1 Mn1 Cu2 S4		MSG 7.27 (P_{ac})	None	
Topology	 U=0 eV AI	 U= 1 eV AI	 U= 2 eV AI	 U= 3 eV AI	 U=4 eV AI

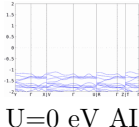
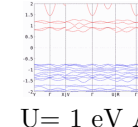
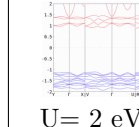
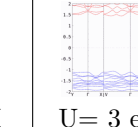
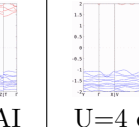
TAB. S302. Topology phase diagram of Ge1 Mn1 Cu2 S4

BCS ID	Formula	ICSD	MSG	T.C.	Picture
1.734	Fe1 Ge1 Cu2 S4		MSG 1.3 (P_S1)	None	
Topology	 U=0 eV AI	 U= 1 eV AI	 U= 2 eV AI	 U= 3 eV AI	 U=4 eV AI

TAB. S303. Topology phase diagram of Fe1 Ge1 Cu2 S4

BCS ID	Formula	ICSD	MSG	T.C.	Picture
1.736	Co1 S2 O8 N4 H10		MSG 2.7 ($P_{S\bar{1}}$)	η_{4I}	
Topology	 U=0 eV AI	 U= 1 eV AI	 U= 2 eV AI	 U= 3 eV AI	 U=4 eV AI

TAB. S304. Topology phase diagram of Co1 S2 O8 N4 H10

BCS ID	Formula	ICSD	MSG	T.C.	Picture
1.741	Ni1 K1 As1 O4		MSG 2.7 ($P_S\bar{1}$)	η_{4I}	
Topology	 U=0 eV AI	 U= 1 eV AI	 U= 2 eV AI	 U= 3 eV AI	 U=4 eV AI

TAB. S305. Topology phase diagram of Ni1 K1 As1 O4

BCS ID	Formula	ICSD	MSG	T.C.	Picture
1.742	Ni1 K1 As1 O4		MSG 2.7 ($P_S\bar{1}$)	η_{4I}	
Topology	 U=0 eV AI	 U= 1 eV AI	 U= 2 eV AI	 U= 3 eV AI	 U=4 eV AI

TAB. S306. Topology phase diagram of Ni1 K1 As1 O4

BCS ID	Formula	ICSD	MSG	T.C.	Picture
1.745	Co3 La2		MSG 61.439 (P_Cbca)	None	
Topology	 U=0 eV ES	 U= 1 eV ES	 U= 2 eV ES	 U= 3 eV ES	 U=4 eV OAI

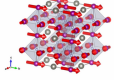
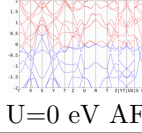
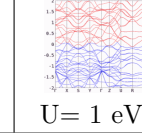
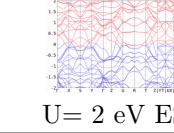
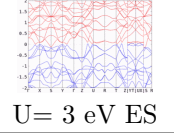
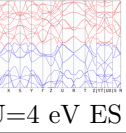
TAB. S307. Topology phase diagram of Co3 La2

BCS ID	Formula	ICSD	MSG	T.C.	Picture
1.746	Mn2 Y1		MSG 4.12 (P_C2_1)	None	
Topology	 U=0 eV AI	 U= 1 eV AI	 U= 2 eV AI	 U= 3 eV AI	 U=4 eV AI

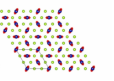
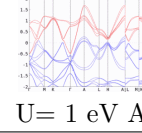
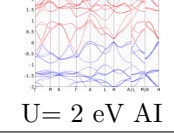
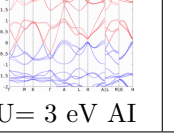
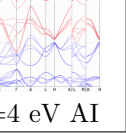
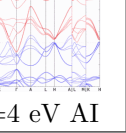
TAB. S308. Topology phase diagram of Mn2 Y1

BCS ID	Formula	ICSD	MSG	T.C.	Picture
1.752	Cs1 Co2 Mo2 O9 H1		MSG 11.55 (P_a2_1/m)	η_{4I}	
Topology	 U=0 eV AI	 U= 1 eV AI	 U= 2 eV NLC (2)	 U= 3 eV AI	 U=4 eV

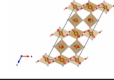
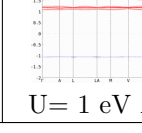
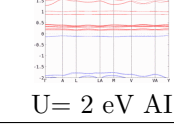
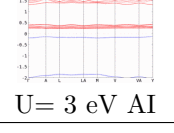
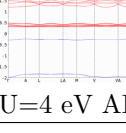
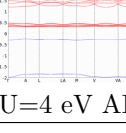
TAB. S309. Topology phase diagram of Cs1 Co2 Mo2 O9 H1

BCS ID	Formula	ICSD	MSG	T.C.	Picture
2.31	Mn3 Zn1 N1		MSG 60.432 ($P_I bcn$)	None	
Topology	 U=0 eV AF	 U= 1 eV ES	 U= 2 eV ES	 U= 3 eV ES	 U=4 eV ES

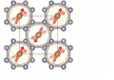
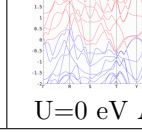
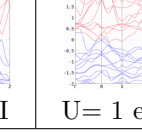
TAB. S310. Topology phase diagram of Mn3 Zn1 N1

BCS ID	Formula	ICSD	MSG	T.C.	Picture
2.35	Cr1 Se1		MSG 157.55 ($P31m'$)	z_{3R}	
Topology	 U=0 eV	 U= 1 eV AI	 U= 2 eV AI	 U= 3 eV AI	 U=4 eV AI

TAB. S311. Topology phase diagram of Cr1 Se1

BCS ID	Formula	ICSD	MSG	T.C.	Picture
2.61	Fe3 F8 O2 H4		MSG 12.62 ($C2'/m'$)	$\eta_{4I} z_{2I,1} z_{2I,2} z_{2I,3}$	
Topology	 U=0 eV	 U= 1 eV AI	 U= 2 eV AI	 U= 3 eV AI	 U=4 eV AI

TAB. S312. Topology phase diagram of Fe3 F8 O2 H4

BCS ID	Formula	ICSD	MSG	T.C.	Picture
2.66	Fe1 Sn2		MSG 68.513 ($Cc'ca$)	None	
Topology	 U=0 eV AI	 U= 1 eV AI	U= 2 eV	U= 3 eV	U=4 eV

TAB. S313. Topology phase diagram of Fe1 Sn2

BCS ID	Formula	ICSD	MSG	T.C.	Picture
2.68	Ge2 Fe1		MSG 56.367 ($Pc'cn$)	None	
Topology	 U=0 eV AI	 U= 1 eV AI		U= 2 eV U= 3 eV U=4 eV	

TAB. S314. Topology phase diagram of Ge2 Fe1

BCS ID	Formula	ICSD	MSG	T.C.	Picture
2.93	Co1 Cr1 O4		MSG 60.417 ($Pbcn$)	η_{4I}	
Topology	 U=0 eV AI	 U= 1 eV AI	 U= 2 eV AI	 U= 3 eV AI	 U=4 eV AI

TAB. S315. Topology phase diagram of Co1 Cr1 O4

BCS ID	Formula	ICSD	MSG	T.C.	Picture
3.24	Ca1 Fe3 Ti4 O12		MSG 148.17 ($R\bar{3}$)	$\eta_{4I}z_{2I,1}z_{2I,2}z_{2I,3}$	
Topology	 U=0 eV AI	 U= 1 eV	 U= 2 eV AI	 U= 3 eV AI	 U=4 eV AI

TAB. S316. Topology phase diagram of Ca1 Fe3 Ti4 O12

BCS ID	Formula	ICSD	MSG	T.C.	Picture
0.237	Er2 Sn2 O7		MSG 141.555 ($I4'_1/AMD'$)	$\eta_{4I}\delta_{2m}$	
Topology					

TAB. S317. Topology phase diagram of Er2 Sn2 O7

BCS ID	Formula	ICSD	MSG	T.C.	Picture
0.238	Er2 Sn2 O7		MSG 141.555 ($I4'_1/AMD'$)	$\eta_{4I}\delta_{2m}$	
Topology					

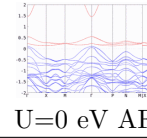
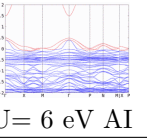
TAB. S318. Topology phase diagram of Er2 Sn2 O7

BCS ID	Formula	ICSD	MSG	T.C.	Picture
0.320	U2 Pd2 In1		MSG 127.394 ($P4'/m'bm'$)	None	
Topology					

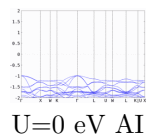
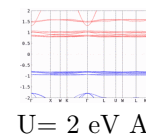
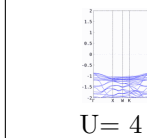
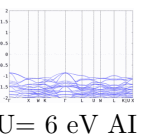
TAB. S319. Topology phase diagram of U2 Pd2 In1

BCS ID	Formula	ICSD	MSG	T.C.	Picture
0.321	U2 Sn1 Pd2		MSG 127.394 ($P4'/m'bm'$)	z_2	
Topology					

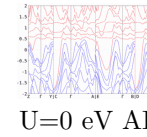
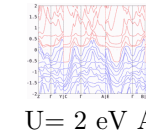
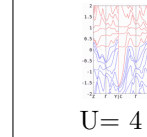
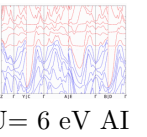
TAB. S320. Topology phase diagram of U2 Sn1 Pd2

BCS ID	Formula	ICSD	MSG	T.C.	Picture
0.324	Cd1 Yb2 S4		MSG 141.551 ($I4_1/AMD$)	$\eta_{4I}\delta_{2m}z_2\eta'_{2I}$	
Topology	 U=0 eV AF	U= 2 eV	U= 4 eV	 U= 6 eV AI	

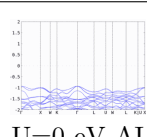
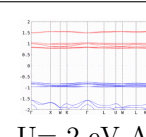
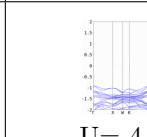
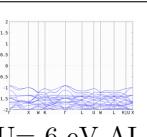
TAB. S321. Topology phase diagram of Cd1 Yb2 S4

BCS ID	Formula	ICSD	MSG	T.C.	Picture
0.326	Nd2 Sn2 O7		MSG 227.131 ($Fd\bar{3}m'$)	η_{4I}	
Topology	 U=0 eV AI	 U= 2 eV AI	 U= 4 eV AI	 U= 6 eV AI	

TAB. S322. Topology phase diagram of Nd2 Sn2 O7

BCS ID	Formula	ICSD	MSG	T.C.	Picture
0.330	Er1 Ge3		MSG 11.53 ($P2_1/m'$)	None	
Topology	 U=0 eV AI	 U= 2 eV AI	 U= 4 eV AI	 U= 6 eV AI	

TAB. S323. Topology phase diagram of Er1 Ge3

BCS ID	Formula	ICSD	MSG	T.C.	Picture
0.339	Nd2 Hf2 O7		MSG 227.131 ($Fd\bar{3}m'$)	η_{4I}	
Topology	 U=0 eV AI	 U= 2 eV AI	 U= 4 eV AI	 U= 6 eV AI	

TAB. S324. Topology phase diagram of Nd2 Hf2 O7

BCS ID	Formula	ICSD	MSG	T.C.	Picture
0.340	Nd ₂ Zr ₂ O ₇		MSG 227.131 ($Fd\bar{3}m'$)	η_{4I}	
Topology	 U=0 eV AI	 U= 2 eV AI	 U= 4 eV AI	 U= 6 eV AI	

TAB. S325. Topology phase diagram of Nd₂ Zr₂ O₇

BCS ID	Formula	ICSD	MSG	T.C.	Picture
0.343	Tb ₁ Ge ₂		MSG 65.483 ($Cm'mm$)	None	
Topology	 U=0 eV AI	 U= 2 eV AI	 U= 4 eV AI	 U= 6 eV AI	

TAB. S326. Topology phase diagram of Tb₁ Ge₂

BCS ID	Formula	ICSD	MSG	T.C.	Picture
0.350	Tb ₁ Al ₁ O ₃		MSG 62.449 ($Pn'm'a'$)	None	
Topology	 U=0 eV ES	 U= 2 eV AI	 U= 4 eV AI	 U= 6 eV AI	

TAB. S327. Topology phase diagram of Tb₁ Al₁ O₃

BCS ID	Formula	ICSD	MSG	T.C.	Picture
0.410	Gd ₁ Al ₁ O ₃		MSG 62.449 ($Pn'm'a'$)	None	
Topology	 U=0 eV AI	 U= 2 eV AI	 U= 4 eV AI	 U= 6 eV AI	

TAB. S328. Topology phase diagram of Gd₁ Al₁ O₃

BCS ID	Formula	ICSD	MSG	T.C.	Picture
0.525	Ce1 Na1 O2		MSG 141.556 ($I4'_1/a'm'd$)	z_2	
Topology					

TAB. S329. Topology phase diagram of Ce1 Na1 O2

BCS ID	Formula	ICSD	MSG	T.C.	Picture
0.527	Er2 Si2 O7		MSG 12.60 ($C2'/m$)	None	
Topology					

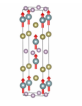
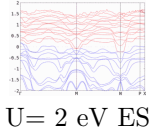
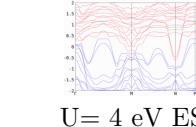
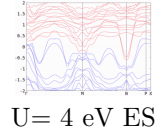
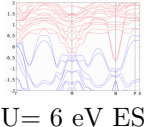
TAB. S330. Topology phase diagram of Er2 Si2 O7

BCS ID	Formula	ICSD	MSG	T.C.	Picture
0.593	U1 Se1 P1		MSG 129.417 ($P4/nm'm'$)	$\eta_{4I}z_{2I,3}z_{2R}z_{4R}z_2z_{4S}$	
Topology					

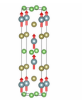
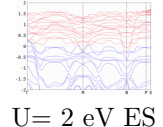
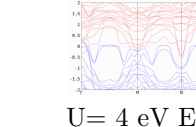
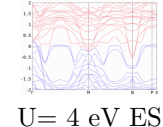
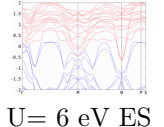
TAB. S331. Topology phase diagram of U1 Se1 P1

BCS ID	Formula	ICSD	MSG	T.C.	Picture
0.594	U1 S1 As1		MSG 129.417 ($P4/nm'm'$)	$\eta_{4I}z_{2I,3}z_{2R}z_{4R}z_2z_{4S}$	
Topology					

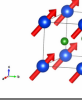
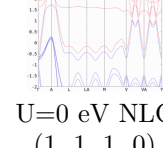
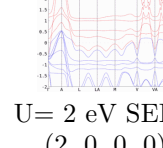
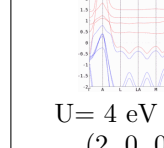
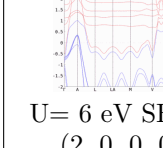
TAB. S332. Topology phase diagram of U1 S1 As1

BCS ID	Formula	ICSD	MSG	T.C.	Picture
0.595	U1 Te1 P1		MSG 139.537 ($I4/mm'm'$)	None	
Topology	U=0 eV				

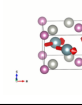
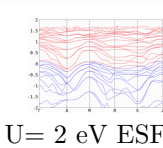
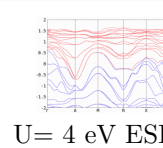
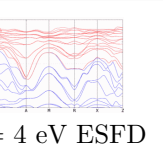
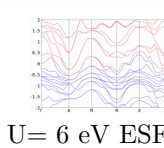
TAB. S333. Topology phase diagram of U1 Te1 P1

BCS ID	Formula	ICSD	MSG	T.C.	Picture
0.596	U1 Te1 As1		MSG 139.537 ($I4/mm'm'$)	None	
Topology	U=0 eV				

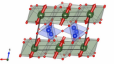
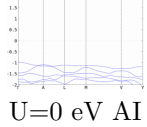
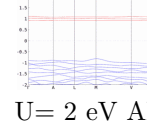
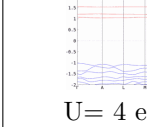
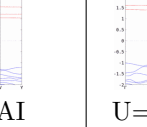
TAB. S334. Topology phase diagram of U1 Te1 As1

BCS ID	Formula	ICSD	MSG	T.C.	Picture
0.616	Ho1 B2		MSG 12.62 ($C2'/m'$)	$\eta_{4I}z_{2I,1}z_{2I,2}z_{2I,3}$	
Topology	U=0 eV NLC (1, 1, 1, 0)				

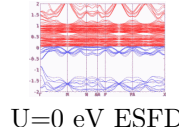
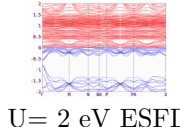
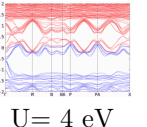
TAB. S335. Topology phase diagram of Ho1 B2

BCS ID	Formula	ICSD	MSG	T.C.	Picture
0.625	U2 In1 Pd2		MSG 127.394 ($P4'/m'bm'$)	None	
Topology	U=0 eV				

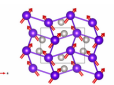
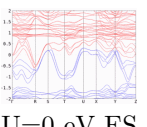
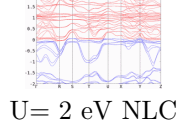
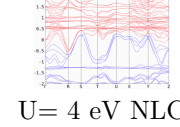
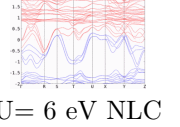
TAB. S336. Topology phase diagram of U2 In1 Pd2

BCS ID	Formula	ICSD	MSG	T.C.	Picture
0.650	Er2 Si2 O7		MSG 12.60 ($C2'/m$)	None	
Topology	 U=0 eV AI	 U=2 eV AI	 U=4 eV AI	 U=6 eV AI	

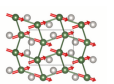
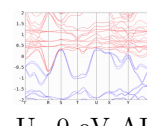
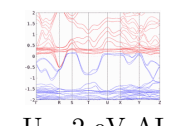
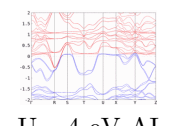
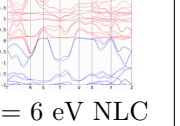
TAB. S337. Topology phase diagram of Er2 Si2 O7

BCS ID	Formula	ICSD	MSG	T.C.	Picture
0.681	Sb3 Ce4		MSG 122.336 ($I\bar{4}'2d'$)	None	
Topology	 U=0 eV ESFD	 U=2 eV ESFD	 U=4 eV	U=6 eV	

TAB. S338. Topology phase diagram of Sb3 Ce4

BCS ID	Formula	ICSD	MSG	T.C.	Picture
0.684	Pt1 Tb1		MSG 62.446 ($Pn'm'a$)	η_{4I}	
Topology	 U=0 eV ES	 U=2 eV NLC (2)	 U=4 eV NLC (2)	 U=6 eV NLC (2)	

TAB. S339. Topology phase diagram of Pt1 Tb1

BCS ID	Formula	ICSD	MSG	T.C.	Picture
0.685	Er1 Pt1		MSG 62.447 ($Pnm'a'$)	η_{4I}	
Topology	 U=0 eV AI	 U=2 eV AI	 U=4 eV AI	 U=6 eV NLC (2)	

TAB. S340. Topology phase diagram of Er1 Pt1

BCS ID	Formula	ICSD	MSG	T.C.	Picture
0.686	Ho1 Pt1		MSG 62.447 ($Pnm'a'$)	None	
Topology	 U=0 eV AI	 U= 2 eV AI	 U= 4 eV AI	 U= 6 eV ES	

TAB. S341. Topology phase diagram of Ho1 Pt1

BCS ID	Formula	ICSD	MSG	T.C.	Picture
0.687	Dy1 Pt1		MSG 62.446 ($Pn'm'a'$)	η_{4I}	
Topology	 U=0 eV ES	 U= 2 eV	 U= 4 eV AI	 U= 6 eV NLC (2)	

TAB. S342. Topology phase diagram of Dy1 Pt1

BCS ID	Formula	ICSD	MSG	T.C.	Picture
0.688	Tm1 Pt1		MSG 62.447 ($Pnm'a'$)	η_{4I}	
Topology	 U=0 eV AF	 U= 2 eV AI	 U= 4 eV AI	 U= 6 eV AI	

TAB. S343. Topology phase diagram of Tm1 Pt1

BCS ID	Formula	ICSD	MSG	T.C.	Picture
0.689	Pt1 Pr1		MSG 63.462 ($Cm'c'm$)	None	
Topology	 U=0 eV ES	 U= 2 eV ES	 U= 4 eV OAI	 U= 6 eV ES	

TAB. S344. Topology phase diagram of Pt1 Pr1

BCS ID	Formula	ICSD	MSG	T.C.	Picture
0.690	Nd1 Pt1		MSG 15.89 ($C2'/c'$)	$\eta_{4I} z_{2I,1} z_{2I,2}$	
Topology	U=0 eV NLC (1, 1, 1)	 U= 2 eV OAI	 U= 4 eV NLC (2, 1, 1)	 U= 6 eV NLC (1, 0, 0)	

TAB. S345. Topology phase diagram of Nd1 Pt1

BCS ID	Formula	ICSD	MSG	T.C.	Picture
0.743	Ho3 Al5 O12		MSG 230.148 ($Ia\bar{3}d'$)	η_{4I}	
Topology	 U=0 eV AF	U= 2 eV	 U= 4 eV AI	U= 6 eV	

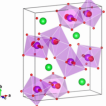
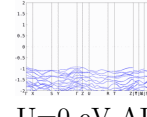
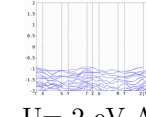
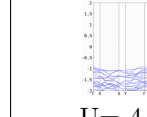
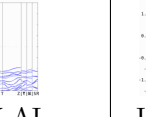
TAB. S346. Topology phase diagram of Ho3 Al5 O12

BCS ID	Formula	ICSD	MSG	T.C.	Picture
0.782	Nd1 Sc1 O3		MSG 62.444 ($Pnm'a$)	None	
Topology	 U=0 eV AI	 U= 2 eV AI	 U= 4 eV AI	 U= 6 eV AI	

TAB. S347. Topology phase diagram of Nd1 Sc1 O3

BCS ID	Formula	ICSD	MSG	T.C.	Picture
0.783	Nd1 In1 O3		MSG 62.444 ($Pnm'a$)	None	
Topology	 U=0 eV AI	 U= 2 eV AI	 U= 4 eV AI	 U= 6 eV AI	

TAB. S348. Topology phase diagram of Nd1 In1 O3

BCS ID	Formula	ICSD	MSG	T.C.	Picture
0.821	Sr1 Gd2 O4		MSG 62.445 ($Pnma'$)	None	
Topology	 U=0 eV AI	 U= 2 eV AI	 U= 4 eV AI	 U= 6 eV AI	

TAB. S349. Topology phase diagram of Sr1 Gd2 O4

BCS ID	Formula	ICSD	MSG	T.C.	Picture
0.832	Ce1 Au1 Ge1		MSG 36.175 ($Cmc'2'_1$)	None	
Topology	 U=0 eV ES	 U= 2 eV AI	 U= 4 eV AI	 U= 6 eV	

TAB. S350. Topology phase diagram of Ce1 Au1 Ge1

BCS ID	Formula	ICSD	MSG	T.C.	Picture
0.842	Dy1 Al1 O3		MSG 62.449 ($Pn'm'a'$)	None	
Topology	 U=0 eV ES	 U= 2 eV AI	 U= 4 eV AI	 U= 6 eV AI	

TAB. S351. Topology phase diagram of Dy1 Al1 O3

BCS ID	Formula	ICSD	MSG	T.C.	Picture
0.854	Gd2 Pt2 O7		MSG 141.555 ($I4'_1/amd'$)	$\eta_{4I}\delta_{2m}$	
Topology	 U=0 eV AI	 U= 2 eV AI	 U= 4 eV AI	 U= 6 eV AI	

TAB. S352. Topology phase diagram of Gd2 Pt2 O7

BCS ID	Formula	ICSD	MSG	T.C.	Picture
0.863	Eu1 Cd2 As2		MSG 12.62 ($C2'/m'$)	$\eta_{4I}z_{2I,1}z_{2I,2}z_{2I,3}$	
Topology	 U=0 eV OAI	 U= 2 eV SEBR (2, 0, 0, 0)	 U= 4 eV SEBR (2, 0, 0, 0)	 U= 6 eV NLC (3, 0, 0, 0)	

TAB. S353. Topology phase diagram of Eu1 Cd2 As2

BCS ID	Formula	ICSD	MSG	T.C.	Picture
0.941	Er2 O3		MSG 206.37 ($Ia\bar{3}$)	η_{4I}	
Topology	 U=0 eV AI	 U= 2 eV AI	 U= 4 eV	 U= 6 eV	

TAB. S354. Topology phase diagram of Er2 O3

BCS ID	Formula	ICSD	MSG	T.C.	Picture
0.950	Er1 La1 O3		MSG 62.441 ($Pnma$)	η_{4I}	
Topology	 U=0 eV AI	 U= 2 eV AI	 U= 4 eV AI	 U= 6 eV AI	

TAB. S355. Topology phase diagram of Er1 La1 O3

BCS ID	Formula	ICSD	MSG	T.C.	Picture
0.952	Yb1 Pd1 Si1		MSG 59.409 ($Pm'm'n$)	$\eta_{4I}z_{2I,3}z_{2R}$	
Topology	 U=0 eV OAI	 U= 2 eV SEBR (2, 0, 0)	 U= 4 eV SEBR (2, 0, 0)	 U= 6 eV SEBR (2, 0, 0)	

TAB. S356. Topology phase diagram of Yb1 Pd1 Si1

BCS ID	Formula	ICSD	MSG	T.C.	Picture
0.972	Ho1 Pd1 In1		MSG 189.225 ($P\bar{6}2'm'$)	None	
Topology	 U=0 eV ES	 U= 2 eV	 U= 4 eV ES	 U= 6 eV	

TAB. S357. Topology phase diagram of Ho1 Pd1 In1

BCS ID	Formula	ICSD	MSG	T.C.	Picture
0.973	Ho1 Pd1 In1		MSG 189.225 ($P\bar{6}2'm'$)	None	
Topology	 U=0 eV ES	 U = 2 eV	 U = 4 eV	 U = 6 eV	

TAB. S358. Topology phase diagram of Ho1 Pd1 In1

BCS ID	Formula	ICSD	MSG	T.C.	Picture
0.974	Er1 Pd1 In1		MSG 189.225 ($P\bar{6}2'm'$)	None	
Topology	 U=0 eV	 U = 2 eV	 U = 4 eV ES	 U = 6 eV	

TAB. S359. Topology phase diagram of Er1 Pd1 In1

BCS ID	Formula	ICSD	MSG	T.C.	Picture
0.975	Er1 Pd1 In1		MSG 189.225 ($P\bar{6}2'm'$)	None	
Topology	 U=0 eV	 U = 2 eV	 U = 4 eV	 U = 6 eV ES	

TAB. S360. Topology phase diagram of Er1 Pd1 In1

BCS ID	Formula	ICSD	MSG	T.C.	Picture
0.976	Nd1 Pd1 In1		MSG 38.191 ($Am'm'2$)	None	
Topology	 U=0 eV ES	 U = 2 eV AI	 U = 4 eV ES	 U = 6 eV ES	

TAB. S361. Topology phase diagram of Nd1 Pd1 In1

BCS ID	Formula	ICSD	MSG	T.C.	Picture
0.977	Nd1 Pd1 In1		MSG 8.34 (Cm')	None	
Topology	 U=0 eV AI	 U= 2 eV AI	 U= 4 eV AI	 U= 6 eV AI	

TAB. S362. Topology phase diagram of Nd1 Pd1 In1

BCS ID	Formula	ICSD	MSG	T.C.	Picture
0.985	Eu1 Pd3 Si2		MSG 74.559 ($Imm'a'$)	None	
Topology	 U=0 eV ES	 U= 2 eV ES	 U= 4 eV ES	 U= 6 eV ES	

TAB. S363. Topology phase diagram of Eu1 Pd3 Si2

BCS ID	Formula	ICSD	MSG	T.C.	Picture
1.288	Ce1 Pd2 Si2		MSG 66.500 (C_{Accm})	$\eta_{4I}\delta_{2m}\eta'_{2I}$	
Topology	 U=0 eV SEBR (2, 1, 1)	 U= 2 eV SEBR (2, 1, 1)	 U= 4 eV AF	 U= 6 eV ES	

TAB. S364. Topology phase diagram of Ce1 Pd2 Si2

BCS ID	Formula	ICSD	MSG	T.C.	Picture
1.290	Ce1 Rh2 Si2		MSG 64.480 (C_{Amca})	$\eta_{4I}\delta_{2m}$	
Topology	 U=0 eV SEBR (2, 1)	 U= 2 eV OAI	 U= 4 eV ES	 U= 6 eV ES	

TAB. S365. Topology phase diagram of Ce1 Rh2 Si2

BCS ID	Formula	ICSD	MSG	T.C.	Picture
1.291	Au2 Ce1 Si2		MSG 128.410 (P_I4/mnc)	None	
Topology	 U=0 eV ES	 U= 2 eV ES	 U= 4 eV ES	 U= 6 eV ES	

TAB. S366. Topology phase diagram of Au2 Ce1 Si2

BCS ID	Formula	ICSD	MSG	T.C.	Picture
1.334	Pr2 Pd2 In1		MSG 62.451 (P_bnma)	None	
Topology	 U=0 eV ES	 U= 2 eV AI	 U= 4 eV ES	 U= 6 eV ES	

TAB. S367. Topology phase diagram of Pr2 Pd2 In1

BCS ID	Formula	ICSD	MSG	T.C.	Picture
1.339	Eu1 As3		MSG 12.63 (C_c2/m)	$\eta_{4I}\delta_{2m}$	
Topology	 U=0 eV OAI	 U= 2 eV OAI	 U= 4 eV OAI	 U= 6 eV SEBR (2, 1)	

TAB. S368. Topology phase diagram of Eu1 As3

BCS ID	Formula	ICSD	MSG	T.C.	Picture
1.361	Dy1 Ge1		MSG 15.90 (C_c2/c)	η_{4I}	
Topology	 U=0 eV OAI	 U= 2 eV SEBR (2)	 U= 4 eV SEBR (2)	 U= 6 eV OAI	

TAB. S369. Topology phase diagram of Dy1 Ge1

BCS ID	Formula	ICSD	MSG	T.C.	Picture
1.367	Pu2 O3		MSG 15.90 (C_c2/c)	η_{4I}	
Topology	U=0 eV SEBR (2) U= 2 eV AI U= 4 eV AI U= 6 eV AI	 			

TAB. S370. Topology phase diagram of Pu2 O3

BCS ID	Formula	ICSD	MSG	T.C.	Picture
1.486	Ce1 Rh1 Al4 Si2		MSG 124.360 (P_c4/mcc)	None	
Topology	U=0 eV U= 2 eV ES U= 4 eV ES U= 6 eV ES	 			

TAB. S371. Topology phase diagram of Ce1 Rh1 Al4 Si2

BCS ID	Formula	ICSD	MSG	T.C.	Picture
1.497	Eu1 Bi2 Mg2		MSG 12.63 (C_c2/m)	$\eta_{4I}\delta_{2m}$	
Topology	U=0 eV SEBR (2, 1) U= 2 eV SEBR (2, 1) U= 4 eV SEBR (2, 1) U= 6 eV SEBR (2, 1)	 			

TAB. S372. Topology phase diagram of Eu1 Bi2 Mg2

BCS ID	Formula	ICSD	MSG	T.C.	Picture
1.505	Gd1 Ag1 Sn1		MSG 33.154 (P_Cna2_1)	None	
Topology	U=0 eV AI U= 2 eV AI U= 4 eV AI U= 6 eV AI	 			

TAB. S373. Topology phase diagram of Gd1 Ag1 Sn1

BCS ID	Formula	ICSD	MSG	T.C.	Picture
1.507	Al2 Pd5 Nd1		MSG 62.450 (P_{anma})	η_{4I}	
Topology	 U=0 eV SEBR (2)	 U= 2 eV SEBR (2)	 U= 4 eV OAI	 U= 6 eV OAI	

TAB. S374. Topology phase diagram of Al2 Pd5 Nd1

BCS ID	Formula	ICSD	MSG	T.C.	Picture
1.530	Ce1 C2		MSG 128.410 (P_I4/mnc)	None	
Topology	 U=0 eV ES	 U= 2 eV ES	 U= 4 eV ES	 U= 6 eV ES	

TAB. S375. Topology phase diagram of Ce1 C2

BCS ID	Formula	ICSD	MSG	T.C.	Picture
1.531	Pr1 C2		MSG 128.410 (P_I4/mnc)	None	
Topology	 U=0 eV ES	 U= 2 eV ES	 U= 4 eV ES	 U= 6 eV ES	

TAB. S376. Topology phase diagram of Pr1 C2

BCS ID	Formula	ICSD	MSG	T.C.	Picture
1.532	Nd1 C2		MSG 128.410 (P_I4/mnc)	None	
Topology	 U=0 eV ES	 U= 2 eV ES	 U= 4 eV ES	 U= 6 eV ES	

TAB. S377. Topology phase diagram of Nd1 C2

BCS ID	Formula	ICSD	MSG	T.C.	Picture
1.536	U1 Pd2 Si2		MSG 128.410 ($P_I\bar{4}/mnc$)	None	
Topology	U=0 eV			U= 4 eV OAI	U= 6 eV OAI

TAB. S378. Topology phase diagram of U1 Pd2 Si2

BCS ID	Formula	ICSD	MSG	T.C.	Picture
1.574	Nd1 Bi1 Pt1		MSG 118.314 ($P_I\bar{4}n2$)	z_2	
Topology	U=0 eV AI			U= 4 eV AI	U= 6 eV AI

TAB. S379. Topology phase diagram of Nd1 Bi1 Pt1

BCS ID	Formula	ICSD	MSG	T.C.	Picture
1.576	O2 S1 Yb2		MSG 12.63 (C_c2/m)	$\eta_{4I}\delta_{2m}$	
Topology	U=0 eV SEBR (2, 1)			U= 4 eV AI	U= 6 eV AI

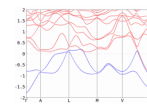
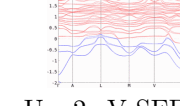
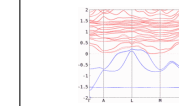
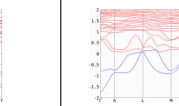
TAB. S380. Topology phase diagram of O2 S1 Yb2

BCS ID	Formula	ICSD	MSG	T.C.	Picture
1.578	K1 Er1 Se2		MSG 12.63 (C_c2/m)	$\eta_{4I}\delta_{2m}$	
Topology	U=0 eV			U= 4 eV AI	U= 6 eV AI

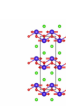
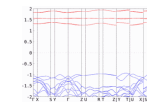
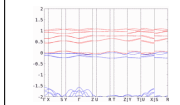
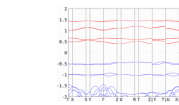
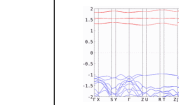
TAB. S381. Topology phase diagram of K1 Er1 Se2

BCS ID	Formula	ICSD	MSG	T.C.	Picture
1.623	Bi2 Eu1 Mg2		MSG 12.63 (C_c2/m)	$\eta_{4I}\delta_{2m}$	
Topology	U=0 eV SEBR (2, 1)	 U = 2 eV SEBR (2, 1)	 U = 4 eV SEBR (2, 1)	 U = 6 eV SEBR (2, 1)	

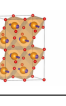
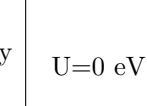
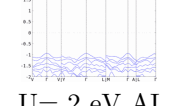
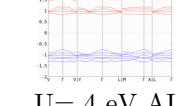
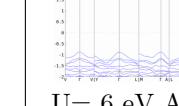
TAB. S382. Topology phase diagram of Bi2 Eu1 Mg2

BCS ID	Formula	ICSD	MSG	T.C.	Picture
1.627	Ce1 K1 S2		MSG 15.90 (C_c2/c)	η_{4I}	
Topology	 U=0 eV AI	 U= 2 eV SEBR (2)	 U= 4 eV AI	 U= 6 eV AI	

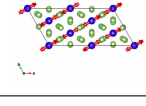
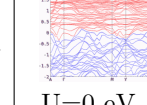
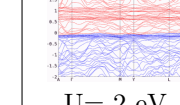
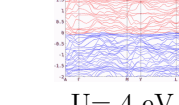
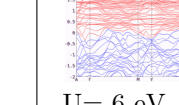
TAB. S383. Topology phase diagram of Ce1 K1 S2

BCS ID	Formula	ICSD	MSG	T.C.	Picture
1.643	Cl1 Dy1 O1		MSG 62.450 (P_anma)	η_{4I}	
Topology	 U=0 eV AI	 U= 2 eV AI	 U= 4 eV AI	 U= 6 eV AI	

TAB. S384. Topology phase diagram of Cl1 Dy1 O1

BCS ID	Formula	ICSD	MSG	T.C.	Picture
1.648	Nd2 O3		MSG 12.63 (C_c2/m)	$\eta_{4I}\delta_{2m}$	
Topology	 U=0 eV	 U= 2 eV AI	 U= 4 eV AI	 U= 6 eV AI	

TAB. S385. Topology phase diagram of Nd2 O3

BCS ID	Formula	ICSD	MSG	T.C.	Picture
1.658	Dy1 Ga3		MSG 15.90 (C_c2/c)	η_{4I}	
Topology	 U=0 eV AI	 U= 2 eV	 U= 4 eV	 U= 6 eV AI	

TAB. S386. Topology phase diagram of Dy1 Ga3

BCS ID	Formula	ICSD	MSG	T.C.	Picture
1.667	U1 Pd1 Ga5		MSG 67.509 (C_a mma)	$\eta_{4I}\delta_{2m}$	
Topology	U=0 eV NLC (2, 1)			U= 4 eV OAI	

TAB. S387. Topology phase diagram of U1 Pd1 Ga5

BCS ID	Formula	ICSD	MSG	T.C.	Picture
1.672	Eu1 Zn2 As2		MSG 12.63 (C_c 2/m)	$\eta_{4I}\delta_{2m}$	
Topology	U=0 eV SEBR (2, 1)			U= 4 eV AI	

TAB. S388. Topology phase diagram of Eu1 Zn2 As2

BCS ID	Formula	ICSD	MSG	T.C.	Picture
1.714	Ce1 Bi2 Au1		MSG 130.432 (P_c 4/ncc)	$\eta_{4I}z_2$	
Topology	U=0 eV ES			U= 4 eV SEBR (2, 1)	

TAB. S389. Topology phase diagram of Ce1 Bi2 Au1

BCS ID	Formula	ICSD	MSG	T.C.	Picture
1.740	Ce1 Au1 Sb2		MSG 39.201 (A_b bm2)	None	
Topology	U=0 eV ES			U= 4 eV AI	

TAB. S390. Topology phase diagram of Ce1 Au1 Sb2

BCS ID	Formula	ICSD	MSG	T.C.	Picture
1.744	Pr1 Pd1 Sn1		MSG 14.80 (P_a2_1/c)	η_{4I}	
Topology	U=0 eV NLC (2) U= 2 eV NLC (2) U= 4 eV NLC (2) U= 6 eV NLC (2)	 			

TAB. S391. Topology phase diagram of Pr1 Pd1 Sn1

BCS ID	Formula	ICSD	MSG	T.C.	Picture
1.747	Er1 In1 Au1		MSG 174.136 ($P_c\bar{6}$)	δ_{3m}	
Topology	U=0 eV U= 2 eV AF U= 4 eV U= 6 eV	 			

TAB. S392. Topology phase diagram of Er1 In1 Au1

BCS ID	Formula	ICSD	MSG	T.C.	Picture
1.749	Ho1 Sb1 Te1		MSG 11.55 (P_a2_1/m)	η_{4I}	
Topology	U=0 eV NLC (2) U= 2 eV U= 4 eV OAI U= 6 eV	 			

TAB. S393. Topology phase diagram of Ho1 Sb1 Te1

BCS ID	Formula	ICSD	MSG	T.C.	Picture
1.753	Ho1 Bi1		MSG 15.90 (C_c2/c)	η_{4I}	
Topology	U=0 eV U= 2 eV AF U= 4 eV U= 6 eV	 			

TAB. S394. Topology phase diagram of Ho1 Bi1

BCS ID	Formula	ICSD	MSG	T.C.	Picture
1.755	K1 Er1 Se2		MSG 12.63 (C_c2/m)	$\eta_{4I}\delta_{2m}$	
Topology	 U=0 eV AI	 U= 2 eV AI	 U= 4 eV AI	 U= 6 eV AI	

TAB. S395. Topology phase diagram of K1 Er1 Se2

BCS ID	Formula	ICSD	MSG	T.C.	Picture
2.100	Ho1 P1		MSG 15.89 ($C2'/c'$)	$\eta_{4I}z_{2I,1}z_{2I,2}$	
Topology	 U=0 eV AF	 U= 2 eV NLC (0, 1, 1)	 U= 4 eV NLC (0, 1, 1)	 U= 6 eV NLC (1, 0, 0)	

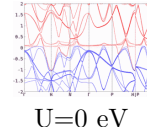
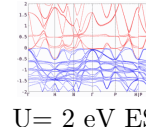
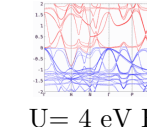
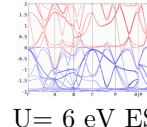
TAB. S396. Topology phase diagram of Ho1 P1

BCS ID	Formula	ICSD	MSG	T.C.	Picture
2.103	Eu3 Pb1 O1		MSG 47.252 ($Pm'm'm$)	None	
Topology	 U=0 eV ES	 U= 2 eV ES	 U= 4 eV OAI	 U= 6 eV OAI	

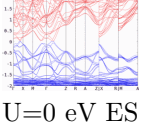
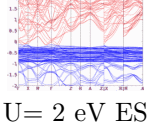
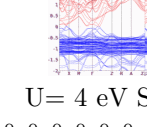
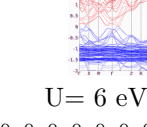
TAB. S397. Topology phase diagram of Eu3 Pb1 O1

BCS ID	Formula	ICSD	MSG	T.C.	Picture
2.71	Ho1 Rh1		MSG 11.57 (P_C2_1/m)	η_{4I}	
Topology	 U=0 eV NLC (2)	U= 2 eV	U= 4 eV	 U= 6 eV AI	

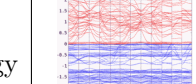
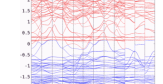
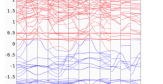
TAB. S398. Topology phase diagram of Ho1 Rh1

BCS ID	Formula	ICSD	MSG	T.C.	Picture
3.21	Ga3 Tm1		MSG 229.143 ($I\bar{m}\bar{3}m'$)	None	
Topology	 U=0 eV  U= 2 eV ES  U= 4 eV ES  U= 6 eV ES				

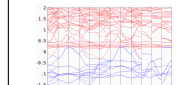
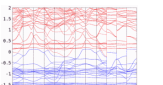
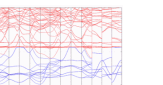
TAB. S399. Topology phase diagram of Ga3 Tm1

BCS ID	Formula	ICSD	MSG	T.C.	Picture
3.23	Eu3 Pb1 O1		MSG 123.345 ($P4/m�'�'$)	$\eta_{4I}z_{2I,3}z_{2R}\delta_{2m}z_{2m,\pi}^-z_{2m,\pi}^+$ $z_{4R}z_2z_{4S}\delta_{4m}z_{4m,\pi}^-z_{4m,\pi}^+$	
Topology	 U=0 eV ES  U= 2 eV ES  U= 4 eV SEBR (0, 0, 0, 0, 0, 0, 0, 0, 0, 2, 0, 0)  U= 6 eV SEBR (0, 0, 0, 0, 0, 0, 0, 0, 0, 0, 2, 0, 0)				

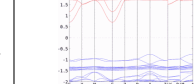
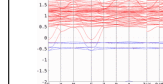
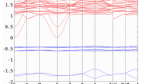
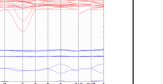
TAB. S400. Topology phase diagram of Eu3 Pb1 O1

BCS ID	Formula	ICSD	MSG	T.C.	Picture
0.231	Tm1 Mn3 O6		MSG 59.410 ($Pmm'n'$)	None	
Topology	 U=0 eV ES	 U= 2 eV ES	 U= 4 eV ES	U= 6 eV	

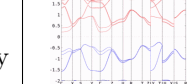
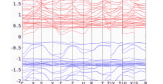
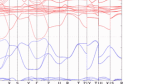
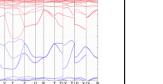
TAB. S401. Topology phase diagram of Tm1 Mn3 O6

BCS ID	Formula	ICSD	MSG	T.C.	Picture
0.232	Tm1 Mn3 O6		MSG 59.409 ($Pm'm'n$)	None	
Topology	 U=0 eV AF	 U= 2 eV ES	 U= 4 eV ES	 U= 6 eV ES	

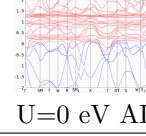
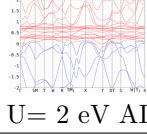
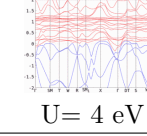
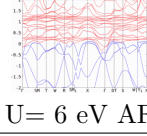
TAB. S402. Topology phase diagram of Tm1 Mn3 O6

BCS ID	Formula	ICSD	MSG	T.C.	Picture
0.235	Mn2 Pr1 Sb1 O6		MSG 86.67 ($P4_2/n$)	$\eta_{4I} z'_{2R} z_2 z_{4S}$	
Topology	 U=0 eV AI	 U= 2 eV AI	 U= 4 eV AI	 U= 6 eV AI	

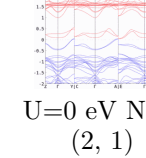
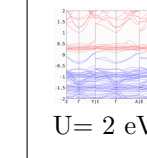
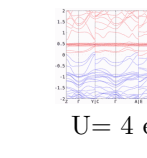
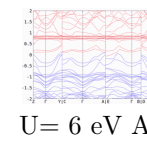
TAB. S403. Topology phase diagram of Mn2 Pr1 Sb1 O6

BCS ID	Formula	ICSD	MSG	T.C.	Picture
0.289	Nd1 Mn1 O3		MSG 62.448 ($Pn'ma'$)	η_{4I}	
Topology	 U=0 eV AF	 U= 2 eV	 U= 4 eV	 U= 6 eV	

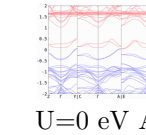
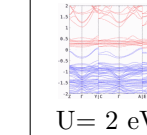
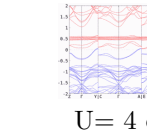
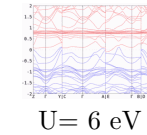
TAB. S404. Topology phase diagram of Nd1 Mn1 O3

BCS ID	Formula	ICSD	MSG	T.C.	Picture
0.290	Ce1 Cu2		MSG 74.560 ($Im'm'a'$)	None	
Topology	    U=0 eV AI U= 2 eV AI U= 4 eV U= 6 eV AF				

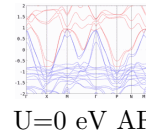
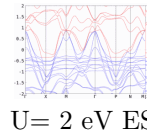
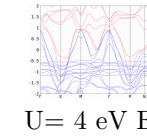
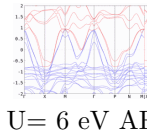
TAB. S405. Topology phase diagram of Ce1 Cu2

BCS ID	Formula	ICSD	MSG	T.C.	Picture
0.318	Tm2 Co1 Mn1 O6		MSG 14.79 ($P2'_1/c'$)	$\eta_{4I}z_{2I,1}$	
Topology	    U=0 eV NLC (2,1) U= 2 eV AI U= 4 eV U= 6 eV AI				

TAB. S406. Topology phase diagram of Tm2 Co1 Mn1 O6

BCS ID	Formula	ICSD	MSG	T.C.	Picture
0.319	Tm2 Co1 Mn1 O6		MSG 14.79 ($P2'_1/c'$)	$\eta_{4I}z_{2I,1}$	
Topology	    U=0 eV AF U= 2 eV AI U= 4 eV U= 6 eV				

TAB. S407. Topology phase diagram of Tm2 Co1 Mn1 O6

BCS ID	Formula	ICSD	MSG	T.C.	Picture
0.367	Eu1 Cr2 As2		MSG 119.319 ($I\bar{4}m'2'$)	None	
Topology	    U=0 eV AF U= 2 eV ES U= 4 eV ES U= 6 eV AF				

TAB. S408. Topology phase diagram of Eu1 Cr2 As2

BCS ID	Formula	ICSD	MSG	T.C.	Picture
0.372	Dy1 Cr1 O4		MSG 15.87 ($C2'/c$)	None	
Topology	 U=0 eV AI	 U= 2 eV AI	 U = 4 eV	 U = 6 eV AI	

TAB. S409. Topology phase diagram of Dy1 Cr1 O4

BCS ID	Formula	ICSD	MSG	T.C.	Picture
0.374	Tb1 Ni4 Si1		MSG 65.486 ($Cmm'm'$)	None	
Topology	 U=0 eV ES	 U= 2 eV ES	 U = 4 eV ES	 U = 6 eV ES	

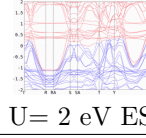
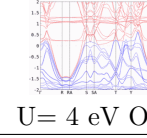
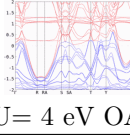
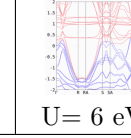
TAB. S410. Topology phase diagram of Tb1 Ni4 Si1

BCS ID	Formula	ICSD	MSG	T.C.	Picture
0.406	Gd1 Ni1 Si3		MSG 65.484 ($Cmmm'$)	None	
Topology	 U=0 eV AI	 U= 2 eV AI	 U = 4 eV AI	 U = 6 eV AI	

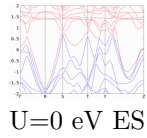
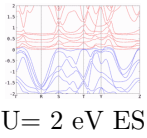
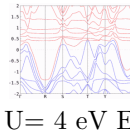
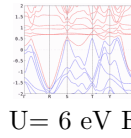
TAB. S411. Topology phase diagram of Gd1 Ni1 Si3

BCS ID	Formula	ICSD	MSG	T.C.	Picture
0.519	Ho1 Cr2 Si2		MSG 139.536 ($I4'/m'm'm$)	None	
Topology	 U=0 eV AF	 U = 2 eV	 U = 4 eV ESFD	 U = 6 eV	

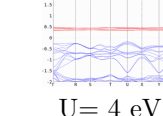
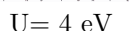
TAB. S412. Topology phase diagram of Ho1 Cr2 Si2

BCS ID	Formula	ICSD	MSG	T.C.	Picture
0.561	Ni1 Nd1 Ge2		MSG 63.462 ($Cm'c'm$)	None	
Topology	U=0 eV				

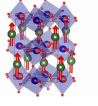
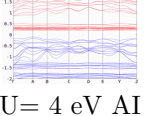
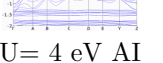
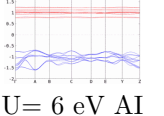
TAB. S413. Topology phase diagram of Ni1 Nd1 Ge2

BCS ID	Formula	ICSD	MSG	T.C.	Picture
0.566	Ge2 Ni1 Tb1		MSG 63.459 ($Cm'cm$)	None	
Topology	U=0 eV ES				

TAB. S414. Topology phase diagram of Ge2 Ni1 Tb1

BCS ID	Formula	ICSD	MSG	T.C.	Picture
0.587	Tm1 Cr1 O3		MSG 62.448 ($Pn'ma'$)	η_{4I}	
Topology	U=0 eV OAI	U= 2 eV		U= 4 eV	

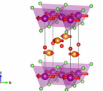
TAB. S415. Topology phase diagram of Tm1 Cr1 O3

BCS ID	Formula	ICSD	MSG	T.C.	Picture
0.590	Er1 Cr1 O3		MSG 11.50 ($P2_1/m$)	η_{4I}	
Topology	U=0 eV	U= 2 eV			

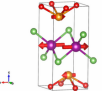
TAB. S416. Topology phase diagram of Er1 Cr1 O3

BCS ID	Formula	ICSD	MSG	T.C.	Picture
0.620	Mn1 Nd1 As1 O1		MSG 129.416 ($P4'/n'm'm$)	z_2	
Topology	U=0 eV SEBR (1)	U= 2 eV	U= 4 eV SEBR (1)	U= 6 eV AI	

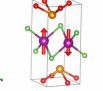
TAB. S417. Topology phase diagram of Mn1 Nd1 As1 O1

BCS ID	Formula	ICSD	MSG	T.C.	Picture
0.621	Mn1 Nd1 As1 O1		MSG 59.407 ($Pm'mn$)	None	
Topology	U=0 eV AI	U= 2 eV AI	U= 4 eV	U= 6 eV AI	

TAB. S418. Topology phase diagram of Mn1 Nd1 As1 O1

BCS ID	Formula	ICSD	MSG	T.C.	Picture
0.622	Mn1 Nd1 As1 O1		MSG 59.407 ($Pm'mn$)	None	
Topology	U=0 eV AI	U= 2 eV AI	U= 4 eV AI	U= 6 eV	

TAB. S419. Topology phase diagram of Mn1 Nd1 As1 O1

BCS ID	Formula	ICSD	MSG	T.C.	Picture
0.623	Mn1 Nd1 As1 O1		MSG 129.416 ($P4'/n'm'm$)	z_2	
Topology	U=0 eV SEBR (1)	U= 2 eV	U= 4 eV SEBR (1)	U= 6 eV AI	

TAB. S420. Topology phase diagram of Mn1 Nd1 As1 O1

BCS ID	Formula	ICSD	MSG	T.C.	Picture
0.656	Nd ₁ Mn ₂ Ge ₂		MSG 44.231 ($Im'm2'$)	None	
Topology	 U=0 eV ES	 U= 2 eV ES	 U= 4 eV	 U= 6 eV ES	

TAB. S421. Topology phase diagram of Nd₁ Mn₂ Ge₂

BCS ID	Formula	ICSD	MSG	T.C.	Picture
0.657	Pr ₁ Mn ₂ Ge ₂		MSG 44.231 ($Im'm2'$)	None	
Topology	 U=0 eV ES	 U= 2 eV ES	 U= 4 eV ES	 U= 6 eV ES	

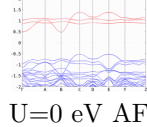
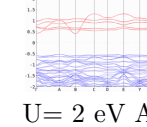
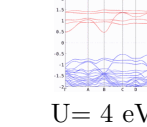
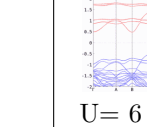
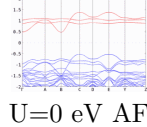
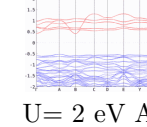
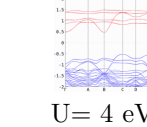
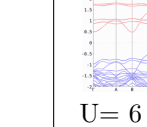
TAB. S422. Topology phase diagram of Pr₁ Mn₂ Ge₂

BCS ID	Formula	ICSD	MSG	T.C.	Picture
0.666	Ce ₁ Mn ₁ Sb ₁ O ₁		MSG 59.407 ($Pm'mn$)	None	
Topology	 U=0 eV AI	 U= 2 eV AI	 U= 4 eV AI	 U= 6 eV AI	

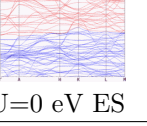
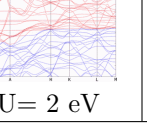
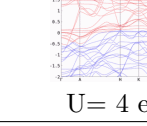
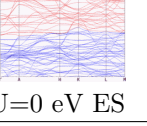
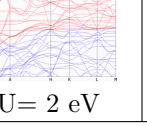
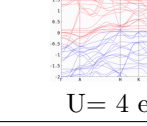
TAB. S423. Topology phase diagram of Ce₁ Mn₁ Sb₁ O₁

BCS ID	Formula	ICSD	MSG	T.C.	Picture
0.668	Pr ₁ Mn ₁ Sb ₁ O ₁		MSG 59.407 ($Pm'mn$)	None	
Topology	 U=0 eV AF	 U= 2 eV AI	 U= 4 eV AI	 U= 6 eV AI	

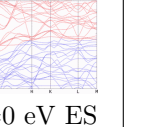
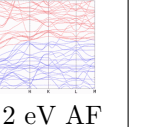
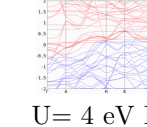
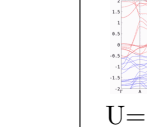
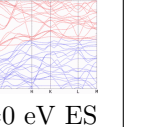
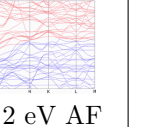
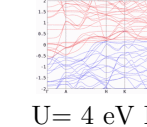
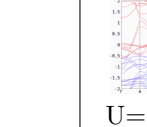
TAB. S424. Topology phase diagram of Pr₁ Mn₁ Sb₁ O₁

BCS ID	Formula	ICSD	MSG	T.C.	Picture
0.671	Sr2 Tm1 Ru1 O6		MSG 14.75 ($P2_1/c$)	η_{4I}	
Topology	   	   	U=0 eV AF U= 2 eV AI U= 4 eV AI U= 6 eV AI		

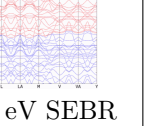
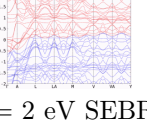
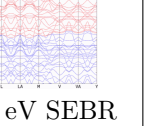
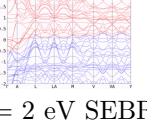
TAB. S425. Topology phase diagram of Sr2 Tm1 Ru1 O6

BCS ID	Formula	ICSD	MSG	T.C.	Picture
0.700	Tb1 Mn6 Sn6		MSG 191.240 ($P6/mm'm'$)	<i>None</i>	
Topology	  	  	U=0 eV ES U= 2 eV U= 4 eV	U= 6 eV	

TAB. S426. Topology phase diagram of Tb1 Mn6 Sn6

BCS ID	Formula	ICSD	MSG	T.C.	Picture
0.701	Tb1 Mn6 Sn6		MSG 191.240 ($P6/mm'm'$)	<i>None</i>	
Topology	   	   	U=0 eV ES U= 2 eV AF U= 4 eV ES U= 6 eV ES		

TAB. S427. Topology phase diagram of Tb1 Mn6 Sn6

BCS ID	Formula	ICSD	MSG	T.C.	Picture
0.703	Ho1 Mn6 Sn6		MSG 12.62 ($C2'/m'$)	$\eta_{4I}z_{2I,1}z_{2I,2}z_{2I,3}$	
Topology	 	 	U= 4 eV	U= 6 eV SEBR (0, 0, 0, 1)	

TAB. S428. Topology phase diagram of Ho1 Mn6 Sn6

BCS ID	Formula	ICSD	MSG	T.C.	Picture
0.704	Ho1 Mn6 Sn6		MSG 12.62 ($C2'/m'$)	$\eta_{4I}z_{2I,1}z_{2I,2}z_{2I,3}$	
Topology	U=0 eV NLC $(3, 0, 0, 1)$	 U= 2 eV SEBR $(2, 0, 0, 0)$	 $U = 4 \text{ eV}$	 $U = 6 \text{ eV NLC}$ $(3, 0, 0, 0)$	

TAB. S429. Topology phase diagram of Ho1 Mn6 Sn6

BCS ID	Formula	ICSD	MSG	T.C.	Picture
0.705	Ho1 Mn6 Sn6		MSG 65.486 ($Cmm'm'$)	<i>None</i>	
Topology	 $U = 0 \text{ eV ES}$	 $U = 2 \text{ eV ES}$	 $U = 4 \text{ eV AF}$	 $U = 6 \text{ eV ES}$	

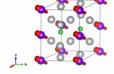
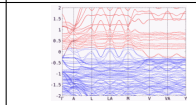
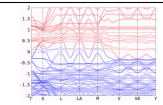
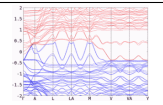
TAB. S430. Topology phase diagram of Ho1 Mn6 Sn6

BCS ID	Formula	ICSD	MSG	T.C.	Picture
0.715	W1 Ho1 Cr1 O6		MSG 33.144 (Pna_2_1)	<i>None</i>	
Topology	 $U = 0 \text{ eV AI}$	 $U = 2 \text{ eV}$	 $U = 4 \text{ eV AI}$	 $U = 6 \text{ eV AI}$	

TAB. S431. Topology phase diagram of W1 Ho1 Cr1 O6

BCS ID	Formula	ICSD	MSG	T.C.	Picture
0.729	Er1 Ni4 B1		MSG 191.240 ($P6/mm'm'$)	<i>None</i>	
Topology	 $U = 0 \text{ eV ES}$	 $U = 2 \text{ eV AF}$	 $U = 4 \text{ eV ES}$	 $U = 6 \text{ eV ES}$	

TAB. S432. Topology phase diagram of Er1 Ni4 B1

BCS ID	Formula	ICSD	MSG	T.C.	Picture
0.730	Tb1 Ni4 B1		MSG 12.62 ($C2'/m'$)	$\eta_{4I} z_{2I,1} z_{2I,2} z_{2I,3}$	
Topology	 U=0 eV SEBR $(0, 0, 0, 1)$	 U= 2 eV SEBR $(2, 0, 0, 0)$	 U= 4 eV SEBR $(2, 0, 0, 0)$	U= 6 eV	

TAB. S433. Topology phase diagram of Tb1 Ni4 B1

BCS ID	Formula	ICSD	MSG	T.C.	Picture
0.731	Ho1 Ni4 B1		MSG 12.62 ($C2'/m'$)	$\eta_{4I} z_{2I,1} z_{2I,2} z_{2I,3}$	
Topology	 U=0 eV SEBR (2, 0, 0, 0)	 U = 2 eV AF	 U = 4 eV NLC (1, 0, 0, 0)	 U = 6 eV NLC (1, 0, 0, 0)	

TAB. S434. Topology phase diagram of Ho1 Ni4 B1

BCS ID	Formula	ICSD	MSG	T.C.	Picture
0.758	Ce1 Fe1 O3		MSG 62.441 ($Pnma$)	η_{4I}	
Topology	 U=0 eV AI	 U = 2 eV AI	 U = 4 eV AI	 U = 6 eV AI	

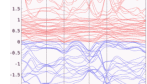
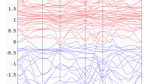
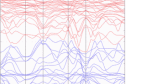
TAB. S435. Topology phase diagram of Ce1 Fe1 O3

BCS ID	Formula	ICSD	MSG	T.C.	Picture
0.759	Ce1 Fe1 O3		MSG 62.441 ($Pnma$)	η_{4I}	
Topology	 U=0 eV AI	 U = 2 eV AI	 U = 4 eV AI	 U = 6 eV AI	

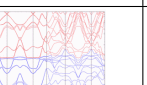
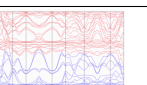
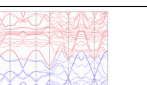
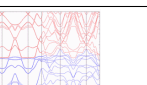
TAB. S436. Topology phase diagram of Ce1 Fe1 O3

BCS ID	Formula	ICSD	MSG	T.C.	Picture
0.771	Pr1 Mn1 Si2		MSG 63.464 ($Cm'cm'$)	None	
Topology	 U=0 eV ES	 U = 2 eV ES	 U = 4 eV ES	 U = 6 eV ES	

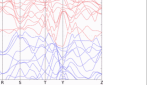
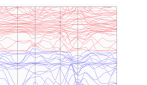
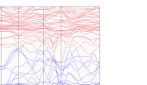
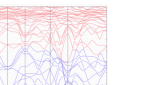
TAB. S437. Topology phase diagram of Pr1 Mn1 Si2

BCS ID	Formula	ICSD	MSG	T.C.	Picture
0.772	Pr1 Mn1 Si2		MSG 63.464 ($Cm'cm'$)	None	
Topology	 U=0 eV ES	 U= 2 eV ES	 U= 4 eV ES	U= 6 eV	

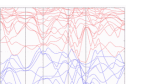
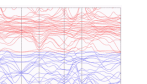
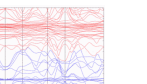
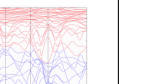
TAB. S438. Topology phase diagram of Pr1 Mn1 Si2

BCS ID	Formula	ICSD	MSG	T.C.	Picture
0.773	Nd1 Mn1 Si2		MSG 12.62 ($C2'/m'$)	$\eta_{4I}z_{2I,1}z_{2I,2}z_{2I,3}$	
Topology	 U=0 eV NLC (3, 0, 0, 0)	 U= 2 eV NLC (3, 1, 1, 0)	 U= 4 eV SEBR (2, 0, 0, 0)	 U= 6 eV SEBR (0, 1, 1, 0)	

TAB. S439. Topology phase diagram of Nd1 Mn1 Si2

BCS ID	Formula	ICSD	MSG	T.C.	Picture
0.774	Nd1 Mn1 Si2		MSG 63.464 ($Cm'cm'$)	$\eta_{4I}z_{2I,1}z_{2I,2}\eta'_{2I}z'_{2R}$	
Topology	 U=0 eV SEBR (0, 1, 1, 0, 1)	 U= 2 eV ES	 U= 4 eV ES	 U= 6 eV ES	

TAB. S440. Topology phase diagram of Nd1 Mn1 Si2

BCS ID	Formula	ICSD	MSG	T.C.	Picture
0.775	Nd1 Mn1 Si2		MSG 63.464 ($Cm'cm'$)	None	
Topology	 U=0 eV ES	 U= 2 eV ES	 U= 4 eV ES	 U= 6 eV ES	

TAB. S441. Topology phase diagram of Nd1 Mn1 Si2

BCS ID	Formula	ICSD	MSG	T.C.	Picture
0.776	Ce1 Mn1 Si2		MSG 63.464 ($Cm'cm'$)	None	
Topology	 U=0 eV ES	 U= 2 eV ES	U= 4 eV	 U= 6 eV ES	

TAB. S442. Topology phase diagram of Ce1 Mn1 Si2

BCS ID	Formula	ICSD	MSG	T.C.	Picture
0.777	Ce1 Mn1 Si2		MSG 63.464 ($Cm'cm'$)	None	
Topology	 U=0 eV ES	 U= 2 eV ES	U= 4 eV ES	 U= 6 eV ES	

TAB. S443. Topology phase diagram of Ce1 Mn1 Si2

BCS ID	Formula	ICSD	MSG	T.C.	Picture
0.781	Ce1 Mn1 Si2		MSG 63.464 ($Cm'cm'$)	None	
Topology	 U=0 eV ES	 U= 2 eV ES	U= 4 eV ES	 U= 6 eV ES	

TAB. S444. Topology phase diagram of Ce1 Mn1 Si2

BCS ID	Formula	ICSD	MSG	T.C.	Picture
0.784	Nd1 Co1 O3		MSG 62.441 ($Pnma$)	η_{4I}	
Topology	 U=0 eV NLC (2)	 U= 2 eV AI	U= 4 eV	 U= 6 eV ES	

TAB. S445. Topology phase diagram of Nd1 Co1 O3

BCS ID	Formula	ICSD	MSG	T.C.	Picture
0.789	Ce1 Cu1 Si1		MSG 63.463 ($Cmc'm'$)	None	
Topology	 U=0 eV ES	 U= 2 eV	 U= 4 eV ES	 U= 6 eV	

TAB. S446. Topology phase diagram of Ce1 Cu1 Si1

BCS ID	Formula	ICSD	MSG	T.C.	Picture
0.791	Sr2 Tb1 Ru1 O6		MSG 14.75 ($P2_1/c$)	η_{4I}	
Topology	 U=0 eV NLC (2)	 U= 2 eV AI	 U= 4 eV AI	 U= 6 eV AI	

TAB. S447. Topology phase diagram of Sr2 Tb1 Ru1 O6

BCS ID	Formula	ICSD	MSG	T.C.	Picture
0.792	Sr2 Ho1 Ru1 O6		MSG 14.75 ($P2_1/c$)	None	
Topology	 U=0 eV ES	 U= 2 eV AI	 U= 4 eV AI	 U= 6 eV AI	

TAB. S448. Topology phase diagram of Sr2 Ho1 Ru1 O6

BCS ID	Formula	ICSD	MSG	T.C.	Picture
0.794	Sr2 Ho1 Ru1 O6		MSG 14.75 ($P2_1/c$)	η_{4I}	
Topology	 U=0 eV ES	 U= 2 eV NLC (2)	 U= 4 eV AI	 U= 6 eV AI	

TAB. S449. Topology phase diagram of Sr2 Ho1 Ru1 O6

BCS ID	Formula	ICSD	MSG	T.C.	Picture
0.840	Dy1 Fe1 O3		MSG 62.441 (<i>Pnma</i>)	η_{4I}	
Topology	 			U = 6 eV	

TAB. S450. Topology phase diagram of Dy1 Fe1 O3

BCS ID	Formula	ICSD	MSG	T.C.	Picture
0.841	Dy1 Fe1 O3		MSG 62.441 (<i>Pnma</i>)	η_{4I}	
Topology	 		U = 4 eV		

TAB. S451. Topology phase diagram of Dy1 Fe1 O3

BCS ID	Formula	ICSD	MSG	T.C.	Picture
0.867	Ir1 Nd2 Ni1 O6		MSG 14.75 (<i>P21/c</i>)	η_{4I}	
Topology	 		U = 4 eV		

TAB. S452. Topology phase diagram of Ir1 Nd2 Ni1 O6

BCS ID	Formula	ICSD	MSG	T.C.	Picture
0.869	Ni1 Ir1 Pr2 O6		MSG 14.75 (<i>P21/c</i>)	<i>None</i>	
Topology	 		U = 4 eV ES		

TAB. S453. Topology phase diagram of Ni1 Ir1 Pr2 O6

BCS ID	Formula	ICSD	MSG	T.C.	Picture
0.870	Ni1 Ir1 Pr2 O6		MSG 14.75 ($P2_1/c$)	None	
Topology	 U=0 eV ES	 U= 2 eV AI	 U= 4 eV AI	 U= 6 eV AI	

TAB. S454. Topology phase diagram of Ni1 Ir1 Pr2 O6

BCS ID	Formula	ICSD	MSG	T.C.	Picture
0.871	Ni1 Ir1 Pr2 O6		MSG 14.75 ($P2_1/c$)	η_{4I}	
Topology	 U=0 eV ES	 U= 2 eV AI	 U= 4 eV NLC (2)	 U= 6 eV AI	

TAB. S455. Topology phase diagram of Ni1 Ir1 Pr2 O6

BCS ID	Formula	ICSD	MSG	T.C.	Picture
0.872	Ni1 Ir1 Pr2 O6		MSG 14.75 ($P2_1/c$)	η_{4I}	
Topology	 U=0 eV AI	 U= 2 eV AI	 U= 4 eV AI	 U= 6 eV AI	

TAB. S456. Topology phase diagram of Ni1 Ir1 Pr2 O6

BCS ID	Formula	ICSD	MSG	T.C.	Picture
0.873	Ni1 Ir1 Pr2 O6		MSG 14.75 ($P2_1/c$)	None	
Topology	 U=0 eV ES	 U= 2 eV AI	 U= 4 eV AI	 U= 6 eV AI	

TAB. S457. Topology phase diagram of Ni1 Ir1 Pr2 O6

BCS ID	Formula	ICSD	MSG	T.C.	Picture
0.874	Ni1 Ir1 Nd2 O6		MSG 14.75 ($P2_1/c$)	None	
Topology	 U=0 eV ES	 U=2 eV AI	 U=4 eV AI	 U=6 eV AI	

TAB. S458. Topology phase diagram of Ni1 Ir1 Nd2 O6

BCS ID	Formula	ICSD	MSG	T.C.	Picture
0.875	Ni1 Ir1 Nd2 O6		MSG 14.75 ($P2_1/c$)	η_{4I}	
Topology	 U=0 eV AI	 U=2 eV AI	 U=4 eV AI	 U=6 eV AI	

TAB. S459. Topology phase diagram of Ni1 Ir1 Nd2 O6

BCS ID	Formula	ICSD	MSG	T.C.	Picture
0.897	Tb1 Mn2 Ge2		MSG 139.537 ($I4/mm'm'$)	None	
Topology	 U=0 eV	 U=2 eV ES	 U=4 eV ES	 U=6 eV ES	

TAB. S460. Topology phase diagram of Tb1 Mn2 Ge2

BCS ID	Formula	ICSD	MSG	T.C.	Picture
0.902	Dy1 Mn2 Ge2		MSG 139.537 ($I4/mm'm'$)	None	
Topology	 U=0 eV ES	 U=2 eV ES	 U=4 eV ES	 U=6 eV ES	

TAB. S461. Topology phase diagram of Dy1 Mn2 Ge2

BCS ID	Formula	ICSD	MSG	T.C.	Picture
0.910	Ni1 Si2 Tb1		MSG 63.459 ($Cm'mcm$)	None	
Topology					

TAB. S462. Topology phase diagram of Ni1 Si2 Tb1

BCS ID	Formula	ICSD	MSG	T.C.	Picture
0.919	Eu1 Mn1 Bi2		MSG 139.536 ($I4'/m'm'm$)	z_2	
Topology					

TAB. S463. Topology phase diagram of Eu1 Mn1 Bi2

BCS ID	Formula	ICSD	MSG	T.C.	Picture
0.920	N1 P1 Mn1 Th1		MSG 129.416 ($P4'/n'm'm$)	z_2	
Topology	U=0 eV				

TAB. S464. Topology phase diagram of N1 P1 Mn1 Th1

BCS ID	Formula	ICSD	MSG	T.C.	Picture
0.922	N1 As1 Mn1 Th1		MSG 129.416 ($P4'/n'm'm$)	z_2	
Topology	U=0 eV				

TAB. S465. Topology phase diagram of N1 As1 Mn1 Th1

BCS ID	Formula	ICSD	MSG	T.C.	Picture
0.923	N1 As1 Mn1 Th1		MSG 129.416 ($P4'/n'm'm$)	z_2	
Topology	 U=0 eV AI	 U= 2 eV AI	U= 4 eV		 U= 6 eV AI

TAB. S466. Topology phase diagram of N1 As1 Mn1 Th1

BCS ID	Formula	ICSD	MSG	T.C.	Picture
0.944	Yb ₂ Ir ₂ O ₇		MSG 166.101 ($R\bar{3}m'$)	$\eta_{4I} z_{2I,1} z_{2I,2} z_{2I,3}$	
Topology	U=0 eV SEBR (2, 0, 0, 0)				

TAB. S467. Topology phase diagram of Yb₂ Ir₂ O₇

BCS ID	Formula	ICSD	MSG	T.C.	Picture
0.945	Yb ₂ Ir ₂ O ₇		MSG 227.131 ($Fd\bar{3}m'$)	η_{4I}	
Topology	U=0 eV NLC (2)				

TAB. S468. Topology phase diagram of Yb₂ Ir₂ O₇

BCS ID	Formula	ICSD	MSG	T.C.	Picture
0.954	Nd ₂ Ir ₂ O ₇		MSG 227.131 ($Fd\bar{3}m'$)	η_{4I}	
Topology	U=0 eV AF				

TAB. S469. Topology phase diagram of Nd₂ Ir₂ O₇

BCS ID	Formula	ICSD	MSG	T.C.	Picture
0.970	Pr ₁ Ru ₂ Si ₂		MSG 139.537 ($I4/mm'm'$)	None	
Topology	U=0 eV ES				

TAB. S470. Topology phase diagram of Pr₁ Ru₂ Si₂

BCS ID	Formula	ICSD	MSG	T.C.	Picture
0.978	Er1 In1 Ni1		MSG 189.225 ($P\bar{6}2'm'$)	None	
Topology	 U=0 eV	 U= 2 eV	 U= 4 eV	 U= 6 eV ES	

TAB. S471. Topology phase diagram of Er1 In1 Ni1

BCS ID	Formula	ICSD	MSG	T.C.	Picture
0.979	Tm1 V1 O3		MSG 62.446 ($Pn'm'a$)	η_{4I}	
Topology	 U=0 eV NLC (2)	 U= 2 eV AI	 U= 4 eV AI	 U= 6 eV	

TAB. S472. Topology phase diagram of Tm1 V1 O3

BCS ID	Formula	ICSD	MSG	T.C.	Picture
0.980	Tm1 V1 O3		MSG 62.446 ($Pn'm'a$)	η_{4I}	
Topology	 U=0 eV NLC (2)	 U= 2 eV	 U= 4 eV	 U= 6 eV	

TAB. S473. Topology phase diagram of Tm1 V1 O3

BCS ID	Formula	ICSD	MSG	T.C.	Picture
0.981	Tm1 V1 O3		MSG 62.441 ($Pnma$)	η_{4I}	
Topology	 U=0 eV NLC (2)	 U= 2 eV NLC (2)	 U= 4 eV AI	 U= 6 eV AI	

TAB. S474. Topology phase diagram of Tm1 V1 O3

BCS ID	Formula	ICSD	MSG	T.C.	Picture
0.982	Tm1 V1 O3		MSG 14.75 ($P2_1/c$)	η_{4I}	
Topology	 U=0 eV NLC (2)	 U= 2 eV ES	 U= 4 eV AI	U= 6 eV	

TAB. S475. Topology phase diagram of Tm1 V1 O3

BCS ID	Formula	ICSD	MSG	T.C.	Picture
0.983	Tm1 V1 O3		MSG 14.75 ($P2_1/c$)	η_{4I}	
Topology	 U=0 eV NLC (2)	 U= 2 eV AI		U= 4 eV	 U= 6 eV AI

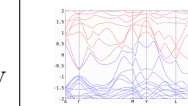
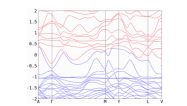
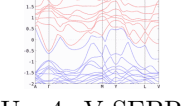
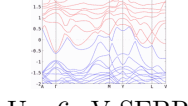
TAB. S476. Topology phase diagram of Tm1 V1 O3

BCS ID	Formula	ICSD	MSG	T.C.	Picture
1.272	Ce1 Ni1 As1 O1		MSG 4.10 (P_{a2_1})	None	
Topology	 U=0 eV AI	 U= 2 eV AI	 U= 4 eV		 U= 6 eV

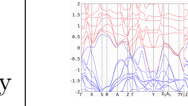
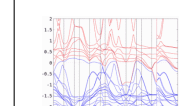
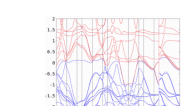
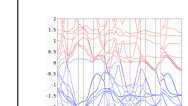
TAB. S477. Topology phase diagram of Ce1 Ni1 As1 O1

BCS ID	Formula	ICSD	MSG	T.C.	Picture
1.292	Ho1 Ni2 B2 C1		MSG 64.480 ($C_A mca$)	$\eta_{4I}\delta_{2m}$	
Topology	 U=0 eV AI	 U= 2 eV AI	 U= 4 eV AI		 U= 6 eV AI

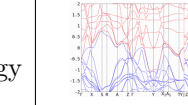
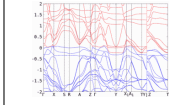
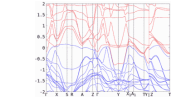
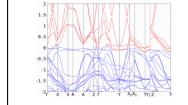
TAB. S478. Topology phase diagram of Ho1 Ni2 B2 C1

BCS ID	Formula	ICSD	MSG	T.C.	Picture
1.293	Nd1 Ni2 B2 C1		MSG 15.90 (C_c2/c)	η_{4I}	
Topology	 U=0 eV	 U= 2 eV OAI	 U= 4 eV SEBR (2)	 U= 6 eV SEBR (2)	

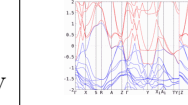
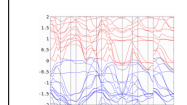
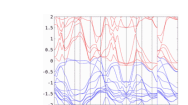
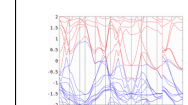
TAB. S479. Topology phase diagram of Nd1 Ni2 B2 C1

BCS ID	Formula	ICSD	MSG	T.C.	Picture
1.294	Ho1 Ni2 B2 C1		MSG 64.480 (C_Amca)	$\eta_{4I}\delta_{2m}$	
Topology	 U=0 eV SEBR (2, 1)	 U= 2 eV AI	 U= 4 eV AI	 U= 6 eV AI	

TAB. S480. Topology phase diagram of Ho1 Ni2 B2 C1

BCS ID	Formula	ICSD	MSG	T.C.	Picture
1.295	Dy1 Ni2 B2 C1		MSG 64.480 (C_Amca)	None	
Topology	 U=0 eV ES	 U= 2 eV AI	 U= 4 eV AI	 U= 6 eV AI	

TAB. S481. Topology phase diagram of Dy1 Ni2 B2 C1

BCS ID	Formula	ICSD	MSG	T.C.	Picture
1.296	Pr1 Ni2 B2 C1		MSG 64.480 (C_Amca)	$\eta_{4I}\delta_{2m}$	
Topology	 U=0 eV SEBR (2, 1)	 U= 2 eV ES	 U= 4 eV AF	 U= 6 eV AF	

TAB. S482. Topology phase diagram of Pr1 Ni2 B2 C1

BCS ID	Formula	ICSD	MSG	T.C.	Picture
1.312	Ho1 Ni2 B2 C1		MSG 64.480 (C_{Amca})	$\eta_{4I}\delta_{2m}$	
Topology	 U=0 eV AI	 U= 2 eV AI	 U= 4 eV AI	 U= 6 eV AI	

TAB. S483. Topology phase diagram of Ho1 Ni2 B2 C1

BCS ID	Formula	ICSD	MSG	T.C.	Picture
1.350	Ba1 Nd2 Co1 O5		MSG 15.90 (C_c2/c)	η_{4I}	
Topology	 U=0 eV AI	 U= 2 eV AI	 U= 4 eV AI	 U= 6 eV AI	

TAB. S484. Topology phase diagram of Ba1 Nd2 Co1 O5

BCS ID	Formula	ICSD	MSG	T.C.	Picture
1.363	Tb1 Cu2 Si2		MSG 2.7 ($P_S\bar{1}$)	η_{4I}	
Topology	 U=0 eV OAI	 U= 2 eV AF	 U= 4 eV	 U= 6 eV OAI	

TAB. S485. Topology phase diagram of Tb1 Cu2 Si2

BCS ID	Formula	ICSD	MSG	T.C.	Picture
1.364	Ho1 Cu2 Si2		MSG 2.7 ($P_S\bar{1}$)	η_{4I}	
Topology	 U=0 eV OAI	 U= 2 eV OAI	 U= 4 eV OAI	 U= 6 eV	

TAB. S486. Topology phase diagram of Ho1 Cu2 Si2

BCS ID	Formula	ICSD	MSG	T.C.	Picture
1.365	Cu2 Si2 Tb1		MSG 2.7 ($P_S\bar{1}$)	η_{4I}	
Topology	 U=0 eV OAI	 U= 2 eV NLC (2)	 U= 4 eV NLC (2)	 U= 6 eV NLC (2)	

TAB. S487. Topology phase diagram of Cu2 Si2 Tb1

BCS ID	Formula	ICSD	MSG	T.C.	Picture
1.366	Cu2 Ho1 Si2		MSG 12.63 (C_c2/m)	None	
Topology	 U=0 eV ES	 U= 2 eV	 U= 4 eV	 U= 6 eV	

TAB. S488. Topology phase diagram of Cu2 Ho1 Si2

BCS ID	Formula	ICSD	MSG	T.C.	Picture
1.369	Ho1 Fe2 Ge2		MSG 64.480 (C_Amca)	$\eta_{4I}\delta_{2m}$	
Topology	 U=0 eV SEBR (2, 1)	 U= 2 eV AF	 U= 4 eV ES	 U= 6 eV ES	

TAB. S489. Topology phase diagram of Ho1 Fe2 Ge2

BCS ID	Formula	ICSD	MSG	T.C.	Picture
1.487	Ce1 Ir1 Al4 Si2		MSG 124.360 (P_c4/mcc)	None	
Topology	U=0 eV	U= 2 eV	 U= 4 eV ES	 U= 6 eV ES	

TAB. S490. Topology phase diagram of Ce1 Ir1 Al4 Si2

BCS ID	Formula	ICSD	MSG	T.C.	Picture
1.488	Ce1 Mn2 Si2		MSG 126.386 (P_I4/nnc)	None	
Topology	 U=0 eV ES	 U=2 eV ES	 U=4 eV ES	 U=6 eV ES	

TAB. S491. Topology phase diagram of Ce1 Mn2 Si2

BCS ID	Formula	ICSD	MSG	T.C.	Picture
1.489	Ce1 Mn2 Si2		MSG 126.386 (P_I4/nnc)	None	
Topology	 U=0 eV ES	 U=2 eV ES	 U=4 eV ES	U=6 eV	

TAB. S492. Topology phase diagram of Ce1 Mn2 Si2

BCS ID	Formula	ICSD	MSG	T.C.	Picture
1.491	Pr1 Mn2 Si2		MSG 126.386 (P_I4/nnc)	None	
Topology	U=0 eV	 U=0 eV ESFD	 U=2 eV ESFD	 U=4 eV ESFD	 U=6 eV ESFD

TAB. S493. Topology phase diagram of Pr1 Mn2 Si2

BCS ID	Formula	ICSD	MSG	T.C.	Picture
1.492	Pr1 Mn2 Si2		MSG 126.386 (P_I4/nnc)	None	
Topology	 U=0 eV ESFD	 U=2 eV ESFD	 U=4 eV ESFD	 U=6 eV ESFD	

TAB. S494. Topology phase diagram of Pr1 Mn2 Si2

BCS ID	Formula	ICSD	MSG	T.C.	Picture
1.493	Pr1 Mn2 Si2		MSG 126.386 (P_I4/nnc)	None	
Topology	U=0 eV				

TAB. S495. Topology phase diagram of Pr1 Mn2 Si2

BCS ID	Formula	ICSD	MSG	T.C.	Picture
1.494	Nd1 Mn2 Si2		MSG 126.386 (P_I4/nnc)	None	
Topology	U=0 eV OAI				

TAB. S496. Topology phase diagram of Nd1 Mn2 Si2

BCS ID	Formula	ICSD	MSG	T.C.	Picture
1.504	Gd1 Cu1 Sn1		MSG 33.154 (P_Cna2_1)	None	
Topology	U=0 eV AI				

TAB. S497. Topology phase diagram of Gd1 Cu1 Sn1

BCS ID	Formula	ICSD	MSG	T.C.	Picture
1.511	Ni2 Tb1 Si2		MSG 64.480 (C_{Amca})	$\eta_4 I \delta_{2m}$	
Topology	U=0 eV SEBR (2, 1)				

TAB. S498. Topology phase diagram of Ni2 Tb1 Si2

BCS ID	Formula	ICSD	MSG	T.C.	Picture
1.516	Er1 Co2 Si2		MSG 58.404 (P_{Innm})	None	
Topology	U=0 eV	U= 2 eV ES	U= 4 eV ES	U= 6 eV AF	

TAB. S499. Topology phase diagram of Er1 Co2 Si2

BCS ID	Formula	ICSD	MSG	T.C.	Picture
1.549	U2 In1 Ni2		MSG 128.408 (P_{c4}/mnc)	None	
Topology	U=0 eV			U= 6 eV	

TAB. S500. Topology phase diagram of U2 In1 Ni2

BCS ID	Formula	ICSD	MSG	T.C.	Picture
1.566	Ba2 Yb1 Ru1 O6		MSG 128.410 (P_{I4}/mnc)	None	
Topology	U=0 eV ES			U= 4 eV	

TAB. S501. Topology phase diagram of Ba2 Yb1 Ru1 O6

BCS ID	Formula	ICSD	MSG	T.C.	Picture
1.567	Ba2 Tm1 Ru1 O6		MSG 128.410 (P_{I4}/mnc)	$\eta_{4I}\delta_{2m}z_2\delta_{4m}$	
Topology	U=0 eV SEBR (0, 0, 0, 2)			U= 4 eV AI	

TAB. S502. Topology phase diagram of Ba2 Tm1 Ru1 O6

BCS ID	Formula	ICSD	MSG	T.C.	Picture
1.568	Cu2 Gd1 Si2		MSG 12.63 (C_{c2}/m)	$\eta_{4I}\delta_{2m}$	
Topology	U=0 eV AF			U= 4 eV AF	

TAB. S503. Topology phase diagram of Cu2 Gd1 Si2

BCS ID	Formula	ICSD	MSG	T.C.	Picture
1.584	Pr1 Fe1 As1 O1		MSG 54.350 (P_{Bcc})	None	
Topology	 U=0 eV OAI	 U= 2 eV OAI	 U= 4 eV OAI	 U= 6 eV ES	

TAB. S504. Topology phase diagram of Pr1 Fe1 As1 O1

BCS ID	Formula	ICSD	MSG	T.C.	Picture
1.585	Pr1 Fe1 As1 O1		MSG 54.350 (P_{Bcc})	η_{4I}	
Topology	 U=0 eV NLC (2)	 U= 2 eV NLC (2)	 U= 4 eV OAI	 U= 6 eV OAI	

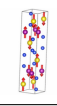
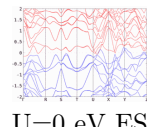
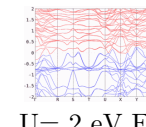
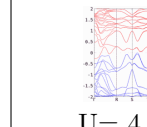
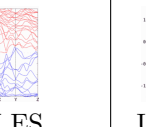
TAB. S505. Topology phase diagram of Pr1 Fe1 As1 O1

BCS ID	Formula	ICSD	MSG	T.C.	Picture
1.586	Pr1 Fe1 As1 O1		MSG 27.85 (P_{Acc2})	None	
Topology	 U=0 eV AI	 U= 2 eV AI	 U= 4 eV AI	 U= 6 eV AI	

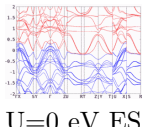
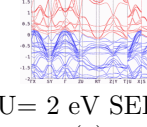
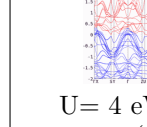
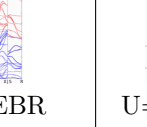
TAB. S506. Topology phase diagram of Pr1 Fe1 As1 O1

BCS ID	Formula	ICSD	MSG	T.C.	Picture
1.596	Tb1 Cu1 Sb2		MSG 2.7 ($P_S\bar{1}$)	η_{4I}	
Topology	 U=0 eV OAI	 U= 2 eV	 U= 4 eV	 U= 6 eV OAI	

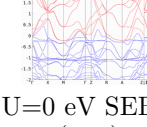
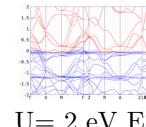
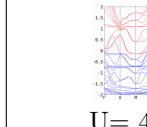
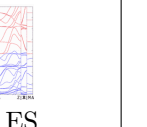
TAB. S507. Topology phase diagram of Tb1 Cu1 Sb2

BCS ID	Formula	ICSD	MSG	T.C.	Picture
1.628	Pr1 Mn1 Si2		MSG 52.318 (P_Bnna)	None	
Topology	 U=0 eV ES	 U= 2 eV ES	 U= 4 eV ES	 U= 6 eV ES	

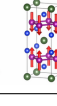
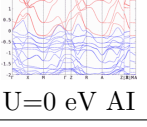
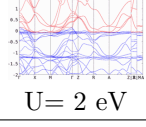
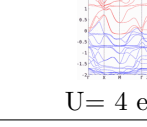
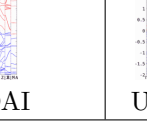
TAB. S508. Topology phase diagram of Pr1 Mn1 Si2

BCS ID	Formula	ICSD	MSG	T.C.	Picture
1.635	Er1 Fe2 Si2		MSG 62.450 (P_anma)	η_{4I}	
Topology	 U=0 eV SEBR (2)	 U= 2 eV SEBR (2)	 U= 4 eV SEBR (2)	 U= 6 eV SEBR (2)	

TAB. S509. Topology phase diagram of Er1 Fe2 Si2

BCS ID	Formula	ICSD	MSG	T.C.	Picture
1.636	Er1 Mn2 Si2		MSG 126.386 (P_I4/nnc)	$\eta_{4I}z_2$	
Topology	 U=0 eV SEBR (2, 1)	 U= 2 eV ES	 U= 4 eV ES	 U= 6 eV OAI	

TAB. S510. Topology phase diagram of Er1 Mn2 Si2

BCS ID	Formula	ICSD	MSG	T.C.	Picture
1.637	Er1 Mn2 Si2		MSG 126.386 (P_I4/nnc)	None	
Topology	 U=0 eV AI	 U= 2 eV	 U= 4 eV OAI	 U= 6 eV ES	

TAB. S511. Topology phase diagram of Er1 Mn2 Si2

BCS ID	Formula	ICSD	MSG	T.C.	Picture
1.638	Er1 Mn2 Ge2		MSG 126.386 (P_{I4}/nn)	$\eta_{4I}z_2$	
Topology	 U=0 eV AI	 U= 2 eV ES	 U= 4 eV SEBR (2, 1)	 U= 6 eV ES	

TAB. S512. Topology phase diagram of Er1 Mn2 Ge2

BCS ID	Formula	ICSD	MSG	T.C.	Picture
1.639	Er1 Mn2 Ge2		MSG 126.386 (P_{I4}/nn)	$\eta_{4I}z_2$	
Topology	 U=0 eV AI	 U= 2 eV SEBR (2, 1)	 U= 4 eV ES	 U= 6 eV ES	

TAB. S513. Topology phase diagram of Er1 Mn2 Ge2

BCS ID	Formula	ICSD	MSG	T.C.	Picture
1.640	Er1 Mn2 Ge2		MSG 126.386 (P_{I4}/nn)	$\eta_{4I}z_2$	
Topology	 U=0 eV AI	 U= 2 eV ES	 U= 4 eV SEBR (2, 1)	 U= 6 eV ES	

TAB. S514. Topology phase diagram of Er1 Mn2 Ge2

BCS ID	Formula	ICSD	MSG	T.C.	Picture
1.664	Dy1 V1 O4		MSG 62.456 (P_{Inma})	η_{4I}	
Topology	 U=0 eV AI	 U= 2 eV AI	 U= 4 eV AI	 U= 6 eV AI	

TAB. S515. Topology phase diagram of Dy1 V1 O4

BCS ID	Formula	ICSD	MSG	T.C.	Picture
1.666	Tb1 Co1 Ga5		MSG 67.509 (C_{mma})	$\eta_{4I}\delta_{2m}$	
Topology	 U=0 eV OAI	 U= 2 eV OAI	 U= 4 eV NLC (2, 1)	 U= 6 eV OAI	

TAB. S516. Topology phase diagram of Tb1 Co1 Ga5

BCS ID	Formula	ICSD	MSG	T.C.	Picture
1.668	Ho1 Co1 Ga5		MSG 67.509 (C_{mma})	$\eta_{4I}\delta_{2m}$	
Topology	 U=0 eV NLC (2, 1)	 U= 2 eV NLC (2, 1)	 U= 4 eV NLC (2, 1)	 U= 6 eV NLC (2, 1)	

TAB. S517. Topology phase diagram of Ho1 Co1 Ga5

BCS ID	Formula	ICSD	MSG	T.C.	Picture
1.670	Np1 Fe1 Ga5		MSG 67.509 (C_{mma})	$\eta_{4I}\delta_{2m}$	
Topology	 U=0 eV AI	 U= 2 eV AI	 U= 4 eV AI	 U= 6 eV NLC (2, 1)	

TAB. S518. Topology phase diagram of Np1 Fe1 Ga5

BCS ID	Formula	ICSD	MSG	T.C.	Picture
1.683	Ga5 Ni1 U1		MSG 140.550 (I_{c4}/mcm)	$\eta_{4I}\delta_{2m}z_2\delta_{4m}z_{4m,0}^+z_4z'_4$	
Topology	 U=0 eV ES	 U= 2 eV SEBR (2, 1, 1, 3, 1, 3, 3)	 U= 4 eV SEBR (2, 1, 1, 3, 1, 3, 3)	 U= 6 eV OAI	

TAB. S519. Topology phase diagram of Ga5 Ni1 U1

BCS ID	Formula	ICSD	MSG	T.C.	Picture
1.690	Tm1 Mn2 Ge2		MSG 126.386 (P_I4/nnc)	None	
Topology	 	U=0 eV AF U= 2 eV ESFD U= 4 eV ESFD U= 6 eV ESFD			

TAB. S520. Topology phase diagram of Tm1 Mn2 Ge2

BCS ID	Formula	ICSD	MSG	T.C.	Picture
1.694	Mn2 Tb1 Ge2		MSG 126.386 (P_I4/nnc)	None	
Topology	 	U=0 eV ESFD U= 2 eV ESFD U= 4 eV ESFD U= 6 eV ESFD			

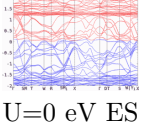
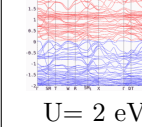
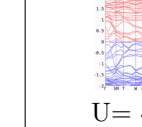
TAB. S521. Topology phase diagram of Mn2 Tb1 Ge2

BCS ID	Formula	ICSD	MSG	T.C.	Picture
1.721	U1 Cu5		MSG 161.72 (R_I3c)	None	
Topology	 	U=0 eV AF U= 2 eV AI U= 4 eV AI U= 6 eV AI			

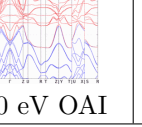
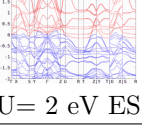
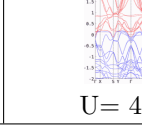
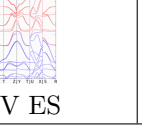
TAB. S522. Topology phase diagram of U1 Cu5

BCS ID	Formula	ICSD	MSG	T.C.	Picture
1.729	Gd2 Fe2 Si2 C1		MSG 12.63 (C_c2/m)	$\eta_{4I}\delta_{2m}$	
Topology	 	U=0 eV SEBR (2, 1) U= 2 eV AF U= 4 eV AF U= 6 eV AF			

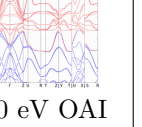
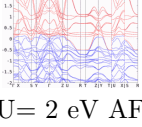
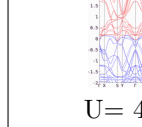
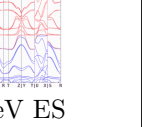
TAB. S523. Topology phase diagram of Gd2 Fe2 Si2 C1

BCS ID	Formula	ICSD	MSG	T.C.	Picture
1.738	Tb1 Al1 Ni1		MSG 46.247 ($I_a ma2$)	None	
Topology	 $U=0 \text{ eV ES}$	 $U=2 \text{ eV}$	 $U=4 \text{ eV AI}$	$U=6 \text{ eV}$	

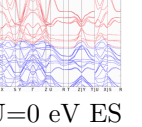
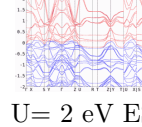
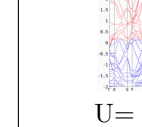
TAB. S524. Topology phase diagram of Tb1 Al1 Ni1

BCS ID	Formula	ICSD	MSG	T.C.	Picture
2.81	Er1 Mn2 Si2		MSG 59.409 ($Pm'm'n$)	None	
Topology	 $U=0 \text{ eV OAI}$	 $U=2 \text{ eV ES}$	 $U=4 \text{ eV ES}$	 $U=6 \text{ eV AF}$	

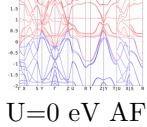
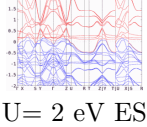
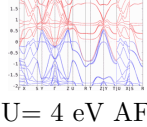
TAB. S525. Topology phase diagram of Er1 Mn2 Si2

BCS ID	Formula	ICSD	MSG	T.C.	Picture
2.82	Er1 Mn2 Si2		MSG 59.409 ($Pm'm'n$)	None	
Topology	 $U=0 \text{ eV OAI}$	 $U=2 \text{ eV AF}$	 $U=4 \text{ eV ES}$	 $U=6 \text{ eV ES}$	

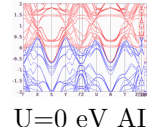
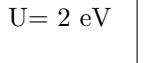
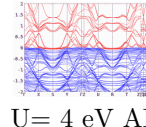
TAB. S526. Topology phase diagram of Er1 Mn2 Si2

BCS ID	Formula	ICSD	MSG	T.C.	Picture
2.83	Er1 Mn2 Ge2		MSG 59.409 ($Pm'm'n$)	None	
Topology	 $U=0 \text{ eV ES}$	 $U=2 \text{ eV ES}$	 $U=4 \text{ eV ES}$	$U=6 \text{ eV}$	

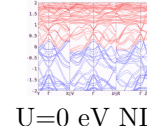
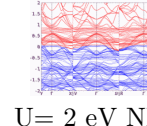
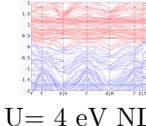
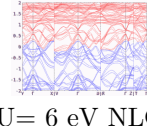
TAB. S527. Topology phase diagram of Er1 Mn2 Ge2

BCS ID	Formula	ICSD	MSG	T.C.	Picture
2.84	Er1 Mn2 Ge2		MSG 59.409 ($Pm'm'n$)	None	
Topology	 U=0 eV AF	 U= 2 eV ES	 U= 4 eV AF	U= 6 eV	

TAB. S528. Topology phase diagram of Er1 Mn2 Ge2

BCS ID	Formula	ICSD	MSG	T.C.	Picture
2.94	Tm1 Mn2 Ge2		MSG 26.70 ($Pm'c'2_1$)	None	
Topology	 U=0 eV AI	 U= 2 eV	 U= 4 eV AI	U= 6 eV	

TAB. S529. Topology phase diagram of Tm1 Mn2 Ge2

BCS ID	Formula	ICSD	MSG	T.C.	Picture
3.20	Mn2 Tb1 Ge2		MSG 2.4 ($P\bar{1}$)	$\eta_{4I}z_{2I,1}z_{2I,2}z_{2I,3}$	
Topology	 U=0 eV NLC (2, 0, 0, 0)	 U= 2 eV NLC (2, 0, 0, 0)	 U= 4 eV NLC (1, 0, 0, 0)	 U= 6 eV NLC (1, 0, 0, 0)	

TAB. S530. Topology phase diagram of Mn2 Tb1 Ge2